Structure and Bonding, Vol. 106 (2004): 1–5
DOI 10.1007/b11301

Axel Christian Klixbüll Jørgensen (1931–2001)

Claus E. Schäffer

University of Copenhagen, Department of Chemistry, Universitetsparken 5, 21000 København, Denmark

Axel to his parents, Christian to his friends, Klixbüll to his country, and C.K.Jorgensen (in Danish C.K.Jørgensen) to the world community of chemists: almost symbolic that a person so much out of the ordinary should have four different given names and two unusual letters, the German ü and the Danish ø in his surname.

Christian was extraordinary even when he was a child. Even though originating from a family without bookshelves, he could read, write and do arithmetic before he entered school. In his early teens, he made personal friends for life among active scientists. At first his curiosity led him to an astronomer who soon taught him about the spectra of stars. With this knowledge, he visited the last atomic spectroscopist of the Niels Bohr Institute, Ebbe Rasmussen, who introduced him to the world of atoms and to how we describe their spectra. At the same time – during the second world war – he carried out chemical experiments in his mother's kitchen while his father served on the Danish school ship under the American flag.

As a freshman, Klixbüll read Jannik Bjerrum's thesis entitled "Metal Amine Formation in Aqueous Solution". He did this overnight and formed his personal opinion about certain points, which he discussed with Bjerrum the following morning. The thesis was a book of 300 pages describing the "ligand method" for the determination of stability constants, not exactly an easy-reader for an almost school boy.

As the first freshman ever to appear regularly as a guest in the scientific laboratories, Klixbüll made himself famous in Chemistry Department A of the Technical University of Denmark. In the beginning, everybody wanted to experience this young wonder and his readiness to discuss any chemical problem. However, he was so engrossed that even direct reference to one's need to do other things could not stop his monologs. Therefore, after a while, he was courted less. This was in 1950.

He not only obtained an unusual degree at the University of Copenhagen, a degree in chemistry, physics, and astronomy, but he also managed to avoid organic laboratory work entirely. This was contrary to the standard training of chemists in Denmark at that time, which was classically experimental with a whole year of practical organic chemistry, three full afternoons a week. But he found this subject uninteresting.

C.K.Jørgensen appeared in the literature as early as 1953 after he had studied the alcohol solvation of metal ions together with his adviser, Jannik Bjerrum,

who was the permanent head of the laboratory. This issue was followed up over a couple of years before the case was closed, unfinished, and with an argument in Nature with L.I. Katzin from Argonne National Laboratory. The nature of the competition between water and anions in alcoholic solution was never properly elucidated, but the story made him skeptical about the general usefulness of the mass action law and sharpened his general critical attitude toward the establishment.

He finished his master's degree in January 1954. There was no such thing as a Danish Ph.D. degree at that time, but in 1957 he delivered his thesis in the Danish tradition, much resembling the British Dr. of Science degree or the German Habilitation. The title was "Energy Levels of Complexes and Gaseous Ions" and attached to the thesis were 11 out of some 30 papers, primarily written by himself alone. Only two years after his master's degree, he had already established himself enough to be invited as a main speaker (Orgel and Nyholm being among the others) at the Xth Solvay Council on the colors of metal compounds. This was just after his 25th birthday.

Also in 1956, Jørgensen entered the 4f and 5f clubs, uniting the two. He did this by a small interdisciplinary note in J.Chem.Phys. In the same year he produced two papers on the 4f spectra as members of a series of ten papers with the common main title "Studies of Absorption Spectra". Jannik Bjerrum had taken the initiative with the first one of these crystal-field papers in collaboration with his student C.J. Ballhausen, and Jørgensen had joined in as a coauthor. This paper treated the copper ammine system and provided a theoretical explanation of the "pentammine effect", which is the unusual phenomenon that the replacement of the copper(II) ion's fifth water molecule by ammonia leads to a red-shift of the absorption band in the visible region. The very discovery of the pentammine and the "pentammine effect" had been instrumental in bringing Jannik Bjerrum on to the scientific scene more than 20 years earlier.

The following "Studies of Absorption Spectra" became a common effort by C.J.Ballhausen and C.K.Jørgensen. However, they mostly acted individually. Ballhausen, who also finished his master's degree in 1954 with Bjerrum as his adviser, was the single author of two of the papers giving an account of how the Ilse and Hartmann's point-charge formalism for d^1 and d^2 systems could be used to handle d^9 and d^8 systems, respectively, and also in a point-dipole formalism. Five of the papers were authored by Jørgensen alone. In three of them, he discussed the shapes of the absorption bands, spin-forbidden transitions, and the relationship between the highest spin-multiplicity energy levels among d^q configurations. In the next two papers he discussed $5f^2$ systems and systems with three and more f-electrons. The series ended with two papers, where Ballhausen and Jørgensen's efforts were united, mainly in discussing the splitting of the energy levels of cubic complexes by crystal fields of lower symmetry.

Klixbüll worked in a cellar room during all his years in Denmark, and I was in the neighboring room. We were the only people in that part of the building and had a lot to do with each other. He was always very kind and an inspiring person to be around, but he created an environment in which it was not too easy to work. He provided almost constant entertainment, sometimes at a high level, while at the same time he would do his other work. It was a strange sensation to be en-

tertained by a person who only looked at you now and then and who quite apparently did other things at the same time. In order to survive these working conditions, I had to make the agreement with him that he kept away on his weekly literature day when he was irritable while excerpting each paper of interest on an index card. When he had his measuring days, which not only involved making up solutions using a graduated cylinder, but also mass action considerations that could be quite complicated, he would often come and beg me to be present so that we could discuss "less trivial matters." But even though he was kind, he was not an easy person to have around. Discussions with him often led him to suggest that "we write about it." Then, by the next morning and at the latest the following Monday morning, he would deliver a draft to a paper embracing our common efforts in his own, often quite original thoughts, whose details were frequently presented in a stream-of-consciousness kind of way. It was never possible for me to join in as a co-author under these conditions and his "method" rarely led to collaboration in any of the usual meanings of the word. However, later in life, he did contribute with his special expertise to papers on many different issues and involving co-authors from several different countries through the years. As to our early years together, when Klixbüll became Christian and Schäffer became Claus, I am grateful in retrospect; and I was lucky enough to be able to develop the nephelauxetic series and the angular overlap model (AOM) together with him.

Jørgensen had the remarkable ability of being able to extract the quintessence of articles not only on chemistry, but also on physics and astrophysics, without necessarily understanding their details. In addition, he could use this comprehension for widening the perspective of his own work. Even though he was like a computer with his encyclopedic memory, he was much more different from a computer than most other humans in that he was often able to correlate not only his stored data, but also concepts, which other people would not have imagined to be related.

His focus on his immediate aims was also exceptional. His most permanent interest was absorption spectra of solutions. Therefore, his first question was inevitably: What is/are the species? And in answering this question he was very astute. Then his only important spectroscopic question was: What are the positions of the absorption bands? In order to obtain a quick answer to this second question, he broke so much with tradition that he was severely criticized at the defense of his thesis. He had decided that since we did not have good theories for the shapes and intensities of the absorption bands, it was, at that stage of our knowledge, a waste to spend much extra time in obtaining these quantities accurately. At the time, he was alone with that attitude, but in retrospect – looking at what he accomplished – one has to conclude that he was right.

Even in his Solvay report (1956), Jørgensen had already collected together experimental evidence that our ligand-field treatment of the 3d elements could be successfully extended to 4d and 5d, a fact which was unexpected at that time. Moreover, the crystal-field series "Studies of Absorption Spectra"(1955) had hardly been finished when he began a crusade against crystal-field theory (the electrostatic model). He always claimed that this model died at the Solvay conference. This was not to say that the theoretical formalism died; the empirical parameters, however, required a different physical interpretation involving the

idea of covalency as a comparative concept. Thereby, a unification of the treatment of the ligand-field spectra of 3d, 4d, 5d, 4f, and 5f complexes was brought about, along with an emphasis on their similarities and differences.

A few years later Jørgensen became one of the pioneers of our understanding of the so-called ligand-to-metal charge transfer spectra, which he called electron transfer spectra because he was able to rationalize them on the basis of molecular-orbital electron configurations which had preponderantly either ligand or metal character. This was a major accomplishment bringing order into an apparent chaos.

He wrote five books in the 1960s bringing his own work into perspective.

In the seventies, when the technique of X-ray photoelectron spectroscopy became commercially available, he again contributed considerably to our knowledge by reviewing almost the whole periodic table. He used his usual technique based upon induction from his new spectral results; this time he was able to obtain knowledge about the energies of certain inner electrons. Again his productivity was overwhelming, but his accuracy and reproducibility were hampered by charging-up effects of his non-conducting solid samples. An impact of this part of his work on the chemical community at large has yet to be seen.

Exotic subjects such as the prediction of the chemistries of quarks and of not yet known trans-uranium elements were among his interests in his later years when he also fraternized with the astrophysicists.

During his early chemistry studies, he had produced philosophical papers on trivalent logic, but it was not until he was established in chemistry that he found a place to publish his contributions in this area.

At the age of 29 he had left Denmark, never to live in that country again. After 2 years at the NATO Science Adviser's office in Paris, where he instituted several of the NATO-sponsored scientific gatherings, he was attached to the new Cyanamid European Research Institute in Cologny, near Geneva, where he was allowed to establish and run a small group of people doing fundamental science. When this institute was closed down eight years later, he moved to the University of Geneva where he spent his remaining active years.

Jørgensen's eagerness to give improvised talks remained a characteristic of him. Moreover, he did this with equal enthusiasm to a large audience and to one or two people in a corridor. These latter monologs had of course a more conversational character and were perhaps his main oral contact with the world outside himself. A black board was his most beloved utensil all through his life, and during a lecture or conversation he could almost paint it white by using up the last bits of empty space. Sometimes his lectures were brilliant: original, inspiring, and communicating a lot of new results from all over the world, often not yet published, his own or those of others. From before his bachelor's degree he corresponded with an unbelievable number of people, and this also led him to his future wife. She was French and felt most comfortable in surroundings where her mother tongue was spoken. Unfortunately, she died when their children were still small.

Christian and I were friends for 50 years and remained feeling like boys, comfortable in each other's company. We always had lots of scientific matters to talk about and did not often touch upon personal matters. Christian was a solitary man.

Jørgensen's experimental and conceptual contributions, especially to ligand-field theory's connection with chemistry and chemical bonding, form one of the success stories of inorganic chemistry of the 20th century. Were it not for his somewhat esoteric style, he would probably not only have been the dominating figure he was, but he would also have left the subject in such a form that reinventions would forever have been unjustified. As it is, many of his original ideas, results, and concepts have become universally accepted, but their origin, history, and context have been forgotten – and thereby the full perspective that lay in his thinking. In spite of this, the 2000 pages he produced during less than two decades (1954–1971) will probably continue to be studied and quoted for a long time to come.

Structure and Bonding, Vol. 106 (2004): 7–18
DOI 10.1007/b11302

Whereof Man Cannot Speak: Some Scientific Vocabulary of Michael Faraday and Klixbüll Jørgensen

Peter Day

The Royal Institution of Great Britain, Davy Faraday Research Laboratory,
Albemarle Street 21, London W1S 4BS, UK
E-mail: pday@ri.ac.uk

Abstract Inventing new words and phrases is an indispensable means of capturing new concepts that arise as science advances. Some comparisons are made between the approaches of the nineteenth century natural philosopher Michael Faraday and the twentieth century spectroscopist Christian Klixbüll Jørgensen in their approach to naming new phenomena.

Keywords Nephelauxetic effect · Oxidation state · Taxological quantum chemistry · Faraday Jørgensen

1 Words for Things

In their pursuit of larger truths, often encapsulated in short aphorisms, even the greatest philosophers can sometimes be guilty of making approximations. Thus, when Ludwig Wittgenstein finished his major work on linguistic philosophy, Tractatus Logico-Philosophicus with the famous phrase 'whereof we cannot speak, thereof we must be silent' [1], he failed to take account of a situation that occurs quite frequently in science, as newly uncovered facts about the world call for new concepts to describe them. In science, when we find something for which

there is no existing vocabulary, it is certainly not customary to remain silent. What is normally done is to invent a new word or phrase.

This procedure of coining new phrases to embrace new facts or new levels of understanding goes back to the very foundations of the scientific enterprise. Indeed, a good case could be made that it is a fundamental part of the whole procedure of gaining intellectual ascendancy over the world of natural phenomena. Astronomers of the era of the scientific revolution were adventurous employers of vocabulary, and the chemists, having such a diverse array of phenomena to encompass, were not far behind: Just think of the potent sway that the concept symbolised by the word 'phlogiston' held over chemical theory up to the late eighteenth century. In the first half of the nineteenth century, one of the most prolific coiners of new phraseology was Michael Faraday. In fact, two quite disparate fields of science still bear the hallmark of his invention till the present day. Early in Faraday's career, electrochemistry (a word that we owe to Faraday's mentor, Humphry Davy) was at the centre of his interests, while two decades later it was magnetism. Before considering some of Jørgensen's contributions to the language of chemistry, it is pertinent to document briefly some of the great contributions by his illustrious forebear.

2
Michael Faraday and Scientific Vocabulary

One of many remarkable features of Faraday's career was his lack of advanced education [2]. Indeed, his formal education ceased at the age of 13, in 1804, when he was apprenticed to a bookseller and bookbinder Mr. Riebau. Consequently, it is not surprising that his knowledge of mathematics remained rudimentary throughout his life, probably not stretching much beyond simple arithmetic. Although his laboratory notes contain geometrical diagrams (for example the lines of induction around magnetised bodies), there is no evidence that he was capable of drawing quantitative conclusions from them. Among the earliest of many protestations found in his voluminous writings about a handicap in comprehending mathematical reasoning is a letter to Ampère in 1822, in which he takes refuge in the primacy of experimental facts, regarding mathematics as a navigational compass of uncertain efficacy. Here is what he wrote [3]:

> I am unfortunate in a want of mathematical knowledge and the power of entering with facility into abstract reasoning. I am obliged to feel my way by facts closely placed together, so that it often happens I am left behind in the progress of a branch of science (not merely from the want of attention) but from the incapability I lay under of following it, notwithstanding all my exertions. It is just now so, I am ashamed to say, with your refined researches on electromagnetism or electrodynamics. On reading your papers and letters, I have no difficulty in following the reasoning, but still at last I seem to want something more on which to steady the conclusions. I fancy the habit I got into of attending too closely to experiment has somewhat fettered my powers of reasoning, and chains me down, and I cannot help now and then comparing myself to a timid ignorant navigator who (though he might boldly and safely steer across a bay or an ocean by the aid of a compass which in its actions and principles is infallible) is afraid to leave sight of the shore because he understands not the power of the instrument that is to guide him.

In contrast to his suspicion of mathematics as a tool, Faraday was intensely concerned with inventing and defining new words to encapsulate the new pheno-

mena that his experiments were opening up. The ironic tone of the following description (in a letter of 1831 to the chemist Richard Phillips [4]) of how the word 'electrotonic', now quite vanished from the scientific vocabulary, came to be coined, should not be taken at face value:

> This condition of matter I have dignified by the term *Electro-tonic*. What do you think of that? Am I not a bold man, ignorant as I am, to coin words? But I have consulted the scholars.

Despite his own propensity for coining words, Faraday was not above casting scorn on others who sought to do the same. The line between illumination and obfuscation in the way that technical language is used remains a narrow one for science even today. William Whewell (the Cambridge historian and classical scholar) frequently gave advice to Faraday about etymology, enveloping the new objects of science in classical language. In one of his letters, Faraday wrote to Whewell as follows [5]:

> Your remarks upon chemical notation, with the variety of systems which have arisen with regard to notation, nomenclature, scales of proportional or atomic number etc., etc., had almost stirred me up to regret publicly that such hindrances to the progress of science should exist. I cannot help thinking it a most unfortunate thing that men who, as experimentalists and philosophers, are the most fitted to advance the general cause of science and knowledge should, by the promulgation of their own theoretical views under the form of nomenclature, notation or scale, actually retard its progress.

Faraday's earliest lasting contribution to scientific nomenclature arose from his experiments in the 1820s and early 1830s on the electrolysis of aqueous solutions. He also sought advice about nomenclature from another friend, William Nicholl, which he passed on in a letter to William Whewell in 1834. That letter contains the first ever mention of the words '*electrode*' and '*electrolyte*'. In contrast it is interesting to observe that another word '*zetode*' did not survive. In his letter to Whewell, he writes [6]:

> I wanted some new names to express my facts in electrical science without involving more theory than I could help, and applied to a friend Dr. Nicholl, who has given me some that I intend to adopt. For instance, a body decomposable by the passage of the electric current, I call an "*electrolyte*", and instead of saying that water is *electro chemically decomposed* I say it is "*electrolysed*". The intensity above which a body is decomposed, beneath which it conducts without decomposition, I call the "*electrolytic intensity*", etc., etc. What have been called the poles of the battery I call the *electrodes*. They are not merely surfaces of metal, but even of water and air, to which the term poles could hardly apply without receiving a new sense. *Electrolytes* must consist of two parts which, during the *electrolysation*, are determined the one in one direction, the other in the other towards the electrodes or poles where they are evolved. These evolved substances I call *zetodes*, which are therefore the direct constituents of electrolytes.

Faraday also accepted other suggestions from Whewell, amongst which *anode, cathode, cation* and *anion* are still with us, and furnish the staple vocabulary of electrochemistry, although others (*dexiode* and *skaiode*) did not stand the test of time. In the following letter thanking Whewell for his help, he is clearly exercised not only about the clarity for the new words but also by their euphony [7]:

> All your names I and my friend approve of (or nearly all) as to sense and expression, but I am frightened by their length and sound when compounded. As you will see, I have taken *dexiode* and *skaiode* because they agree best with my natural standard East and West. I like Anode and

Cathode better as to sound, but all to whom I have shown them have supposed at first by *Anode* I meant *No way*.

I have taken your advice, and the names used are *anode, cathode, anions, cations* and *ions*; the last I shall have but little occasion for. [How wrong he was in that prediction!]. I had some hot objections made to them here and found myself very much in the condition of the man with his son and ass who tried to please everybody; but when I held up the shield of your authority, it was wonderful to observe how the tone of objection melted away.

Twenty years on from his electrochemical experiments, Faraday was working on magnetism. This period gave us two more words, used in the physical sciences to this day, *diamagnetism* and *paramagnetism*. The concept that lines of magnetic induction are more closely packed together inside a paramagnetic body than in free space, and less so in a diamagnetic one, remains valid after 150 years. Again, he reported his choice of words in a letter to Whewell, at the same time hazarding the idea that paramagnetic oxygen in the atmosphere might contribute to the earth's magnetism (now we know that it does not). It should also be noted how defensive he sounds about sharing his ideas until they are fully worked out for publication – a thought that resonates strongly with the modern world! The 1850 letter to Whewell reads as follows [8]:

I have been driven to assume for a time, especially in relation to the gases, a sort of conducting power for magnetism. Mere space is Zero. One substance being made to occupy a given portion of space will cause more lines of force to pass through that space than before, and another substance will cause less to pass. The former I now call *paramagnetic* and the latter are the *diamagnetic*. The former need not of necessity assume a polarity of particles such as iron has when magnetic, and the latter do not assume any such polarity either direct or reverse. I do not say more to you just now because my own thoughts are only in the act of formation, but this I may say: that the atmosphere has an extraordinary magnetic constitution, and I hope and expect to find in it the cause of the annual and diurnal variations, but *keep this to yourself* until I have time to see what harvest will spring from my growing ideas.

My reason for documenting these thoughts is not in any way to belittle the accomplishments of Klixbüll Jørgensen in the much narrower field of science in which he operated, but rather to illustrate how important it is to enlarge language to symbolise new concepts. Before describing some of Jørgensen's creative flights with language, however, it is pertinent to recall a few facts about his origins.

3
Klixbüll Jørgensen and the Language of Science

3.1
Beginnings

In almost no respect did Jørgensen's upbringing and education resemble that of Faraday, save that both were precocious students [9, 10]. Jørgensen's father was an officer on a naval training ship but the family moved to Copenhagen, where he went to school and to university. He was a voracious pupil, with an early interest in science fostered by experiments at home with a chemistry set, much as in Faraday's case. It was there that he began his lifelong interest in the lanthanides, which he tried to separate by fractional crystallisation. His interest in optical spectroscopy was also kindled by a member of the staff of the Niels Bohr

Laboratory in Copenhagen. At the University of Copenhagen he quickly moved beyond the reading set by his lecturers to include, for example, the doctoral dissertation of the then Head of Department, Professor Jannik Bjerrum, who later supervised Jørgensen's research. One can imagine how surprised the eminent professor must have been at being interrogated by one of his students about the details of his own thesis.

Jørgensen's first publications concerned thermodynamic properties in collaboration with Bjerrum [11, 12], but apart from a few theoretical works co-authored with Ballhausen [13–15], practically all the publications from the early part of his career (and, indeed, many subsequently) carry his name alone. In this respect at least, his career does resemble that of Faraday, who worked and published mostly alone. A further point of resemblance is in speed of working: in the first five years of his career, Jørgensen published 44 papers, bearing out Faraday's famous maxim, 'work, finish, publish'. Of course, the compass of Jørgensen's interest was narrower than Faraday's, but it is certainly fair to say that, at the earliest part of both men's careers, they had the good fortune (or, more probably, good judgement) to find themselves at the point of entering into a new chemical landscape; in Faraday's case it was electrochemistry, in Jørgensen's, chemical spectroscopy. In intellectual terms, both fields were at that early stage where practically any new observation opens a new horizon for speculation. That suited Jørgensen's style of working very well: he was in the fortunate position that the then newly developed technology of photoelectric detectors made it possible for the first time to record visible-ultraviolet spectra of metal complexes in solution, where the absorption bands were often weak and rather broad. Almost any compound taken from the bottle and dissolved in water would have a spectrum exhibiting some new feature. More important than that, the technology made it possible quickly to build up series of spectra of closely related compounds and hence establish correlations of the kind that form the traditional methodology of inorganic chemistry.

In the hands of the unimaginative, that may be called 'stamp collecting' but, as a prelude to comprehending the manifold factors contributing to a given outcome, it is an essential first step. And Jørgensen, like the young Faraday, was committed from the start not just to interrogate nature but to comprehend it. That, of course, meant theory, but the theory of electronic structure of many electron systems like transition metals and their complexes was not then (or even now) susceptible to exact solution. Judgements as to approximations were therefore fundamental to the process of extracting the maximum of insight with the minimum of complexity. Jørgensen's own view of the place of theory in chemistry is expressed in characteristically graphic terms in the following [16]:

> Chemistry is very young as a science, and the most plausible and coherent hypotheses about the nature of chemical bonding have changed very rapidly. However, the waves of new discoveries have deposited a sediment of theory, which is not so thixotropic as sand though it is not as firm as rock.

So it was in pursuit of understanding chemical bonding by means of informed approximation that Jørgensen embarked on his relentless accumulation of spectroscopic data. In this he proclaims his purpose, in the very first sentence of the

Preface to his first book 'Absorption Spectra and Chemical Bonding in Complexes' (as, indeed, also in the title) [17]:

> Our knowledge of the electron clouds of gaseous atoms and ions is based on the energy levels, studied in atomic spectroscopy. It has been generally realised among chemists that the study of energy levels, i.e. the absorption spectra, is equally fruitful in helping our understanding of the chemical bonding, not only in transition group complexes, but in every type of molecule.

We find the same sentiment at the end of his fascinating book 'Oxidation Numbers and Oxidation States' [18]:

> Since the properties of matter surrounding us are essentially dependent of the electronic structure alone, the combination of chemistry and spectroscopy is of utmost importance for our preliminary and provisional, but ever progressing understanding of our complicated and fascinating world.

Let us now examine a few of the new concepts and the imaginative new terminology that Jørgensen coined to describe them.

3.2 Insight from Neologisms

3.2.1 *Preponderant Configurations and Ionic Colours*

Jørgensen was never much taken with the minutiae of optical spectroscopy; polarisation selection rules, cryogenics, magneto-optics and so on concerned him little. The energies and intensities of transitions were sufficient for his purposes of identifying what he called *preponderant configurations* [19]. Indeed, completely qualitative observations were sometimes brought to bear, as in his coining of the phrase *'additivity of ionic colours'* [20]. By that he meant cases where, for example, a blue cationic complex formed a salt with a yellow anionic one, creating a green solid and indicating that not only did the complexes retain their electronic integrity in the new environment, but that there was no significant electronic interaction between them. Conversely, where there was non-additivity, such interaction existed and was manifested either in substantial spectral shifts or the appearance of new absorption bands. A famous case of the former is Magnus' Green Salt, $Pt(NH_3)_4PtCl_4$, formed from a colourless cation and a pink anion [21] and of the latter the many instances of intervalence transitions in mixed valency compounds [22].

3.2.2 *The Nephelauxetic Effect*

Of all the words and phrases invented or applied by Jørgensen to encapsulate the phenomena that he was uncovering in the electronic spectra of inorganic complexes, the one which is likely to prove the most durable is *'nephelauxetic'*. In a few favourable cases the energy of a particular ligand field transition is determined only by a variation in interelectron repulsion, rather than orbital excitation. Such

transitions are called intraconfigurational since they correspond to a change in the total spin quantum number within a given configuration. Examples are:

$^6A_{1g} \rightarrow {}^4A_{1g}, {}^4E_g$ in octahedral Mn(II)

$^4A_{2g} \rightarrow {}^2E_g, {}^2T_{1g}$ in octahedral Cr(III)

Since there are very large numbers of each kind, and the transitions are relatively easy to identify in the spectra, placing them in an empirical series is straightforward. In fact, the corresponding effect in 4f complexes had been known for half a century [23], and some discussion of the difference between hexaquo- and hexammino-complexes had already taken place [24]. Adding a much larger number of ligands to the series, however, served to emphasise a qualitative correlation with their reducing character and, since the transition energy depends only on the interelectron repulsion, served to emphasise change in the effective radius of the 3d orbital going from the gaseous ion to the complex. The more reducing the ligand, the lower the repulsion and the larger the effective radius [25].

Just as Faraday approached Whewell for words to add classical dignity to his new results, so Jørgensen turned to Professor K. Barr of the University of Copenhagen. What emerged was *'nephelauxetic'* from the Greek for 'cloud expanding'. It was further noted that the nephelauxetic ratio β (being the ratio of the electron repulsion parameter B or C found in the complex to that of the gaseous ion in the same oxidation state, i.e. same preponderant configuration) was determined by the interplay of two phenomena, to which Jørgensen gave the further labels *'central field'* and *'symmetry restricted'* covalency. The former implies the invasion (Jørgensen's word) of the central ion by electrons from the ligand forming bonding molecular orbitals and hence decreasing its effective charge, while the latter arises from the contribution of the ligand atomic orbitals to the antibonding molecular orbital containing the unpaired electrons. Somewhat later Schaeffer proposed the ratio of ligand field splitting to electron repulsion ($\triangle$/B) as a measure of ligand field strength, to which he assigned the symbol Σ [26]. This brought forth from Jørgensen a further linguistic flourish [27]. He pointed out that the latter is the first letter of the Greek work σφοδρότης, meaning 'force applied against a resistance', in this case interelectron repulsion acting against spin pairing. Correspondingly, $\triangle$ can be thought of as the first letter of δύναμις, meaning force as a potential ability. Finally (even more whimsically), the letter β might easily have been chosen for the nephelauxetic ratio for the word βάτραχος (frog) from the legend about the frog wanting to blow himself up to the size of an ox! Unfortunately, what Jørgensen calls 'this mnemotechnic derivation' is, as he writes, *a posteriori*.

3.2.3 *Innocent Ligands*

Other well judged epithets for phenomena connected with the distribution of charge and its rearrangement after electronic excitation flowed from Jørgensen's copious imagination. Thus, in an adjective still widely used, he distinguished ligands like H_2O with closed shells, making complexes with unambiguously

defined oxidation states, from ones like NO and maleonitrile-dithiolate, where the degree of electron donation is uncertain, by calling the former *innocent* [28]. Sadly he never labelled the antithesis – would it have been *guilty*? Where more than one non-innocent ligand is attached to a central metal atom, he also found it helpful to speak of the ligand array as being *'collectively oxidised'*. In the excited state of an electron transfer transition, such as that of $IrCl_6^{2-}$, where an electron has been transferred from a ligand-based molecular orbital to the metal 5d shell, the same situation applies, i.e. to a good approximation we have $(Cl)_6^{5-}$. Likewise, the tendency of hard or non-polarisable ligands to come together around a metal centre, or of soft with soft, he correctly called *symbiosis,* extending the meaning of the word beyond its usual biological context of two species interdependent on one another [29]. Thus, for example, $Mn(CO)_5X$ are far more stable for X=I, H, CH_3 and have not been synthesised for X=F.

3.2.4 *Oxidation Numbers and Oxidation States*

The phrase *oxidation state* goes right to the heart of inorganic chemistry, and was current for very many years before Jørgensen came on the scene. There is no doubt though that it has been defined in a variety of ways and hence employed in quite an ambiguous fashion. Jørgensen applied himself to setting it in the context of modern theories of chemical bonding, in particular in one of his most eloquent and insightful books 'Oxidation Numbers and Oxidation States' (already referenced several times), which provides us with further examples of his analytical and expository style. In the course of the first few pages of text he introduces no fewer than five different concepts related to oxidation [30]. First are formal oxidation numbers, to be written as superscript small Roman numerals such as Cu^{II}, Cr^{III} though with the anachronism that zero and negatives can be added. These are to be distinguished from *(spectroscopic) oxidation states*, which are derived from the excited states observed in the visible-ultraviolet spectrum. In that case the Roman figures are written on the line and in parenthesis, such as Cr(III) and may also occur in the description of *chromophores* like $Cr(III)O_6$, occurring in $KCr(SO_4)_2 12H_2O$ and Cr_2O_3. Next came *conditional oxidation states*, defined with respect to the parent configuration found from atomic spectroscopy, but taking account only of the partly filled shell having the smallest ionic radius. Thus the three configurations of Ti^{2+}, Ti^{+} and Ti^{0} (respectively $[Ar]3d^2$, $[Ar]3d^24s$ and $[Ar]3d^24s^2$) would all be counted as being Ti[II] (note the square brackets). One reason for this classification is the simultaneous occurrence of localised and delocalised electrons in some solids, e.g. metallic PrI_2, which would be counted as Pr[III] from its magnetic properties, or even the lanthanide elements themselves. It also makes contact with the concept of preponderant configuration mentioned earlier.

The two final definitions, *quanticle oxidation states* and *distributed quanticle oxidation states*, take us into more controversial territory. The word *quanticle* was coined by Fajans [31] to denote one or more (most frequently an even number) of electrons quantised with respect to one or more nuclei. Where only one nucleus is concerned, of course this is synonymous with nl-configurations, but

where there are more it can be taken as representing the molecular orbitals of the valence shell. Jørgensen writes the atomic constituent lacking all the electrons taking part in the bonding quanticles as, e.g. N{III} in NH_3 and N{V} in NH_4^+, while the 'distributed' variant is obtained by sharing each two-electron quanticle equally between the two atom bonds, e.g. $N\langle 0\rangle$ in NH_3 and NF_3, $N\langle 1\rangle$ in NH_4^+.

Apart from his having accepted a contract to write a book on 'Oxidation Numbers and Oxidation States', and a decision to enter fully into all the ways in which such terms could be defined, it is hard to imagine from our current perspective why the author should have devoted such intellectual energy to these arcane distinctions. Quanticles have certainly taken the same path to oblivion as Faraday's zetode. However, it is nevertheless fascinating to observe the performance and the manner of deploying a formidable body of factual information and theoretical insight. As he acknowledges, 'there seems to be a kind of inverse variation of the physical content of various possible definitions of oxidation states and the number of compounds to which these definitions can be applied' [32].

3.3 Chemical Taxonomy and Taxological Quantum Chemistry

As we have seen in earlier sections of this brief appreciation, two themes run through Jørgensen's approach to chemical theory. These are, first, a reliance on spectroscopic evidence to establish 'preponderant configurations', naturally of the excited states themselves, but by extension also the ground state. By 'spectroscopy' we mean, in the first instance, excitations within and around the valence shell (frontier orbitals in the organic chemist's phraseology) observed by electronic absorption and emission spectra up to (say) about 6 eV. Towards the end of his career as an experimenter, Jørgensen turned to the then newly invented photoelectron spectroscopy in an effort to broaden the horizon of energy levels being brought into consideration, but his results are less illuminating, in part because of experimental difficulties in respect of surface damage and charging, so they are not referred to here. The second impulse driving his science was the desire to comprehend, through classification, what were the major factors governing not just the appearance of the spectra that he empathised with so closely, but the quantum chemical bonding principles that determine them. In this, he aligned himself with the traditional approach of the inorganic chemist (or, as he once described himself to the author, 'inorganic physicist') [33]:

> … if people still devote their efforts to try to understand chemistry, there is hope. The empirical facts of chemistry have been fashioned into many theoretical descriptions with time; most of these descriptions have been abandoned again; but there remain always some pleasant memories.

Classification means labelling, and labelling often means finding new words. The eighteenth and nineteenth centuries represented the apogee of taxonomy, when biologists imposed order on a vast array of newly found species by inventing botanical and zoological appellations. Jørgensen had a similar conception of chemistry beginning as natural history but progressing to understanding through classification, and introduced the new word *taxology*, which he defined as follows [34]:

When we use the word *taxology* about quantum chemistry, we are trying to draw attention to the meta-theoretical, the higher-type aspect in Bertrand Russell's sense, propensity of preponderant electron configurations suitably chosen to *classify correctly* the symmetry types of the ground state and lowest excited states .... No criterion is safer for the presence of a definitive spectroscopic oxidation state than the observation of such a complicated manifold of excited levels with the predicted symmetry types. The paradoxical situation is that this classification works even though we know that Ψ of many electron systems do not correspond to well-defined configurations … The whole theory of such configurations is a masquerade played by Nature; it is *as if* the preponderant configurations are taxologically valid.

The mention of Bertrand Russell in the above quotation is representative of a deeper interest in the philosophy of classification, which emerges in the following [35]:

Whereas Aristotle was interested both in formal logics and in botany, there has not in recent times been a very strong interaction between chemistry and formal logics … the British philosopher Jevons pointed out that the natural sciences in actual practice frequently use definitions of the type 'metals are materials having the properties common to sodium, iron and gold' … the examples are chosen as different as possible and yet compatible with the intention … Both Aristotle and the reflecting chemist immediately start wondering about essential and accidental properties.

What is interesting here is that Jørgensen, good chemist as he was, makes no mention of the simple theory-based definition that a metal is a solid in which one can define a Fermi surface. However, the problem can be posed when defining oxidation states from preponderant electron configurations, and Jørgensen comes back again to Bertrand Russell's theory of types, i.e. that it is the class itself and not its members individually which may be numerous. Thus the ground and low lying excited states of IrF_6 all belong to the situation where three 5d-like electrons and hence the oxidation state Ir(VI) is a good descriptor. Without committing any judgement about the fractional charge of the central atom (probably between 2 and 3), higher energy excited states belong to a preponderant configuration with four 5d-like electrons and hence designated Ir(V), probably with a similar fractional charge on the Ir.

As an amusing aside on essential and accidental properties, Jørgensen invites us to consider the class of halogens: it is certainly a chemically interesting statement that all halogens have odd atomic numbers. Given the laws of atomic structure, it is inconceivable that any newly discovered halogen would not. On the other hand, it is certainly an accident (as Jørgensen says, only of interest to someone having access to just the first volume of the Chemical Abstracts index) that the English names of all the halogens begin with one of the first ten letters of the alphabet! The key issue regarding the validity of definitions or classifications is thus their stability against future discoveries. Astatine could equally well have been called syntomine (from the Greek 'brief') or taxyboline (from the Greek 'rapid gun-fire') according to Jørgensen, but the point about atomic number remains robust.

4
Chemistry, Philosophy and Language

Although the phrase 'natural philosophy' has a long and honourable pedigree, the words 'chemical' and 'philosophy' are not associated very much. In part, perhaps,

that is because chemistry (at least in earlier times) had more the character of natural history, that is, of a dense and fascinating jungle of compounds and phenomena, through the trees of which it was often quite difficult to see the wood. Even today, it remains notoriously hard to predict the crystal structure of a new molecular compound from a knowledge of its chemical formula. Chemistry, therefore, remains wonderfully capable of springing surprises (fullerenes and molecular superconductors, to name but two relatively recent examples). Or, as Jørgensen wrote in the late 1960s, 'at one time, the class of non-metallic ferromagnets was thought to be as empty as earlier the class of aerostats heavier than air' [36]. So description and classification founded on quantum-mechanically-based approximation remains a viable (indeed, in many cases the only) option. A final quotation [37]:

> It is not reasonable for the chemist to sit down and wait for the pure theorists to deduce everything *ab initio*; experience shows clearly that the preliminary steps of approximate calculation have an unfortunate tendency of producing non-sensical results from incorrect assumptions, unless these are strictly governed by a realistic knowledge of the experimental facts.

Classification and description need words, both the facility to manipulate the existing ones and an ability to coin new ones. I have tried to show in this brief memoir that Jørgensen was a master of language, albeit on occasions a somewhat idiosyncratic one. At no point up till now has any reference been made to the fact that English was not his first language. Like so many of his compatriots, however, he was equally fluent in several languages, though with a pronunciation that remained resolutely Danish. Access to the instincts of vocabulary in a more general sense must be a prerequisite to coining new words and phrases for scientific purposes. A glance at Faraday's voluminous writings shows that he too had that instinct for language [2, 3]. There is no doubt that both men enriched our scientific vocabulary greatly while searching to encompass their new findings.

Acknowledgements I wish to pay tribute to a multitude of fascinating conversations and extensive correspondence over many years with Klixbüll Jørgensen, which did much to form my own approach to chemistry and science in general.

5 References

1. Wittgenstein L (1961) Tractatus logico-philosophicus. Translated by Pears DF, McGuiness BF. Routledge, London
2. For accounts of Faraday's life and work see, e.g. Pearce Williams L (1987) Michael Faraday: a biography. New York, Basic Books. Reprinted by Da Capo Press Inc; Day P (1999) The philosopher's tree: Michael Faraday's life and work in his own words. Bristol, Institute of Physics Publishing
3. James FALJ (ed) The correspondence of Michael Faraday. Vol 1. Institute of Electrical Engineers, London, p 287
4. James FALJ (ed) The correspondence of Michael Faraday. Vol 1. Institute of Electrical Engineers, London, p 590
5. James FALJ (ed) The correspondence of Michael Faraday. Vol 1. Institute of Electrical Engineers, London, p 549
6. James FALJ (ed) The correspondence of Michael Faraday. Vol 2. Institute of Electrical Engineers, London, p 176

7. James FALJ (ed) The correspondence of Michael Faraday. Vol 2. Institute of Electrical Engineers, London, p 181
8. James FALJ (ed) The correspondence of Michael Faraday. Vol 4. Institute of Electrical Engineers, London, p 176
9. Williams AF (2001) Chimia 55:472
10. Day P (2003) Coord Chem Rev 238–239; 3–8
11. Bjerrum J, Jørgensen CK (1953) Acta Chem Scand 7:951
12. Jørgensen CK (1954) Acta Chem Scand 8:175–191
13. Bjerrum J, Ballhausen CJ, Jørgensen CK Acta Chem Scand (1954) 8:1275
14. Ballhausen CJ, Jørgensen CK (1955) Acta Chem Scand 9:397
15. Ballhausen CJ, Jørgensen CK (1955) Mat Fys Medd Dan Vid Selskab (1955) 29:14
16. Jørgensen CK (1969) Oxidation numbers and oxidation states. Springer, Berlin Heidelberg New York, p 1
17. Jørgensen CK (1962) Absorption spectra and chemical bonding in complexes. Pergamon Press, Oxford, p vii
18. Jørgensen CK (1969) Oxidation numbers and oxidation states. Springer, Berlin Heidelberg New York, p 269
19. Jørgensen CK (1969) Oxidation numbers and oxidation states. Springer, Berlin Heidelberg New York, p 189
20. Jørgensen CK (1962) Absorption spectra and chemical bonding in complexes. Pergamon Press, Oxford, p 203
21. Day P, Orchard AF, Thomson AJ, William RJP (1965) J Chem Phys 42:1973–1979
22. Robin MB, Day P (1967) Adv Inorg Chem Radiochem 10:248
23. Hofmann KA, Kirmreuther H (1910) Z Physik Chem 71:312
24. For example: Tanabe Y, Sugano S (1954) J Phys Soc Japan 9:753,766
25. Schäffer CE, Jørgensen CK (1958) J Inorg Nucl Chem 8:143
26. Schäffer CE (1967) Proc Roy Soc (London) A297:96
27. Jørgensen CK (1969) Oxidation numbers and oxidation states. Springer, Berlin Heidelberg New York, p 92
28. Jørgensen CK (1969) Oxidation numbers and oxidation states. Springer, Berlin Heidelberg New York, p 153
29. Jørgensen CK (1964) Mol Phys 7:417
30. Jørgensen CK (1969) Oxidation numbers and oxidation states. Springer, Berlin Heidelberg New York, pp 2–4
31. Fajans K (1959) Chimia 13:349
32. Jørgensen CK (1969) Oxidation numbers and oxidation states. Springer, Berlin Heidelberg New York, p 252
33. Jørgensen CK (1969) Oxidation numbers and oxidation states. Springer, Berlin Heidelberg New York, p 269
34. Jørgensen CK (1969) Oxidation numbers and oxidation states. Springer, Berlin Heidelberg New York, p 268
35. Jørgensen CK (1969) Oxidation numbers and oxidation states. Springer, Berlin Heidelberg New York, p 178
36. Jørgensen CK (1969) Oxidation numbers and oxidation states. Springer, Berlin Heidelberg New York, p 176
37. Jørgensen CK (1962) Absorption spectra and chemical bonding in complexes. Pergamon Press, Oxford, p 19

Structure and Bonding, Vol. 106 (2004): 19–35
DOI 10.1007/b11303

The Variation of Slater-Condon Parameters F^k and Racah Parameters B and C with Chemical Bonding in Transition Group Complexes

Hans-Herbert Schmidtke

Heinrich-Heine-Universität Düsseldorf, Institut für Theoretische Chemie, Universitätsstrasse 1, 40225 Düsseldorf, Germany
E-mail: schmidtke@theochem.uni-duesseldorf.de

Abstract The present work focuses on the treatment of electron-electron repulsion which is part of the interpretation (analysis) of electronic spectra of transition group complexes using ligand field theory or the angular overlap model. Relative values of parameters which represent the strength of the d-d electron interaction in these models are considered, in particular the change of these parameters due to chemical bonding is discussed. Predictions on the variation of these parameters from the free central ions to the complex compounds are made, using an effective electron repulsion operator $(r_<+q)^k/(r_>+q)^{k+1}$ in the integrals which due to chemical antibonding leads for $q>0$ to a higher weighting of d-electron density at larger electron-nuclear distances. A comparison to experimentally determined parameters F^k or B and C, which are available from literature, shows that all data fulfill the predicted relative sizes $\Delta F^2>\Delta F^4$ and $\Delta C>\Delta B$, the symbols representing the parameter changes due to complex formation of metal ions. Disagreement with these relations can be taken as an indication of wrong level assignments or incorrect theoretical analyses.

Keywords Racah parameters · Ligand field theory · Nephelauxetic effect · Model parameter relations

List of Abbreviations

AOM Angular Overlap Model
LFT Ligand Field Theory

1 Introduction

A basis for interpretation of chemical bonding, electronic spectra, magnetic susceptibilities, and other properties of molecular compounds is obtained by computing reliable energy level schemes using a well established quantum mechanical model. This covers the calculation of molecular orbitals, the electron-electron repulsion, and, if applicable, spin-orbit coupling and interactions with external fields. In ab initio calculations which in general use self-consistent field method, the molecular orbitals and electron-electron repulsion part are processed in a joint procedure yielding energy levels (multiplets) and sets of orbitals which are in general different for each level. In most of the semiempirical models the molecular orbital energies and electron repulsions are calculated separately. The set of molecular orbitals remains rigid and is not changed nor optimized for each of the energy levels on calculation of the electron interaction part. The multiplet energies result from different occupations of orbitals which contain bonding and antibonding contributions between the atoms in the molecule.

Main procedures up to date for investigating the electronic structure of transition group complexes in the ground state and excited states are primarily semiempirical methods which are appropriately adapted to the type of molecule considered. Ab initio and eventually density function calculations of molecules, as large as those with ligands and metal ions in the center, are carried out only for supplementary purposes and deal for the most part with the electronic ground state.

Among semiempirical methods primarily the ligand field theory LFT [1–3] must be mentioned together with its subsequent variation usually addressed as "Angular Overlap Model" (AOM) [4–6] which is the today's most common version used for calculations. The importance of this method is demonstrated by its large flexibility which allows for establishing different extensions for various purposes which are, e.g., introduction of the phase-coupling concept [7], considering s-d and p-d orbital mixing [8], regarding misdirected valency [9] and even use for molecules of extended structures (chains, layers, etc.) [10]. In this context the cellular ligand field (CLF) [11] should also be mentioned which abandons the idea of introducing parameters purely depending on metal-ligand atomic pairs that are characteristic for the AOM and all of its varieties.

All these semiempirical methods have in common that they only calculate orbital energies. The electron-electron repulsion part necessary for obtaining energy levels (multiplets) is left to a second part of the calculation. Procedures for handling this problem which furnish satisfactory results obtaining experimental standards, have been proposed in earlier days at various occasions. The earliest, and straightforward way is to use the repulsion part of d-electrons from the free central ions and neglect the intricacies arising from the molecular sym-

metry which necessarily is lower than spherical. For an ion with d-electrons in a molecule of D_4 symmetry, for instance, a total of ten non-vanishing interelectronic repulsion integrals of the type

$$\left\langle \mathrm{ac} \left| \frac{1}{r_{12}} \right| \mathrm{bd} \right\rangle \tag{1}$$

(in atomic units) evolves which gives rise to an equal number of different parameters in a semiempirical model [12, 13]. This emerges, e.g., from introducing different radial parts $R(Z_*)$ in the Slater functions (central-field covalency) and/or applying orbital reduction factors c_M attached to the central metal ion function ψ_M (symmetry-restricted covalency) arriving at molecular orbitals (LCAOs) as [13, 14]:

$$\psi_{MO} = c_M \psi_M(\mathrm{nd}, Z_*) + c_L \sum \psi_L \tag{2}$$

The function combines central metal d functions with a sum of ligand functions ψ_L of appropriate symmetry. The consideration of reduction factors c_M or Stevens delocalization coefficients as they are also called [14] causes an inflation of parameters. However, if they are introduced in a limited number where orbital intermixing is essential, they can be quite useful for explaining low symmetry splittings. In the case of Cr(III) ammonia complexes of C_{4v} symmetry this has been demonstrated for transitions within the t_{2g}^3 (octahedral) electron configuration where level splittings in first order perturbation only depend on electron-electron repulsion integrals [15].

The number of relevant parameters is drastically reduced when the interelectronic part of the model is approximated by assuming entire spherical symmetry using the corresponding integral types valid for the free ions of the central metals. This is justified since transition group elements when forming chemical bonds largely maintain their d-electrons localized on the central ion. Therefore parameters representing integrals over radial wave functions in spherical symmetry can be further used for the complex compounds although their numerical values are distinctly reduced compared to those of the free metal ions (nephelauxetic effect [2, 16]). In this case the number of parameters for d-electron structures is limited to three, where either Slater-Condon parameters F^k (k=0,2,4) [17] or Racah parameters A, B, and C [18] may be used. Although the parameters F^0 or A, respectively, cancel when differences of energy levels are considered, as in the case of explaining electronic spectra, the remaining parameters sets of two, i.e., F^2, F^4, or B, C, seem to be for most of the authors still inconveniently large. Therefore, for same reason they further cut down the number of interelectronic parameters to one by assuming the relation γ=C/B to be constant for the free transition metal ions and all their compounds. This drastic approximation has its origin from the classical work of Tanabe and Sugano [19] who derived from the spectra of free ions of the first transition series γ values of 4 to 5. They calculated a relation of γ=3.97 largely independent from the effective nuclear charge when evaluating the integrals from Slater-type radial functions. More extensive calculations which include spin-orbit coupling in general came to lower γ relations when the integrals were adapted to experimental results, e.g.,

Liehr reports ϒ values of 3.9 to 4.4 of free V(III), Cr(III), Co(II), and Ni(II) [20]. Jørgensen in the majority of his work used ϒ=4 for all transition metals that he applied for free ions as well as for complex compounds [14, 16, 21, 22]. This assumption was taken over by many other authors [23].

For obtaining better agreement between theory and experiment, Jørgensen introduced different B parameters for each set of energy levels which arise from an electron configuration (e.g., using tetrahedral group theoretical symbols, $t_2^n \equiv \gamma_5^n$ or, for a mixed electron configuration, $t_2^n e^m \equiv \gamma_5^n \gamma_3^m$) [14, 16, 22]. The nephelauxetic quotients

$$\beta = B_{compl}/B_{free\ ion} \tag{3}$$

relating the B parameters obtained by fitting the spectra of the complexes to those of the free central ions therefore may be different which is indicated by β_{55}, β_{35}, and β_{33}. Some of these data are listed in the tables of the articles mentioned. Since the more drastic requirement keeping ϒ a constant was maintained, the electronic repulsion parameter set is only increased from one to three members (instead of six if the Cs were allowed to vary freely as well). The empirical model of different β_{ij} parameters for explaining intra- and interconfigurational electronic transitions, however, has not been accepted by the scientific community to the same extent as other ideas of Jørgensen.

Since semiempirical models are well appreciated when they can explain a maximum of experimental data from a minimal number of parameters and this with sufficient accuracy, any introduction of further parameters should be avoided unless it promises a comparatively higher precision or a lot more insight into the system. This is, however, not expected from present procedures. Therefore we consider at the present time the model which assumes well accomplished spherical symmetry conditions for the electron-electron interaction part of the theory and which allows the parameter sets F^2, F^4 or B, C, respectively, to vary independently when adapting these parameters to the experiment. We shall not differentiate between orbitals of different d-electron subshells. Consequently this investigation applies only to cases of d-electrons highly localized on the central metal. The main subject of the present investigation is to look at relative sizes of the F^2 and F^4 (or B and C) parameter values and, in particular, demonstrate how these parameters change individually, one larger than the other, with covalent bonding when metal ions are forming complex compounds.

2 Theory

2.1 Parameter Definitions

The treatment of the electron-electron repulsion part in quantum mechanical calculations requires the solution of two electron integrals of Eq. (1):

$$\left\langle ac \left| \frac{1}{r_{12}} \right| bd \right\rangle = \int\int a^*(1) b(1) \frac{1}{r_{12}} c^*(2) d(2) d\tau_1 d\tau_2 \tag{4}$$

For Slater or hydrogen functions which are in general used for free atoms and in LCAO approximations of molecular orbitals as those in Eq. (2), the integration over angular parts of Eq. (4) is straightforward and easily carried out. The solution of the radial part with Slater functions $R_{nl}(r;Z_*)$ leads to non-vanishing integrals of the type

$$F^k = \iint R_a{}^2(r_1, Z_*{}^a)\,\frac{r_<{}^k}{r_>{}^{k+1}}\,R_c{}^2(r_2, Z_*{}^c)\,r_1{}^2\,dr_1\,r_2{}^2\,dr_2$$

$$G^k = \iint R_a(r_1, Z_*{}^a)\,R_c(r_1, Z_*{}^c)\,\frac{r_<{}^k}{r_>{}^{k+1}}\,R_a(r_2, Z_*{}^a)\,R_c(r_2, Z_*{}^c)\,r_1{}^2\,dr_1\,r_2{}^2\,dr_2 \tag{5}$$

with k=0, 2, 4, 6,…, where $r_<$ (or $r_>$) is the smaller (larger) distance r_1 or r_2 of two interacting electrons from the atomic nucleus [12, 17] which is the origin of the coordinate system. Both integrals are shown to be positive [17] as is expected from expressions representing electron-electron repulsion energies. When dealing with equivalent electrons within a given electron configuration (R_a=R_c), the two types of integrals of Eq. (5) are identical (for given k), i.e.,

$$F^k \equiv G^k \tag{6}$$

This is the case, for instance, for an atomic d-shell; however, at lower symmetry when dealing with electrons in molecules, different effective charges Z_* are to be attributed to the d-orbitals of different sub-shell configurations, for instance $Z_*{}^{t_2}$ and $Z_*{}^e$ in $t_2{}^n e^m$ for cubic symmetry. This again casts some doubts on the conceptive standard when introducing different B parameters in the expressions of intra- and intershell electron transitions ($\beta_{55}\neq\beta_{35}\neq\beta_{33}$) as outlined above. In this case exchange integrals G^k cannot be identified with coulomb integrals F^k as set in Eq. (6).

The integrals F^k in principle can be calculated from wave function by the use of

$$F^K = \int_0^\infty \left[\int_0^{r_2} R_a{}^2(r_1)\,\frac{r_1{}^k}{r_2{}^{k+1}}\,r_1{}^2\,dr_1 + \int_{r_2}^\infty R_a{}^2(r_1)\,\frac{r_2{}^k}{r_2{}^{k+1}}\,r_1{}^2\,dr_1\right] R_c{}^2(r_2)\,r_2{}^2\,dr \tag{7}$$

However, since radial parts of the wave functions in general are not well known, a straightforward solution of these integrals is not carried out. Instead they are considered as parameters which are determined by fitting to the electronic spectra of the compounds. In semiempirical theories the integrals over radial parts are known as Slater-Condon parameters.

For obtaining more convenient numerical sizes, parameters F_k instead of F^k were introduced which for d orbitals are converted by

$$F_2 = \frac{1}{49}\,F^2 \quad \text{and} \quad F_4 = \frac{1}{441}\,F^4 \tag{8}$$

The coefficients are the reciprocal of integrals over the angular parts of Eq. (4) which in the calculations is always attached to each F^k integral. Sizes of F^k parameters for f orbitals can be reduced correspondingly [12, 13]. For an investiga-

tion of relative magnitudes of integrals and its changes by varying the radial parts, which is the main object of the present investigation, we must, however, deal with F^k parameters (see below).

Another useful set of parameters has been introduced by Racah [18]:

$$A = F^0 - 49\,F_4\,,\; B = F_2 - 5F_4, \quad \text{and } C = 35\,F_4\,. \tag{9}$$

They have some advantages, in particular because energy differences between levels with maximal spin quantum number S arising from an electron configuration are always multiples of the parameter B only. As Slater-Condon parameters the Racah parameters necessarily must also be positive since physically they describe electron-electron repulsions. This immediately has the consequence that relations such as

$$F^0 > 49\,F_4 \quad \text{and} \quad F_2 > 5F_4 \tag{10}$$

must hold. Unless F_2 is unusually large compared to F_4 we can conclude from Eq. (9) that

$$C > B \tag{11}$$

is generally valid. Detailed parameter relations will be discussed in Sects. 2.2. and 3 where model parameters determined from the experiment are considered.

2.2 Parameter Relations

The main subject of the present article deals with the investigation of relative sizes and expected changes of the electron-electron repulsion parameters due to chemical bonding that can be compared by extrapolation from the electronic spectra of complex compounds. Predictions to be made are based on the discussion of integrals originating from the wavemechanical treatment of electrostatic interelectron repulsion given in Eq. (5).

2.2.1 *Slater-Condon Parameters F^k*

For an investigation of dependences of the integrals in Eq. (5) on a general parameter z, we proceed as used in the derivation of the Hellmann-Feynman theorem [24, 25]. Accordingly, the variation of F^k, when assuming R_a=R_b=R, is

$$\frac{\partial F^k}{\partial z} = 2\iint \frac{\partial R^2(r_1)}{\partial z}\,\frac{r_<^{\,k}}{r_>^{\,k+1}}\,R^2(r_2)\,r_1^{\,2}dr_1\,r_2^{\,2}dr_2 + \iint R^2(r_1)\,\frac{\partial}{\partial z}\left(\frac{r_<^{\,k}}{r_>^{\,k+1}}\right)R^2(r_2)\,r_1^{\,2}dr_1\,r_2^{\,2}dr_2 \tag{12}$$

Therefore we can consider the variation due to wavefunctions and to the operator separately. For a rigorous analysis the analytical z-dependences of the wavefunction and the operator should be known.

2.2.1.1 *Variation with k*

Considering the variation with k putting k=z in Eq. (12), the first integral vanishes since the function R(r) definitely does not depend on k. The operator in the second integral is when we set $r_</r_> \equiv x$:

$$\frac{1}{r_>}\frac{\partial}{\partial k}x^k = \frac{1}{r_>}x^k \ln x \tag{13}$$

Since x by definition is limited by

$$0 < x < 1 \quad \text{and} \quad \ln x < 0 \tag{14}$$

Eq. (13) is a decreasing function with k for each k>0. For larger k this decline is smaller than for smaller ks because, due to Eq. (14),

$$x^{k+1} < x^k \tag{15}$$

must hold. Since the operators x^k and $\frac{\partial}{\partial k}x^k$ are weighted in the integrals of Eq. (12) by the wavefunction R(r) independently of k, we safely conclude that the F^k parameters are decreasing with increasing k as the operator x does.

This result, valid for any (p,d,f,…) orbitals, supplies the sequence

$$F^0 > F^2 > F^4 > F^6 \ldots \tag{16}$$

which has been quoted by Jørgensen [26], although without giving a proof. Griffith argues barely on the basis of the function $r_<^k/r_>^{k+1}$ which decreases with k, from which he concludes $F^k > F^{k'}$ for $k<k'$ [27].

Correspondingly for the reduced parameters F_k of Eq. (8) the sequence

$$F^0 > 49\,F_2 > 441\,F_4 \tag{17}$$

is established for d-orbitals which predicts an F_k sequence decreasing more strongly than the series of the F^k parameters in Eq. (16).

2.2.1.2 *Variation with Chemical Bonding*

Since the strength of (covalent) bonding or antibonding cannot possibly be identified with a single parameter z which would be necessary for applying Eq. (12), we must use an approximation. Covalent and possibly ionic bonding (e.g., screening effects) is usually reflected by the wave functions while the operators in general remain unchanged. In LFT and AOM the radial parts of wavefunctions are largely unknown; instead they are in general handled by introducing parameters as substitutes for their integrals [1–5]. These are determined from the experiment. For applying Eq. (12), we use a model in which chemical (anti-)bonding is dealt with by introducing appropriate changes into the operator which is as well common for semiempirical methods.

Since we can also interpret the integrals of Eq. (5) by an infinite summation of radial function products weighted by the operator $r_<^k/r_>^{k+1}$ at each $r_<$ and $r_>$, we

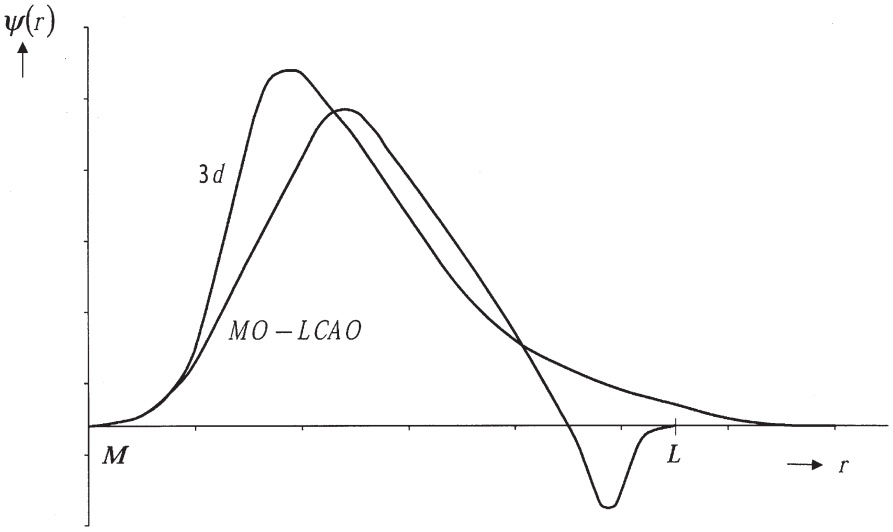

Fig. 1 Radial part of the central metal 3d-function and molecular orbital, MO-LCAO, resulting from linear combination with ligand functions, Eq. (2)

may simulate the expansion of the central metal atomic function due to covalent bonding (central field and/or symmetry restricted covalency [13, 14]) by an increased weighting of functionals at larger distances r→r+q (cf. Fig. 1). We therefore substitute the electron-electron (electrostatic) repulsion operator from Eq. (5) by

$$V(q;k) = \frac{1}{r_> + q}\left(\frac{r_< + q}{r_> + q}\right)^k \quad \text{with } q > 0 \tag{18}$$

and investigate its variation with q for each k, proceeding in a similar way as carried out in the foregoing section where the variation of V(0;k) with k was considered.

Differentiation of V(q;k) obtains

$$\frac{\partial V(q;k)}{\partial q} = \frac{1}{(r_> + q)^2} w^k \left(-1 - k + \frac{k}{w}\right) \tag{19}$$

where

$$w = \frac{r_< + q}{r_> + q} < 1 \tag{20}$$

which must be a function of q which is negative, because electron repulsion (Slater-Condon-) parameters become smaller with covalent bonding (nephelauxetic effect [16]). This is introduced as a physical condition which is fulfilled when

$$\left(-1 - k + \frac{k}{w}\right) < 0 \tag{21}$$

limiting w in the present case (d-orbitals) by

$$\begin{aligned} &1 > w > 0 && \text{for } k = 0 \\ &1 > w > \left(\frac{2}{3}\right) && \text{for } k = 2 \\ &1 > w > \left(\frac{4}{5}\right) && \text{for } k = 4 \end{aligned} \tag{22}$$

This moves w closer to 1 favoring larger q values. Notice as well that main contributions to the F^k integrals are those with $r_< \approx r_>$ ($w \approx 1$) and weights near the maximum of radial functions. This is particularly well fulfilled when the electrons are located close to the metal nucleus. An addition, because the bracket Eq. (21) is more negative for larger k within the limits given by Eq. (22), and maintaining the mathematical condition $w<1$, Eq. (20), we can conclude that V(q;k) is a stronger decreasing function with q for smaller values of k. Since this holds for the operator Eq. (18), it must be valid for the integrals of Eqs. (5) and (12) as well. Because the wavefunctions are not assumed to depend on q in the present model, the result will also hold for the F^k parameters. Therefore chemical bonding must affect the electron repulsion parameters differently; in detail F^k parameters are decreased by smaller amounts for higher values of k. If we define these changes as a result of bonding by

$$\Delta F^k = F^k{}_{ion} - F^k{}_{compl} \tag{23}$$

for each k, the series of ΔF^k is given by

$$\Delta F^0 > \Delta F^2 > \Delta F^4 \tag{24}$$

The ΔF^k parameters increase with q with different slopes which is depicted in Fig. 2.

An investigation of $\dfrac{\partial V(q;k)}{\partial q}$, Eq. (19), whether it is a generally decreasing function with k from an inspection of the second derivative

$$\frac{\partial^2 V(q;k)}{\partial q \partial k} = \frac{1}{(r_> + q)^2} w^{k-1} (1 - w) \left[1 + \left(k - \frac{w}{1 - w} \right) \ln w \right] \tag{25}$$

does not lead to a rigorous answer, since relative sizes of various terms which determine the sign of this expression cannot be estimated using the limits $w<1$ and $k>0$ as the only conditions.

2.2.2 *Racah Parameters A, B, and C*

In this section we shall discuss the Racah parameters correspondingly as in Sect. 2.2.1, i.e., their relative quantities and the different variations with covalent bonding when we use the results as obtained above for the Slater-Condon parameters F^k. Since these parameters are linear combinations of the F^k (or F_k), they depend on the action of operators $w^k=(r_</r_>)^k$ with different ks supplying posi-

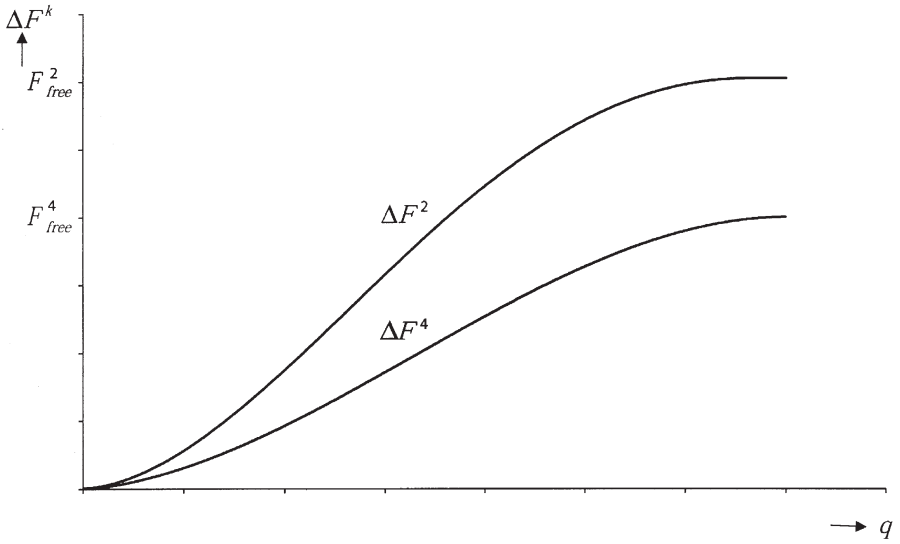

Fig. 2 Variation of parameters ΔF^k, Eq. (23), with the increment q of chemical bonding introduced in Eq. (18) (schematic). For (unrealistically) high values of q the F^k parameters of the complex vanish, i.e., ΔF^k approaches F^k of the free ions. Similar dependences also hold for the Racah parameter changes ΔB and ΔC

tive and negative contributions to the sums (cf. Eqs. (8) and (9)). This complicates the discussion somewhat restricting the results due to closer limits.

2.2.2.1 *Relative Parameter Sizes*

Relations of Racah parameters depending on the F^ks are calculated for d-electrons from Eqs. (8) and (9) giving

$$\frac{A}{C} = \frac{63}{5}\frac{F^0}{F^4} - \frac{7}{5} \tag{26}$$

$$\frac{B}{C} = \frac{9}{35}\frac{F^2}{F^4} - \frac{1}{7} \tag{27}$$

For the extreme case $F^0=F^2=F^4$, we obtain

$$\frac{A}{C} = \frac{56}{5} \quad \text{and} \quad \frac{B}{C} = \frac{4}{35} \quad \text{yielding} \quad \frac{A}{B} = \frac{392}{4} \tag{28}$$

such that

$$A >> B < C \tag{29}$$

However, since in fact the F^ks differ according to Eq. (16) decreasing with larger k, we must consider the relation B/C when F^2/F^4 now exceeds one making B/C

larger. In the same way A/C in fact is more increased due to $F^0/F^4 > F^2/F^4$, which supports the relation Eq. (29) also for real F^k parameters. Evidently, for $F^2 = \frac{40}{9} F^4$ we obtain B=C and the relation given by Eq. (29) is not valid any more. However, since this F^2/F^4 relation is extremely large – realistic values never exceed $F^2/F^4 \cong 2$ as supported by data adjusted from the experiment (see Sect. 3) –, we can safely conclude that the relation B<C as given in Eq. (29) holds for all possible F^k series of Eq. (16). This is realized in all complex systems known for which their electronic spectra are fitted to LFT or AOM energy levels.

2.2.2.2
Variation with Chemical Bonding

For an investigation of Racah parameter changes from the free central metal ion to the complex compound, also described by the nephelauxetic effect [16], we define as in Eq. (23)

$$\Delta A = A_{ion} - A_{compl} \tag{30}$$

and correspondingly for B and C.

For these changes ΔF^k and ΔA etc., the expressions Eqs. (26) and (27) hold as well: since these conversion formulas from F^k parameters to Racah parameters are the same for the free central ion as they are for complex compounds, they must also be valid for the respective parameter changes ΔF^k (k=0,2,4) and ΔA, ΔB, and ΔC. Therefore, following the same procedure as pointed out for the F^k and Racah parameters in Sect. 2.2.2.1, when assuming equal bonding effects on each F^k independent of k, i.e., $\Delta F^0 = \Delta F^2 = \Delta F^4$, the same relations as those of Eqs. (26) and (27) must hold for ΔA, ΔB, and ΔC as well. Hence we obtain a corresponding series applying for the parameter changes

$$\Delta A >> \Delta B < \Delta C \tag{31}$$

Now, as arguing above, if we take the true sequence, Eq. (24), as a basis with ΔF^k values decreasing with k, the relations of Eq. (31) will remain valid, unless F^2 exceeds the unrealistically high value of $\Delta F^2 = \frac{40}{9} \Delta F^4$. A check on the data obtained from the experiments show that this extreme is far from ever being reached in reality. Therefore it is generally concluded that the parameter decrease due to the nephelauxetic effect is larger for C than it is for B parameters, i.e., $\Delta C > \Delta B$. An inspection of dependencies of ΔB and ΔC on the bonding increment q supplies similar curves as those depicted for ΔF^k in Fig. 2 with corresponding limits for large q approaching the B and C parameters for the free ions.

3
Comparison with the Experiment

In this section we will check the theoretical predictions outlined in Sect. 2 by comparing these results with the pertaining parameters determined from the ex-

periment. The latter parameters are obtained by fitting the d-electron absorption or reflectance spectra with the electronic levels calculated by LFT or the AOM. The first complete listing of LFT energy matrix elements for octahedral complexes can be found in the work of Tanabe and Sugano [19]; for tetragonal fields the corresponding tables have been provided by Otsuka [28]. A computer program applicable for LFT or AOM calculations, valid for all possible molecular symmetries and geometrical structures, has been established by Hoggard [29]; it is available by Adamsky from the present institute [30]. The parameters of the semiempirical models are adapted to the maxima of the measured spectra using an appropriate fitting program which includes optimization procedures for calculated mean square errors.

The number of LFT and AOM parameters reported in the literature which are calculated from adjusting both parameters B and C independently is, however, rather limited. The bulk of the data includes the approximation where C/B is assumed to be a constant which in general refers to the free ion and is not varied during the fitting procedure [19, 23]. These results cannot be used for the present analysis. We shall see that this approximation turns out to be a short cut which cannot be accepted for all compounds we are dealing with.

However, also the data which are reported from independent evaluation of B and C (and of parameters F^k as well) can only be compared with some reservations because they are obtained in general by using different approximations. Some of these fittings use only parts of the level systems when comparing with the experiment; others include spin-orbit coupling and/or Trees correction [31] or use more sophisticated extensions of LFT or AOM. The data to be compared with therefore do not strictly reflect the same physical meaning in full identity; they are, however, up to some significant figures, good mean values for the model parameters investigated in the present approximation. This assumption is in general common for all compilations of data collected from different references used for comparing parameters with theoretical results.

3.1
Check on Slater-Condon Parameters

In Table 1 the Slater-Condon parameters F^k of some complexes of transition metal ions are compiled for which the electron-electron repulsion parameters are reported to be fitted independently. In the majority of cases it was the Racah parameters B and C which had been adapted to the experiment. The F^k values listed in Table 1 therefore result from applying the conversion formulas Eqs. (8) and (9). Changes of these parameters due to the effect of chemical bond obtained from the difference to the corresponding parameters of the free central metal ion, Eq. (23), are listed in the ΔF^k columns. The parameters of the free ions are taken from [19], although occasionally other data for same of the ions can be found in the literature as well. For V(III), Cr(III), Co(II), and Ni(II), e.g., the C parameters, calculated from a model including spin-orbit coupling [20], are somewhat smaller (5–15%) than those listed in [19]. On the other hand, the B parameter values are remarkably similar independent on the model approximation used.

Table 1 Slater-Condon parameters F^k and their variations ΔF^k due to chemical bonding as calculated from a fit to the experiment (in 1000 cm^{-1})

No.	Compound	F^2	F^4	ΔF^2	ΔF^4	Ref
1	$K_2NaScF_6:V^{3+}$	54.8	35.2	14.2	12.9	32
2	$K_2LiScCl_6:V^{3+}$	49.3	34.1	19.6	13.9	32
3	$Cs_2LiScBr_6:V^{3+}$	48.6	32.3	20.3	15.8	32
4	$Cs_2NaYCl_6:Cr^{3+}$	51.5	39.7	22.5	12.4	33
5	$K_3[Cr(CN)_6]$	44.5	33.4	29.4	18.7	34
6	$[Cr(NH_3)_5NCO](NO_3)_2$	55.6	43.2	18.3	8.85	35
7	tr-$[Cr(NH_3)_4(CN)_2](ClO_4)$	53.4	44.9	20.5	7.15	36
8	$NaMnF_3$	62.7	38.3	6.39	10.2	23
9	$(Me_4N)_2MnCl_4$	52.8	37.7	16.3	10.8	23
10	$(Me_4N)_2MnBr_4$	52.0	38.1	17.1	10.4	23
11	Na_6MnS_4	47.8	40.3	21.3	81.9	37
12	MnS_4[a]	49.3	39.4	19.8	9.07	23
13	$(PPh_4)FeCl_4$	40.9	34.4	42.5	26.1	38
14	$(Me_4N)FeBr_4$[b]	35.9	23.1	47.5	37.4	23
15	Na_5FeS_4	35.1	22.7	48.2	37.8	38
16	$Cs[Co(H_2O)_6](SO_4)_2{\cdot}6H_2O$	54.8	53.7	33.2	10.8	23
17	$[Co(NH_3)_6]Cl_3$	51.7	38.9	36.3	25.6	23
18	$[Coen_3]Cl_3$	49.2	36.5	38.8	28.0	23
19	$Codtp_3$	30.9	20.4	57.1	44.1	23
20	Na_6CoS_4	46.5	33.4	32.6	23.3	39
21	$(Et_4N)_2NiCl_4$	60.5	38.3	23.9	22.8	40
22	$Ni[R'_2P(NR)_2]_2$	58.1	44.2	26.3	16.9	41
23	$(Bu_3Ph)NiBr_3(Bu_3P)$	44.0	30.7	40.4	30.4	40
24	$Ni(N_3)_6^{4-}$	56.9	35.4	27.5	25.7	23
25	$Ni(hist)_2(H_2O)_2$	64.0	46.1	20.5	15.0	23

[a] $(Tetraphenyldithioimidodiphosphinato)_2$.
[b] With Me_3NH, Me_2NH_2, $MeNH_3$ counter ions as well.

Table 1 refers only to complex compounds of ions of the first transition series. Since "there is no essential difference between the energy levels of complexes in the three transition groups" (quotation from Jørgensen [22]), corresponding results should be obtained as well for higher transition group complexes. However, since the F^k parameter values for the free ions are not known as well as for the first transition series, a discussion of parameter changes ΔF^k due to chemical bonding, which strongly depend through Eq. (23) on reliable data for these parameters, would be less conclusive. The difficulties for determining good electron-electron repulsion parameters arise from the intermediate coupling. The inclusion of spin-orbit coupling in the model competing with electron-electron repulsion, which is of the same order for higher transition group elements, causes serious band assignment problems which are difficult to solve. A consideration of rare earth complexes along the lines of the present work would probably be more promising.

An inspection of Table 1 shows that in all cases the predictions on relative sizes of F^k parameters proposed by Eq. (16), and on its variations ΔF^k indicated by Eq. (24), are fulfilled by the experiment, i.e., in more detail:

The F^2 parameter values are always larger than the F^4 values and, more specifically, the $\triangle F^2$ are larger than the $\triangle F^4$ parameter changes.

All parameter relations agree well with one exception: for the compound No. 8, $NaMnF_3$ the relation for the parameter changes, when calculated from the parameters compiled in [23], is reversed compared to what is predicted. A check on the original paper, [42], shows, however, that the LFT analysis carried out on the optical spectrum of this compound cannot be correct. For high-spin d^5 complexes in octahedral environments, an evaluation of F^2 and F^4 (or B and C) parameters is straightforward. Since transitions into $^4E_g(G)$, $^4E_g(D)$, and $^4A_{2g}(F)$ only depend on the electron-electron repulsion parameters, because they result from the same electron configuration as the ground state, a full adaptation including ligand field parameters is not necessary, if spin-orbit coupling is neglected. For the assignment of the spectra made in [42] using the 80 K data reported in that work, we calculate (in 1000 cm^{-1})

$$F^2 = 60.0 \quad \text{and} \quad F^4 = 45.5 \tag{32}$$

This supplies an F^2/F^4=1.32 relation which is much closer to that given for other Mn(II) complexes (cf. those in Table 1). With the corrected data the parameter changes due to bonding, Eq. (23) are

$$\Delta F^2 = 9.0 \quad \text{and} \quad \Delta F^4 = 3.1 \tag{33}$$

which agree well with the relative orders predicted in Eq. (24).

Since relative values of model parameters must follow simple orders, as given in Eqs. (16) and (24), these relations therefore can be used for testing the validity or correctness of an LFT or AOM analysis which is carried out on the electronic spectra of complex compounds.

3.2 Check on Racah Parameters

In Table 2 the Racah parameters B and C together with their changes $\triangle$B and $\triangle$C due to chemical bonding are compiled correspondingly as in Table 1. The compound numbers refer to those of Table 1. In addition the nephelauxetic quotients (B and C parameters of the complexes relative to those for the free transition metal ions) are listed. In all cases the theoretical predictions on relative orders given by Eqs. (29) and (31) are fulfilled, i.e.,

the Racah parameters B are smaller than C parameters and parameter changes $\triangle B$ due to chemical bonding of central ions are smaller than the changes $\triangle C$.

The different behavior of compound No. 8, which in the preceding section is attributed to an incorrect fitting to experimental results in [42], is manifested by an unusually low parameter B=15 cm^{-1}. An adaptation carried out as in the preceding section using only intraconfigurational transitions leads to (all in cm^{-1})

$$B = 710 \quad \text{and} \quad C = 3608 \tag{34}$$

and for the parameter changes

$$\Delta B = 150 \quad \text{and} \quad \Delta C = 242 \tag{35}$$

Table 2 Racah parameters and their variations due to chemical bonding as calculated from a fit to the experiment (in cm^{-1})

Compound No.[a]	B	C	△B	$\frac{B}{B_{ion}}$	△C	$\frac{C}{C_{ion}}$
1	719	2790	143	0.83	1025	0.73
2	620	2710	242	0.72	1105	0.71
3	626	2560	236	0.73	1255	0.67
4	600	3150	318	0.65	983	0.76
5	529	2650	389	0.58	1483	0.64
6	645	3430	273	0.70	703	0.83
7	580	3565	338	0.63	568	0.86
8	845	3040	15	0.98	810	0.79
9	650	2990	210	0.76	860	0.78
10	630	3025	230	0.73	825	0.79
11	519	3200	341	0.60	650	0.83
12	559	3130	301	0.65	720	0.81
13	444	2728	571	0.44	2072	0.43
14	470	1833	545	0.46	2967	0.38
15	460	1800	555	0.45	3000	0.38
16	510	4264	555	0.48	856	0.83
17	615	3087	450	0.58	2033	0.60
18	590	2897	475	0.55	2223	0.57
19	400	1620	665	0.38	3500	0.32
20	570	2651	401	0.59	1846	0.59
21	800	3040	230	0.78	1810	0.63
22	686	3505	344	0.67	1345	0.72
23	550	2435	480	0.53	2415	0.50
24	760	2812	270	0.74	2038	0.58
25	783	3657	247	0.76	1193	0.75

[a] Numbers as indicated in Table 1.

matching the parameters of other Mn(II) complexes as No. 8 to 12 compounds much better than before. It also takes into account that a small nephelauxetic effect is expected for the fluoride complex [2, 16].

Furthermore, we may look at decreases of B and C parameters somewhat closer by considering relative values with respect to their free ion parameters. From the B/B_{ion} and C/C_{ion} columns listed in Table 2, we see that these values for most of the compounds are relatively similar. There are, however, some compounds, e.g., the Cr(III) complexes Nos. 6 and 7, Mn(II) complexes Nos. 11 and 12, the Co(III) complex No. 16 and the Ni(II) complex No. 24, for which these quotients differ significantly. Obviously it cannot be predicted which of the two quotients, B/B_{ion}or C/C_{ion}, is expected to be larger. In any case, for complexes, where these quotients differ considerably, the approximation of setting C=4B, as usually anticipated in the LFT and AOM analyses [14, 16, 21, 22], cannot be valid. Since this assumption is common in much of the related work, these analyses should be considered with care or eventually must be revised. A theoretical re-evaluation by varying B and C independently in general should not cause any dif-

ficulties, provided the experimental results allow this. This could further contribute to gaining more physical insight into the bonding properties of complex compounds.

4 Conclusions

The analyses of electronic spectra of transition metal complexes by fitting the measured band maxima to the energy levels calculated from LFT or AOM have proved to be strongly worthwhile. The parameters to be evaluated supply important information about the structure, chemical bonding, electron distribution, and other properties of these compounds. Among the parameters of the semiempirical models obtained, more attention should be directed to the parameters describing the d electron-electron interaction. Similar to LFT parameters as well as to any other model parameters describing orbital energy differences due to ligand field splitting, Slater-Condon or Racah parameters also have to obey certain rules, e.g., their values either follow some sequences independent of the central metal ion (nephelauxetic series) or they must fulfill some fundamental conditions concerning relative sizes as it is dealt with in the present chapter. If these principles are not complied with, the disagreement may be taken as an indication of wrong band assignments or, alternatively, that the theoretical analysis carried out proves to be incorrect. An example for the latter case is demonstrated in the present work. Corresponding checks are recommended for earlier and any forthcoming LFT or AOM analyses of optical spectra which will be undertaken.

5 References

1. Ballhausen CJ (1962) Introduction to ligand field theory. McGraw Hill, New York
2. Jørgensen CK (1962) Absorption spectra and chemical bonding in complexes. Pergamon Press, Oxford London New York Paris
3. Schläfer HL, Gliemann G (1967) Einführung in die Ligandenfeldtheorie. Akademische Verlagsgesellschaft, Frankfurt/Main
4. Jørgensen CK, Pappalardo R, Schmidtke HH (1963) Chem Phys 39:1422
5. Schmidtke HH (1964) Z Naturforsch A 19:1502
6. Schäffer CE, Jørgensen CK (1965) Mol Phys 9:401
7. Ceulemans A, Dendooven M, Vanquickenborne LG (1985) Inorg Chem 24:1153
8. Smith DW (1972) Struct Bond (Berlin) 12:49
9. Duer MJ, Fenton ND, Gerloch M (1990) Int Rev Phys Chem 9:227
10. Atanasov MA, Schmidtke HH (1988) Chem Phys 124:205
11. Bridgeman AJ, Gerloch M (1997) Prog Inorg Chem 45:179
12. Griffith JS (1961) The theory of transition metal ions. University Press, Cambridge
13. Jørgensen CK (1962) Orbitals in atoms and molecules. Academic Press, London,New York
14. Jørgensen CK (1966) Struct Bond (Berlin) 1:3
15. Schmidtke HH, Adamsky H, Schönherr T (1988) Bull Chem Soc Jpn 61:59
16. Jørgensen CK (1962) Prog Inorg Chem 4:73
17. Condon EU, Shortley GH (1959) The theory of atomic spectra. University Press, Cambridge
18. Racah G (1943) Phys Rev 63:367
19. Tanabe Y, Sugano S (1954) J Phys Soc Jpn 9:753,766

20. Liehr AD (1963) J Phys Chem 67:1314
21. Jørgensen CK (1962) Solid State Phys 13:375
22. Jørgensen CK (1963) Adv Chem Phys 5:33
23. Lever ABP (1984) Inorganic electronic spectroscopy, 2nd edn. Elsevier Science, Amsterdam
24. Hellmann H (1937) Einführung in die Quantenchemie. Deuticke, Leipzig, Wien
25. Feynman RP (1939) Phys Rev 56:340
26. Jørgensen CK (1956) Mat Fys Medd Dan Vid Selsk 30 No 22
27. From [12] p 78, note the mistake therein where $F^k > F^{k'}$ for $k > k'$ is wrongly noted
28. Otsuka J (1966) J Phys Soc Jpn 21:596
29. Hoggard PE. AOMX program, Santa Clara University, Department of Chemistry, Santa Clara, CA 95053
30. Adamsky H (1982) AOMX – a Fortran computer program for ligand field calculations – within the angular overlap model. Heinrich Heine University, Düsseldorf
31. Trees RE (1951) Phys Rev 83:756
32. Reber C, Güdel HU, Meyer G, Schleid T, Daul CA (1989) Inorg Chem 28:3249
33. Schwartz RW (1976) Inorg Chem 15:2817
34. Hoggard PE (1986) Coord Chem Rev 70:85
35. Schönherr T, Wiskemann R, Mootz D (1994) Inorg Chim Acta 221:93
36. Schönherr T, Itoh M, Urushiyama A (1995) Bull Chem Soc Jpn 68:2271
37. Rosellen U, Schmidtke HH (2002) Inorg Chem 41:856
38. Packroff R, Schmidtke HH (1993) Inorg Chem 32:654
39. Packroff R (1991) PhD Thesis, Heinrich Heine University, Düsseldorf
40. Mink HJ (1996) PhD Thesis, Heinrich Heine University, Düsseldorf
41. Mink HJ, Schmidtke HH (1998) Chem Phys Lett 291:202
42. Srivastava JP, Mehra A (1972) J Chem Phys 57:1587

Structure and Bonding, Vol. 106 (2004): 37–57
DOI 10.1007/b11304

Angular Overlap Model Parameters

Patrick E. Hoggard

Santa Clara University, Department of Chemistry, Santa Clara California 95053, USA
E-mail: phoggard@scu.edu

Abstract Since the introduction of the Angular overlap model (AOM) in the mid-1960s, expressing *d* orbital energies in terms of the σ- and π-antibonding parameters e_σ and e_π, the AOM has failed to supplant crystal field theory as the standard model to explain structure and electronic spectra in transition metal complexes. This is so despite the much more obvious connection in the AOM between structure and *d* orbital energies, the pictorial simplicity of the AOM approach, and the more consistent transferability of AOM parameters from one complex to another. The main reason is probably that AOM parameters cannot be determined uniquely when all the ligands are on the Cartesian axes. The scales for e_σ and e_π must then be fixed arbitrarily, as is done automatically in the crystal field model. A number of experimental approaches have evolved to solve, or at least evade, the nonuniqueness problem, including: (a) the assignment of e_π for saturated amines to zero, reflecting their inability to π-bond; (b) the simultaneous use of magnetic and spectroscopic data; (c) the inclusion of data from sharp, spin-forbidden lines in Cr(III) spectra, along with application of the exact geometry and full d^n configuration interaction in computations, or any combination of these; (d) the use of charge transfer bands involving $d\pi$ orbitals to determine e_π values. As of yet, the level of consistency among different techniques leaves something to be desired, and even with a common technique, reported AOM parameter values for particular metal-ligand combinations show a much higher variability than one would like, given even minimum expectations for transferability. Some of the variability can be ascribed to differences in the other ligands present. Even with these variations, AOM parameter sets can be usefully correlated with kinetic and thermodynamic data from both photochemical and thermal reactions.

Keywords Angular overlap model · Parameters · Ligand field theory

1 In the Beginning

One can scarcely imagine a more obscure venue than *Det Kongelige Danske Videnskabernes Selskab, Matematisk-fysiske Meddelelser* for the landmark paper on the angular overlap model (AOM). Appearing in 1965, "Energy Levels of Orthoaxial Chromophores and the Interrelation Between Cubic Parent Configurations", by Claus Erik Schäffer and Christian Klixbüll Jørgensen, laid out the now familiar one-electron ligand field matrix elements for orthoaxial (all ligands on the Cartesian axes) complexes in terms of AOM parameters [1]:

$$\langle d_{z^2}|\,V\,|d_{z^2}\rangle = e_{\sigma z} + \tfrac{1}{4}\,(e_{\sigma x} + e_{\sigma y}) + \tfrac{3}{4}\,(e_{\delta x} + e_{\delta y}) \tag{1}$$

$$\langle d_{x^2-y^2}|\,V\,|d_{x^2-y^2}\rangle = \tfrac{3}{4}\,(e_{\sigma x} + e_{\sigma y}) + e_{\delta z} + \tfrac{1}{4}\,(e_{\delta x} + e_{\delta y}) \tag{2}$$

$$\langle d_{xz}|\,V\,|d_{xz}\rangle = e_{\pi x} + e_{\pi z} + e_{\delta y} \tag{3}$$

$$\langle d_{yz}|\,V\,|d_{yz}\rangle = e_{\pi y} + e_{\pi z} + e_{\delta x} \tag{4}$$

$$\langle d_{xy}|\,V\,|d_{xz}\rangle = e_{\pi x} + e_{\pi y} + e_{\delta x} \tag{5}$$

$$\langle d_{z^2}|\,V\,|d_{x^2-y^2}\rangle = \tfrac{\sqrt{3}}{4}\,(e_{\sigma x} - e_{\sigma x} + e_{\delta x} - e_{\delta y}) \tag{6}$$

These matrix elements follow directly from the central premise of the angular overlap model, which is that each ligand exerts its effects separately on the metal *d* orbitals, and the net result for the metal ion can be taken as a sum of the effects of all ligands. Much of the molecular orbital (MO) basis for this approach was set forth in 1963 in an article by Jørgensen et al. [2]. Just prior to the appearance of the *Mat Fys Medd* paper, the *d*-electron matrix elements, $\langle d_i|\,V\,|d_j\rangle$, for a ligand at an arbitrary angular position was published by Schäffer and Jørgensen [3] using polar coordinates for ligand angular positions. This was preceded by an often neglected article by Schmidtke, who derived the same matrix elements using Eulerian angles to specify the ligand coordinates [4].

The $e_{\lambda x}$, $e_{\lambda y}$, and $e_{\lambda z}$ (λ=σ, π, δ) AOM parameters in Eqs. (1)–(6) which, based on a Wolfsberg-Helmholtz approximation, are intended to be proportional to the square of the overlap between metal and ligand orbitals, each represent the sum of the contributions from both ligands on the axis.

The *Mat Fys Medd* paper demonstrated the equivalence between AOM parameters [1] and the ligand field tetragonal parameters *Ds* and *Dt* [5], the equivalence for *Dq* having already appeared [3]:

$$Dq = \tfrac{1}{20}(3e_{\sigma x} - 4e_{\pi x}) \tag{7}$$

$$Ds = \tfrac{1}{7}(e_{\sigma x} + e_{\pi x} - e_{\sigma z} - e_{\pi z}) \tag{8}$$

$$Dt = \tfrac{1}{35}(3e_{\sigma x} - 4e_{\pi x} - 3e_{\sigma z} + 4e_{\pi z}) \tag{9}$$

The doubtless more familiar relation, $10Dq = 3e_\sigma - 4e_\pi$, refers to values for individual ligands rather than axis pairs. It should be noted that not all authors use the same sign conventions for *Ds* and *Dt* [6–8]. It should also be noted that the

delta-bonding e_δ terms from Eqs. (1)–(6) are neglected, or, more precisely, incorporated as part of the e_σ parameters. The term "tetragonal complexes" actually refers to complexes with the "holohedrized symmetry" D_{4h}. That term was introduced in the *Mat Fys Medd* paper to describe the concept that the effective molecular symmetry with respect to the *d* orbitals can be much greater than the actual molecular symmetry, because the *d* orbitals themselves have inversion symmetry. Thus the effects of ligands on the $+x$ and $-x$ axes are separately indistinguishable [1, 9]. The notion that ligand effects average across the axes for *d* orbitals had circulated previously [6, 10], probably the earliest reference being a paper by Ballhausen and Jørgensen in 1955 in *Matematisk-fysiske Meddelelser* [11].

It had already been recognized [6, 10] that *cis*-MA_4B_2, *trans*-MA_4B_2, and MA_5B complexes could all be classified as tetragonal complexes, and that their spectra could be interpreted in terms of the ligand field parameters *Dq, Ds,* and *Dt*. The idea of holohedral symmetry generalized this, showing, for example, that any six-coordinate complex with 90° angles between ligands has at least an effective D_{2h} symmetry. With this concept firmly in place, complexes with off-axis ligands could later be naturally analyzed in terms of the holohedral, rather than the actual, symmetry.

Finally, the 1965 *Mat Fys Medd* paper presented all the matrix elements for the $t_{2g}\rightarrow e_g$ spin-allowed transitions in d^3 and d^6 systems in all possible MA_nB_{6-n} geometries on an octahedral framework. This provided perhaps the most important connection to experiment, since experimental spectroscopic transition energies could be matched with unambiguous expressions in terms of AOM parameters together with interelectron repulsion parameters. For Cr(III) the situation is particularly simple for the lowest energy spin-allowed transition, because there is no interelectronic repulsion contribution at all [12].

The most important achievement of the *Mat Fys Medd* paper was the establishment of a simple conceptual relationship between structure and energy levels. This is still lacking in conventional ligand field theory, despite valiant attempts [13, 14]. The simplicity can be illustrated with the example of a *trans*-CrA_4B_2 complex. The energies of the five *d* orbitals, from Eqs. (1)–(6), ignoring the delta bonding terms, are

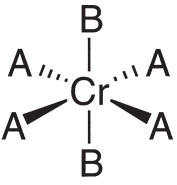

$$E(d_{z^2}) = e_{\sigma A} + 2e_{\sigma B} \tag{10}$$

$$E(d_{x^2-y^2}) = 3e_{\sigma A} \tag{11}$$

$$E(d_{xy}) = 4e_{\pi A} \tag{12}$$

$$E(d_{xz}) = E(d_{yz}) = 2e_{\sigma A} + 2e_{\pi B} \tag{13}$$

The transition energies for the three components of the $^4A_{2g}\rightarrow{}^4T_{2g}$ transition may be written as cyclic coordinate permutations of the $t_{2g}\rightarrow e_g$ transition $(xy)\rightarrow(x^2-y^2)$, another contribution from Schäffer and Jørgensen's *Mat Fys Medd* paper. The requisite energies are easily determined in a completely analogous manner:

$$E(d_{y^2-z^2}) = E(d_{z^2-x^2}) = \tfrac{3}{2}\,(e_{\sigma A} + e_{\sigma B}) \tag{14}$$

Thus the three component energies are

$$E(d_{x^2-y^2}) - E(d_{xy}) = 3e_{\sigma A} - 4e_{\pi A}) \tag{15}$$

$$E(d_{y^2-z^2}) - E(d_{yz}) = (\tfrac{3}{2}e_{\sigma A} - 2e_{\pi A}) + (\tfrac{3}{2}e_{\sigma B} - 2e_{\pi B}) \tag{16}$$

$$E(d_{z^2-x^2}) - E(d_{zx}) = (\tfrac{3}{2}e_{\sigma A} - 2e_{\pi A}) + (\tfrac{3}{2}e_{\sigma B} - 2e_{\pi B}) \tag{17}$$

and the splitting between the two observable components is

$$\Delta E = (\tfrac{3}{2}e_{\sigma A} - 2e_{\pi A}) - (\tfrac{3}{2}e_{\sigma B} - 2e_{\pi B}) \tag{18}$$

This corresponds, in ligand field terms, to $5Dq_A - 5Dq_B$.

The pictorial simplicity is enhanced further by expressing Eqs. (1)–(5) in the following terms, neglecting off-diagonal matrix elements when the holohedral symmetry is less than tetragonal. A ligand in the xy plane alters the energy of the x^2–y^2 orbital by $3e_\sigma/4$, the energy of the z^2 orbital by $e_\sigma/4$, the energy of the xy orbital by e_π, and the energy of the other t_{2g} orbital with which it overlaps by the same amount. A ligand on the z axis alters the energy of the z^2 orbital by e_σ and the energies of the two t_{2g} orbitals with which it overlaps by e_π. The same procedure is followed for permuted axes.

Not only are the orbital energies easily derived from and associated with the structure, the AOM formulation allows one to predict readily the energy order of the components of excited states, given some idea of the parameter values. Because the overlap of a given ligand with a given metal ion may be presumed to be somewhat similar even when the remaining ligands are different, AOM parameters have a degree of transferability not possessed by ligand field parameters, with the exception of Dq. Thus the acquisition of experimental AOM parameter values can be quickly rewarded with a predictive capability unachievable in the point charge model.

Given these attributes, it might be regarded as something of an accident of history that the crystal field model was developed earlier and has remained the standard model in textbooks that discuss the bonding and electronic spectra of coordination compounds. Two of the few to adopt the AOM approach were Drago's *Physical Methods in Chemistry* [15], though only after an extensive development of crystal field theory, and Purcell and Kotz's *Inorganic Chemistry*, which did away with crystal field theory altogether [16]. Jørgensen is quoted at great length in the latter text on the reasons why crystal field theory has remained the model of choice [9]. Purcell and Kotz is especially noteworthy in having used AOM parameters in the formulation of structure preference energies that successfully predict the coordination type for various d^n complexes.

Though Jørgensen thought it mainly a matter of inertia, there are probably sound reasons why AOM methods have not caught on as a basic explanation of excited state behavior. Often there is little interest in lower symmetry complexes at the textbook level, and crystal field theory suffices nicely to explain the spectra and magnetic properties of octahedral and tetrahedral complexes. The octahedral parameter Dq has a large degree of transferability and predictability, about which Jørgensen himself expounded at length [17]. In addition, Dq values are useful in predicting a number of non-spectroscopic properties, such as the spin

of the ground state and enthalpies of complexation [18]. Yet the angular overlap model can do all that and more.

2 The Problem of Nonunique Parameter Values

There is one problem that presents itself from the outset. Especially when dealing with orthoaxial complexes, there are more AOM parameters than there are unique spectroscopic energy differences. This is rather obvious for octahedral complexes, for which there is one unique energy difference, equal to $3e_\sigma - 4e_\pi$. Neither e_σ nor e_π can be determined uniquely.

In traditional crystal field theory, the problem vanishes, because the center of gravity of the *d* orbitals is set to zero. For octahedral complexes, the relevant diagram is

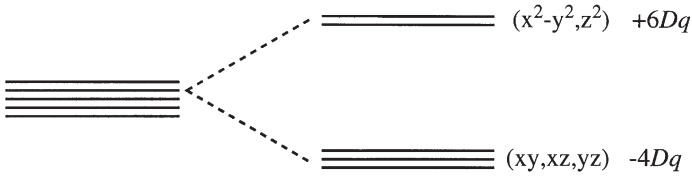

In the angular overlap model, the (x^2-y^2) and (z^2) orbitals increase in energy because they have σ-antibonding character in the molecular orbitals formed between the *d* orbitals and the ligand lone pairs. The (xy), (xz), and (yz) orbitals may go up or down through π-interaction with ligand lone pairs, ligand π-bonding orbitals, or ligand π-antibonding orbitals. The energy diagram above is replaced by

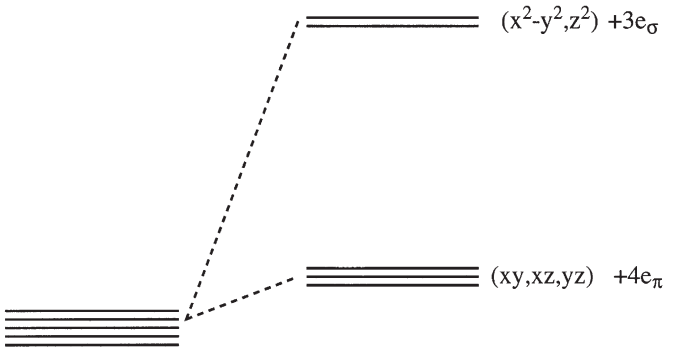

In this diagram, the isotropic increase in the energy of all the *d* orbitals is not pictured. The e_π parameter may be negative through interaction with π-antibonding orbitals. Spectroscopy measures only energy differences, and there is only one energy difference.

Lowering the symmetry to tetragonal does not alter the outcome. There are four AOM parameters for an MA_4B_2 complex: $e_{\sigma A}$, $e_{\pi A}$, $e_{\sigma B}$, and $e_{\pi B}$. However, there

are just three unique energy differences, as can be seen from the $\langle d_i|V|d_j\rangle$ ligand field potential matrix for *trans*-MA_4B_2.

$$\begin{pmatrix} 4e_{\pi A} & 0 & 0 & 0 & 0 \\ 0 & 2e_{\pi A}+2e_{\pi B} & 0 & 0 & 0 \\ 0 & 0 & 2e_{\pi A}+2e_{\pi B} & 0 & 0 \\ 0 & 0 & 0 & 3e_{\sigma A} & 0 \\ 0 & 0 & 0 & 0 & e_{\sigma A}+2e_{\pi B} \end{pmatrix}$$

The basis functions for this matrix are in the order (xy), (xz), (yz), $(x^2\text{-}y^2)$, (z^2). The diagonal elements are arbitrary to within an additive constant and there are four distinct diagonal elements; thus we can say there are three spectroscopically independent parameters [19]. The three crystal field parameters *Dq, Ds,* and *Dt* are therefore unambiguous (assuming a correct orbital assignment), while the AOM parameters cannot be individually determined, clearly a major handicap in the general case. It would be even worse if the actual symmetry were lower, but the holohedral symmetry were the same. A *trans(C)*-$MA_2B_2C_2$ complex, with two identical A-M-B axes, would have a potential matrix similar to that of MA_4B_2, but there would be six AOM parameters.

The D_{2h} complex, all-*trans*-$MA_2B_2C_2$, has more spectroscopically independent parameters, but still not enough. The potential matrix, from Eqs. (1)–(6), is

$$\begin{pmatrix} 2e_{\pi B}+2e_{\pi C} & 0 & 0 & 0 & 0 \\ 0 & 2e_{\pi A}+2e_{\pi C} & 0 & 0 & 0 \\ 0 & 0 & 2e_{\pi A}+2e_{\pi B} & 0 & 0 \\ 0 & 0 & 0 & \frac{3}{2}(e_{\sigma B}+e_{\sigma C}) & \frac{\sqrt{3}}{4}(e_{\sigma B}-e_{\sigma C}) \\ 0 & 0 & 0 & \frac{\sqrt{3}}{4}(e_{\sigma B}-e_{\sigma C}) & 2e_{\sigma A}+\frac{1}{2}(e_{\sigma B}+e_{\sigma C}) \end{pmatrix}$$

There are five spectroscopically independent parameters, four from the diagonal plus the off-diagonal element. No crystal field approach has been proposed for this system, and indeed it would be awkward, but five parameters could, in principle, be defined. It is another question whether there would be sufficient, and sufficiently good, experimental data to determine these five parameters, but the AOM formulation is, from the very beginning, insoluble.

The lack of a uniquely determinable set of parameters for complexes with simple (orthoaxial) geometry, but a general, unrestricted set of ligands, may provide the actual reason why the angular overlap model has not caught on as the standard explanatory model for the spectra of transition metal complexes. AOM parameters have a simple, comprehensible origin and are readily correlated with structures and spectra, but the relationship tends to be one-way. Knowing the AOM parameter values, one might predict the spectrum of a particular complex, but it may well be impossible to determine the parameter values from the spectrum. With crystal field-based ligand field theory, on the other hand, the parameters, aside from *Dq*, may have little meaning and little transferability, but for a particular complex they can be determined readily from a spectrum. With

crystal field theory it would be quite difficult to estimate a set of parameters for a new complex and predict the spectrum, something that is particularly easy with the angular overlap model.

3 Experimental Approaches to AOM Parameter Values

Despite the grim outlook in the orthoaxial general case, there are several approaches to the problem of nonunique AOM parameters for particular types of complexes.

3.1 Anchor Parameters by Setting e_π for Saturated Amines to Zero

The earliest approach was offered by Schäffer and Jørgensen in the *Mat Fys Medd* paper. They reasoned that a saturated amine like NH_3 has no ability to interact with π-symmetry *d* orbitals, and therefore the e_π value for NH_3 can be set equal to zero in all ammine (and aliphatic amine) complexes. Even if the reasoning were faulty (and potential problems have been noted [20, 21]), fixing one AOM parameter by agreement could solve the nonuniqueness problem. Even though a complex without an ammine ligand would still be, in principle, indeterminate, if e_σ and e_π for one of the ligands could be determined from an ammine complex, and if the AOM parameter values are indeed transferable, then the remaining AOM parameter values could also be determined. That might be stretching the model, but it does mean that the situation is not hopeless.

Indeed, through the observation of splitting in at least one of the two $t_{2g} \rightarrow e_g$ spin-allowed bands of $[CrA_5X]^{2+}$ or *cis*- or *trans*-$[CrA_4X_2]^+$ complexes (A=NH_3 or one arm of ethylenediamine), AOM parameters for a fair number of ligands have been determined [22–25]. A similar effort has not been made for Co(III) complexes, because two interelectronic repulsion parameters are required to fit the two spin-allowed bands, rather than the one required for Cr(III) complexes. Thus even if each of the four tetragonal components of the two spin-allowed bands, $^1A_{1g} \rightarrow {}^1T_{1g}$ and $^1A_{1g} \rightarrow {}^1T_{2g}$, are observed experimentally (generally by going to low temperature) and correctly assigned, there are still not enough data to determine three AOM and two interelectronic repulsion parameters. For this reason, a great deal of effort has been expended on Cr(III) complexes, with the hope that these will serve, with a suitable scale factor, for complexes of other metal ions.

A comparison of AOM parameter values from several sources determined as above reveals some degree of consistency. The value of $e_{\sigma N}$ for NH_3, for example, varied only from 6950 to 7220 cm^{-1} among several different compounds, different investigators, and different techniques [23–25]. On the other hand, $e_{\sigma N}$ for ethylenediamine was assigned values between 6640 and 7830 cm^{-1}, varying substantially with the other ligand present [23, 24]. Within a series of *trans*-$[CrA_4F_2]^+$ complexes with different amines, $e_{\sigma F}$ was assigned values between 7450 and 8480 cm^{-1}, and $e_{\pi F}$ values between 1620 and 2050 cm^{-1} [24]. The precision with which the component peaks within a broad band can be located is not high even

Table 1 Average AOM parameter values for Cr(III), determined from the splitting of spin-allowedbands in amine complexes [22–27]

Ligand	e_σ, cm^{-1}	e_π, cm^{-1}
NH_3	7010	(0)
F^-	7870	1880
Cl^-	5610	910
Br^-	5050	690
I^-	4140	670
OH^-	7510	1400
H_2O	7490	1390
en	7290	(0)
dmso	6770	1650
NCS^-	6240	380
CN^-	8310	–290
py	5800	–580

at low temperature and even for single crystals. Despite this variability, the ranges are restricted enough to make comparisons between ligands possible. Average values for some AOM parameters are shown in Table 1.

3.2 Use Both Magnetic and Spectroscopic Data

Ni(II) and Co(II) share with Co(III) the problem that there is an insufficient amount of spectroscopic data to determine two interelectronic repulsion parameters and all AOM parameters. An ingenious methodology has been brought to bear by Gerloch and coworkers on d^7, d^8, and high spin d^6 complexes, supplementing spectral data with magnetic susceptibility data [20, 28–33]. By determining the orientation of the principal axes of the magnetic susceptibility on single crystals, and repeating this over a wide temperature range, the AOM parameters are no longer underdetermined. The susceptibility tensor, $\chi_{\alpha\beta}$, is a complicated, temperature-dependent function of the magnetic moment matrix elements between energy eigenstates, $\langle i|k\mathbf{L}+2\mathbf{S}|j\rangle$ [28], where **L** and **S** are the orbital and spin angular momentum, and k is the Stevens orbital reduction factor [34]. Given the assumption that the magnetism arises within the metal d orbitals, these reduce to functions of the matrix elements over the d orbitals, $\langle d_i|k\mathbf{L}+2\mathbf{S}|d_j\rangle$,which are readily derived [20, 35]. The AOM parameters enter into the energy terms in the temperature factors, $\exp(-E_i/kT)$, for the different states i, as well as influencing the eigenvectors for these states. A related technique uses the g values and hyperfine splittings from EPR spectra to overcome the insufficiency of spectroscopic data [36, 37].

The method has proved to be as successful as the solely spectroscopic analysis of Cr(III) orthoaxial complexes – more so, in fact, because a number of more sophisticated factors, such as the orientation of ligand π orbitals, can be deter-

Table 2 Average AOM parameters for ligands intetrahedral nickel(II) complexes derived from electronic spectra and magnetic susceptibility measurements [21, 38, 39]

Ligand	e_σ, cm^{-1}	e_π, cm^{-1}
Cl^-	4000	2000
Br^-	3400	700
I^-	2000	600
PPh_3	5500	–1500

mined from the combined spectroscopic and magnetic data available. Gerloch's AOM computations frequently are based on the actual molecular geometry rather than an idealized structure [33]. A further advantage is that this overcomes the limitations of Cr(III) as a hard metal ion that will not bind to many soft ligands. Table 2 presents a sampling of AOM parameters derived from nickel(II) complexes by these techniques.

3.3 Include Sharp-line Spin-forbidden Bands, Exact Geometry, and CI

A third technique to get around the insufficiency of data from spin-allowed electronic bands is to use data from sharp-line spin-forbidden bands. These arise from electronic transitions within the same configuration, so that the excited state and the ground state have very similar geometries. Chromium(III) spectra have eight such transitions, all $(t_{2g})^3 \rightarrow (t_{2g})^3$, and under favorable conditions all eight may be found (in O_h: $^4A_{2g} \rightarrow {}^2E_g$, $^2T_{1g}$, $^2T_{2g}$). Sharp electronic lines have an additional advantage that they correspond one-to-one with particular excited states. The broad spin-allowed bands, on the other hand, consist of several components, especially when spin-orbit coupling is considered, and are never fully resolved. Thus there are always severe approximations to the assignment of a particular band maximum to an electronic transition.

Even with numerous sharp lines supplementing the broad spin-allowed bands, electronic spectra can yield up no more than the spectroscopically independent terms in the $\langle d_i | V | d_j \rangle$ potential matrix [19]. So, in principle, the sharp lines add only redundancy to the data set for orthoaxial complexes. If, however, the complex is not orthoaxial, and the geometry is known, a number of off-diagonal terms arise [19, 40]. The number of spectroscopically independent terms can then equal or exceed the number of parameters in the model. If those terms can be determined experimentally, they can suffice to calculate the AOM parameters of which the potential matrix is composed [41]. They may even suffice to determine in addition one or two bond angles, if the entire geometry can be expressed in terms of those angles [41–43].

A number of chromium(III) complexes have been analyzed in this fashion, including configuration interaction (CI) by use of the full 120×120 d^3 ligand field matrix [41, 43, 44]. It is even possible to determine angular overlap parameters for octahedral complexes by this technique, provided that the complex does not

sit at a site of O_h symmetry. To do this, the influence of the environment, at least the nearest counterions, must be accounted for in the analysis [45].

Table 3 surveys some of the AOM parameter values determined by sharp-line techniques, using either the exact geometry from the crystal structure or the approximate geometry from molecular modeling, or representing the geometry in terms of one or more angles varied as part of the analysis. The first question to be asked has to do with consistency. How close are parameter values reported for the same ligating group in similar complexes, in dissimilar complexes, in the same complexes studied in different laboratories? Given differences such as those in Table 3, how much can be ascribed to experimental variability and how much is actually chemically significant? It would be convenient if a particular ligand always had the same parameter values with a given metal ion, but Bridgeman and Gerloch have argued convincingly in a recent review article [40] not only that AOM parameter values must vary with the other ligands present, but that they are altered in a somewhat predictable way.

All the parameters in Table 3 were determined through a fitting process. Best-fit algorithms will happily yield answers with a precision of 1 cm^{-1}. The real uncertainties in the AOM parameter values can be estimated from the propagation of error from the uncertainties in the spectroscopic data [62], assuming of course that bands are correctly assigned. From reported values of propagated uncertainties it appears that 30 cm^{-1} is typical. Considering the different theoretical and computational techniques brought to bear in different laboratories, we may infer a still higher degree of uncertainty, perhaps 50 to 100 cm^{-1} or more. However, the values in Table 3 have been rounded to the nearest 10 cm^{-1} to reflect the most optimistic of reported error limits. A comparison of a significant number of similar complexes is necessary to be able to distinguish variations in parameter

Table 3 AOM parameter values for Cr(III) complexes from an analysis based in large part on the sharp line spin-forbidden transitions in the electronic spectrum

Parameter	Value (cm^{-1})	Complex	Ref
$e_{\sigma N}$ (Amine)	7590	$[Cr(en)_3]Cl_3$	35
	7610	$[Cr(tacn)_2]Cl_3$	46
	7510	$[Cr(chxn)_3]Cl_3$	47
	7050	[Cr(tcta)]	46
	7370(dpt)	[Cr(dpt)(glygly)]ClO_4	48
	7290	$[Cr(cyclam)(N_3)_2]N_3$	49
	7520	$[Cr(cyclam)(ONO)_2]NO_3$	50
	7510	$[Cr(cyclam)(ONO_2)_2]NO_3$	51
	7350 (cyclam)	$[Cr(cyclam)(pn)](ClO_4)_3$	52
	7540	$[Cr(diammac)](ClO_4)_3$	53
	7230	$[Cr(his)_2]NO_3$	54
	7240	$[Cr(gly)_3]$	55
	6620	$[Cr(ser)_3]$	55
	6750	$[Cr(leu)_3]$	55
$e_{\sigma N}$ (Imine)	6820	Na[*cis*-$Cr(ida)_2$]	56
	6850	Na[*trans*-$Cr(mida)_2$]	57

Table 3 (continued)

Parameter	Value (cm^{-1})	Complex	Ref
$e_{\sigma O}$ (Carboxylate)	7110	$K_3[Cr(ox)_3]$	58
	6750	$K[Cr(ox)_2(py)_2]$	59
	7150	$K_3[Cr(mal)_3]$	58
	7910	[Cr(tcta)]	46
	7770	$[Cr(his)_2]NO_3$	54
	7730	Na[*cis*-$Cr(ida)_2$]	56
	7960	Na[*trans*-$Cr(mida)_2$]	57
	7280	$[Cr(gly)_3]$	55
	7400	$[Cr(ser)_3]$	55
	7120	$[Cr(leu)_3]$	55
$e_{\pi O}$ (Carboxylate)	1440	$K_3[Cr(ox)_3]$	58
	700	$K[Cr(ox)_2(py)_2]$	59
	1880	$K_3[Cr(mal)_3]$	58
	2040	[Cr(tcta)]	46
	1910	$[Cr(his)_2]NO_3$	54
	1910	Na[*cis*-$Cr(ida)_2$]	56
	1110	Na[*trans*-$Cr(mida)_2$]	57
	1510	$[Cr(gly)_3]$	55
	640	$[Cr(ser)_3]$	55
	1240	$[Cr(leu)_3]$	55
$e_{\sigma C}$ (CN^-)	9990	$K_3[Cr(CN)_6]$	45
	7480	$[Cr(NH_3)_5CN]ClClO_4$	60
$e_{\pi C}$ (CN^-)	600	$K_3[Cr(CN)_6]$	45
	–890	$[Cr(NH_3)_5CN]ClClO_4$	60
$e_{\sigma N}$ (Peptide)	7430	[Cr(dpt)(glygly)]ClO_4	45
	7350	[Cr(dpt)(progly)]ClO_4	61
$e_{\pi N}$ (Peptide)	500	[Cr(dpt)(glygly)]ClO_4	48
	580	[Cr(dpt)(progly)]ClO_4	61

Ligandabbreviations:
en=ethylenediamine
H_2ox=oxalic acid
H_2mal=malonicacid
tacn=1,4,7-triazacyclononane
H_3tcta=1,4,7,-triazacyclononane-N′,N″,N‴-triaceticacid
py=pyridine
dpt=di(3-aminopropyl)amine
H_2glygly=glycylglycine
Hhis=L-histidine
chxn=*trans*-1,2-cyclohexanediamine
Hgly=glycine
Hser=L-serine
Hleu=L-leucine
H_2ida=iminodiaceticacid
H_2mida=*N*-methyliminodiaceticacid
H_2glygly=glycylglycine
H_2progly=L-prolylglycine

values due to different environments from variations ascribable to expected experimental uncertainties.

When very similar complexes are compared, the variability seems to fall within experimental (i.e., propagated) error. The three complexes $[Cr(en)_3]^{3+}$, $[Cr(chxn)_3]^{3+}$, and $[Cr(tacn)_2]^{3+}$ have rather similar environments, except for the actual geometry of the six saturated nitrogens around the chromium. The geometry is, however, factored into the analysis. The three values for e_σ are between 7510 and 7610 cm^{-1} [35, 46, 47]. This is a considerably narrower range of values than is typical of either of the two experimental methods discussed above. This is not apparent from Tables 1 and 2, because they show only average values. Values of e_σ for saturated amines do not provide the best test, however, because e_π was set to zero in all cases. When both e_σ and e_π are allowed to vary, while the difference, $3e_\sigma–4e_\pi$, is fairly well known from the spin-allowed bands and also likely to be fairly consistent from complex to complex, a more severe test is created.

Indeed, the reported e_σ and e_π values for carboxylate ligands show a much greater variability. The variability in e_σ is roughly comparable to that seen in the data behind Tables 1 and 2. The variability in e_π is so great as to leave some doubt that the spectra of all the carboxylate complexes in Table 3 were correctly assigned. It should be noted that the values of 10Dq are no more consistent, ranging from 13,900 to 19,600 cm^{-1} among the carboxylates in Table 3. Some consistencies emerge. Values of e_σ are quite similar for oxalate and malonate, although malonate exhibits a higher value of e_π [58]. This might be interpreted to mean that malonate is a better π-donor because the carboxylates are not conjugated as they are in oxalate.

The cyanide ligand offers an interesting discrepancy, though as yet based on limited data. The e_σ value was found to be 9990 cm^{-1} in $[Cr(CN)_6]^{3-}$ but 7480 cm^{-1} in $[Cr(NH_3)_5CN]^{2+}$ [45, 60]. That is a very considerable difference, matched by the reported differences in e_π, +600 cm^{-1} in the former, and –890 cm^{-1} in the latter. The difference in $10Dq$ is slighter: 27,570 cm^{-1} for $[Cr(CN)_6]^{3-}$ and 26,000 cm^{-1} for $[Cr(NH_3)_5CN]^{2+}$. Differences in parameter values might be due to incorrect spectral assignments, or to differences in the computational techniques used by dif-

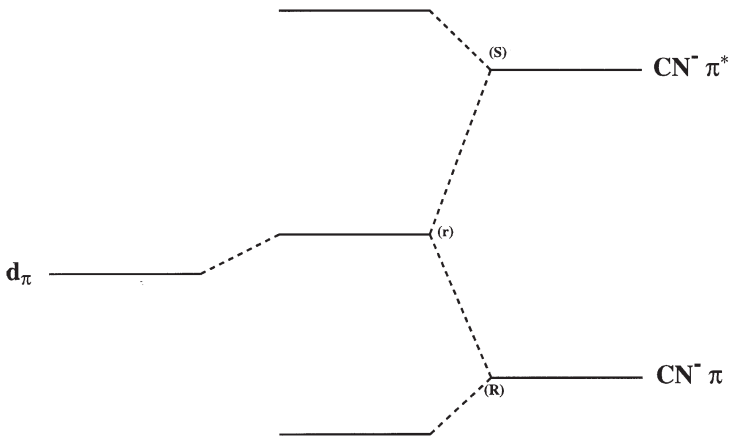

ferent laboratories. They may, however, be due to the different environments. The value of e_π derives from the sum of the interactions of the Cr^{3+} ion with the cyanide π-bonding orbitals, raising e_π (since the metal t_{2g} orbitals are higher in energy), and with the cyanide π-antibonding orbitals, lowering e_π.

One argument for the variation in e_π values goes like this: the higher in energy the metal t_{2g} orbitals are, the greater the interaction with the π^* orbitals, and the more negative, or less positive, the value of e_π will be. When the other five ligands are ammines, assumed not to affect the t_{2g} orbital energies, cyanide shows itself to be a net π acceptor, and the e_π value of –890 cm^{-1} is reasonable. When the other five ligands are π-withdrawing, their net effect is to depress the energies of the t_{2g} orbitals, allowing the interaction with the cyanide bonding orbitals to increase in importance, leading to a positive value of e_π.

This simple argument may seem self-contradictory, because the aggregate effect of the π-withdrawing cyanides is a positive value of e_π, which would make CN^- a net π-donor. Whether e_π=0 does indeed represent the demarcation between net π-donors and acceptors is questionable, and related to this is the difference in the application of AOM methods to the two complexes being compared, $[Cr(NH_3)_5CN]^{2+}$ and $[Cr(CN)_6]^{3-}$. The analysis of the latter complex included effects from the 14 nearest K^+ ions [45], which (in that treatment) lower the energies of the $d\pi$ orbitals, mimicking a negative value of e_π at (empty) positions on the Cartesian axes. Had the cations not been included, a correspondingly more negative value of e_π for cyanide would presumably have resulted, though it is hard to carry this argument to completion, because the spectrum could not have been fitted at all well.

It is considerations such as these that make an evaluation of the proposition of transferability of AOM parameters tricky. Nevertheless, Bridgeman and Gerloch [40] make a very good case, both theoretically and empirically, that e_π for a given ligand will increase the more π-electron withdrawing the other ligands are, and much of the experimental data behind this derives from neutral complexes, so that counterion effects can be neglected.

An additional perspective on cyanide coordinated to Cr(III) can be gleaned from the original spectral data from which the values in Table 1 were derived [25, 26]. They were determined specifically from the spectra of cyanoaqua complexes, especially $[Cr(H_2O)_5CN]^{2+}$ and $[Cr(H_2O)(CN)_5]^{2-}$ [63]. If the value of e_π for cyanide becomes more negative when π-donor ligands coordinate to the metal, then, all else being equal, this should be reflected in a larger value for $10Dq=3e_\sigma-4e_\pi$. Comparing the spectra of $[Cr(CN)_6]^{3-}$, $[Cr(H_2O)(CN)_5]^{2-}$, and $[Cr(H_2O)_5CN]^{2+}$, we find $10Dq$ equal to 26,500, 26,500, and 27,900 cm^{-1} [63]. If e_σ (CN^-) remained constant, that would amount to an e_π value 350 cm^{-1} more negative in the pentaaqua complex than in the other two, consistent with expectations.

For purposes of comparison with the ligands shown in Table 3, Table 4 presents data for some additional ligands, each derived from a single Cr(III) complex by a spectroscopic analysis including sharp lines, and using full d^n configuration interaction.

AOM parameters have been compiled for a number of other metal ions from detailed electronic spectra, calculations in the full d^n basis set, and often the exact

Table 4 AOM parameter values from an analysis involving Cr(III) sharp line spectra for some additional ligands

Ligand	Complex	e_σ, cm^{-1}	e_π, cm^{-1}	Ref
NCO^-	$[Cr(NH_3)_5NCO](NO_3)_2$	6060	420	64
$HBpz_3(N)$	$[Cr(HBpz_3)_2(ClO_4)_3$	8350	1300	42
N_3^-	$[Cr(cyclam)(N_3)_2]N_3$	5080	290	49
ONO^-	$[Cr(cyclam)(ONO)_2]NO_3$	6160	670	50
ONO_2^-	$[Cr(cyclam)(ONO_2)_2]NO_3$	5850	790	51
Urea (O)	$[Cr(urea)_6]Br_3$	6200	1400	65

Ligandabbreviations:
cyclam=1,4,8,11-tetraayaczclotetradecane,
$HBpz_3$=hydrotris(1-pyrazolyl)borate.

ligand geometry. As discussed above, calculations are still limited by the form of the ligand field potential matrix. No matter how many bands are identified, they can be used to determine no more than the number of spectroscopically independent terms in the matrix. In some systems, especially orthoaxial complexes, this may mean that one or more AOM parameters must be fixed arbitrarily.

Perhaps the most systematic study on systems other than chromium(III) was carried out by Zink and coworkers on square planar Pt(II) complexes of the type PtX_3L^-, investigated by single crystal polarized spectroscopy [66–70]. AOM parameter values are shown in Table 5.

In these computations, e_π values for amines were not set to zero. It is rather striking, therefore, to see that trimethylamine, with no available π-symmetry lone pairs, has an e_π value of 5100 cm^{-1} in this series, larger even than Cl^- and Br^-, which are π-donors in Cr(III) systems. Of course, both can also act as π-acceptors, a function liable to be much more pronounced in Pt(II) complexes. The large e_π value for NMe_3 supports the contention that both σ and π orbitals are raised in energy by electrostatic interactions with the ligand. This can be further seen in the value for e_π of ethylene near zero, although it clearly qualifies as a strongly π-withdrawing ligand.

Table 5 AOM parameters for ligands (L) in $[PtX_3L]^-$ complexes, X=halide, from single crystal polarized spectra [66–70]

Ligand	e_σ, cm^{-1}	e_π, cm^{-1}[a]
Cl^-	11,800	2900
Br^-	10800	2600
NMe_3	21700	5100
PPh_3	20000	1500
$AsPh_3$	18000	1100
CO	14500	–1750
PEt_3	23500	2750
C_2H_4	15000	0

[a] As an average of perpendicular and parallel components.

3.4 Use Charge Transfer Bands to Find e_π

Yet another approach is to examine metal-to-ligand charge transfer (MLCT) bands in a series of similar complexes. This was tried for complexes of the type *cis*-[Ru(bpy)$_2$X$_2$], bpy=2,2′-bipyridine [71]. All of these are strong field d^6 complexes, and the lowest energy charge transfer band can be represented as $t_{2g} \rightarrow \pi^*(bpy)$. The basic assumption is that the bipyridine π^* orbitals remain at a constant energy throughout the series, while the t_{2g} orbitals are raised or lowered in energy through interaction with the ligand X. A reference is still necessary (e_π for ethylenediamine was set to zero in this study), but no resolution of broad bands must be undertaken in order to derive parameters. Values for e_σ can then be estimated by finding 10*Dq* for a particular ligand [71], a generally much easier task than the spectral resolution required when *d-d* bands are analyzed. Representative values of e_π are shown in Table 6.

One use one might want to make of these parameters is to transfer them to another metal. Jørgensen is particularly well known for compiling evidence that the ligand field parameter 10*Dq* transfers rather well from one metal ion to another, given only a single scaling factor [17]. A comparison of Table 6 with Table 1, both of which set e_π for ammines to zero, shows that this would not work very well for AOM parameters if the two metal ions are Ru^{2+} and Cr^{3+}. Note first that the scaling factor for 10*Dq* has been given by Jørgensen as 0.87 upon going

Table 6 Values of e_π derived from MLCT bands in [Ru(bpy)$_2$X$_2$] [71]

X[a]	e_π cm^{-1}
F^-	570
HCO_3^-	490
$acac^-$	490
Cl^-	470
$CH_3CO_2^-$	410
$C_2O_4^{2-}$	370
BrO_3^-	370
Br^-	340
I^-	320
CO_3^{2-}	160
en	[0]
N_3^-	–20
SO_3^{2-}	–110
IO_3^-	–110
HCO_2^-	–200
NCS^-	–330
$NCSe^-$	–490
CN^-	–620
NO_2^-	–1160
bpy	–1600

[a] Ligandabbreviations:
Hacac=24-pentanedioneen=12-diaminoethane.

from Ru^{2+} to Cr^{3+} [72]. However, ligands that are π-donors tend to have much larger values of e_π with Cr^{3+} than with Ru^{2+}, a factor of three in the case of fluoride ion. On the other hand, ligands that have π-antibonding orbitals tend to have considerably more negative values of e_π with Ru^{2+}.

A perhaps too simple explanation of this phenomenon is that it is not just empty ligand and metal orbitals that interact with each other. The occupation of the *d* orbitals is also important. To some extent, e_σ and e_π, though derived strictly as energy parameters, represent electron donation or withdrawal to or from the metal *d* orbitals. Ru^{2+}, with a $(t_{2g})^6$ configuration, is resistant to donation, but more receptive to withdrawal than Cr^{3+}.

4 Applications of AOM Parameters

If the AOM parameters actually function as electron donation/withdrawal parameters, there should be several areas of application of a predictive nature in kinetics and thermodynamics, similar to the use of Hammett σ and ρ functions [73]. Perhaps the best known at this time is the theoretical treatment of the photochemical reactions of transition metal complexes by Vanquickenborne and Ceulemans [26, 74, 75]. This has proved singularly successful in predicting the selection rules and stereochemical outcome of photochemical reactions, including cases that did not fit the older empirical rules of Adamson [76] and the somewhat more refined rules of Zink [77, 78].

In the treatment of Vanquickenborne and Ceulemans, AOM parameters are used to estimate the energy of each of the *d* orbitals, as in Eqs. (1)–(6), before and after promotion of an electron during excitation. By rearrangement (ligand stabilization energies can be assumed to be the negative of metal destabilization energies), the net change in the bond energy of each ligand upon excitation can be determined, and the leaving group predicted. The five-coordinate intermediate may then rearrange, and again the AOM parameters can be used to identify the most stable arrangement. From the geometry of the intermediate one can then straightforwardly predict where the entering group will attack [74, 75].

A particular triumph of this model was that it provided a logical explanation for the remarkable empirical observation that *trans* Cr(III) complexes almost invariably rearranged to *cis* upon the photochemical loss of one of the *trans* ligands [79]. This had been a considerable puzzle, but the proposition by Vanquickenborne and Ceulemans that the intermediate will rearrange to its most stable geometry, that is, the geometry with the greatest net bond energy, provided the missing link.

Given the success of AOM parameters with photochemical reactions, it seems somewhat odd that they have not been used as much for thermal reactions. Yet their function as electron donor/acceptor parameters would appear to make them ideally suitable for this task. Consider the famous graph of hydrolysis rates of $[Co(en)_2LCl]^+$ complexes as a function of the electron-donating or -accepting power of the ligand L from Basolo and Pearson's monograph [80], reproduced in Fig. 1.

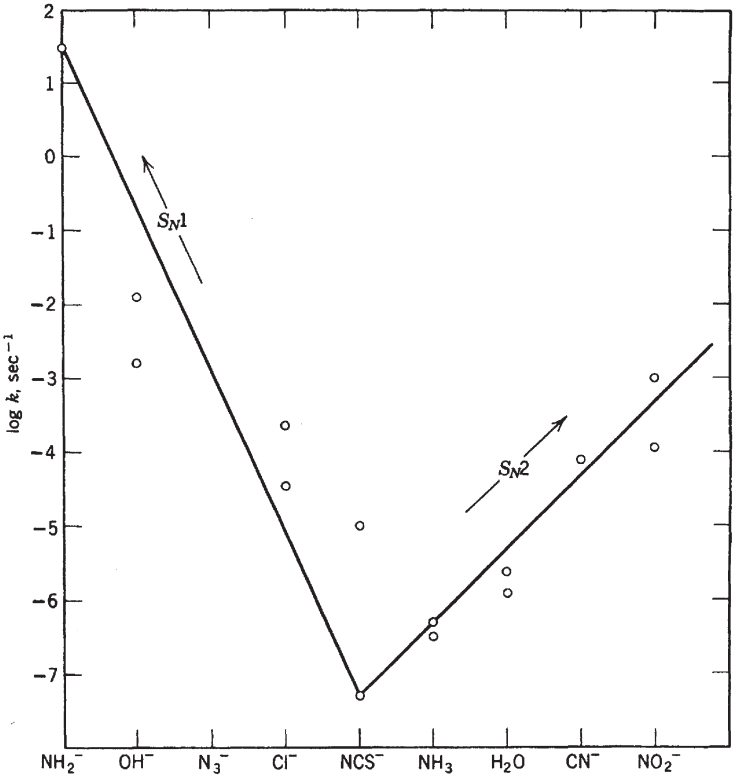

Fig. 1 Rates of hydrolysis of $[Co(en)_2LCl]^+$as a function of the ligand L [80]

The ligands L are arranged on the *x*-axis in what was perceived to be the order of increasing electron-withdrawing character. In AOM terms, it appears that what Basolo and Pearson were attempting to represent was specifically the π-withdrawing or π-donor character. With reference to Table 6, NO_2^- is clearly the best π acceptor and CN^- the second best among this group. On the left side, NH_2^- and OH^- are similar to F^-, that is, strong π donors. The ordering in the center appears from our vantage point to be uncertain, if not arbitrary. For example, it is unclear why H_2O was ranked as a weaker donor, or stronger acceptor, than NH_3. At any rate, the point was that both strong donors and strong acceptors seemed to react quickly. Therefore, they deduced that there were two mechanisms involved. The strong acceptors promoted association of a seventh ligand, thus an S_N2 reaction. The strong donors promoted dissociation of the chloride, thus an S_N1 reaction [80].

At the very least, AOM parameters would allow the ligands on the *x*-axis to be placed in order of e_π, which may represent rather well what was intended. On the other hand, when one notices that the ordering, which was largely intuitive, wound up primarily a measure of π-donation and π-withdrawal, the natural question is to ask about the neglected effects of σ-bonding. In fact, σ-donation

should be more important than π-donation in labilizing another ligand in the coordination sphere, because σ effects are so much larger. Looking at all the tables above, one might note that the ligands on both the right and the left side of the diagram are reasonably strong σ donors (NO_2^- is not shown in the tables, but e_σ is very high [71]). This suggests that perhaps we are dealing with just a single mechanism, S_N1, and the appropriate gauge of electron donor ability ought to be some combination of e_σ and e_π. Both *cis* and *trans* complexes are represented in the diagram above. Looking at the *d* orbitals that overlap with both L and Cl^-, one would surmise that $e_\sigma+2e_\pi$ might be appropriate for *trans* complexes, and $e_\sigma+4e_\pi$ appropriate for *cis* complexes, if the π interaction is symmetric about the M-L axis. Ligands that π-bond anisotropically would require individual analysis that must take into account the orientation of the π orbitals on the ligand. Unfortunately, there is not yet a set of AOM parameters for Co(III) sufficiently precise or extensive to allow a quantitative approach to this question.

The reader might note that AOM parameters were discussed in the previous two paragraphs as if they were essentially fixed attributes of the ligand when bound to a particular metal ion. As mentioned earlier, however, we can expect some, perhaps considerable, variation due to the other ligands in the coordination sphere [40]. This accentuates the problem of carrying out a quantitative correlation of kinetic or other data with AOM parameter values. The $[Co(en)_2LCl]^+$data described above ought to have the fewest problems in this regard, because AOM parameters could, in principle, be determined spectroscopically for just this series of complexes.

Another straightforward application of AOM parameters is to the *trans* effect in square planar complexes. Lee has outlined some AOM formulations applicable both to the relative weakening of bonds *trans* to particular ligands and to the stabilization of the 5-coordinate intermediate from an associative substitution process (the kinetic *trans* effect) [81]. He concluded that when the *trans* ligand is not a π-acceptor, the *trans* effect has a negative correlation with e_σ, at least qualitatively. The higher the value of e_σ, the smaller the *trans* labilization. This may seem counterintuitive, since σ-donation will raise the energy of the $(x^2–y^2)$ orbital and destabilize the other three ligands in the *xy* plane, although not specifically the *trans* ligand.

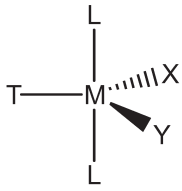

Lee's argument is more sophisticated. Consider the complex above, in which ligand T is varied and its influence on the labilization of X investigated. When a ligand Y associates with this complex, it then rearranges to a trigonal bipyramid transition state. The energy difference for the ligands, equal to the negative of the energy difference for the metal *d* electrons [81] is

$$E_{tbp} - E_{sp} = e_{\sigma T} + e_{\sigma X} - e_{\sigma L} - \tfrac{1}{2} e_{\sigma Y} \qquad (19)$$

If everything but T remains the same, the greater the value of $e_{\sigma T}$, the higher in energy the ligands are in the transition state, and the slower the reaction will go [81].

5 Concluding Remarks

There are now hundreds of AOM parameter values to be found in the literature, only a small fraction of which are included in the tables above. They cover a wide variety of ligands and metal ions. They have been determined using some quite different experimental techniques and theoretical frameworks. Because of this, and because of the general problem of where and how (and whether) to anchor the AOM parameter scales, they lack the kind of universal comparability about which Jørgensen has written profusely [17, 72].

To this author, perhaps the biggest problem is the common assumption that e_π for NH_3 or saturated amines is zero, upon which the values in Tables 1, 3, 4, and 6 depend, as well as many other literature values. There are both experimental and conceptual reasons to be skeptical of this assumption beyond any consideration of electrostatic effects in the first coordination sphere. In an early paper, Vanquickenborne and Ceulemans allowed e_π for NH_3 in some Pt(II) complexes to vary, ending with a positive value [21]. Later Zink's group assigned positive values of e_π (Table 5) to several π-acids, PEt_3 and $AsPh_3$, for example, in other Pt(II) complexes, and a correspondingly larger positive value to NMe_3 [66–70]. Conceptually, there are perturbations on the energies of the $d\pi$ orbitals from beyond the first coordination sphere, which may come from counterions [45], nonbound atoms in a coordinating molecule [35], or electron density from neighboring complexes in the crystal. The "amine assumption", if it were valid at all, should apply only when all these effects are accounted for. Their neglect, though quite practical, would properly cause e_π for amines to be nonzero.

To permit comparison between different metal ions, different experimental techniques, and different computational assumptions, $e_{\pi N}$ for amines ought not to be fixed, but should be determined by experiment. Several of the procedures discussed are capable of doing this, although how well they are capable of producing reliable parameter values is a separate question. At the very least, much of the experimental data on which Tables 3 and 4 are based could be reexamined, and the "amine assumption" discarded. For the Table 1 data this is impossible, because the parameters are otherwise underdetermined. The parameters in Tables 2 and 5 were determined without the "amine assumption", though sometimes with other assumptions involving the transferability of parameters between complexes.

In order to correlate AOM parameter values with other types of experimental data, it is not necessarily required that all parameters everywhere be derived in a like manner. The most important difference between different approaches is in the location of the zero values for the parameter scales. A series of similar experiments with different ligands but the same metal ion, if done properly, ought to place the ligands in the correct sequence, and e_σ and e_π values might be corrected primarily by common additive terms. Thus correlations of other properties with e_σ or e_π should still be feasible.However, another common assumption

that positive values of e_π imply net π-electron donation from ligand to metal, and negative values imply the reverse should probably be abandoned.

With this in mind, the question discussed earlier about the value of e_π for CN^- in different complexes may be easier to resolve. If a negative value of e_π does not imply opposite behavior from a positive value of e_π, it is not inconsistent for cyanide to have a small negative value in $[Cr(NH_3)_5CN]^{2+}$, but a small positive value in $[Cr(CN)_6]^{3-}$.

Difficulties in achieving reliable sets of AOM parameter values have doubtless hindered the application of AOM parameters to the understanding of other types of experiments. The few examples presented above, however, serve as evidence that this could be a fertile field in the future.

Based on the insights in Bridgeman and Gerloch's paper [40], as well as much of Gerloch's body of work on the transferability of AOM parameters, or lack thereof, and reinforced directly or indirectly by the observations of others, there is one direction in which the opportunities appear to be great for AOM parameters to gain in significance. If the influence of each of the ligands in the coordination sphere on the effective AOM parameter values of the others could be incorporated into the analytical treatment, the AOM parameters might regain a great deal of the transferability that was hoped for when Jørgensen and others first conceived of the angular overlap model.

6 References

1. Schäffer CE, Jørgensen CK (1965) Mat Fys Medd Dan Vid Selsk 34(13)
2. Jørgensen CK, Pappalardo R, Schmidtke H-H (1963) J Chem Phys 39:1422
3. Schäffer CE, Jørgensen CK (1965) Mol Phys 9:401
4. Schmidtke H-H (1964) Z Naturforsch 19A:1502
5. Ballhausen CJ, Moffitt W (1956) J Inorg Nucl Chem 3:178
6. Ballhausen CJ (1962) Introduction to ligand field theory. McGraw-Hill, New York
7. Perumareddi JR (1967) J Phys Chem 71:3144
8. Lever ABP (1968) Coord Chem Rev 3:119
9. Jørgensen CK (1971) Modern aspects of ligand field theory. North Holland, Amsterdam
10. Yamatera H (1958) Bull Chem Soc Jpn 31:95
11. Ballhausen CJ, Jørgensen CK (1955) Mat Fys Medd Dan Vid Selsk 29(14)
12. Tanabe Y, Sugano S (1954) J Phys Soc Jpn 9:753
13. Krishnamurthy R, Schaap WB (1969) J Chem Ed 46:799
14. Donini JC, Hollebone BR, Lever ABP (1977) Progr Inorg Chem 22:225
15. Drago RS (1977) Physical methods in chemistry. Saunders, Philadelphia
16. Purcell KF, Kotz JC (1977) Inorganic chemistry. Saunders, Philadelphia
17. Jørgensen CK (1962) Absorption spectra and chemical bonding in complexes. Pergamon, Oxford
18. Kettle SFA (1969) Coordination compounds. Thomas Nelson, London
19. Hoggard PE (1994) Top Curr Chem 171:113
20. Gerloch M (1983) Magnetism and ligand-field analysis. Cambridge University Press
21. Vanquickenborne LG, Ceulemans A (1981) Inorg Chem 20:796
22. Fee WW, Harrowfield JNM (1969) Aust J Chem 23:1049
23. Keeton M, Chou F-C, Lever ABP (1970) Can J Chem 49:192
24. Barton TJ, Slade RC (1975) J Chem Soc Dalton 650
25. Glerup J, Mønsted O, Schäffer CE (1976) Inorg Chem 15:1399
26. Vanquickenborne LG, Ceulemans A (1977) J Am Chem Soc 99:2208
27. Perumareddi JR (1969) Coord Chem Rev 4:73

28. Gerloch M, McMeeking RF (1975) J Chem Soc Dalton 2443
29. Gerloch M, Hanton LR (1980) Inorg Chem 19:1692
30. Gerloch M, Morgenstern-Badarau I, Audiere J-P (1979) Inorg Chem 18:3220
31. Gerloch M, Morgenstern-Badarau I, Audiere J-P (1979) Inorg Chem 18:3225
32. Gerloch M, Manning M (1981) Inorg Chem 20:1051
33. Fenton ND, Gerloch M (1987) Inorg Chem 26:3273
34. Stevens KWH (1954) Proc R Soc London 219A:542
35. Hoggard PE (1988) Inorg Chem 27:3476
36. Bencini A, Benelli C, Gatteschi D (1984) Coord Chem Rev 60:131
37. Bencini A, Benelli C, Gatteschi D, Zanchini C (1983) Inorg Chem 22:2123
38. Gerloch M, Hanton LR (1981) 20:1046
39. Davies JE, Gerloch M, Phillips DJ (1979) J Chem Soc Dalton 1836
40. Bridgeman AJ, Gerloch M (1997) Prog Inorg Chem 45:179
41. Hoggard PE (1986) Coord Chem Rev 70:85
42. Fujihara T, Schönherr T, Kaizaki S (1996) Inorg Chim Acta 249:135
43. Schönherr T (1997) Top Curr Chem 191:87
44. Schmidtke H-H, Adamsky H, Schönherr T (1988) Bull Chem Soc Jpn 61:59
45. Hoggard PE, Lee K-W (1988) Inorg Chem 27:2335
46. Lee K-W, Hoggard PE (1991) Transition Met Chem 16:377
47. Choi J-H (1994) Bull Korean Chem Soc 15:145
48. Choi J-H, Hoggard PE (1992) Polyhedron 11:2399
49. Choi J-H (2000) Spectrochim Acta 56A:1653
50. Choi J-H (2000) Chem Phys 256:29
51. Choi J-H (1997) Bull Korean Chem Soc 18:819
52. Choi J-H, Oh I-G, Yeh J-H (1996) Ungyong Mulli 9:728
53. Choi J-H, Oh I-G (1997) Bull Korean Chem Soc 18:23
54. Lee K-W, Eom K-I, Park S-J (1997) Inorg Chim Acta 254:131
55. Park S-J, Choi Y-K, Han S-S, Lee K-W (1999) Bull Korean Chem Soc 20:1475
56. Park S-J, Lee K-W (1996) Chem Phys 202:15
57. Lee K-W, personal communication
58. Lee K-W (1989) Dissertation, North Dakota State University
59. Schönherr T, Degen J (1990) Z. Naturforsch A 45:161
60. Urushiyama A, Mutsuyoshi I, Schönherr T (1995) Bull Chem Soc Jpn 68:594
61. Choi J-H, Hong YP, Park YC (2002) Spectrochim Acta 58A:1599
62. Clifford AA (1973) Multivariate error analysis. Wiley-Halstad, New York
63. Krishnamurthy R, Schaap WB, Perumareddi JR (1967) Inorg Chem 6:1338
64. Schönherr T, Wiskemann R, Mootz D (1994) Inorg Chim Acta 221:93
65. Park S-J, Oh B-K, Park Y-D, Lee K-W (1999) Bull Korean Chem Soc 20:943
66. Chang T-H, Zink JI (1984) J Am Chem Soc 106:287
67. Chang T-H, Zink JI (1985) Inorg Chem 24:2499
68. Chang T-H, Zink JI (1986) Inorg Chem 25:2736
69. Chang T-H, Zink JI (1987) J Am Chem Soc 109:692
70. Phillips J, Zink JI (1986) Inorg Chem 25:1503
71. Hoggard PE, Clanet PP (1987) Polyhedron 6:1621
72. Jørgensen CK (1969) Oxidation numbers and oxidation states. Springer, Berlin Heidelberg New York
73. Hammett LP (1940) Physical organic chemistry. McGraw Hill, New York
74. Vanquickenborne LG, Ceulemans A (1978) J Am Chem Soc 100:475
75. Vanquickenborne LG, Ceulemans A (1978) Inorg Chem 17:2730
76. Adamson AW (1967) J Phys Chem 71:798
77. Zink JI (1972) J Am Chem Soc 94:8039
78. Zink JI (1974) J Am Chem Soc 96:4464
79. Kirk AD (1973) Mol Photochem 5:127
80. Basolo F, Pearson RG (1967) Mechanisms of inorganic reactions, 2nd edn. Wiley, New York, p 172
81. Lee L (1994) J Chem Ed 71:644

Structure and Bonding, Vol. 106 (2004): 59–70
DOI 10.1007/b11305

Influence of Crystal Field Parameters on Near-Infrared to Visible Photon Upconversion in Ti^{2+} and Ni^{2+} Doped Halide Lattices

Oliver S. Wenger · Hans U. Güdel

Universität Bern, Departement für Chemie und Biochemie, Freiestrasse 3, 3000 Bern, Switzerland
E-mail: guedel@iac.unibe.ch

Abstract The near-infrared to visible photon upconversion properties of Ti^{2+} and Ni^{2+} doped chloride and bromide lattices are summarized and discussed. They are used to illustrate the young and emerging field of transition metal based upconversion systems. It is demonstrated that transition metal upconversion properties can be tuned by chemical and structural variation. The change from NaCl to $MgCl_2$ as a host for Ti^{2+} induces a crossover in the intermediate metastable excited state of Ti^{2+} from $^3T_{2g}$ to $^1T_{2g}$, leading to an order of magnitude enhancement of the 15 K near-infrared to visible upconversion efficiency. The change from $CsCdCl_3$ to $MgBr_2$ as host lattices for Ni^{2+} dopant ions induces a crossover in the upper emitting excited state of Ni^{2+} from $^1T_{2g}$ to $^1A_{1g}$, manifesting itself in a change from broad-band to sharp-line visible upconversion luminescence. These results are rationalized on the basis of varying covalency and crystal field strength.

Keywords Upconversion · Luminescence · Transition metal ions · Crystal field · Excited state absorption

List of Abbreviations

GSA Ground state absorption
ESA Excited state absorption
ESE Excited state excitation

1 Introduction

Light emission is always in competition with nonradiative relaxation processes. In transition metal complexes such as for example $Ru(bpy)_3^{2+}$ (bpy=2,2′-bipyridine) or $Pt(CN)_4^{2-}$ efficient luminescence is observed at room temperature [1, 2]. Other complexes, e.g. $V(urea)_6^{3+}$ exhibit luminescence only at cryogenic temperatures [3], because the transformation of electronic energy into vibrational energy and eventually heat is dominant at room temperature. High energy vibrations such as O-H, N-H and C-H stretches as well as other common vibrations in organic groups are extremely efficient luminescence killers. A commonly followed strategy for improving the efficiency of light emitting materials therefore involves the use of so-called low-phonon hosts for transition metal or rare earth dopant ions [4]. Typical low-phonon hosts are fluorides, chlorides, bromides or even iodides. The term low-phonon host derives from the fact that in these systems the highest energy vibrations are typically around 400, 300, 200 and 160 cm^{-1}, respectively, i.e. substantially lower than the vibrations encountered in organic materials. In contrast to $V(urea)_6^{3+}$, VCl_6^{3-} (the active luminophore in V^{3+} doped Cs_2NaYCl_6) is an efficient room temperature emitter [5], and this nicely illustrates the power of this approach in terms of optimising luminescence efficiencies. Further illustrative examples are found among trivalent lanthanide doped systems [6, 7], and among a large number of transition metal doped systems which have become important solid state laser materials [8]. For a relatively small number of transition metal ions the use of low-phonon host lattices results in particularly interesting and unusual luminescence properties. In octahedral fluoro-, chloro- and bromo-coordination Ni^{2+}, Mo^{3+}, Re^{4+} and Os^{4+} emit light from multiple excited states when cooled below 50–150 K [9–12]. The same is true for Ti^{2+} in hexachloro-coordination [13]. Thus these systems are exceptions to Kasha's rule, which states that luminescence is to be expected, if at all, only from the lowest energetic excited state in condensed systems [14]. All of the above systems have higher excited states which are separated from their next lower lying excited state by several thousand wavenumbers. These large energy gaps, in combination with low vibrational energies, are of key importance for their unusual photophysical properties.

With their multiple metastable excited states, Ti^{2+}, Ni^{2+}, Mo^{3+}, Re^{4+} and Os^{4+} doped halide lattices have recently come into the focus of several upconversion studies [15]. Photon upconversion is a nonlinear optical process used to convert low energy input light into higher energy output radiation [16]. In contrast to the better known second harmonic generation, the existence of at least two metastable excited states is a fundamental prerequisite for upconversion processes. The lower energy metastable state, typically located in the near-infrared spectral region, is used as an energy storage reservoir from which upconversion to an energetically higher lying emitting excited state occurs. In 1960 Auzel first reported on such upconversion processes in rare earth doped materials [17]. Since then a large number of upconversion studies involving rare earths, in particular trivalent lanthanides, has appeared. This is because the existence of multiple metastable f-f excited states is a very common phenomenon

among rare earth systems [18]. Upconversion processes have been exploited to build several near-infrared solid-state lasers, which emit in the visible spectral range [18–20]. Further applications involve infrared quantum counters, display phosphors and a 3D imaging display [21, 22]. Upconversion in transition metal based systems is a young research area, which is very actively explored in our group.

In this contribution we report on the low temperature upconversion properties of the $3d^2$ and $3d^8$ ions Ti^{2+} and Ni^{2+} in chloride and bromide host lattices. They illustrate the main difference between transition metal and rare earth upconversion systems. In the latter the spectroscopically active 4f and 5f electrons are shielded by the outer 5s, 5p and 6s, 6p electrons, respectively [23]. Chemical and structural changes in their crystal field environments therefore have relatively little impact on the energy level structure of the rare earth ions. In transition metal ions, by contrast, the spectroscopically active d-electrons play a decisive role in chemical bonding. Environmental changes may therefore dramatically alter the energy level structure of these systems, and in the case of Ti^{2+} and Ni^{2+} doped halide lattices this allows a chemical tuning of their upconversion properties.

2 Upconversion in Ti^{2+} Doped Chlorides: Crystal Field Strength Dependence of Upconversion Efficiencies

Figure 1a shows an energy level diagram for octahedrally coordinated d^2 ions [24].

The ground state is $^3T_{1g}(t_{2g}^2)$ and two spin-allowed one-electron absorption transitions to $^3T_{2g}(t_{2g}e_g)$ and $^3T_{1g}(t_{2g}e_g)$ (thick lines in Fig. 1a) are expected.

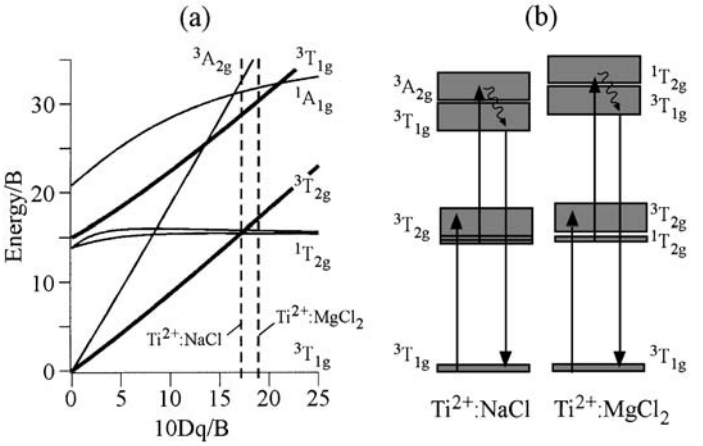

Fig. 1 **a** Energy level diagram for octahedrally coordinated d^2 ions [24]. The left and right dashed vertical lines indicate the positions of Ti^{2+} doped into NaCl and $MgCl_2$, respectively [30]. **b** Schematic representations of the upconversion processes in the two Ti^{2+} doped systems. Solid upward arrows represent ground- and excited-state absorption transitions, wavy arrows stand for nonradiative relaxation, and the solid downward arrows indicate luminescence

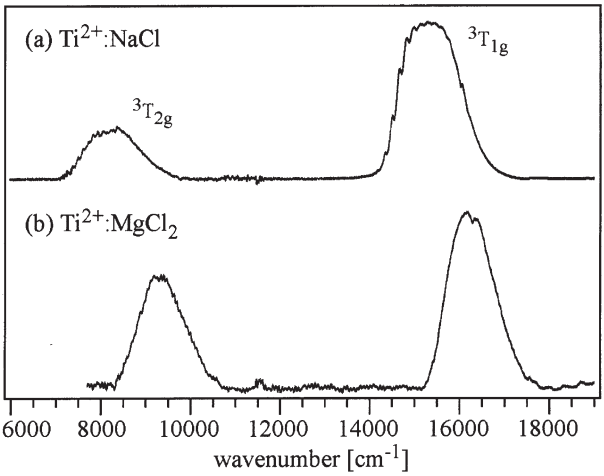

Fig. 2a,b The 15 K survey d-d absorption spectra of: **a** 0.8% Ti^{2+}:NaCl; **b** 0.1% Ti^{2+}:$MgCl_2$ (axial) [26, 28]

Figure 2 shows the 15 K absorption spectra of (a) 0.8% Ti^{2+}:NaCl and (b) 0.1% Ti^{2+}:$MgCl_2$ (axial) [25, 26]. Both spectra are comprised of two broad absorption bands with oscillator strengths of the order of 10^{-5}. They are assigned to the above two spin-allowed transitions, respectively. Due to their weakness, no spin-forbidden triplet-singlet absorptions are observed in either crystal. In Ti^{2+}:$MgCl_2$ both absorption bands are blue-shifted by roughly 1000 cm^{-1} with respect to Ti^{2+}:NaCl. This is a manifestation of the stronger crystal field acting on the Ti^{2+} ion in $MgCl_2$ relative to NaCl.

This is rationalized by a simple comparison of ionic radii [27]: Ti^{2+} (r=1.00 Å) is smaller than Na^+ (r=1.16 Å), but larger than Mg^{2+} (r=0.86 Å). Neglecting the trigonal distortion of the $TiCl_6^{4-}$ units caused by the crystal structure of $MgCl_2$, a simple O_h crystal field calculation yields 10Dq=10,180 cm^{-1}, B=527 cm^{-1} and C/B=3.76 for Ti^{2+}:$MgCl_2$ [26]. As shown in Table 1, an analogous calculation for Ti^{2+}:NaCl yields very similar B and C values, but 10Dq=9064 cm^{-1} [27]. Thus one calculates a 10Dq/B ratio of 17.1 for Ti^{2+}:NaCl and 19.3 for Ti^{2+}:$MgCl_2$. This places the former a little to the left of the $^3T_{2g}(t_{2g}e_g)/^1T_{2g}(t_{2g}^2)$ crossing point in the d^2

Table 1 Approximate octahedral crystal field parameters (in cm^{-1}) for Ti^{2+} in NaCl and $MgCl_2$, respectively, extracted from fits to the experimental 15 K absorption energies (Fig. 2). A detailed description of the fit procedures is given in [26] and [28]

	Ti^{2+}:NaCl	Ti^{2+}:$MgCl_2$
10Dq	9,064	10,180
B	530	527
C/B	3.9	3.76

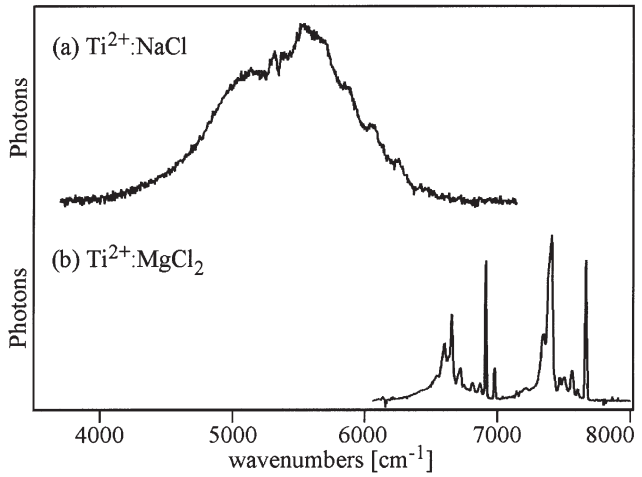

Fig. 3a,b The 15 K near-infrared luminescence spectra of: **a** 0.2% Ti^{2+}:NaCl; **b** 0.1% Ti^{2+}:$MgCl_2$ (axial) obtained after continuous-wave laser excitation at 15,454 cm^{-1} and 19,436 cm^{-1}, respectively [28, 29]

energy level diagram of Fig. 1a, whereas Ti^{2+}:$MgCl_2$ is located to the right of this crossing point, see the dashed vertical lines in Fig. 1a. This fact can account for the vastly different 15 K near-infrared luminescence spectra observed from 0.2% Ti^{2+}:NaCl on the one hand and 0.1% Ti^{2+}:$MgCl_2$ on the other hand; compare Fig. 3a and Fig. 3b. Excitation of 0.2% Ti^{2+}:NaCl around 15,454 cm^{-1} induces broad-band near-infrared $^3T_{2g}(t_{2g}e_g) \rightarrow {}^3T_{1g}(t_{2g}^2)$ luminescence extending from 6750 to almost 4000 cm^{-1} [28]. This is the reverse of the near-infrared absorption transition in Fig. 2a, and therefore it has a very similar band shape. In contrast, the 15 K near-infrared luminescence spectrum of 0.1% Ti^{2+}:$MgCl_2$ (Fig. 3b) is comprised of a series of sharp lines distributed over an energy range of about 1500 cm^{-1} and assigned to the t_{2g}^2 intra-configurational $^1T_{2g} \rightarrow {}^3T_{1g}$ luminescence transition [26]. The complicated line structure is due to the trigonal crystal field and spin-orbit splitting of the $^3T_{1g}(t_{2g}^2)$ ground state [29]. Thus 15 K near-infrared luminescence is spin-allowed in Ti^{2+}:NaCl and spin-forbidden in Ti^{2+}:$MgCl_2$, and this is also reflected in their 15 K lifetimes of 1.4 ms and 109 ms, respectively. Since these two states serve as energy storage reservoirs for near-infrared to visible upconversion in Ti^{2+}:NaCl and Ti^{2+}:$MgCl_2$, respectively, this has direct consequences on the relative upconversion efficiencies of these two materials (see below).

The 15 K upconversion luminescence spectra of the two Ti^{2+} doped systems are presented in Fig. 4. They were obtained after pulsed Nd^{3+}:YAG laser excitation into $^3T_{2g}(t_{2g}e_g)$ at 9399 cm^{-1} [30]. Broad luminescence bands centred at 12,800 cm^{-1} for Ti^{2+}:NaCl (Fig. 4a) and at 13,300 cm^{-1} for Ti^{2+}:$MgCl_2$ (Fig. 4b) are observed, and they are assigned to the $^3T_{1g}(t_{2g}e_g) \rightarrow {}^3T_{1g}(t_{2g}^2)$ transition in both cases. These luminescences, which are also observed after direct $^3T_{1g}(t_{2g}e_g)$ (HeNe laser) excitation at 15,803 cm^{-1}, only occur because there are large energy gaps of approximately 5000 cm^{-1} between $^3T_{1g}(t_{2g}e_g)$ and the next lower lying excited

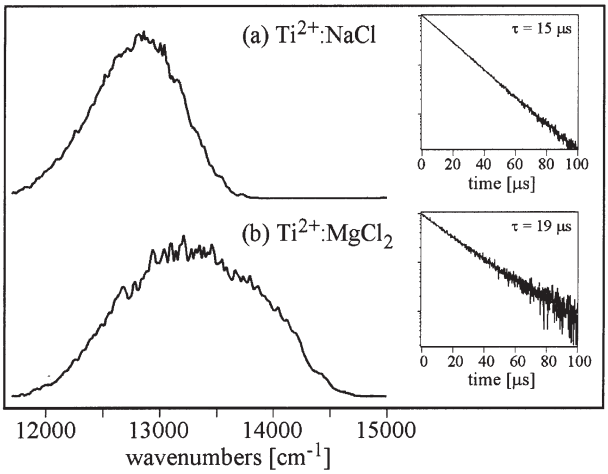

Fig. 4a,b 15 K $^3T_{1g}(t_{2g}e_g) \rightarrow {}^3T_{1g}(t_{2g}{}^2)$ upconversion luminescence spectra of: **a** 0.2% Ti^{2+}:NaCl; **b** 0.1% Ti^{2+}:$MgCl_2$ (axial) obtained after 10 ns pulsed excitation at 9,399 cm^{-1} [30]. The insets show the respective 15 K upconversion luminescence decays in semilogarithmic representation

states; see Fig. 2. Thus luminescence becomes competitive with nonradiative relaxation. Nevertheless, a substantial amount of $^3T_{1g}(t_{2g}e_g)$ depopulation occurs via multiphonon relaxation processes, leading to a shortening of the $^3T_{1g}(t_{2g}e_g)$ lifetimes [13, 28]. The 15 K $^3T_{1g}(t_{2g}e_g)$ lifetimes in 0.2% Ti^{2+}:NaCl and 0.1% Ti^{2+}:$MgCl_2$ are 15 and 19 μs, respectively; see the insets in Fig. 4. These transients were obtained after 10 ns pulsed excitation at 9399 cm^{-1} [30], and they exhibit an instantaneous decay of the $^3T_{1g}(t_{2g}e_g)$ population after the near-infrared excitation pulse. This shows that the whole upconversion process takes place within the 10 ns duration of the laser pulse, i.e. in these systems upconversion occurs via a sequence of radiative ground- and excited state absorption (GSA/ESA) steps. The upconversion relevant ESA transition for 9399 cm^{-1} excitation is a triplet-triplet transition in Ti^{2+}:NaCl and a singlet-singlet transition in Ti^{2+}:$MgCl_2$; see Fig. 1b [30]. This difference is due to the different spin multiplicities of the first metastable excited states and the relative strictness of the spin-selection rule in 3d systems.

Recent continuous-wave excitation experiments have shown that the 15 K upconversion efficiency of 0.1% Ti^{2+}:$MgCl_2$ exceeds that of 0.2% Ti^{2+}:NaCl by at least an order of magnitude [30], and this is because at 15 K energy storage in the first metastable excited state is roughly a factor of 80 more efficient in 0.1% Ti^{2+}:$MgCl_2$ than in 0.2% Ti^{2+}:NaCl. Thus the chemically induced crossover from weak-field Ti^{2+} with a $^3T_{2g}(t_{2g}e_g)$ to strong-field with a $^1T_{2g}(t_{2g}{}^2)$ first excited state, and the associated large increase in the first excited state lifetime has a huge effect on the Ti^{2+} upconversion efficiency.

3
Comparison of the Ni^{2+} Upconversion Luminescence Properties in Chloride and Bromide Host Lattices: Covalency and Crystal Field Effects

Figure 5 shows 15 K axial survey absorption spectra of (a) 5% Ni^{2+}:$CsCdCl_3$ and (b) 5% Ni^{2+}:$MgBr_2$ [31, 32]. In both systems the Ni^{2+} dopant ions are in trigonally distorted octahedral halide coordination [33, 34]. Figure 6a shows an energy level scheme for d^8 ions in octahedral coordination [24], and it can be used to assign the absorption bands in Fig. 5. In $MgBr_2$ all Ni^{2+} d-d absorption oscillator strengths are higher than in $CsCdCl_3$ by about a factor of 3. This is attributed to the closer energetic proximity of ungerade charge transfer states in the bromide from which the d-d intensity is stolen. The onset of LMCT absorptions is around 25,000 cm^{-1} in Ni^{2+} doped bromides and around 33,000 cm^{-1} in Ni^{2+} doped chlorides [35].

Apart from the different absorption intensities there are two other striking differences between the two absorption spectra in Fig. 5. Whereas in Ni^{2+}:$CsCdCl_3$ the $^3T_{1g}(^3F)$ and ^1E_g absorptions are energetically well separated from each other (Fig. 5a), this is not the case in Ni^{2+}:$MgBr_2$ (Fig. 5b). Instead, one single broad band with vibrational fine structure on its high energy side is observed. This phenomenon is well documented in the literature and occurs in Ni^{2+} systems whenever there is a strong interaction between spinors of $^3T_{1g}(^3F)$ and ^1E_g [36]. More important for our upconversion-oriented study is the following. In Ni^{2+}:$CsCdCl_3$ at 15 K the $^3A_{2g} \rightarrow {}^1A_{1g}$ absorption peak occurs at 19,029 cm^{-1} and is thus roughly 800 cm^{-1} *above* the $^3A_{2g} \rightarrow {}^1T_{2g}$ absorption band maximum; see Fig. 5a. In Ni^{2+}:$MgBr_2$ at 15 K, on the other hand, the $^1A_{1g}$ peak is at 17,355 cm^{-1} and thus about 900 cm^{-1} *below* the $^1T_{2g}$ maximum; see Fig. 5b. As illustrated in Fig. 6a, the $^1T_{2g}$ energy primarily depends on the crystal field strength 10Dq, whereas the $^1A_{1g}$ energy is essentially determined by the magnitude of the Racah

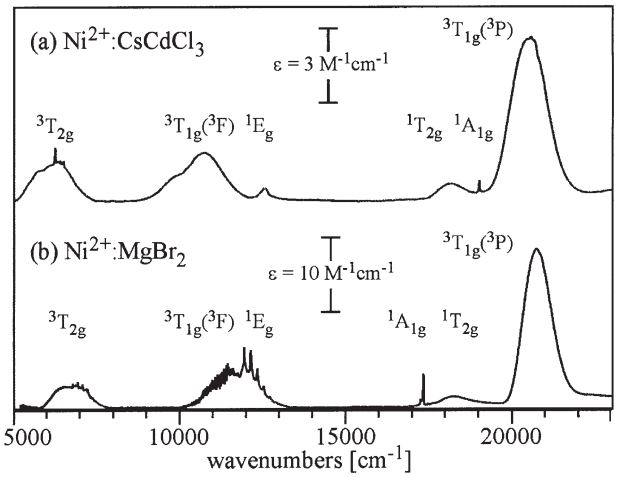

Fig. 5a,b 15 K axial survey d-d absorption spectra of: **a** 5% Ni^{2+}:$CsCdCl_3$; **b** 5% Ni^{2+}:$MgBr_2$ [31, 32]

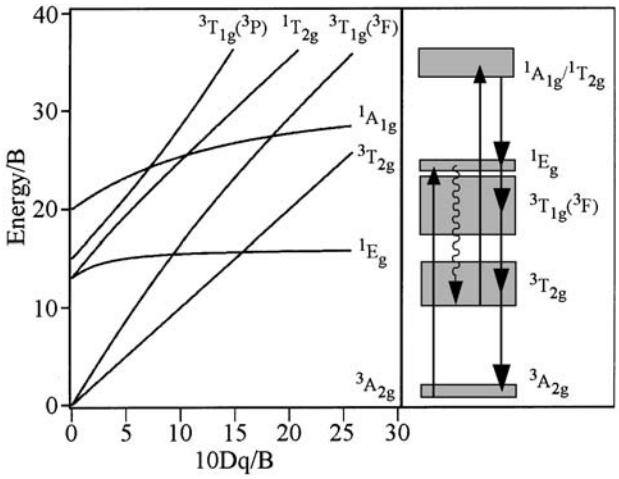

Fig. 6 **a** Energy level diagram for octahedrally coordinated d^8 ions [24]. **b** Schematic illustration of the upconversion mechanisms in Ni^{2+}:$CsCdCl_3$ and Ni^{2+}:$MgBr_2$. Solid upward arrows represent ground- and excited-state absorption transitions, the wavy arrow stands for nonradiative relaxation, and the solid downward arrows indicate luminescence transitions [31]

parameters. Crystal field parameters obtained from simple O_h crystal field calculations for Ni^{2+}:$CsCdCl_3$ and Ni^{2+}:$MgBr_2$ are given in Table 2. In going from Ni^{2+}:$CsCdCl_3$ to Ni^{2+}:$MgBr_2$ there is an 11% increase in 10Dq and a 10% decrease in the magnitude of B. The former is a manifestation of the smaller dopant site for Ni^{2+} in $MgBr_2$ compared to $CsCdCl_3$. The smaller B-value in the bromide reflects the more covalent nature of the Ni^{2+}-X^- interaction than in the chloride [37], i.e. it is a manifestation of the so-called nephelauxetic effect as first introduced by Jørgensen [38, 39]. The net result of these two effects is a reversed order of the $^1T_{2g}$ and $^1A_{1g}$ higher excited states.

Figure 7 shows 15 K upconversion luminescence spectra of (a) 0.1% Ni^{2+}:$CsCdCl_3$ and (b) 0.1% Ni^{2+}:$MgBr_2$. These spectra were obtained after continuous-wave laser excitation around 12,000 cm^{-1} [31, 32]. A broad and structureless luminescence band centred at about 16,300 cm^{-1} with a full width at half maximum of roughly 800 cm^{-1} is observed for the chloride, whereas the bromide spectrum is comprised of a series of sharp lines, the most prominent one being

Table 2 Approximate octahedral crystal field parameters (in cm^{-1}) for Ni^{2+}:$CsCdCl_3$ and Ni^{2+}:$MgBr_2$, respectively. These parameters were extracted from fits to experimental 15 K absorption energies (Fig. 5)

	Ni^{2+}:$CsCdCl_3$	$Ni^{2+}MgBr_2$
10Dq	6340	7060
B	800	720
C/B	3.93	4.04

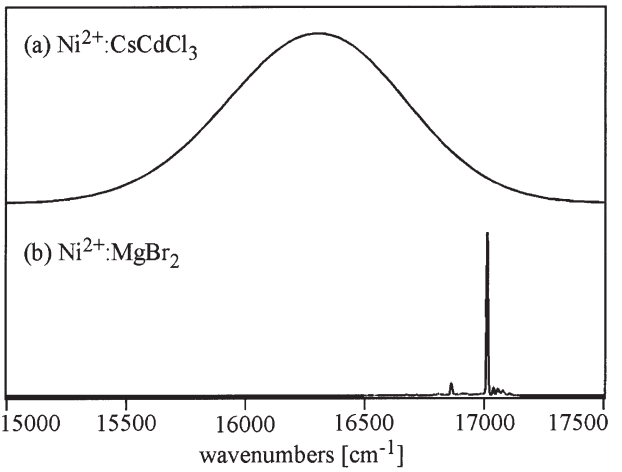

Fig. 7a,b The 15 K unpolarized upconversion luminescence spectra of: **a** 0.1% Ni^{2+}:$CsCdCl_3$; **b** 0.1% Ni^{2+}:$MgBr_2$. Excitation occurred at 12,344 and 11,940 cm^{-1}, respectively

located at 17,014 cm^{-1}. From the foregoing discussion, this vast difference in upconversion luminescence spectra is easily understood. In Ni^{2+}:$CsCdCl_3$ visible upconversion luminescence is due to $^1T_{2g} \rightarrow {}^3A_{2\,g}$ [31], and this is an electronic transition involving an electron promotion from a strongly antibonding e_g to a weakly antibonding t_{2g} orbital. Thus the $NiCl_6^{4-}$ unit undergoes a compression upon de-excitation from $^1T_{2g}$ to $^3A_{2g}$, and this is the reason for the broadness of the chloride emission. In Ni^{2+}:$MgBr_2$, by contrast, $^1A_{1g}$ lies energetically lower than $^1T_{2g}$ and upconversion luminescence is due to $^1A_{1g} \rightarrow {}^3A_{2g}$, a so-called spin-flip transition within the $t_{2g}{}^6e_g{}^2$ orbital configuration. As such it yields a luminescence spectrum consisting of sharp lines. The multitude of lines in Fig. 7b is due to the occurrence of several vibronic origins which enable the parity-forbidden $^1A_{1g} \rightarrow {}^3A_{2g}$ transition [32]. Note that luminescence from the $^1T_{2g}$ and $^1A_{1g}$ excited states is only observed because these states are energetically separated from their next lower lying excited states by more than 4,000 cm^{-1}, see Fig. 5. This makes radiative emission competitive with nonradiative relaxation processes. Nonetheless, the latter account for at least 50% of the total depopulation of these emissive states even at 15 K [32, 40], leading to excited state lifetimes of only around 50–85 μs.

Figure 8d shows a near-infrared excitation spectrum of 15 K visible $^1A_{1g} \rightarrow {}^3A_{2g}$ upconversion luminescence in 0.1% Ni^{2+}:$MgBr_2$. Its rather unusual band shape is explained as follows. Excitation around 11,500–13,000 cm^{-1} occurs into the high-energy side of the $Ni^{2+3}A_{2g} \rightarrow {}^3T_{1g}({}^3F)/{}^1E_g$ ground-state absorption band; see Fig. 5b. Figure 8a shows this spectral region in more detail. The physical origin of the sharp vibrational fine structure features has been mentioned above. Figure 8b shows a 15 K $^3T_{2g} \rightarrow {}^1A_{1g}/{}^1T_{2g}$ excited state excitation (ESE) spectrum of 0.1% Ni^{2+}:$MgBr_2$. This spectrum was obtained as follows. Intense laser excitation (200 mW) at 11,000 cm^{-1} was used to produce a high steady state population in the $Ni^{2+3}T_{2g}$ first metastable excited state, but without inducing any upconversion

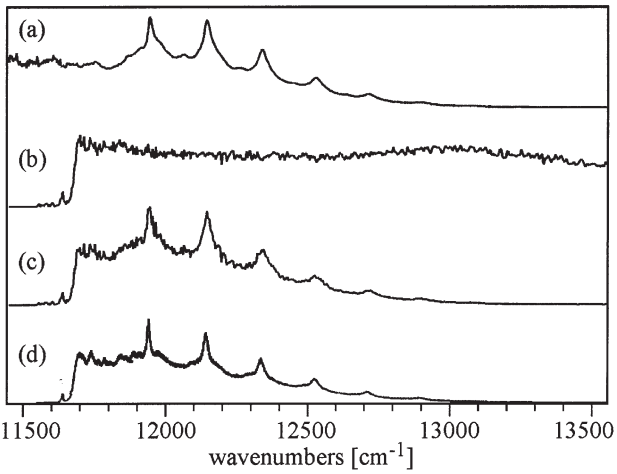

Fig. 8 **a** High-energy side of the 15 K $^3A_{2g} \rightarrow {}^3T_{1g}(^3F)/{}^1E_g$ (axial) ground state absorption (GSA) spectrum of 5% Ni^{2+}:$MgBr_2$. **b** 15 K $^3T_{2g} \rightarrow {}^1A_{1g}/{}^1T_{2g}$ (axial) excited state excitation (ESE) spectrum of 0.1% Ni^{2+}:$MgBr_2$. In this experiment one (intense) Ti^{3+}:sapphire laser was used to provide a high $^3T_{2g}$ population by pumping into the $^3T_{1g}(^3F)$ absorption at 11,000 cm^{-1}. $^1A_{1g} \rightarrow {}^3A_{2g}$ luminescence at 17,014 cm^{-1} was monitored as second (weak) probe laser was scanned from 11,500 to 13,500 cm^{-1}. **c** Calculated product of a and b. **d** Experimental 15 K (axial) excitation spectrum of $Ni^{2+1}A_{1g} \rightarrow {}^3A_{2g}$ upconversion luminescence, monitored at 17,014 cm^{-1} , in 0.1% Ni^{2+}:$MgBr_2$ [32]

for energetic reasons. At 15 K, energy storage in $^3T_{2g}$ is possible due to its lifetime of around 4 ms. A weak probe laser (1 mW) was scanned from 11,450 to 13,550 cm^{-1}, while the intensity of 15 K $Ni^{2+1}A_{1g} \rightarrow {}^3A_{2g}$ upconversion luminescence at 17,014 cm^{-1} was monitored. This second laser promotes $^3T_{2g}$-excited Ni^{2+} ions to $^1A_{1g}$ and $^1T_{2g}$, and by monitoring the $^1A_{1g} \rightarrow {}^3A_{2g}$ luminescence intensity one essentially obtains the $^3T_{2g} \rightarrow {}^1A_{1g}/{}^1T_{2g}$ excited state absorption spectrum. It is similar to previously reported Ni^{2+} ESE spectra [41]. Figure 8c is the calculated product of the GSA and ESE spectra from Fig. 8a,b. Its agreement with the experimental 15 K upconversion excitation spectrum in Fig. 8d is very good, and we conclude that upconversion in Ni^{2+}:$MgBr_2$ occurs as schematically illustrated in Fig. 6b. $^3A_{2g} \rightarrow {}^3T_{1g}(^3F)/{}^1E_g$ GSA (solid upward arrow) is followed by fast nonradiative relaxation to $^3T_{2\,g}$ (wavy downward arrow). From there, $^3T_{2g} \rightarrow {}^1A_{1g}/{}^1T_{2g}$ excited state absorption occurs (second solid upward arrow), and this is followed by emission from $^1A_{1g}$ to all energetically lower lying states (solid downward arrows) [32]. Analogous experiments have been performed with 0.1% Ni^{2+}:$CsCdCl_3$, and they reveal an identical upconversion mechanism for this system [41]. Thus the main difference between the two upconversion systems considered here lies in the identity of the emitting state.

4 Summary and Conclusions

At cryogenic temperatures Ti^{2+} doped chloride hosts as well as Ni^{2+} doped chlorides and bromides are capable of exhibiting near-infrared to visible upconversion phenomena. The change from NaCl to $MgCl_2$ as a host lattice for Ti^{2+} leads to a crossover in the first metastable excited state from $^3T_{2g}(t_{2g}e_g)$ to $^1T_{2g}(t_{2g}^2)$. This is due to a 12% increase in 10Dq in Ti^{2+}:$MgCl_2$. The 15 K $^1T_{2g}(t_{2g}^2)$ lifetime in 0.1% Ti^{2+}:$MgCl_2$ is a factor of 80 longer than the 15 K $^3T_{2g}(t_{2g}e_g)$ lifetime in 0.2% Ti^{2+}:NaCl, i.e. energy storage is 80 times more efficient in the former. As a consequence, upconversion at 15 K is more than an order of magnitude more efficient in 0.1% Ti^{2+}:$MgCl_2$ than in 0.2% Ti^{2+}:NaCl.

The change from $CsCdCl_3$ to $MgBr_2$ as a host for Ni^{2+} leads to a crossover in a higher excited emitting state of Ni^{2+}. In Ni^{2+}:$CsCdCl_3$ the upconverted energy is emitted from $^1T_{2g}$, whereas in Ni^{2+}:$MgBr_2$ upconversion luminescence is emitted from $^1A_{1g}$. This crossover is due to an 11% increase in 10Dq and a simultaneous 10% decrease in Racah B when going from $CsCdCl_3$ to $MgBr_2$. It manifests itself in a change from broad-band visible upconversion luminescence in the chloride to sharp-line luminescence in the bromide.

These two Ti^{2+} and Ni^{2+} case studies demonstrate the broader principle of environmental control of transition metal upconversion properties using chemical means to take advantage of the accessibility of their spectroscopically active d-orbitals [42, 43].

Acknowledgment This work was financially supported by the Swiss NSF.

5 References

1. Hager RW, Crosby GA (1975) J Am Chem Soc 97:7031
2. Gliemann G, Yersin H (1985) Struct Bond 62:87
3. Flint CD, Greenough P (1972) Chem Phys Lett 16:369
4. Güdel HU, Pollnau M (2000) J Alloy Compd 303/304:307
5. Reber C, Güdel HU (1988) J Lumin 42:1
6. Cockroft NJ, Jones GD, Nguyen DC (1992) Phys Rev B 45:5187
7. Chivian JS, Case WE, Eden DD (1979) Appl Phys Lett 35:124
8. Kück S (2001) Appl Phys B 72:515
9. Buñuel MA, Cases R (1999) J Chem Phys 110:9695
10. Flint CD, Paulusz AG (1981) Mol Phys 44:925
11. Flint CD, Paulusz AG (1981) Mol Phys 43:321
12. Flint CD, Paulusz AG (1980) Mol Phys 41:907
13. Jacobsen SM, Güdel HU (1989) J Lumin 43:125
14. Kasha M (1950) Discuss Faraday Soc 9:14
15. Gamelin DR, Güdel HU (2000) Acc Chem Res 33:235
16. Wright JC (1976) Top Appl Phys 15:239
17. Auzel FE (1960) C R Acad Sci Paris 262:1016, 263:819
18. Blasse G, Grabmaier BC (1994) Luminescent materials, 1st edn. Springer, Berlin Heidelberg New York
19. Macfarlane RM, Tong F, Silversmith AJ, Lenth W (1988) Appl Phys Lett 52:1300
20. Joubert MF (1999) Opt Mater 11:181

21. Chivian JS, Chase WE, Eden DD (1979) Appl Phys Lett 35:124
22. Downing E, Hesselink L, Ralston J, Macfarlane R (1996) Science 273:1185
23. Hüfner S (1978) Optical spectra of transparent rare earth compounds, 1st edn. Academic Press, New York San Francisco London
24. Sugano S, Tanabe Y, Kamimura H (1970) Multiplets of transition metal ions in crystals. 1st edn. Academic Press, New York London
25. Brown DH, Hunter A, Smith WE (1979) J Chem Soc Dalton Trans 1:79
26. Jacobsen SM, Güdel HU, Daul CA (1988) J Am Chem Soc 110:7610
27. Shannon RD (1976) Acta Cryst A 104:7624
28. Wenger OS, Güdel HU (2001) J Phys Chem B 105:4187
29. Jacobsen SM, Smith WE, Reber C, Güdel HU (1986) J Chem Phys 84:5205
30. Wenger OS, Güdel HU (2001) Inorg Chem 40:5747
31. Wenger OS, Gamelin DR, Güdel HU (2000) J Am Chem Soc 122:7408
32. Wenger OS, Bénard S, Güdel HU (2002) Inorg Chem 41:5968
33. Chang JR, McPherson GL, Atwood JL (1975) Inorg Chem 14:3079
34. Anderson A, Lo YW (1981) Spec Lett 14:603
35. Coutts AG, Day P (1968) Phys Status Solidi B 88:767
36. Bussière G, Reber C (1998) J Am Chem Soc 120:6306
37. Jørgensen CK (1962) Absorption spectra and chemical bonding in complexes. Pergamon, Oxford
38. Jørgensen CK (1966) Struct Bond 1:3
39. Schäffer CE, Jørgensen CK (1958) J Inorg Nuclear Chem 8:143
40. May PS, Güdel HU (1991) J Chem Phys 95:6343
41. Wenger OS, Güdel HU (2001) Inorg Chem 40:157
42. Wenger OS, Valiente R, Güdel HU (2001) Phys Rev B 64:235116
43. Wenger OS, Wermuth M, Güdel HU (2002) J Alloy Compd 341:342

Structure and Bonding, Vol. 106 (2004): 71–79
DOI 10.1007/b11306

Electronic Structures and Reduction Potentials of Cu(II) Complexes of [N,N′-Alkyl-bis(ethyl-2-amino-1-cyclopentenecarbothioate)] (Alkyl=Ethyl, Propyl, and Butyl)

Ricardo R. Contreras[1] · Trino Suárez[1] · Marisela Reyes[1] · Fernándo Bellandi[1] · Pedro Cancines[1] · Jenny Moreno[1] · Mona Shahgholi[2] · Angel J. Di Bilio[2] · Harry B. Gray[2] · Bernardo Fontal[1]

[1] Universidad de Los Andes, Laboratorio de Organometálicos, Departamento de Química, Facultad de Ciencias, La Hechicera, 5101 Mérida, 9 Venezuela
[2] Beckman Institute, Pasadena CA 91125 USA
E-mail: hbgray@caltech.edu

Abstract Copper(II) complexes of *N,N'*-alkyl-bis(ethyl-2-amino-1-cyclopentenecarbodithioate) [alkyl=ethyl (L2), propyl (L3), and butyl(L4)] ligands have been synthesized and characterized. Analytical data for all three complexes show 1:1 copper-ligand stoichiometry. Well-resolved EPR spectra were recorded in toluene, benzene, and methylene chloride solutions at room temperature and in glassy toluene or toluene-methylene chloride mixtures in the range 20–150 K. The superhyperfine pattern unambiguously demonstrates coordination of two nitrogen atoms to copper; and the spin-Hamiltonian parameters [CuL2, $g_{\|}$=2.115, $A_{\|}$=187×10^{-4} cm^{-1}; CuL3, $g_{\|}$=2.128, $A_{\|}$=165×10^{-4} cm^{-1}; CuL4, $g_{\|}$=2.138, $A_{\|}$=147×10^{-4} cm^{-1}] are as expected for a CuN_2S_2 coordination core. Quasi-reversible electrochemical behavior was observed in methylene chloride: the Cu(II)/Cu(I) reduction potentials increase from –1.17 V (E° vs $Ag/AgNO_3$) for CuL2 to –0.74 V for CuL4, indicating greater stabilization of Cu(I) in CuL4. Taken together, these data demonstrate that lengthening the *N,N'*-alkyl chain distorts the planar CuN_2S_2 core (CuL2) toward a flattened tetrahedral geometry (CuL4).

Keywords Copper complexes · Reduction potentials · Electronic structures · EPR spectra

1 Introduction

In a seminal paper published in 1961, James and Williams reported the dependence of Cu(II)/Cu(I) reduction potentials on ligand type and coordination geometry [1]. These authors showed that nitrogen π-acceptors and sulfur donors generally raise the potential, thereby stabilizing Cu(I), whereas anionic ligands act in the opposite direction. Importantly, bulky ligands that lead to a distortion of the coordination sphere often increase the potential, especially in cases where the geometry is forced toward tetrahedral. Indeed, several workers have shown that there is a correlation between the positions of the lowest d-d states and the reduction potentials of Cu(II) complexes [2].

The connection of such correlations with C. K. Jørgensen's many interests in coordination chemistry is that he was among the first to discuss the *d-d* band positions in the electronic spectra of Cu(II) complexes in terms of their solution structures [3]. In this tribute to him, we report an extension of research on certain Cu(II)N_2S_2 complexes [4–7] to include those with *N,N′*-alkyl-bis(ethyl-2-amino-1-cyclopentenecarbodithioate) [alkyl=ethyl (L2), propyl (L3), and butyl (L4)] ligands. We believe that Cu(II) complexes in the series L2–L4 would have been of interest to Jørgensen, as their *d-d* spectra and reduction potentials can be interpreted readily in terms of systematic variations in coordination geometry.

2 Experimental

Reagents and solvents (Aldrich, Merck, Baker and Eastman) were used directly. Carbon disulfide was purified as described previously [8]. Ligands ethyl-*N,N′*-alkyl-bis(2amino1cyclopentencarbodithioate [alkyl=ethyl (L2); propyl (L3); butyl (L4)] and their copper(II) complexes were prepared by literature procedures [9, 10].

Precaution: all synthetic procedures should be carried out in a fume hood.

2.1 Physical Measurements

UV-visible absorption spectra were obtained with a LAMBDA 3 Perkin-Elmer spectrophotometer. Vibrational spectra (5000–400 cm^{-1}, KBr pellets) were recorded with a Fourier Transform Perkin-Elmer 1725X spectrophotometer. Room temperature ^1H NMR spectra (DMSO, TMS internal standard) were obtained with a Bruker Avance DRX 400-MHz spectrometer. Electron spin resonance spectra were measured with a Bruker EMX EPR spectrometer equipped with an Oxford (ESR 900) helium cryostat. Mass spectra were obtained with a Hewlett-Packard gas chromatograph-mass spectrometer, GC-MS Model 5988A, using chemical ionization. Electrochemical experiments were carried out with a BAS100B/W system. Measurements were conducted employing an H cell, a vitreous carbon working electrode, and an $Ag/AgNO_3$ reference electrode;

methylene chloride was used as solvent and tetrabutylammonium tetrafluoroborate (TBAFB) as supporting electrolyte. Conductivity measurements were made with a Schott Gerate C6857 conductance bridge.

2.2
Synthesis of Carboxydithioic Acid from Cyclopentanone

To 25 ml (0.3 mol) of cyclopentanone dissolved in 100 ml of ammonium hydroxide (29%) were added 28 ml (0.5 mol) of carbon disulfide and the mixture stirred for 6 h at 0 °C. The orange ammonium salt of the carboxydithioic acid was filtered and redissolved in water. Yellow carboxydithioic acid precipitates on acidification to pH 4 with 2 mol/l HCl. Yield: 30.8 g (65%); m.p.: 97–98 °C. **IR** (KBr pellet, cm^{-1}): ν_a(S-H), 2487w; ν_a(C=O), 1614s; ν_a(C=S), 1354m; ν_a(CSSH), 917s. **MS** (EI): M^+ m/z (%), $C_6H_9NS_2$ 160.2(7).

2.3
Synthesis of the Ethyl Ester

To 6.8 g (0.04 mol) of the carboxydithioic acid dissolved in 50 ml of 1 mol/l sodium hydroxide were added 2.6 ml (0.02 mol) of dimethylsulfate with stirring for 20 min at 5 °C. A golden yellow solid ester was filtered and recrystallized from dioxane. Yield: 6.6 g (96%), m.p.: 35–36 °C. **IR** (KBr pellet, cm^{-1}): ν_a(C=O), 1660s; ν_a(C=S), 1343m; ν_a(S-CH_2-), 1292m; ν_a(CSS-), 921w; δ(S-CH_2-), 481w. **MS** (EI): M^+ m/z (%), $C_8H_{14}NS_2$ 174.02(11).

2.4
Synthesis of the Ligands (L2, L3, L4)

Condensation of the methyl ester (0.02 mol) dissolved in 15 ml of methanol was carried out with the appropriate diamine (0.01 mol; 1,2 diaminoethane for L2; 1,3 diaminopropane for L3and 1,4 diaminobutane for L4) with stirring for 72 h at room temperature. The compounds (yellow solids) were dried under vacuum and re-crystallized from methanol. L2, yield: 1.44 g (36%); m.p.: 152–153 °C; L3, yield: 0.75 g (18%); m.p.: 96–99 °C; L4, yield: 2.06 g (48%); m.p.: 128–130 °C. ^{1}H NMR, 400 MHz, DMSO-d_6 (s=singlet, d=doublet, t=triplet, c=quartet, q=quintet, m=multiplet, br=broad): L2: δ 8.20 (br s, 2H), 3.59 (m, 4H), 3.07(c, 4H, J=7.54 Hz), 2.72 (t, 4H, J=7.50 Hz), 2.60 (t, 4H, J=7.1), 1.71 (q, 4H, J=7.46 Hz), 1.17 (t, 6 H, J=7.16). L3: δ 12.40 (br s, 2H,), 3.50 (c, 4H, J=6.38 Hz), 3.20 (c, 4H, J=7.41 Hz), 2.77 (t, 4H, J=7.31 Hz), 2.69 (t, 4H, J=7.65 Hz), 2.00 (q, 2H, J=6,49 Hz), 1.84 (q, 4H, J=7.46 Hz), 1.30 (t, 6H, J=7.39 Hz). L4: δ 8.30 (br s, 2H), 3.80 (c, 4H, J=7.09 Hz), 3.06 (c, 4H, J=7.65 Hz), 2.74 (t, 4H, J=7.5 Hz), 2.62 (t, 4H, J=7.07 Hz), 1.75 (q, 4H, J=7.56 Hz), 1.16 (t, 4H, J=7.1 Hz), 1.09 (t, 6H, J=7.06 Hz). **MS** (EI): M^+ m/z (%), L2, $C_{18}H_{26}N_2S_4$ 400(6.0); L3, $C_{19}H_{28}N_2S_4$ 414(17.0); L4, $C_{20}H_{30}N_2S_4$ 428(8.0).

2.5
Synthesis of Copper(II) Complexes

A suspension of 0.22 g (0.001 mol) of copper acetate in 15 ml of methanol was added dropwise with stirring to a solution of the appropriate ligand (0.001 mol) in 20 ml of methanol. Colored solids formed after 1 h reflux were dissolved in dichloromethane, filtered in a glass fiber filter and vacuum dried. The complexes were precipitated from solution with a minimum amount of methanol and suction collected using a millipore (0.8 UM) filter, vacuum dried and recrystallized from methanol. The complexes are not thermally stable above 150 °C. CuL2, green, yield 0.37 g (79%); CuL3, brown, yield 0.31 g (65%); CuL4, dark brown, yield 0.44 g (89%). **MS** (CI): M^+ m/*z* (%), CuL2: $CuC_{18}H_{26}N_2S_4$ 461.2(3); CuL3: $CuC_{19}H_{28}N_2S_4$ 475.2(4) and CuL4: $CuC_{20}H_{30}N_2S_4$ 489.3(3).

3
Results and Discussion

3.1
Mass Spectra

The Cu(II) complexes are neutral, as evidenced by their low Λ_M (Ω^{-1} cm^2 mol^{-1}) [CuL2, 1.2; CuL3, 0.8; CuL4, 1.3] values in nitrobenzene solution. Chemical ionization mass spectra show typical fragmentation patterns, indicating neutral losses of [C_3H_5S] and 2[C_3H_5S] from the molecular species [11]. Mass scans up to 2000 m/z were carried out to check for cluster impurities. The masses of the copper complexes and their respective prominent fragment ions are set out in Table 1.

Table 1 Mass spectral data

Complexes	M^+ (m/z)	M^+-[C_2H_5S] (m/z)	M^+-2[C_2H_5S] (m/z)
CuL2	461.2	400.5	339.4
CuL3	475.2	414.2	353.7
CuL4	489.3	428.5	367.3

3.2
Infrared Spectra

The bands in the IR spectra of the ligands and metal complexes are listed in Table 2. Compounds L2 and L3show a strong broad band around 1588 cm^{-1} that is assigned to ν_a(C=C)+ν_a(C=N) stretching and a weak broad band centered at 3500 cm^{-1} that corresponds to ν(N-H) in secondary amines [12]; the positions of these bands indicate extensive electron delocalization from the cyclopentene to the amino and *S-cis* thiocarboxylate groups. Metal imine complexation with L2 and L3 is supported by the disappearance of ν(N-H) and the red shift of the

Table 2 FTIR spectral data

Vibration	L2	CuL2	L3	CuL3	L4	CuL4
νN-H	3452 (m, br)	–	3502 (m, br)	–	3532 (m, br)	–
ν_a(C=C)+ν_a(C=N)	1586 (s)	1581 (s)	1589 (s)	1584 (s)	1589 (s)	1573 (s)
ν_s (C=C)	1479 (m)	1462 (s)	1484 (m)	1453 (s)	1480 (s)	1451 (s)
ν_s(C=N)+ν_a(C=S)	1313 (w)	1310 (s)	1322 (m)	1309 (w)	1336 (s)	1339 (m)
ν_a(S-CH_2-)	1270 (s)	1274 (s)	1274 (m)	1279 (m)	1271 (s)	1256 (m)
ρ-CH_2	948 (m)	949 (w)	949 (m)	947 (m)	951 (m)	947 (w)
ν_a(CSS-)	919 (m)	911 (m)	915 (m)	906 (m)	911 (m)	908 (s)
ν_s(CSS-)	757 (m)	788 (w)	774 (w)	765 (w)	761 (w)	767 (w)
ν_a(M-N), B_2	–	507 (w)	–	525 (w)	–	538 (w)
ν_s(M-N), A_1	–	420 (w)	–	424 (w)	–	436 (w)

1588 cm^{-1} band, due to the reduction in C=N character, but maintaining the C=C bond. The ν_a(C-S) band splitting and the blue shift of the ν_s(CS-S) band in the CSS-R moiety, compared with the free ligand, indicate a monodentate dithio group, similar to dithiocarbamate complexes reported by Nag [4]. Assuming C_{2v} core coordination, the three Cu(II)N_2 bands are: B_2,ν_a(M(II)N) stretching near 520 cm^{-1}; A_1, ν_a(Cu(II)N) stretching near 490 cm^{-1}, similar to values reported for Cu(II)N [4, 5]; and A_1, δ(Cu(II)N) bending, appearing in the far infrared, along with three Cu(II)S_2 bands [12].

3.3 EPR Spectra

Well-resolved EPR spectra were recorded at room temperature in toluene, benzene, and methylene chloride solution. The isotropic EPR spectrum of CuL2 in methylene chloride is shown in Fig. 1 (inset). Note that each of the four ^{63}Cu (I=3/2, 69.2% abundance)/^{65}Cu (I=3/2, 30.8% abundance) hyperfine lines is split into five components (this splitting, however, is not obvious for the broad lowest-field hyperfine line). This superhyperfine structure in the EPR spectrum is ascribable to interaction of the Cu(II) unpaired electron with two nearly equivalent ^{14}N (I=1, 98% abundance) donors. The EPR spectrum unambiguously demonstrates coordination of two nitrogen atoms to copper. Well-resolved EPR spectra in glassy toluene and toluene-methylene chloride mixtures were recorded in the range 20–150 K (Fig. 1).

The spin-Hamiltonian parameters (Table 3) are within the range expected for a CuN_2S_2 coordination core [13]. The increase in $g_{\|}$ and concomitant decrease in $A_{\|}$ on going from CuL2 to CuL4 suggests increasing distortion from CuN_2S_2 planarity in the order CuL3<CuL4 [14].

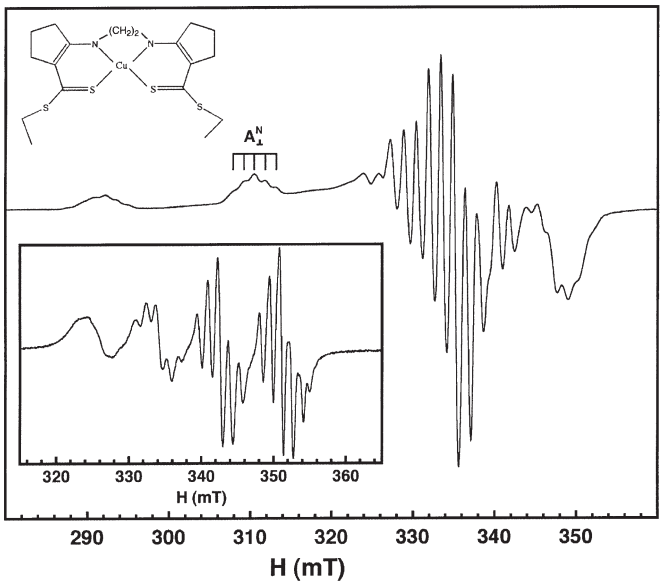

Fig. 1 EPR spectrum of CuL2 in glassy toluene at 20 K (*inset*, isotropic spectrum in toluene at room temperature)

Table 3 Spin-Hamiltonian parameters

Complex	g_{iso}	$A_{iso}(^{63}Cu)$	$A_{iso}(^{65}Cu)$	$A_{iso}(N)$	$g_{\parallel}$	$A_{\parallel}(^{63}Cu)$
CuL2	2.060	81.0	86.0	13.0	2.115	187
CuL3	2.064	66.5	72.0	11.5	2.128	165
CuL4	2.068	59.0	64.0	10.0	2.138	147

Isotropic EPR spectra were measured at 22 °C.
EPR spectra inglassy toluene solutions were measured at 20 K.
The hyperfine coupling constants (in 10^{-4} cm^{-1} units) and *g* values were estimated by simulations using WINEPR *Simfonia* (Version 1.25, Bruker Analytische Messtechnik GmbH).

3.4 Electronic Absorption Spectra

Values of absorption maxima in the UV-visible spectra of the ligands and their copper complexes are set out in Table 4. Electronic absorptions of the ligands were assigned by reference to energies of molecular orbitals obtained from a calculation using the *PC SPARTAN* Plus program [15]. Ligand localized electronic transitions are as follows: C=C $\pi \rightarrow \pi^*$ (37 kK); S-CH_2CH_3 $n \rightarrow \sigma^*$ (31 kK); C=N $\pi \rightarrow \pi^*$ (26 kK); and C=S $\pi \rightarrow \pi^*$ (24 kK). Bands attributable to these transitions are red shifted from their normal positions [16], due to strong charge delocalization among the cyclopentene double bond, the nitrogen group, and the carbodithioate group. In addition to charge-transfer absorptions, broad bands attributable to *d-d* transitions

Table 4 Electronic spectra

Ligands[a]	E, kK (ε ($M^{-1}cm^{-1}$))
L2	37.87 (9,100), 31.35 (7,300), 26.32 (9,900), 24.63 (12,200)
L3	31.35 (13,800), 26.32 (19,900), 24.69 (18,000)
L4	31.66 (15,700), 26.32 (24,400), 24.45 (18,400)
Complexes[b]	
CuL2	45.45(13,500), 31.84(15,600), 26.47(11,700), 24.87(4,030), 14.50(300), 12.41(76)
CuL3	44.83(10,100), 34.71(12,600), 31.20(13,700) 24,57(2,980), 21.19(1,660), 10.7(50)
CuL4	45,82(18,800), 31.85(11,600), 26.74(12,100), 24.39(1,990), 10.5(89)

[a] 1×10^{-3} mol/l CH_2Cl_2 solutions.
[b] 1×10^{-3} to 1×10^{-4} mol/l 1:1 DMSO-CH_2Cl_2 solutions.

Table 5 Calculated bond angles (degrees)

L	CuSS′	CuNN′	CuSN	CuS′N′	CuN′S	CuNS′
2	84.17	88.30	145.27	137.96	86.34	76.80
3	86.98	91.09	173.30	165.83	91.56	88.73
4	94.69	94.80	140.48	141.40	95.05	100.95

are observed in the near IR region: CuL2, 12.41 kK; CuL3, 10.7 kK; and CuL4, 10.5 kK (the corresponding *d-d* bands in the spectra of planar [*N,N′*-ethylene-bis(methyl-2-amino-1-cyclopentenedithiocarboxylate)]Cu(II) complexes are above 12 kK [7]). The red-shifted absorptions in the CuL3 and CuL4 spectra strongly suggest that the core CuN_2S_2 structures of these complexes are distorted toward a flattened tetrahedral geometry [17–20], consistent with the copper-ligand angles obtained from computations (Table 5, Fig. 2) [15].

3.5 Reduction Potentials

Cyclic voltammetry of the Cu(II) complexes shows that the $[Cu^{II}L]^{2+}\rightarrow[Cu^{I}L]^{+}$ reduction potential is in the –1.17 to –0.74 V range (Table 6). Peak current ratios

Table 6 Reduction potentials

Complex	E_{ox}, V	E_{red}, V	$E_{1/2}$, V
CuL2	–	–1.17	–
CuL3	–0.75	–0.86	–0.81
CuL4	–0.61	–0.74	–0.68

Potentials are vs $Ag/AgNO_3$ (range +1.3 to –1.2 V; scan rate of 100 mV s^{-1}).
Measurements were made in 0.1 mol/l TBAFB/CH_2Cl_2 solutions (1×10^{-4} mol/l complex).

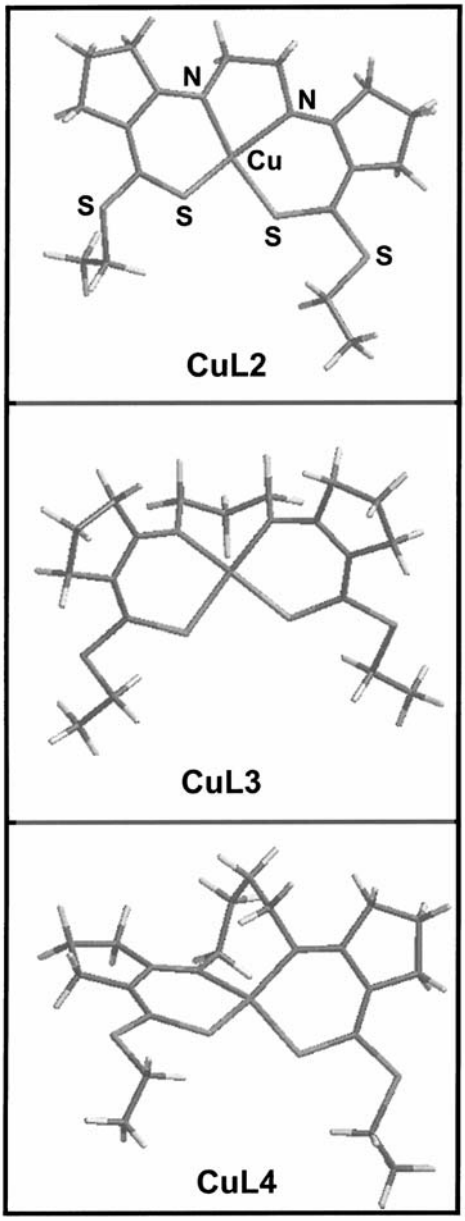

Fig. 2 Structures of the copper(II) complexes

(i_{pc}/i_{pa}) for 500 to 50 mV s^{-1} scan rates and peak to peak separations indicate a quasi-reversible electrochemical process [21]. The reduction potential increases with addition of methylene groups in the *N*,*N*'-alkyl chain (–1.17 V for CuL2 to –0.74 V for CuL4). In the planar core coordination of CuL2, Cu(II) is stabilized, while in a flattened tetrahedral geometry (L3and L4), Cu(II) is destabilized. Cu(II)/Cu(I) potentials also are affected by the electronic nature of the donor atoms: nitrogen donor interactions stabilize Cu(II), whereas sulfur ligation stabilizes Cu(I) [22]. In the blue copper proteins, which contain distorted trigonal CuN_2S complexes, Cu(II)/Cu(I) potentials are all positive (>0.2 V vs NHE) [2].

Acknowledgements This work was supported by CDCHT-ULA (C-1108–01-A), the NSF, NIH, and the Arnold and Mabel Beckman Foundation.

4 References

1. James BR, Williams RJP (1961) J Chem Soc 2007
2. Gray HB, Malmström BG, Williams RJP (2000) JBIC 5:551
3. Jørgensen CK (1971) Modern aspects of ligand field theory. North-Holland Publishing, Amsterdam
4. Nag K, Joardar DS (1975) Inorg Chim Acta 14:133
5. Nag K, Joardar DS (1976) Can J Chem 54:2827
6. Martin EM, Bereman RD (1991) Inorg Chim Acta 188:221
7. Martin EM, Bereman RD (1991) Inorg Chim Acta 188:233
8. Gordon A, Ford R (1972) The chemist companion. Wiley, New York
9. Bordás B, Sohár P, Matolcsy G, Berencsi P (1972) J Org Chem 37:1727
10. Mondal N, Mitra S, Gramilich V, Ozra Ghodsi S, Abdul Malik KM (2001) Polyhedron 20:135
11. Mondal SK, Joardar DS, Nag K (1978) Inorg Chem 17:191
12. Nakamoto K (1997) Infrared and Raman spectra of inorganic coordination compounds. Wiley-Interscience Publication, New York
13. Bencini A, Gatteschi D (1982) Transition Met Chem 8:97
14. Yokoi H, Addison AW (1977) J Am Chem Soc 16:1341
15. SPARTAN (2000) Wavefunction, Irvine, California
16. Silverstein RM, Bassler GC, Morrill TC (1998) Spectrophotometric identification of organic compounds. Wiley, New York
17. Raper ES (1994) Coord Chem Rev 129:91
18. Raper ES (1997) Coord Chem Rev 165:475
19. Mandal S, Das G, Singh R, Shukla R, Bharadwaj PK (1997) Coord Chem Rev 160:191
20. Drago RS (1965) Reinhold, New York
21. Gosser DK (1993) Cyclic voltammetry. VCH Publishers, New York
22. Ambundo EA, Deydier MV, Grall AJ, Aguera-Vega N, Dressel LT, Cooper TH, Heeg MJ, Ochrymowycz LA, Rorabacher DB (1999) Inorg Chem 38:4233

Structure and Bonding, Vol. 106 (2004): 81–96
DOI 10.1007/b11307

Fine Tuning the Electronic Properties of $[M(bpy)_3]^{2+}$ Complexes by Chemical Pressure ($M=Fe^{2+}$, Ru^{2+}, Co^{2+}, bpy=2,2′-Bipyridine)

Andreas Hauser · Nahid Amstutz · Sandra Delahaye · Asmaâ Sadki · Sabine Schenker · Regula Sieber · Mohamed Zerara

Université de Genève, Bâtiment de Science II, Département de chimie physique, Quai Ernest Ansermet, 301211 Genève, Switzerland
E-mail: andreas.hauser@chiphy.unige.ch

Abstract The optical and photophysical properties of three classic transition metal complexes, namely $[Fe(bpy)_3]^{2+}$, $[Ru(bpy)_3]^{2+}$ and $[Co(bpy)_3]^{2+}$, can be fine-tuned by doping them into a variety of inert host lattices. The effects of the guest-host interactions are discussed in terms of a chemical pressure. In this chapter we show how this chemical pressure can accelerate the high-spin→low-spin relaxation in the iron complex by more than three orders of magnitude, how it can increase the activation energy of the thermal quenching of the famous orange luminescence of the ruthenium complex by a factor of two, and how it can push the high-spin cobalt complex to become a spin-crossover complex.

Keywords $[Fe(bpy)_3]^{2+}$ · $[Ru(bpy)_3]^{2+}$ · $[Co(bpy)_3]^{2+}$ · Intersystem crossing · Spin-crossover · Luminescence · Radiationless deactivation · Chemical pressure · Guest-host interactions

1 Introduction

Christian Klixbüll Jørgensen has been one of the pioneers in the elucidation of the electronic structure of transition metal complexes [1]. The concepts of the spectrochemical series [2], which classifies ligands in order of increasing ligand-field strength, and the nephelauxetic series [3], which classifies them with respect to the covalency of the metal ligand bond, are key concepts for our understanding of chemical bonding in coordination compounds. They are equally important for the understanding of their photo-physical and photo-chemical properties.

The aim of such general concepts is not to delve into the fine details of the electronic structure of a given complex, but to describe the most important contributions to the overall evolution of given properties within a series of compounds. Thus, Jørgensen's product rule [4] for estimating the value of the ligand-field parameter for a given metal-ligand combination can, for instance, predict low-spin or high-spin complexes. It is, however, too crude to be able to predict a given complex to be a spin-crossover system, because the effective energy difference between the high-spin and the low-spin state is also influenced by the second coordination sphere. Indeed, many physical properties of transition metal complexes are strongly influenced by the surrounding medium. More often than not this influence is rather difficult to quantify. In particular in solution with static and dynamic solvent/solute interactions, simple continuum models very often do not do justice to the complexity of the problem. In this chapter, dedicated to the memory of our colleague Christian Klixbüll Jørgensen, we present three examples of how the electronic properties of three simple complexes, namely $[Fe(bpy)_3]^{2+}$, $[Ru(bpy)_3]^{2+}$ and $[Co(bpy)_3]^{2+}$ can be tuned in a controlled way by doping them into a series of host lattices.

2 Intersystem Crossing in $[Fe(bpy)_3]^{2+}$

The iron(II) complex $[Fe(bpy)_3]^{2+}$ is considered a typical low-spin complex having a $^1A_1$ ground state with all of the six d electrons nicely paired up in the t_{2g} orbitals [2]. The absorption spectrum of this complex is dominated by an intense

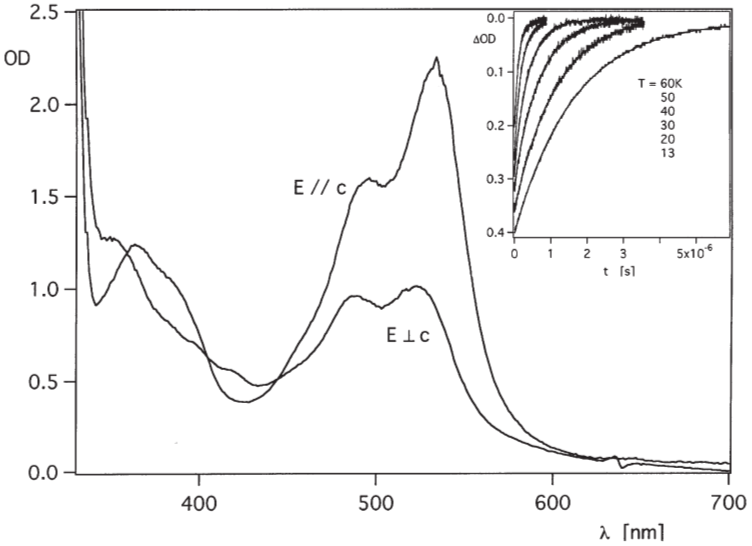

Fig. 1 Polarised single crystal absorption spectra at 293 K of $[Fe(bpy)_3]^{2+}$ doped into $[Zn(bpy)_3](PF_6)_2$ with the characteristic MLCT band centred at 530 nm. *Insert*: transient absorption monitored at 500 nm following pulsed laser excitation at 532 nm

band centred at 530 nm. This band has first been assigned to a metal-ligand $d \rightarrow \pi^*$ charge transfer (MLCT) transition by Jørgenson [5]. Palmer and Piper [6] confirmed this assignment on the basis of polarised single crystal absorption spectra of $[Fe(bpy)_3]^{2+}$ doped into a variety of inert host lattices. Indeed, based on the half width, they concluded that all observed spectral features in the visible are of an MLCT nature. Figure 1 shows the polarised single crystal absorption spectra of $[Fe(bpy)_3]^{2+}$ doped into $[Zn(bpy)_3](PF_6)_2$. The host crystallises in the trigonal space group $P3_1$ [7]. However, the molecular trigonal axes of the complexes are not parallel to the trigonal axis of the crystal. Rather, the unit cell contains three formula units, and the $[Zn(bpy)_3]^{2+}$ complexes are arranged in such a way that the molecular trigonal axes are perpendicular to the trigonal axis of the crystal. This is reflected in the relative intensities of the σ (E⊥c) and the π (E//c) spectrum of 1:2, due to the fact that the MLCT transitions in tris-bipyridine complexes are polarised exclusively perpendicular to the molecular trigonal axis [8].

The ligand-field strength for $[Fe(bpy)_3]^{2+}$ is not too far away from the spin-crossover region, and, as shown in Scheme 1, ligand-field theory predicts a number of low-lying ligand-field states in addition to the MLCT state. As mentioned above, the corresponding d-d transitions are not directly observable in the absorption spectrum as their intensities are too low relative to the intense MLCT band. Nevertheless, they play an important role for the photophysical properties of $[Fe(bpy)_3]^{2+}$ in so far as they provide a ladder of close lying states for efficient non-radiative decay. In fact, the photophysical behaviour of $[Fe(bpy)_3]^{2+}$ [9] is quite similar to the one of iron(II) spin-crossover systems [10]. As indicated in

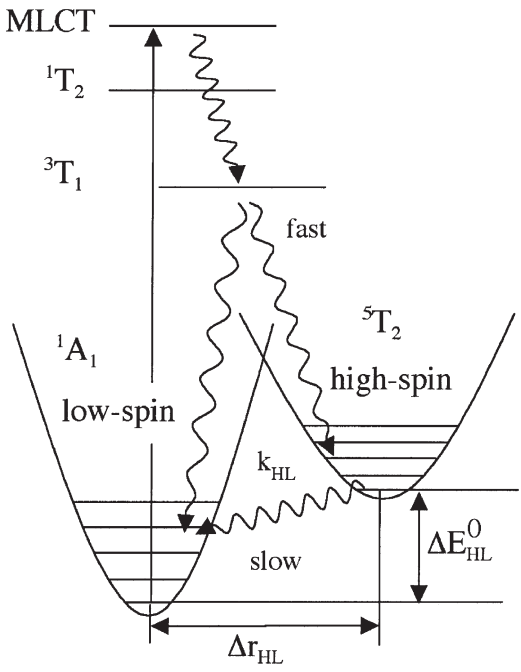

Scheme 1 The electronic structure of $[Fe(bpy)_3]^{2+}$ including the low-spin $^1A_1(t_{2g}^6)$ ground state, excited ligand-field states, and the low-lying MLCT state giving this complex its red colour. *Curly arrows* indicate the pathway for the extremely efficient radiationless relaxation from higher excited states down to the high-spin $^5T_2(t_{2g}^4e_g^2)$ state. The subsequent high-spin→low-spin relaxation is orders of magnitude slower

Scheme 1, following the initial excitation into the MLCT band, a subpicosecond [11] and thus highly non-adiabatic double intersystem crossing step can take the complex to the lowest excited d-d state, which is the classic high-spin state of the d^6 configuration, namely the $^5T_2(t_{2g}{}^4e_g{}^2)$ state. Even though the $^3T_1$ state does not have an observable lifetime [11] it mediates the double intersystem crossing step [12]. Due to the large difference in metal-ligand bond length between the high-spin and the low-spin state and the resulting energy barrier between them, the non-radiative relaxation from the high-spin state back to the low-spin ground state is comparatively slow. For spin-crossover compounds having a very small zero-point energy difference, ΔE^0_{HL}, between the high-spin state and the low-spin state, the light-induced high-spin state can have lifetimes of up to several days at liquid helium temperatures [10]. In the $[Fe(bpy)_3]^{2+}$ low-spin system, the driving force for the relaxation is somewhat larger, and therefore the relaxation back to the ground state is considerably faster. This is exemplified by the series of relaxation curves recorded between 10 and 50 K for $[Fe(bpy)_3]^{2+}$ doped into $[Zn(bpy)_3](PF_6)_2$ shown in the insert of Fig. 1. These curves were recorded by monitoring the transient bleaching of the MLCT band at 500 nm following pulsed excitation with the second harmonic of a Nd:YAG laser at 532 nm. All relaxation curves are perfectly single exponential, and the corresponding high-spin→low-spin relaxation rate constants are plotted on a logarithmic scale vs 1/T (Arrhenius plot) in Fig. 2 for temperatures between 15 and 150 K and, in addition, at 295 K using a picosecond set-up. The room temperature lifetime of 640 ns of the transient state of $[Fe(bpy)_3]^{2+}$ doped into $[Zn(bpy)_3](PF_6)_2$ is very close to the value of 830 ns for the transient state of $[Fe(bpy)_3]^{2+}$ in aqueous solution previously reported by Kirk et al. [13] and Creutz et al. [14]. As already pointed out by these authors, the transient bleaching of the MLCT band merely indicates that there is a short-lived metastable state at some energy above the ground state, without actually identifying its nature. At the time, both Kirk et al. as well as Creutz et al. favoured the $^3T_1$ ligand-field state as transient state, although Kirk et al. thought it could also be a ^{3}MLCT state, and Creutz et al. did not entirely exclude the $^5T_2$ ligand-field state. The comparison of the lifetime of the transient state of $[Fe(bpy)_3]^{2+}$ doped into the inert $[Mn(bpy)_3](PF_6)_2$ host lattice as determined using pulsed laser excitation with the one determined using Mössbauer emission spectroscopy put an end to speculation as it allowed a clear cut identification of the transient state as the $^5T_2$ high-spin state [15].

Figure 2 not only shows the high-spin→low-spin relaxation rate constants for $[Fe(bpy)_3]^{2+}$ doped into the $[Zn(bpy)_3](PF_6)_2$ host but into the whole series of isostructural, and within the spectral range of interest photophysically inert host lattices $[M(bpy)_3](PF_6)_2$, M=Co, Zn, Mn, and Cd. As expected from the theory of non-adiabatic multi-phonon relaxation in the strong coupling limit [16], that is with a large value of the difference in equilibrium bond lengths and a small value of the zero-point energy difference between the two states, the relaxation proceeds via an almost temperature independent tunnelling process below approximately 50 K and becomes thermally activated at elevated temperatures [10, 17]. The most striking aspect of the data shown in Fig. 2 is the wide spread of the low temperature tunnelling rate constants ranging from 6.2×10^3 s^{-1} (τ=162 μs) for the

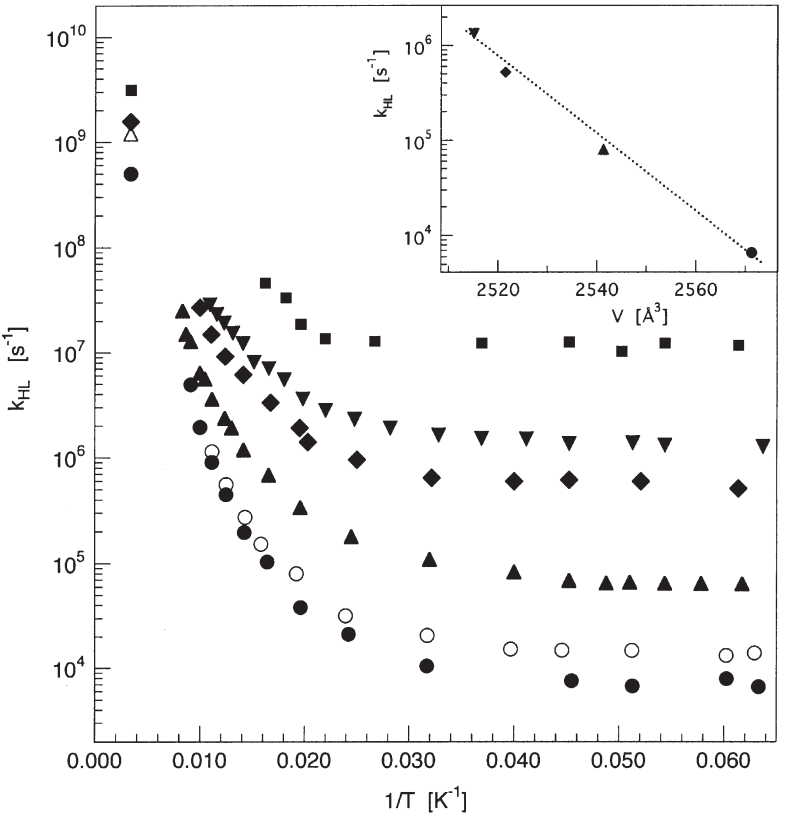

Fig. 2 The high-spin→low-spin relaxation rate constant k_{HL} plotted on a logarithmic scale against 1/T (Arrhenius plot) for $[Fe(bpy)_3]^{2+}$ doped into $[M(bpy)_3](PF_6)_2$, M=Co (*filled inverted triangles*), Zn (*filled diamonds*), Mn (*filled triangles*), Cd (*filled circles*), and into the three-dimensional oxalate network $[NaRh(ox)_3][Zn(bpy)_3]$ (*filled squares*) at ambient pressure, and for the Cd host at an external pressure of 1 kbar (*open circles*), in aqueous solution at room temperature (*open squares*). Insert: the low-temperature tunnelling rate constant $k_{HL}(T\rightarrow 0)$ vs the unit cell volume of the host lattice for $[Fe(bpy)_3]^{2+}$ doped into $[M(bpy)_3](PF_6)_2$ (M=Co, Zn, Mn, Cd)

Cd host to 1.4×10^6 s^{-1} (τ=720 ns) for the Co host. Phenomenologically, the low-temperature tunnelling rate constant increases with a decreasing unit cell volume of the host lattice. As shown in the insert of Fig. 2, k_{HL} plotted on a logarithmic scale vs the unit cell volume of the host results in a perfectly linear correlation. The physical interpretation of this result is straightforward. As the cavity provided by the host lattice for guest becomes smaller and smaller, the high-spin state of the iron(II) complex, with its considerably larger volume as compared to the low-spin state, becomes more and more destabilised. As a result the driving force for the high-spin→low-spin relaxation increases and therefore the corresponding rate constant also increases. Thus the effect of the different host lattices on the guest can be viewed as a variation of an internal or chemical pressure. This

chemical pressure can be compared to the effect of an external pressure. Figure 2 includes the relaxation rate constants observed in the Cd host at an external pressure of 1 kbar. In the low-temperature tunnelling regime, this pressure increases the relaxation rate constant by a mere factor of 2. Thus, the increase in relaxation rate constant by a factor of ~250 between the Cd and the Co host indicates an internal pressure variation corresponding to ~8 kbar. Unfortunately, it is not possible to verify this experimentally by increasing the external pressure, because above 1 kbar the external pressure induces a crystallographic phase transition, which is accompanied by a discontinuous jump in the relaxation rate constant. However, the hypothesis can be tested by doping $[Fe(bpy)_3]^{2+}$ into the even more confining host lattice of the oxalate network $[Zn(bpy)_3][NaRh(ox)_3]$ [18]. The oxalate network provides a very tight fitting cavity for the tris-bipyridine cation, and as shown by the data included in Fig. 2, for this host lattice the low-temperature tunnelling rate constant increases by yet another order of magnitude to 1.3×10^7 s^{-1} (τ=81 ns).

At room temperature the relaxation rate constant for the investigated systems as well as for $[Fe(bpy)_3]^{2+}$ in solution [13, 14] falls into the comparatively narrow range of 0.5 to 3×10^9 s^{-1} (τ=0.35–2.0 ns). This is in accordance with the theory of non-adiabatic multi-phonon relaxation in the strong coupling limit. At elevated temperatures, tunnelling proceeds via thermally populated vibrational levels of the high-spin state, and in the high-temperature limit the variation of the driving force has less of an effect on the rate constant than in the low-temperature tunnelling region. The variation in zero-point energy difference between the two states of $[Fe(bpy)_3]^{2+}$ doped into the various host lattices can be estimated to be of the order of 2000 cm^{-1} as compared to an average driving force of the order of a few thousand wavenumbers [9, 14, 17].

3
The Quencher State in $[Ru(bpy)_3]^{2+}$

The excited state electronic structure of the $[Ru(bpy)_3]^{2+}$ (bpy=2,2′-bipyridine) complex has been the subject of a large number of papers over the past 30 years [19]. Whereas the ground state of $[Ru(bpy)_3]^{2+}$ in a strong octahedral ligand field is the diamagnetic $^1A_1$ (t_{2g}^6) state, it is generally acknowledged that the lowest excited state, from which the famous orange luminescence originates, is an MLCT state having a triplet character (see Scheme 2). Based on low-temperature data, Harrigan et al. [20] proposed that this ^{3}MLCT state actually consists of a multiplet with three well-defined electronic levels split by ~10 and ~60 cm^{-1}, respectively, each having its own radiative lifetime and luminescence quantum efficiency, and having an increasing admixture of singlet character with increasing energy. Extrapolation of the low temperature data to room temperature yields limiting values for the ^{3}MLCT lifetime and the luminescence quantum efficiency of ~2.8 µs and ~0.5, respectively. This is in contrast to experimental results. Typically, the luminescence quantum efficiency starts to decrease rapidly above ~200 K and, in parallel, the lifetime drops to well below the 2.8 µs. This behaviour has been interpreted as being due to a close lying d-d state which becomes thermally populated at elevated temperatures, thereby quenching the ^{3}MLCT lu-

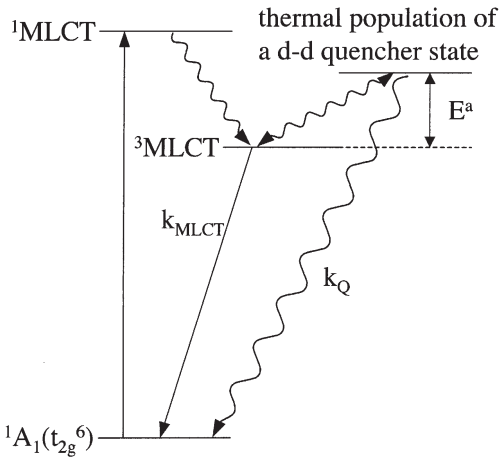

Scheme 2 The electronic structure of $[Ru(bpy)_3]^{2+}$. The much higher ligand-field strength as compared to $[Fe(bpy)_3]^{2+}$ pushes the excited ligand-field states to energies which are above the energy of the lowest excited ^{3}MLCT state. As a result, there is luminescence from this ^{3}MLCT state. At low temperatures the quantum efficiency of the luminescence is quite high, but at elevated temperatures thermally activated quenching sets in. This quenching is thought to proceed via the thermal population of close lying ligand-field states

minescence via non-radiative processes [21]. In a more refined model, Lumpkin et al. [22] proposed an additional higher lying MLCT state of predominantly singlet character making significant contributions to the non-radiative decay at elevated temperatures. This was subsequently confirmed by the detailed spectroscopic investigations of Yersin et al. [23] on the basis of polarised absorption and emission spectra.

Maruszewski et al. [24] noticed that the energy of d-d quencher state depends critically upon the second coordination sphere, showing that for instance insertion of $[Ru(bpy)_3]^{2+}$ into the cavities of a zeolite effectively moves it to substantially higher energy. To date there is no hard experimental evidence for the assignment of this state, but it is generally assumed to be a triplet ligand-field state belonging formally to the $t_{2g}^5e_g^1$ configuration. The recent publication by Thompson et al. [25] in fact addresses this problem explicitly. In a two photon absorption experiment these authors achieve a direct population of the quencher state followed by relaxation to the emitting MLCT state within 100 ns on the one hand and expulsion of one arm of a bipyridine ligand followed by recombination within 80 µs on the other.

Figure 3 shows the polarised single crystal absorption spectrum at room temperature of $[Ru(bpy)_3]^{2+}$ doped into $[Zn(bpy)_3](PF_6)_2$ at a level of 0.1%. As for the iron(II) complex, the spectrum in the visible is dominated by the intense spin-allowed ^{1}MLCT band centred at 452 nm, and as for the iron(II) complex doped into the same host lattice, the ratio of the E//c to the E⊥c intensity is 2:1 due to the MLCT transition being polarised perpendicular to the molecular trigonal axis [8] and to the crystal packing with the molecular trigonal axis perpendicular to the crystal c axis [7]. Figure 3 includes the luminescence spectra at 11 K of

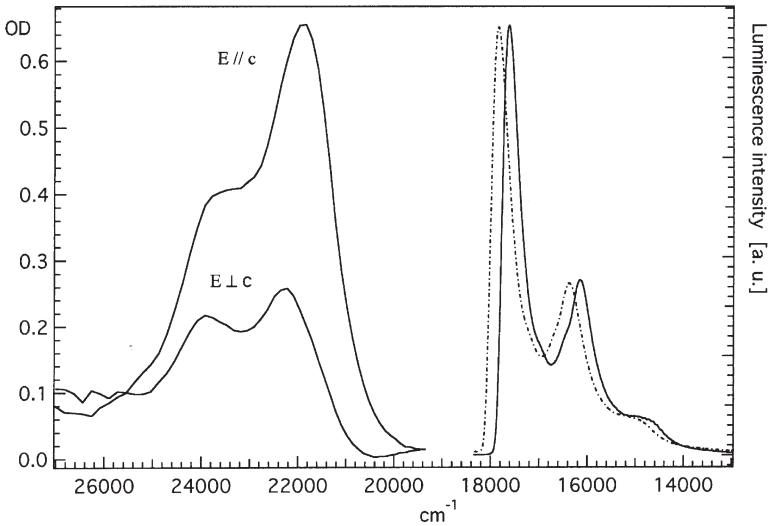

Fig. 3 Polarised single crystal absorption spectra at 295 K and luminescence spectra at 11 K of $[Ru(bpy)_3]^{2+}$ doped into $[Zn(bpy)_3](PF_6)_2$

$[Ru(bpy)_3]^{2+}$ doped both into $[Zn(bpy)_3](PF_6)_2$ and $[Cd(bpy)_3](PF_6)_2$. Apart from a slight shift of ~250 cm^{-1} towards higher energy for the latter, the two spectra are very similar.

Figure 4 shows the luminescence lifetime of the ^{3}MLCT state of $[Ru(bpy)_3]^{2+}$ doped into the two above-mentioned crystalline hosts as well as into the oxalate network $[Zn(bpy)_3][NaAl(ox)_3]$ as a function of temperature between 10 and 520 K. Below 180 K the curves are superimposable and follow the behaviour reported for $[Ru(bpy)_3]^{2+}$ in a poly-methacrylate glass [13]. For the $[Cd(bpy)_3](PF_6)_2$ host, thermal quenching sets in at ~180 K, for $[Zn(bpy)_3](PF_6)_2$ at ~270 K, and for the oxalate network $[Zn(bpy)_3][NaAl(ox)_3]$ at ~380 K. In addition, under an external pressure of 30 kbar, the $[Ru(bpy)_3]^{2+}$ luminescence in the oxalate network is not quenched all the way up to 520 K!

Again, the key difference between the three hosts lattices lies in the different volumes they provide for the guest complexes and thus a variation of the chemical pressure felt by the guest complexes. As before, the $[Zn(bpy)_3](PF_6)_2$ host exerts a larger chemical pressure than $[Cd(bpy)_3](PF_6)_2$, and the tight fit of the tris-bipyridine cations in the oxalate network results in a larger chemical pressure still. The quenching temperature thus follows the increasing chemical pressure, and in the oxalate network an additional external pressure removes the quencher state altogether. Both chemical and physical pressures shift the quencher state to higher energies. Qualitatively, it therefore has a larger molecular volume than the MLCT states, as expected for a d-d excited state. According to Eq. 1,

$$k_{obs}(T) = k_{MLCT}(T) + k_Q(T) = k_{MLCT}(T) + A \times e^{-E^a/k_BT} \quad (1)$$

the observed relaxation rate constant, $k_{obs}(T)$, can be expressed as the sum of the direct relaxation rate constant of the MLCT manifold, $k_{MLCT}(T)$, comprising both

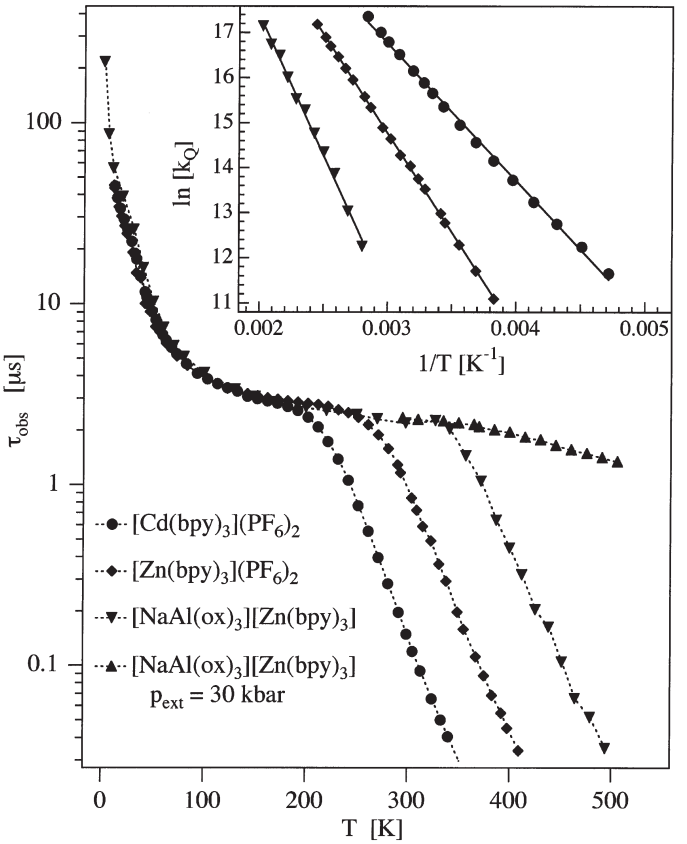

Fig. 4 Excited state lifetimes (on a logarithmic scale) vs temperature for $[Ru(bpy)_3]^{2+}$ doped into $[M(bpy)_3](PF_6)_2$ (M=Cd, Zn) and into the three-dimensional oxalate network $[Zn(bpy)_3][NaAl(ox)_3]$. For the latter system the lifetime at an external pressure of 30 kbar is included. *Insert*: the thermal quenching rate constant k_Q of $[Ru(bpy)_3]^{2+}$ plotted on a logarithmic scale vs 1/T

radiative and non-radiative processes, and the thermally activated quenching process, $k_Q(T)$ [22]. The temperature dependence of the direct decay at elevated temperatures is accessible experimentally as the lifetime of the $[Ru(bpy)_3]^{2+}$ luminescence in $[Zn(bpy)_3][NaAl(ox)_3]$ under the external pressure of 30 kbar. Thus, k_Q (T) can be extracted from the experimental data. The insert of Fig. 4 shows the Arrhenius plots as $\ln[k_Q(T)]$ vs 1/T for the three host lattices. They are all perfectly linear with activation energies E^a of 2110(30) cm^{-1} for the $[Cd(bpy)_3](PF_6)_2$ host, 3045(20) cm^{-1} for the $[Zn(bpy)_3](PF_6)_2$ host and 4310(80) cm^{-1} for the $[Zn(bpy)_3][NaAl(ox)_3]$ host, respectively. Such a large variation in activation energy, as compared to the rather small shift of the ^{3}MLCT luminescence, indicates that the molecular volume of $[Ru(bpy)_3]^{2+}$ in the quencher state is substantially larger than in the luminescent state. As the ^{3}MLCT state equilibrium geometry is not very much different from the ground state geometry

[26], it can be concluded that the molecular volume of the quencher state is also very much larger than the one of the $^1A_1$ (t_{2g}^6) ground state. Indeed, the variation of the activation energy is of the same order of magnitude as for the zero-point energy difference between the high-spin and the low-spin state in the corresponding iron(II) systems discussed in the previous section. Thus the commonly assumed assignment of the d-d quencher state to the lowest energy triplet state originating from the $t_{2g}^5e_g^1$configuration is not conclusive. The large variation of the activation energy on the surrounding medium indicates that it could also be the quintet high-spin state originating from the $t_{2g}^4e_g^2$ configuration. Of course, the ligand-field strength for $[Ru(bpy)_3]^{2+}$ at the ground state equilibrium bond length is typically 50% larger than for $[Fe(bpy)_3]^{2+}$. Thus, vertically from the ground state equilibrium bond length, the first excited d-d state is indeed the $^3T_1$ ($t_{2g}^5e_g^1$) state. However, it is not the Franck-Condon energy that is of interest here, but the zero-point energy difference. As for iron(II) spin-crossover systems the difference in volume between the two states translates into a difference in metal-ligand bond length, and therefore at the equilibrium geometry of the quencher state the ligand-field strength is substantially reduced as compared to the one at the ground state geometry. This results in a ligand-field strength in the vicinity of the crossover point in the Tanabe-Sugano diagram, and thus at the equilibrium geometry of the quencher state the first excited d-d state could indeed be the $^5T_2$ ($t_{2g}^4e_g^2$) high-spin state. *

Of course, the results presented here do not constitute hard experimental evidence for such a reassignment of the d-d quencher state either. The reassignment would, however, explain as to why for $[Ru(bpy)_3]^{2+}$ and its numerous derivatives there is not a single case for which luminescence from a d-d state has been observed. Based on the above ligand-field theoretical arguments the zero-point energy difference between the triplet and the quintet state is expected to be quite small. Indeed, it is conceivable that in solution the dissociative Jahn-Teller coordinate of the triplet state is responsible for the thermal quenching of the MLCT luminescence whereas in the solid state such a distortion is inhibited by the host lattice.

4 Turning $[Co(Bpy)_3]^{2+}$ into a Spin-Crossover Complex

In contrast to the iron(II) complex, $[Co(bpy)_3]^{2+}$ generally is a typical d^7 high-spin complex with a $^4T_1$ ($t_{2g}^5e_g^2$) ground state [2]. The corresponding absorption spectrum in the region of the d-d transitions consists of one weak band at around 11,500 cm^{-1} (830 nm) assigned to the $^4T_1 \rightarrow {}^4T_2$ d-d transition [6]. This is exemplified in the spectra of the cobalt complex doped in the three-dimensional oxalate network structure $[Co(bpy)_3][NaRh(ox)_3]$ shown in Fig. 5a.

However, the ligand-field strength for $[Co(bpy)_3]^{2+}$ is not too far away from the spin-crossover point and, as indicated in Scheme 3, the zero-point energy difference between the ground state and the corresponding $^2E(t_{2g}^6e_g^1)$ low-spin state must therefore be quite small. The by now obvious strategy to push $[Co(bpy)_3]^{2+}$ towards a spin-crossover or even a low-spin system is to increase the chemical

* See note added in proof.

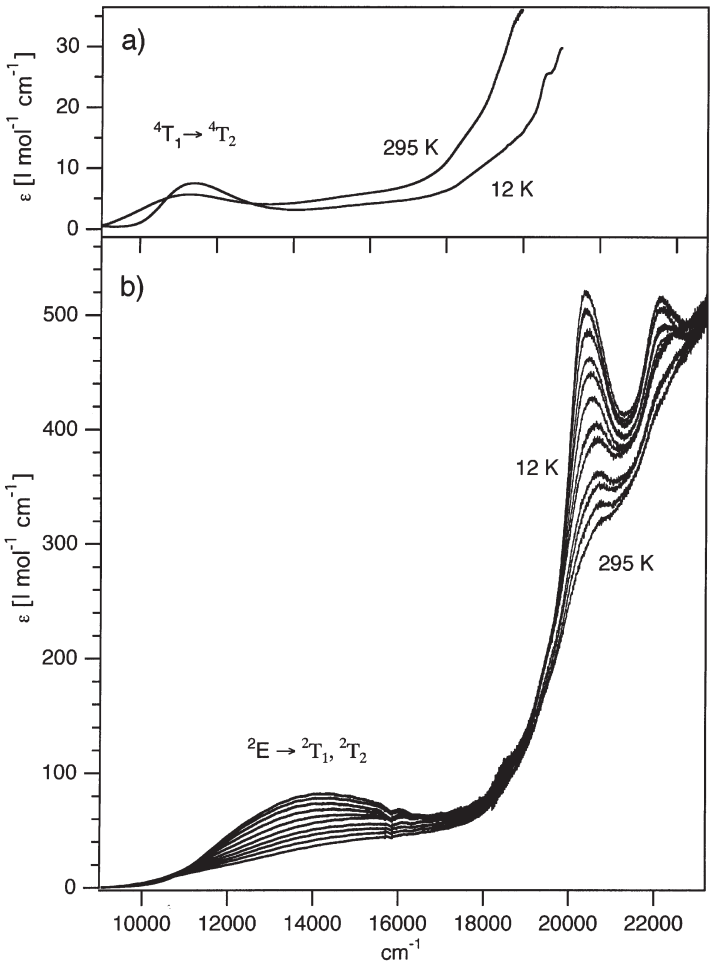

Fig. 5 **a** Single crystal absorption spectra of $[Co(bpy)_3][NaRh(ox)_3]$ at 10 and at 295 K. **b** Variable temperature single crystal absorption spectra of $[Co(bpy)_3][LiRh(ox)_3]$

pressure in order to destabilise the high-spin state with respect to the low-spin state!

Mizuno and Lunsford [27] as well as Tiwary and Vasudevan [28] demonstrated the feasibility of this approach by inserting $[Co(bpy)_3]^{2+}$ into zeolites. The three-dimensional oxalate networks are likewise suited for this, as by varying the combination of metal ions on the oxalate backbone, the size of the cavity can be adjusted. The variable temperature absorption spectra of $[Co(bpy)_3][LiRh(ox)_3]$ in Fig. 5b demonstrate that this strategy actually works [29]. They are very different from the spectra of Fig. 5a, indicating that the sought for change in electronic ground state has indeed occurred. At the lowest temperature there is a comparatively intense band centred at 14,400 cm^{-1} (700 nm). This band can be assigned to the $^2E \rightarrow {}^2T_1, {}^2T_2$ transitions of the low-spins species. The temperature dependent

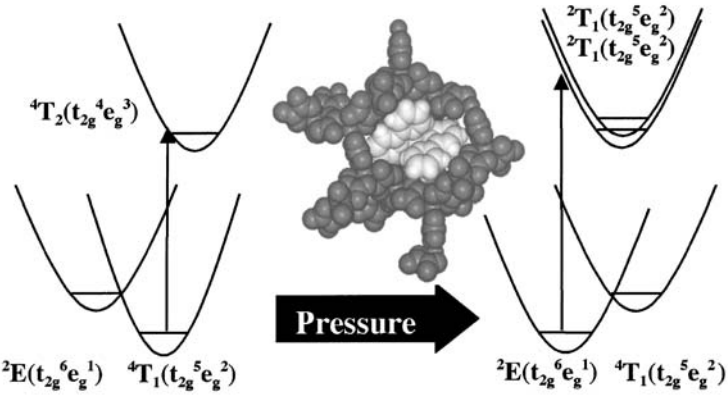

Scheme 3 The electronic structure of $[Co(bpy)_3]^{2+}$ with a high-spin ground state and the effect of chemical pressure provided by the cavities of the oxalate network which destabilises the high-spin state (with picture of cavity)

bands at higher energy clearly belong to the same species as the band at 14,400 cm^{-1}, but they are not as straightforward to assign. With extinction coefficients of ~600 M^{-1} cm^{-1} they are rather too intense for d-d transitions. Furthermore, ligand-field theory does not predict any spin-allowed d-d transitions in this region, and their half width is substantially smaller than the one of the $^2E \rightarrow {}^2T_1$, $^2T_2$ transitions even taking into account the broadening due to the energy difference of ~600 cm^{-1} between the two excited states. They are thus more likely to correspond to MLCT transitions of the low-spin species. As the temperature is increased the intensity of all bands gradually decreases. This indicates a depopulation of the low-spin state with increasing temperature. That this is indeed due to a spin transition is borne out by the magnetic susceptibility, plotted as the product χT (rather than $\mu_{eff} = \sqrt{8\chi T}\mu_B$) vs temperature for $[Co(bpy)_3][NaCr(ox)_3]$ and $[Co(bpy)_3][LiCr(ox)_3]$ [28] in Fig. 6a. After subtracting the spin-only contribution of $[Cr(ox)_3]^{3-}$ using $[Fe(bpy)_3][LiCr(ox)_3]$ as reference, the χT curve of the former follows the typical behaviour of an octahedral cobalt(II) complex in the high-spin state, exceeding the spin only value for S=3/2 of 1.88 cm^3 mol^{-1} K (μ_{eff}=3.87 μ_B) due to the comparatively strong and temperature dependent orbital contribution [30]. For the latter, the χT value at 10 K of 0.38 cm^3 mol^{-1} K (μ_{eff}=1.73 μ_B) corresponds to the spin-only value of an S=1/2 state, as expected for the low-spin state of cobalt(II). As the temperature increases, χT increases and tends towards the characteristic value of the high-spin state at room temperature. Thus, the increase in internal pressure exerted on the $[Co(bpy)_3]^{2+}$ complex upon substitution of Na^+ by the smaller Li^+ does indeed destabilise the high-spin state of $[Co(bpy)_3]^{2+}$ sufficiently for the low-spin state to become the electronic ground state of the system. The actual zero-point energy difference is quite small such that the entropy driven thermal population of the high-spin state approaches 80% at room temperature.

In addition to χT as a function of temperature for the three neat compounds, Fig. 6a shows χT for the mixed crystal series $[Fe_{1-x}Co_x(bpy)_3][LiCr(ox)_3]$, x=0.8,

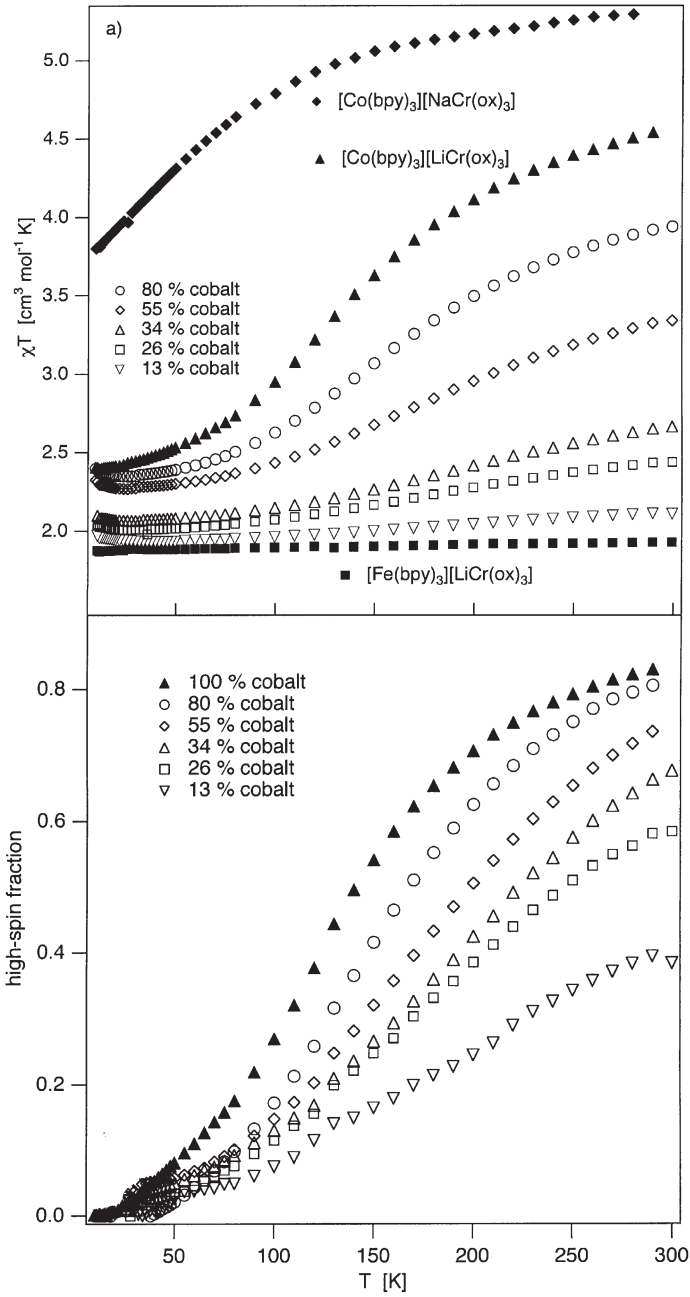

Fig. 6 **a** Variable temperature magnetic susceptibility, plotted as the product χT, in neat $[Co(bpy)_3][NaCr(ox)_3]$, and $[Co(bpy)_3][LiCr(ox)_3]$, as well as in the mixed crystal series $[Fe_{1-x}Co_x(bpy)_3][LiCr(ox)_3]$. For comparison, the data for $[Fe(bpy)_3][LiCr(ox)_3]$ are included. **b** Spin-transition curves for neat $[Co(bpy)_3][LiCr(ox)_3]$ and for the mixed crystals $[Fe_{1-x}Co_x(bpy)_3][LiCr(ox)_3]$ from magnetic susceptibility measurements

0.63, 0.37, 0.23 and 0.13. Obviously, by diluting the paramagnetic complexes with the diamagnetic iron complex, χT decreases with decreasing cobalt concentration. A more meaningful way to plot the data is first to subtract the contribution of chromium(III) complex and then to normalise to the respective mole fraction of cobalt(II) complexes. Figure 6b shows the resulting spin transition curves, plotted as the fraction of cobalt(II) complexes in the high-spin state vs temperature, for the neat compound as well as for the mixed crystal series. Two observations can immediately be made: with increasing dilution, the spin transition moves to higher temperatures and becomes more gradual. The first observation is a direct consequence of the concept of an increasing internal pressure with an increasing concentration of $[Fe(bpy)_3]^{2+}$. This is to be expected, because the Fe-N bond length of 1.96 Å is shorter than the Co-N bond lengths of 2.03 and 2.14 Å for $[Co(bpy)_3]^{2+}$ in the low-spin state in the high-spin state, respectively. The corresponding unit cell volumes are 3642.7 $Å^3$ and 3527.8 $Å^3$ for $[Co(bpy)_3][LiCr(ox)_3]$ at 293 and 10 K, respectively, and 3520.6 $Å^3$ and 3472.4 $Å^3$ for $[Fe(bpy)_3][LiCr(ox)_3]$ at 293 and 10 K. Therefore, an increase in the $[Fe(bpy)_3]^{2+}$ concentration results in a contraction of the lattice and thus to an increase in internal pressure relative to the neat cobalt(II) compound. The second observation is the consequence of so-called cooperative effects due to elastic interactions between the spin changing complexes. These can be viewed as a modulation of the internal pressure as a function of the fraction of complexes in the high-spin state. As the complexes in the high-spin state are larger than those in the low-spin state, the whole lattice expands upon thermal population of the high-spin state, and as a consequence thereof, the internal pressure decreases, making the conversion of the remaining low-spin complexes to the high-spin state easier [10, 31]. Thus, the spin transition in the neat cobalt compound is less gradual than in the mixed crystal systems.

5 Conclusions

Lattice forces can be substantial. Just by substituting the metal ion of the inert hosts, the effect of the chemical difference in pressure can be equivalent to several kbar of external pressure. Ordering of electronic levels can be inverted and therefore magnetic, optical and photophysical properties can be tuned. With our series we have done so in a controlled and understandable way. In this respect the solid state has several advantages over solution and polymer matrices: a) the accessible temperature interval is much larger, b) there are less complications due to phase transitions, glass points and softening of the matrix and c) there is less inhomogeneous broadening of electronic energy levels. Of course, the concept of internal pressure is very crude, and constitutes only a first approximation to the complex problem of guest-host interactions. Advances in computational power should lead to a better understanding of such interactions in the not too distant future. The three examples chosen here are instructive in showing quantitatively by how much energy levels can shift, and how dramatic the effect of seemingly minor chemical changes can be: a) several orders of magnitude variation in rate constant of the high-spin→low-spin relaxation in $[Fe(bpy)_3]^{2+}$, b) a large varia-

tion in activation energy for the thermal quenching of the luminescence in $[Ru(bpy)_3]^{2+}$, suggesting an alternative assignment of the quencher state and c) outright crossover of the electronic ground state for $[Co(bpy)_3]^{2+}$. For all three the importance lies in the fact that ground and excited states have different equilibrium geometries and therefore respond differently to external perturbations. The three examples show how much progress has been made in our understanding of chemical bonding in coordination compounds since the day of the early models for which the concepts developed by our colleague C.K. Jørgensen were instrumental.

Acknowledgements We thank P. Brodard for room temperature picosecond work on the iron(II) systems, G. Bernardinelli for the X-ray work on the host lattices, R. Toomey and I. Y. Chan for the pressure work on the oxalate network and A. Schindler for the magnetic susceptibility measurements. The picture of the oxalate network is by courtesy of S. Decurtins. This work was supported by the Swiss National Science Foundation.

Note added in proof

DFT calculations using one of the latest functionals (rPBE) and a high-quality basis set indicate, that the original assignment of the quencher state in $[Ru(bpy)_3]^{2+}$ to the $^3T_1(t_{2g}{}^5e_g{}^1)$ state is, after all, correct. However, they also indicate that the Ru-N bond length difference between the ^{3}MLCT and the ^{3}dd state is as large as 0.15 Å. This is substantially larger than for a one electron excitation of first row transition metal complexes. It is, in fact, large enough to explain the observed variation in activation energy for the thermal quenching of the $[Ru/(bpy)_3]^{2+}$ luminescence in the different host lattices.

6 References

1. Jørgensen CK (1962) Absorption spectra and chemical bonding in complexes. Pergamon Press, Oxford
2. a) Schläfer HL, Gliemann G (1980) Einführung in die Ligandenfeldtheorie. Akad Verlagsgesellschaft, Wiesbaden; b) Lever ABP (1984) Inorganic electronic spectroscopy, studies in physical and theoretical chemistry 33. Elsevier, Amsterdam
3. Schaffer CE, Jorgensen CK (1958) J Inorg Nucl Chem 8:143
4. Huhey JE (1979) Inorganic chemistry: principles of structure and reactivity. Harper and Row, New York
5. Jørgensen CK (1957) Acta Chem Scand 9:1362
6. Palmer RA, Piper TS (1966) Inorg Chem 5:864
7. Breu J, Domel H, Stoll A (2000) Eur J Inorg Chem 2401
8. Ferguson J, Herren F, Krausz ER, Mäder M, Vbrancich J (1982) Coord Chem Rev 46:159
9. a) Hauser A (1992) Chem Phys Lett 92:65; b) Schenker S, Hauser A, Wang W, Chan IY (1998) Chem Phys Lett 297:281
10. Gütlich P, Hauser A, Spiering H (1994) Angew Chem Int Ed Engl 33:2024
11. McCusker JK, Walda KN, Dunn RC, Simon JD, Magde D, Hendrickson DN (1992) J Am Chem Soc 114:6919; McCusker JK, Walda KN, Dunn RC, Simon JD, Magde D, Hendrickson DN (1993) J Am Chem Soc 115:298
12. Hauser A (1991) J Chem Phys 94:2741
13. Kirk AD, Hoggard PE, Porter GB, Rockley MG, Windsor MW (1976) Chem Phys Lett 37:199
14. Creutz C, Chou M, Netzel TL, Okumura M, Sutin N (1980) J Am Chem Soc 102:1309
15. Deisenroth S, Hauser A, Spiering H, Gütlich P (1994) Hyperfine Inter 93:1573
16. Buhks E, Navon G, Bixon M, Jortner J (1980) J Am Chem Soc 102:2918

17. Hauser A (1995) Comments Inorg Chem 17:17
18. Decurtins S, Schmalle HW, Schneuwly P, Ensling J, Gütlich P (1994) J Am Chem Soc 116:9521
19. Juris A, Balzani V, Barigelletti F, Campagna S, Belser P, von Zelewski A (1988) Coord Chem Rev 84:85
20. Harrigan RW, Hager GD, Crosby GA (1973) Chem Phys Lett 21:487
21. Van Houten J, Watts RJ (1976) J Am Chem Soc 98:4853
22. Lumpkin RS, Kober EM, Worl LA, Murtaza Z, Meyer TJ (1990) J Chem Phys 94:239
23. a) Schönherr T, Degen J, Gallhuber E, Hensler G, Yersin H (1989) Chem Phys Lett 158:519, b) Yersin H, Gallhuber E, Vogler A, Kunkely H (1983) J Am Chem Soc 105:4155
24. Maruszewski K, Strommen DP, Kincaid JR (1993) J Am Chem Soc 115:8345
25. Thompson DW, Wishart JF, Brunschwig BS, Sutin N (2001) J Phys Chem A 105:8117
26. a) Dressick WJ, Cline J, Demas JN, DeGraff BA (1986) J Am Chem Soc 108:7567; b) Yersin H, Humbs W, Strasser J (1997) Coord Chem Rev 159:325
27. Mizuno K, Lunsford JH (1983) Inorg Chem 22:3484
28. Tiwary SK, Vasudevan S (1998) Inorg Chem 37:5239
29. Sieber R, Decurtins S, Stoeckli-Evans H, Wilson C, Yufit D, Howard JAK, Capelli SC, Hauser A (2000) Chem Eur J 6:361
30. Earnshaw A (1963) Introduction to magnetochemistry. Academic Press, London
31. Spiering H, Meissner E, Köppen H, Müller EW, Gütlich P (1982) Chem Phys 68:65

Structure and Bonding, Vol. 106 (2004): 97–125
DOI 10.1007/b11308

A DFT Based Ligand Field Theory

M. Atanasov[1,2] · C. A. Daul[2,3] · C. Rauzy[2]

[1] Bulgarian Academy of Sciences, Institute of General and Inorganic Chemistry, Acad. G. Bontchev Str. Bl.11, 1113 Sofia, Bulgaria
[2] Université de Fribourg, Département de Chimie, Perolles, 1700 Fribourg, Switzerland
E-mail: Claude.Daul@unifr.ch
[3] Author to whom correspondence should be addressed

Abstract A general and user-oriented ligand field (LF) theory – LFDFT with parameters adjusted to DFT energies of separate Slater Determinants (SD) of the partly filled d^n shell [n=2(8), 3(7), 4(6) and 5] of transition metals (TM) complexes – is developed and tested using 22 well documented examples from the literature. These include Cr^{III}, d^3 and Co^{II} d^7 in octahedral and Cr^{IV}, Mn^{V}, Fe^{VI} d^2, Co^{II} d^7, Mn^{II} d^5, Ni^{II} d^8 in tetrahedral complexes for which reliable values of d-d transition energies available from high-resolute ligand field spectra of complexes with halogenide (F, Cl, Br and I), oxide and cyanide ligands have been reported. The formalism has been implemented and consists of three steps allowing provision of geometries, ligand field Kohn-Sham orbitals and SD-energies in a way consistent with the LF phenomenology. In a fourth step LF parameters are utilized to yield multiplet energies using a full CI LF program. Comparing SD energies from DFT with those calculated using the LF parameter values, we can state for all considered cases, that the LF parameterization scheme is remarkably compatible with SD energies from DFT; standard deviations between DFT SD-energies and their LFDFT values being calculated between 0.016 and 0.124 eV. We find that, when based on the average of configuration with n/5 occupancy of each MO dominated by TM d-orbitals and on geometries with metal-ligand bond lengths from experiment, the 10Dq parameter values (cubic symmetry) are very close to the ones obtained from a fit to reported ligand field transitions. In contrast, when using common functionals such as LDA or gradient corrected ones (GGA) we find that the parameters B and C deduced from a fit to the SD energies are systematically lower than experimental. Thus spin-forbidden transitions which are particularly sensitive to B and C are calculated to be by 2000 to 3000 cm^{-1} at lower energies compared to experiment. Based on DFT and experimental B and C values we propose scaling factors, which allow one to improve the agreement between DFT and experimental transition energies, or alternatively to develop a DFT theory based on effective LF functionals and/or basis sets. Using a thorough analysis of the dependence of the Kohn-Sham orbital energy on the orbital occupation numbers, following Slater theory, we propose a general LFDFT scheme allowing one to treat, within the same formalism low symmetric ligand fields as well. Test examples, which illustrate the efficiency of this approach, include C_s distorted CrO_4^{4-} and D_{2d} distorted MnO_4^{3-} chromophores. Finally, for cubic LF we propose a hybrid LFDFT model (HLFDFT) which leads to an improvement of the existing DFT-multiplet theories. We show, taking low-spin $Co(CN)_6^{3-}$ as an example, that the new model yields better results as compared to time-depending DFT (TDDFT). A discussion of the LFDFT method in the context of other CI-DFT approaches is given.

Keywords Ligand field theory · Density functional theory · Electronic transition energies · Ligand field parameters

1 Introduction

In this contribution we present a general theory of transition metal (TM) complexes which is based on DFT calculations of the manifold of all Slater determinants (SD) originating from a given d^n configuration of a transition metal complex. These results are used as a data base allowing one to reformulate the ligand field problem within the DFT framework and to determine and interpret its parameters using DFT data prior to experiment. We study the performance of the presently available functionals and we explore the possibility of accounting for both the dynamic and the non-dynamic correlation by a combined use of DFT and configuration interaction (CI) treatments, respectively. A comparison of some well characterized systems in the literature with other developments for calculating ground and excited states properties using DFT, such as time-depending DFT [1] and CI-DFT [2], is used to demonstrate the impact of this new approach.

Ligand field theory (LFT) has been and still is a useful tool for interpreting optical and magnetic properties of TM complexes. The predominantly ionic picture,

based on metal ions perturbed by surrounding anions (ligands) encountered in crystal field theory (CFT) [3], later supplemented by metal-ligand covalency in the Angular-Overlap Model (AOM) [4], provides an adequate description of the optical d-d transition, paramagnetism, magnetic interactions and electronic spin resonance (ESR). Yet, LFT is an empirical approach gaining its parameters by comparison with existing experimental data and its justification lies in its ability to reproduce these data. Thus, all LF approaches, both CFT and AOM are tools for interpreting rather than tools for predicting electronic phenomena in TM complexes. The demand for a predictive theory in this respect is mostly tangible for systems, such as active sites of enzymes, where little or no structural and/or spectroscopic data in high resolution are known. The need for a model which is *parameter free* on one site but compatible with the usual ligand field formalism on the other site becomes increasingly pronounced in view of the new developments in bio-inorganic chemistry [5, 6]. Density Functional Theory (DFT) is such a model. In an extension of previous studies [7] it has been shown using numerous examples by C. Daul [8], that the multiplet theory of TM ions and complexes is compatible with the DFT formalism. In turn, recipes have been proposed [9–11] to link the latter formalism in the form of SD energies obtained within DFT with the energies of various multiplets of the free TM atom or ion or TM complex. In this introduction, we will briefly summarize, for readers less familiar with LF theory, the existing LF approaches covering the CFT and AOM and reaching up-to-date DFT based multiplet theory developments. Later we will describe our theory and, following that, extensive applications will be given.

1.1
The Conventional Ligand Field Theory CFT [3] and AOM [4]

The physical background of the existing LF models stems from the rather localized character of the wavefunction of the d-electrons allowing one to consider a d^n-configuration as well defined. It gives rise to a number of SD (i.e. 45, 120, 210 and 252 SD for n=2(8), 3(7), 4(6) and 5). They are used as a basis for expanding the many electron wavefunction for the ground and the excited states. The expectation values of the energy within this basis are obtained from the solution of the eigenvalue problem using the operator Eq. (1):

$$H_{LF} = \sum_{(i)} h(i) + \sum_{(i,j)} G(i,j) \tag{1}$$

Equation (1) includes the one electron, ligand field Hamiltonian h(i) and the two-electron G(i,j) operator which takes account of the Coulomb interactions between d-electrons (via the $1/r_{ij}$ operator); summation is carried out over the d-electrons i<j=1, 2, 3, 4 and 5.

We note that the operators h and G are left unspecified in Eq. (1) and various LF models differ in the way they approximate these operators. When acting on the SD the operator V_{LF} leads to matrix elements h_{ab} for the d-orbitals and G_{abcd}:

$$h_{ab} = \int a^*(1)h(1)b(1)\,d\tau_1$$
$$G_{abcd} = \iint a^*(1)b^*(2)G(1,2)\,c(1)\,d(2)d\tau_1\,d\tau_2 \tag{2}$$

In Eq. (1) and Eq. (2) we use symbols i, j (or 1,2) and a, b, c, d in order to distinguish between electrons and orbitals occupied by electrons, respectively. Within the CFT, the h_{ab} matrix elements reflect the electrostatic perturbation of surrounding ligands on the d-electrons in terms of Coulombic interaction. For an octahedral ligand field and a basis of real d-orbitals, the 5×5 matrix is diagonal with matrix elements of ε_e=(3/5) 10Dq for the e_g ($\varepsilon=d_{x2-y2}$, $\theta=d_{z2}$) and ε_t=–(2/5) 10Dq for the t_{2g}($\xi=d_{yz}$, $\eta=d_{zx}$ and $\zeta=d_{xy}$) orbitals obeying the barycentre rule ($2\varepsilon_e+3\varepsilon_t=0$). The $\varepsilon_e-\varepsilon_t$ orbital energy difference is the cubic ligand-field splitting parameter 10Dq.

In the central field approximation the G_{abcd} integrals are expressed in terms of the Racah parameters A, B and C, pertaining to the spherical symmetry (see the Table in the Appendix), or alternatively, the more physical Slater-Condon parameters F_0, F_2 and F_4).

Within the Angular Overlap Model, the h_{ab} matrix is calculated using orbital overlap energies for σ ($\varepsilon_e=3e_\sigma$) and π ($\varepsilon_t=4e_\pi$) antibonding leading to the same diagonal h_{ab} matrix and $10Dq=3e_\sigma-4e_\pi$. The great advantage of using overlap arguments when parameterizing h_{ab} lies in the fact, that overlap energies may be expressed in terms of parameters e_σ and e_π which reflect the strength of the metal-ligand bond and thus the M–L bond distance. The angular dependence is given by the rotational transformation properties of the d-orbitals since ligand-ligand interaction is neglected. Thus coordination polyhedra of complexes with lower symmetry can be treated on the same footing as the higher symmetric ones, the h_{ab} matrix being expressed in terms of angular factors and the e_σ and e_π parameters. The great merit of such a model is its ability to treat systems with little or no symmetry. Its drawback lies in the large number of model parameters to be determined from experiment for such systems, resulting in a complex parameterization. Later we will develop recipes allowing one to use DFT data in order to approximate the h_{ab} matrix from DFT and thus to overcome these shortcomings.

1.2
The Electron Repulsion Parameterization of Griffith [12]

A more refined treatment of the G(i,j) term of the LF-operator beyond the central field approximation considers the dependence of G_{abcd} on symmetry. As has been shown by one of us, making use of Wigner-Eckhart's theorem [8], the 120 G_{abcd} integrals can be expressed in the case of cubic symmetry in terms of 10 independent (reduced) matrix elements R_i(i=1 to 10) and symmetry factors given by the cubic Clebsh-Gordon coefficients. The transformation used here consists simply in choosing a set of 10 merely independent $G_{abcd}(g_i)$ out of the 120 and to express the unphysical reduced matrix elements R_i in terms of the g_i using the corresponding linear mapping. In Table 1 we list all these parameters along with the parameters (a) to (j) proposed by Griffith [12]. In this Table we also include the relations of $R_i(g_i)$ to the electronic configuration, expressing these variables in terms of A, B, C specific for a given configuration.

We also notice that only one parameter, g_{10} cannot be related to any given micro-states.

Table 1 Symmetry independent interelectronic repulsion g_1 to g_{10} parameter definitions in a ligand field of cubic symmetry and their expressions in terms of reduced matrix elements (R_1 to R_{10}) from [8],the A, B and C parameters allowing for their dependence on the electronic-configuration (A_e, B_e, C_e for e^2, A_{te}, B_{te}, C_{te} for $e^1t_2^1$ and A_t, B_t, C_t for t_2^2) as well as with the original Griffith's parameters (a to j)[a]

c_i parameters	Configuration type	Reduced parameters R_i[c]	Racah parameters	Original Griffiths parameters
$g_1=[uu\|uu]$	e^2	$R_1/2+R_2/4$	$A_e+4B_e+3C_e$	e
$g_2=[uv\|uv]$	e^2	$R_2/4$	$4B_e+C_e$	f
$g_3=[u\xi\|u\xi]$	$e^1t_2^1$	$R_5/4+R_6/12$	$B_{te}+C_{te}$	g
$g_4=[u\xi\|v\xi]$	$e^1t_2^1$	$(1/4\sqrt{3})$ (R_5-R_6)	$-\sqrt{3}B_{te}$	–h
$g_5=[uu\|\xi\xi]$	$e^1t_2^1$	$(1/\sqrt{6})R_3+(1/4\sqrt{3})R_4$	$A_{te}+2B_{te}+C_{te}$	$d+(2/\sqrt{3})c$
$g_6=[uv\|\xi\xi]$	$e^1t_2^1$	$R_4/4$	$2\sqrt{3}B_{te}$	c
$g_7=[\xi\xi\|\xi\xi]$	t_2^2	$R_7/3+(2/9)R_8$	$A_t+4B_t+3C_t$	a
$g_8=[\xi\eta\|\xi\eta]$	t_2^2	$R_9/6$	$3B_t+C_t$	j
$g_9=[\xi\xi\|\eta\eta]$	t_2^2	$R_7/3-R_8/9$	$A_t-2B_t+C_t$	b
$g_{10}=[\xi\eta\|u\zeta]$	–	$R_{10}/(3\sqrt{2})$	$-2\sqrt{3}B'$[b]	–2i

[a] $[ab|cd]=\int\int a(1)b(1)(1/r_{12})c(2)d(2)\, d\tau_1\, d\tau_2$.
[b] Value of B′ cannot be assigned to a given electronic configuration.
[c] Reduced matrix elements of interelectronic repulsion as defined by : $R_1=\langle e^2||a_1||e^2\rangle$; $R_2=\langle e^2||e||e^2\rangle$; $R_3=\langle e^2||a_1||t_2^2\rangle$; $R_4=\langle e^2||e||t_2^2\rangle$; $R_5=\langle et_2||t_1||et_2\rangle$; $R_6=\langle et_2||t_2||et_2\rangle$; $R_7=\langle t_2^2||a_1||t_2^2\rangle$; $R_8=\langle t_2^2||e||t_2^2\rangle$; $R_9=\langle t_2^2||t_2||t_2^2\rangle$; $R_{10}=\langle t_2^2||t_2||et_2\rangle$ [8].

In Table 2 we list expressions of the various SD for a d^2 complex of cubic symmetry using the two approaches, along with DFT values for the energies of all independent SD for the MO_4^z (M,z=Cr^{IV}, –4, Mn^V, –3 and Fe^{VI}, –2) model clusters.

1.3 Calculations of Multiplet Energies Using DFT

The wavefunction of multiplets arising from a given configuration is in general a linear combination of SD formed from the Kohn-Sham spin orbitals given by DFT. It follows that DFT calculations cannot yield multiplet energies directly. Following [7] the energy of a multiplet can be expanded in first order as a weighted sum of single determinant energies. The energy of a single determinant can be replaced by the corresponding statistical energy as obtained by the DFT. In order to illustrate the method, as a first example, we consider the singlet and triplet energies arising from an a^1b^1 configuration. While spin-unrestricted calculations with two up (+) spins, $|a^+b^+|$, yields directly the energy of the S=1, M_s=1 state, a calculation with one spin-up (+) and one spin-down (–), $|a^+b^-|$ (or equivalently $|a^-b^+|$) gives the average energy between the S=0 and S=1 with M_s=0 for both states:

$$E\left(|a^+b^+|\right) = E\left(ab\,^3B; M_s = 1\right) \tag{3}$$

$$E\left(|a^+b^-|\right) = (1/2)\left[E\left(ab\,^3B; M_s = 0\right) + E\left(ab, {}^1B\right)\right]$$

Table 2 Energy expressions for the DFT distinguishable Slater determinants of a d^2-configuration in cubic ligand field and their DFT energies for tetrahedral CrO_4^{4-}, MnO_4^{3-} and FeO_4^{2-} clusters (the energy of the $|\theta^+\varepsilon^+|$ ground state is taken at zero) using Kohn-Sham orbitals from a $e^{4/5}t_2^{6/5}$ SCF calculation. The energy expressions of each determinant within the conventional LFT model (B, C, 10Dq parameterization) and within an extended ligand field-model utilizing the 10 independent Griffiths parameters of interelectronic repulsion (g_i, i=1 to 10 and 10Dq) are also included

Slater determinant[b]	DFT energies			LF B, C, 10Dq model	Expression extended model (Griffith)
	CrO_4^{4-}	MnO_4^{3-}	FeO_4^{2-}		
$\|\theta+\theta-\|$, $\|\varepsilon+\varepsilon-\|$	1.571, 1.557	1.302, 1.293	1.006, 1.002	12B+3C	$3\ g_2$
$\|\theta+\varepsilon+\|$	0	0	0	0	0
$\|\theta+\varepsilon-\|$	0.379	0.311	0.241	4B+C	g_2
$\|\theta+\xi+\|$	1.564	1.732	1.754	9B+10Dq	$3\ g_2-g_3+(g_5-g_1)+10Dq$
$\|\theta+\xi-\|$	1.905	2.025	1.999	10B+C+10Dq	$3\ g_2+(g_5-g_1)+10Dq$
$\|\theta+\varsigma+\|$	1.154	1.397	1.508	10Dq	$3\ g_2-g_3+\sqrt{3}\ g_4+(g_5-g_1)-\sqrt{3}\ g_6+10Dq$
$\|\theta+\varsigma-\|$	1.506	1.707	1.780	4B+C+10Dq	$3\ g_2+(g_5-g_1)-\sqrt{3}\ g_6+10Dq$
$\|\varepsilon+\xi+\|$	1.288	1.507	1.589	3B+10Dq	$3\ g_2-g_3+(2/\sqrt{3})g_4+(g_5-g_1)-(2/\sqrt{3})g_6+10Dq$
$\|\varepsilon+\xi-\|$	1.633	1.809	1.851	6B+C+10Dq	$3\ g_2+(g_5-g_1)-(2/\sqrt{3})g_6+10Dq$
$\|\varepsilon+\varsigma+\|$	1.690	1.837	1.832	12B+10Dq	$3\ g_2-g_3-(1/\sqrt{3})g_4+(g_5-g_1)+(1/\sqrt{3})g_6+10Dq$
$\|\varepsilon+\varsigma-\|$	2.031	2.127	2.070	12B+C+10Dq	$3\ g_2+(g_5-g_1)+(1/\sqrt{3})g_6+10Dq$
$\|\xi+\xi-\|$	3.573	3.879	3.932	12B+3C+20Dq	$(g_7-g_1)+20Dq$
$\|\xi+\eta+\|$	2.471	2.894	3.075	3B+20Dq	$-g_8+(g_9-g_1)+20Dq$
$\|\xi+\eta-\|$	2.811	3.198	3.347	6B+C+20Dq	$(g_9-g_1)+20Dq$

[a] LDA calculations utilizing experimental metal-oxygen bond distances of 1.77 Å (Cr-O), 1.700 Å (Mn-O) and 1.650 Å (Fe-O).
[b] θ, ε, ξ, η and ζ are shorthand notations for the dz^2, dx^2-y^2, dyz, dxz and dxy orbitals.

From these equations the energy of $E_{S=0}(M_s=0)$ can be extracted as the weighted sum

$$E\,(ab\,^1B) = 2\,E\,(|a^+\,b^-|) - E\,(|a^+\,b^+|) \tag{4}$$

The situation becomes more involved when going to a TM complex with highly degenerate orbitals. However arguments presented earlier allow one to exploit fully the symmetry in order to simplify the relation between the multiplet splitting and SD energies. In general, we can write the multiplet wavefunction as

$$\psi_k = |\alpha\,\Gamma\,m_\Gamma\,S\,M_S> \tag{5}$$

where Γ and S denote the space and spin part of the wavefunction, respectively, and m_Γ and M_s denote their components in the case of degeneracy. The relation between multiplet first order energies, $E(\psi_k)$and the energies of some symmetry independent (non-redundant) SD $E(\varphi_\mu)$ is given by Eq. (6), where the coefficient $F_{k\mu}$ are the symmetry dependent weights.

$$E\,(\psi_k) = \sum_{(k)} F_{k\mu}\,E\,(\varphi_\mu) \tag{6}$$

Instead of representing the general theory (see [8] for more details) we consider an example, i.e. that of a d^2 configuration in a tetrahedral ligand field. Using symmetry-adapted wavefunctions listed elsewhere [13], the term energies can be expressed to first order as a function of the energies of the SD in Table 3 and of additional mixed terms (Table 3). These terms differ in two orbitals and can correspondingly be expressed in terms of the parameters of interelectronic repulsion for cubic symmetry g_2, g_3, g_4 and g_8 (see Appendix). From the expressions of the SD energies in terms of g_i (i=1 to 9) we can conversely write down g_2, g_3, g_4 and g_8 in function of the former ones (Eq. 7). We, thus, arrive after substitution for g_i to a weighted sum of SD: yielding the first order energy of each term in Table 3, where, for the sake of illustration, numerical values for CrO_4^{4-} are also included:

$$g_2 = E(\theta^+\,\varepsilon^-) = (1/3)\,E(\theta^+\,\theta^-) = (1/3)\,E(\varepsilon^+\,\varepsilon^-) \tag{7.1}$$

$$g_2 = E(\theta^+\,\xi^-) - E(\theta^+\,\xi^+) \tag{7.2}$$

$$g_4 = (\sqrt{3}/2)\,[E\,(\varepsilon^+\,\xi^+) - E(\theta^+\,\xi^+) + (2/3)\,E(\theta^+\,\xi^-) - (2/3)\,E(\theta^+\,\xi^-)] \tag{7.3}$$

$$g_8 = E(\xi^+\,\eta^-) - E(\xi^+\,\eta^+) \tag{7.4}$$

Two different problems deserve discussion here. First of all, we notice a small deviation from the symmetry conditions imposed by the high cubic symmetry. We note also that the $E(\theta^+\varepsilon^-)$, $E(\varepsilon^+\varepsilon^-)$ and $E(\theta^+\theta^-)$ are not symmetry independent, but are related by symmetry (Eq. 7.1); we note that the ground state determinant $E(\theta^+\varepsilon^+)$ is taken as reference. However, the energies of these SD determinants resulting from the DFT calculations deviate somehow from these conditions yielding very close, yet different energies for $\theta^+\theta^-$ and $\varepsilon^+\varepsilon^-$ (cf Table 2) and a ratio of $E(\theta^+\theta^-)/E(\theta^+\varepsilon^-)=4.14$ instead of 3. The violations from the redundancy (symmetry) conditions are due to the approximate character of the functionals in use. In Table 3 we used an adjusted value of g_2 given by Eq. (8) which corresponds to the best fit:

$$g_2^{eff} \approx (1/3)\,E(\theta^+\,\varepsilon^-) + (1/9)\,E(\theta^+\,\theta^-) + (1/9)\,E(\varepsilon^+\,\varepsilon^-) \tag{8}$$

Table 3 First order expressions for the electronic transition energy in terms of the DFT distinguishable Slater determinants (DDSD) of a d^2 system, their expressions in terms of B, C and 10Dq from DFT calculations, and the values of these energies for CrO_4^{4-} including CI in the case of the B, C, 10Dq model[a]

Electronic transition	First order expression in terms of DDSD	CrO_4^{4-} values	First order expressions B, C, 10Dq model	CrO_4^{4-} values		
				First order [b]	Full CI	Exp. [29]
$^3A_2(e^2) \rightarrow {}^1E(e^2)$	$(1/2)E(\theta^+\theta^-)+(1/2)E(\varepsilon^+\varepsilon^-)-g_2$	8,791	8B+2C	7,964	7,844	–
$\rightarrow {}^1A_1(e^2)$	$(1/2)E(\theta^+\theta^-)+(1/2)E(\varepsilon^+\varepsilon^-)+g_2$	16,436	16B+4C	15,928	13,412	14,730
$\rightarrow {}^3T_2(e^1t_2^1)$	$E(\theta^+\zeta^+)$	9,307	10Dq	8,847	8,847	9,087
$\rightarrow {}^3T_1(e^1t_2^1)$	$E(\varepsilon^+\zeta^+)$	13,630	12B+10Dq	13,971	12,892	13,887
$\rightarrow {}^1T_2(e^1t_2^1)$	$E(\theta^+\zeta^-)+g_3-\sqrt{3}\,g_4$	14,767	8B+2C+10Dq	16,811	16,580	–
$\rightarrow {}^1T_1(e^1t_2^1)$	$E(\varepsilon^+\zeta^-)+g_3+g_4/\sqrt{3}$	19,170	12B+2C+10Dq	18,519	18,519	–
$\rightarrow {}^1A_1(t_2^2)$	$E(\xi^+\xi^-)+2\,g_8$	34,300	18B+5C+20Dq	36,750	39,265	–
$\rightarrow {}^1E(t_2^2)$	$E(\xi^+\xi^-)-g_8$	26,074	9B+2C+20Dq	26,085	26,204	–
$\rightarrow {}^3T_1(t_2^2)$	$E(\xi^+\eta^+)$	19,929	3B+20Dq	18,975	20,053	–
$\rightarrow {}^1T_2(t_2^2)$	$E(\xi^+\eta^-)+g_8$	25,413	9B+2C+20Dq	26,085	26,314	–

[a] Calculation for CrO_4^{4-} with a R(Cr-O) bond distance (1.77 Å) taken from experiment.
[b] DFT best fit B, C and 10Dq values of 427 cm^{-1}, 2274 cm^{-1} and 8847 cm^{-1}, respectively.

The second problem inherent in Table 3 is the neglect of configuration interaction between terms of the same symmetry. Such mixing does appear, e.g. for the $^3T_1$ and $^1T_2$ terms due to CI; we have to consider 2×2 matrices rather than first order (diagonal) matrix elements. The off-diagonal mixing terms cannot be obtained from Coulomb and exchange integrals and are thus not amenable in the SD DFT approach. An attempt to introduce this second order correction using Kohn-Sham orbitals has lead to rather large (non-screened) electrostatic matrix elements [14]. Utilizing the formalism described in the next section, we note that off-diagonal terms are crucial in the case of the $^1A_1$ and $^3T_1$ terms. The account of the CI mixing for these terms leads to a better agreement between theory and experiment (Table 3) as will be shown below.

2 The LFDFT Theory

2.1 Cubic $d^{2(8)}$ Systems

We present the main ideas behind our approach using a simple example, that of a d^2 TM in a tetrahedral coordination. Recalling the effective nature of LF Hamiltonian we can write down equations for all SD energies in terms of the parameters B, C and 10Dq. Thus we obtain a system of 45 linear equations with 3 unknown parameters (Eq. 9). We note that only 15 SD energies are different at the DFT level (Table 2); however we take all 45 equations into account. In doing so, we provide a better statistical weight for those SD which have the same energy. In addition, an arbitrary shift of all DFT energies compared to the LF for each SD energy has to be considered due to the different gauge origins. This is most elegantly done by introducing one additional regression coefficient. This yields a system of over-determined linear equations (Eq. 9), where $\underline{X}$ stores the ligand field parameters, $\underline{E}$ the energies of the SD and **A** the coefficients of the linear relation between E and X. This system has to be solved in the least square sense (Eq. 10) to obtain B, C, 10Dq:

$$\underline{E} = \mathbf{A}\underline{X} \tag{9}$$

$$\underline{X} = (\mathbf{A}^T\mathbf{A})^{-1}\,\mathbf{A}^T\underline{E} \tag{10}$$

For CrO_4^{4-} we get B=427 cm^{-1}, C=2274 cm^{-1} and 10Dq=8847 cm^{-1}. A comparison between the SD energies calculated using B, C and 10Dq values with the DFT data shows a nice fit (Fig. 1) with a rather small standard deviation (StDev=0.039 eV). This result illustrates the consistency between the DFT formalism and the parameterization by LF theory. DFT values of B, C and 10Dq have been introduced into an LF program which takes account of configuration interaction (CI) within the LF manifold. The results from these calculations have the advantage that both dynamical (via the DFT) and non-dynamical correlation (via the CI) are taken into account. It follows that the present approach is superior to the usual procedure in which multiplet energies from DFT calculations being confined to a given configuration neglect CI mixing with terms of the same symmetry (see above).

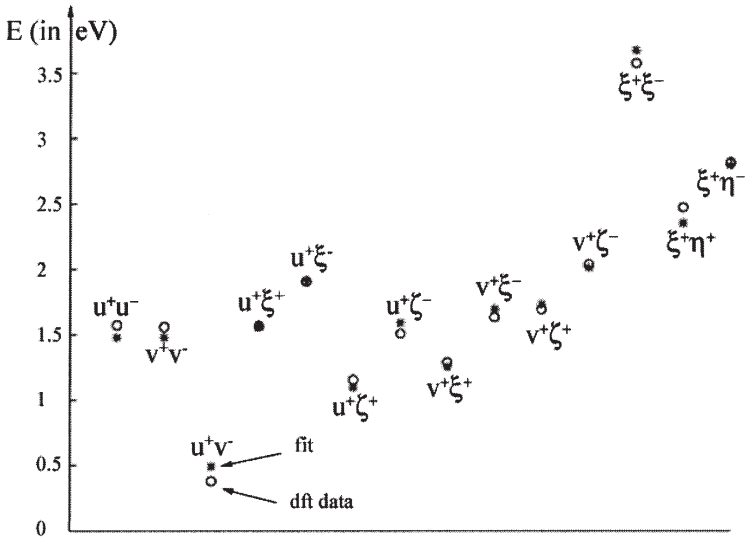

Fig. 1 Calculated (DFT-LDA, *circles*) and reproduced (using best fit B=427 cm^{-1}, C=2274 cm^{-1}, 10Dq=8847 cm^{-1}, *stars*) values of the SD energies of CrO_4^{4-} (R_{Cr-O}=1.77 Å), the energy of the $\varepsilon^+\theta^+$ is taken as energy reference

To generate the Kohn-Sham (KS) orbitals needed in the calculations of the SD energies we use a spin-restricted self-consistent field (SCF) calculation of the average over the whole d^n configurations – we occupy each d-orbital (as recognized as such by the dominating d-character in a population analysis) with n/5 electrons. In doing so, we ensure a good starting approximation; here we comply with the spherical symmetry inherent when approximating matrix elements of G(i,j) in terms of B and C; we thus assign any energetic effect due to deviation of the LF orbitals from the spherical symmetry to contributions to the one-electron, LF matrix h_{ab} [15]. This recipe is consistent with the prerequisites of the LF approach, where orbital relaxation is only taken into account at the level of averaging the electron density to provide proper LF orbitals, while all SD energies for latter LF treatment are calculated without SCF iteration (see the analysis in [15]).

The G_{abcd} Coulomb matrix elements do not change on going from two electrons (d^2) to two holes (for a d^8 complex), while those of the LF h_{ab} change their sign. The same expressions in Table 2 also apply for $d^{2(8)}$ octahedral complexes with a sign reversion of 10Dq from T_d to O_h. A summary of sign-relations between $d^{2(8)}$ and T_d and O_h is given in Eq. (11):

$$(10Dq)\,T_d, d^2 = -\,(10Dq)\,T_d, d^8 = -\,(10Dq)\,O_h, d^2 = (10Dq)\,O_h, d^8 \qquad (11)$$

2.2 Cubic $d^{3(7)}$, $d^{4(6)}$ and d^5 Systems

The procedure just described has also been extended to $d^{3(7)}$, $d^{4(6)}$ and d^5 TM complexes. The 120, 210 and 252 SD that result for these configurations have been ex-

pressed in terms of 10Dq and B, C. A best fit minimizing least square deviations between DFT and calculated SD energies following Eq. (10) has been performed for each case, yielding values of B, C and 10Dq; standard deviations have been used to check the consistency of the parametric model in each case. The procedure has been implemented in a series of programs written in MATLAB 6.1 [16]. Resulting values of the model parameters have been used in combination with our favourite LF program to yield all multiplet energies of a given complex. Electronic transition energies calculated in such a way have been compared with experimental data from literature. In an independent step, B, C and 10Dq fitted directly to experimental LF transition energies (which we call "experimental") have been compared with the DFT ones.

2.3 Generalization to Low Symmetric LF and Poly-Nuclear TM Complexes

A comparison of 10Dq values, obtained from a best fit to DFT SD [10Dq(DFT)] energies with KS-LF orbital energy differences [10Dq(KS)=ε_{t2}-ε_e, in T_d] leads to the following result: 10Dq(DFT) is accurately approximated (within an error of less than 2%!) by 10Dq(KS). The reason for this is as follows; using the theory developed by Slater [17] we can expand the total energy $\langle E \rangle$ in a series of occupation number changes around the energy of a reference configuration which we denote by $\langle E \rangle_o$:

$$\langle E \rangle = \langle E \rangle_0 + \sum_{(i)} (\partial E/\partial n_i)_0 dn_i + (1/2) \sum \sum_{(i,j)} (\partial^2 E/\partial n_i \partial n_j)_0 dn_i dn_j \tag{12}$$

Following Janack's [18] theorem, the derivative $(\partial E/\partial n_i)_o$ equals the energy of the KS orbital i, ε_i. This theorem is intrinsic of DFT; it is valid as long as the exchange-correlation potential V_{XC} equals $(\partial E_{XC}[\rho]/\partial\rho)$, the functional derivative of the exchange-correlation energy, E_{XC} vs the density ρ. The second derivative $(\partial^2 E/\partial n_i \partial n_j)_o$ of the total energy vs the occupation of KS orbitals i and j can be identified with the Coulomb interaction energy between electrons occupying i and j, G_{ijij} and similarly $G_{iiii(jjjj)}=(\partial^2 E/\partial n_{i(j)}^2)_o$. Considering a tetrahedral d^2 complex, we start from a $e^{4/5}t_2^{6/5}$ configuration as reference one ($n_e{}^o=4/5$, $n_{t2}{}^o=6/5$); with $dn_e{}^o=6/5$, $dn_{t2}{}^o=-6/5$ (ground state occupation leading to the energy $\langle E \rangle_{gr.st}$) and with $dn_e{}^o=+1/5$, $dn_{t2}{}^o=-1/5$ (excited state occupation leading to the energy $\langle E \rangle_{ex.st.}$) we obtain after substitution in Eq. (12):

$$\langle E \rangle_{gr.st} = (6/5)\varepsilon_e - (6/5)\varepsilon_{t2} + (6/5)^2 [(1/2) G_{ee} + (1/2) G_{t2t2} - G_{t2e}] \tag{13}$$

$$\langle E \rangle_{ex.st} = (1/5)\varepsilon_e - (1/5)\varepsilon_{t2} + (1/5)^2 [(1/2) G_{ee} + (1/2) G_{t2t2} - G_{t2e}]$$

This yields for the energy of the $e \rightarrow t_2$ electronic transition, $(\Delta E, T_d)e \rightarrow t_2$:

$$(\Delta E, T_d)\ e \rightarrow t_2 = (\varepsilon_{t2} - \varepsilon_e) - (7/5) [(1/2) G_{ee} + (1/2) G_{t2t2} - G_{t2e}] \tag{14}$$

Numerical calculations show that G_{ee}, G_{t2t2} and G_{t2e} are very close in energy such that the second term in Eq. (14) vanishes to a good approximation. We have observed that for the $d^{3(7)}$, $d^{4(6)}$ and d^5 configurations in T_d and O_h geometries, the 10Dq parameters obtained by least squares is approximately equal to the differ-

ence between the corresponding KS orbital energies. This result enables us to approximate the h_{ab} LF matrix in making use of the five KS orbitals with dominant metal character and effective Hamiltonian theory [19]. That is, we can extract from the matrix of the average-of-configuration (AOC) KS orbitals a 5×5 matrix containing the MO coefficients of the d-functions corresponding to the five MOs with dominant metal character. Let us denote this matrix by **U** and the diagonal matrix containing the energy of the ligand field levels (obtained in the fitting procedure) by $\mathbf{\Lambda}$. From there we can generate an effective LF Hamiltonian. We introduce the overlap matrix **S** (Eq. 15):

$$\mathbf{S} = \mathbf{U}\mathbf{U}^T \tag{15}$$

One can easily find $\mathbf{S}^{\pm(1/2)}$ using the following recipe and get eigenvalues $\mathbf{\Lambda}_s$ (diagonal) and eigenvectors (in columns) $\mathbf{U}_s$ matrices. $\mathbf{S}^{-(1/2)}$ is then given by Eq. (16). As has been shown by Des Cloizeaux [20] the effective LF matrix $\mathbf{h}=\{h_{ab}\}$ (a,b run over the five d-orbitals) is given by Eq. (17):

$$\mathbf{S}^{-(1/2)} = \mathbf{U}_s \Lambda_s^{-(1/2)} \mathbf{U}_s^T \tag{16}$$

$$\mathbf{h} = \mathbf{S}^{-(1/2)} \mathbf{U}\Lambda\mathbf{U}^T \mathbf{S}^{-(1/2)} \tag{17}$$

The effective d-eigenvectors given by the columns of matrix **C** (Eq. 18):

$$\mathbf{C} = \mathbf{S}^{-(1/2)} \mathbf{U} \tag{18}$$

can be used to express each SD energy in terms of the parameters B and C yielding linear equations for these parameters similar to Eq. (9). Let us denote KS spin-orbitals by $\chi_i\sigma_i$ (σ_i=α,β) and eigenvalues by ε_i. The energy of $SD_k=|(\chi_i\sigma_i)(\chi_j\sigma_j)|$ is given by

$$E(SD_k) = e_0 + \varepsilon_i + \varepsilon_j + J_{ij} - K_{ij}\delta_{\sigma i \sigma j} \tag{19}$$

where, again, an arbitrary energy is introduced and handled as described earlier. Taking the expression for $\chi_{i(j)}$ (Eq. 20) and substituting into Eq. (19) we obtain a linear equation for B and C (Eq. 21); here β_{ij} and γ_{ij} are calculated according Eq. (22), using $c_{\mu i}$ coefficients and the $\beta_{\mu\nu\lambda\rho}$ and $\gamma_{\mu\nu\lambda\rho}$ as defined by the two-electron integrals for pure d-orbitals (see Appendix):

$$\chi_{i(j)} = \sum c_{\mu i(j)} d_\mu \tag{20}$$

$$E(SD_k) - e_0 - \varepsilon_i - \varepsilon_j = \beta_{ij}(k)\,B + \gamma_{ij}(k)\,C \tag{21}$$

$$\beta_{ij}(k) = \sum_\mu \sum_\nu \sum_\lambda \sum_\varrho c_{\mu i} c_{\nu j} c_{\lambda i} c_{\varrho j} (\beta_{\mu\nu\lambda\varrho} + \delta_{\sigma i \sigma j}\beta_{\mu\nu\varrho\lambda}) \tag{22}$$
$$\gamma_{ij}(k) = \sum_\mu \sum_\nu \sum_\lambda \sum_\varrho c_{\mu i} c_{\nu j} c_{\lambda i} c_{\varrho j} (\gamma_{\mu\nu\lambda\varrho} + \delta_{\sigma i \sigma j}\gamma_{\mu\nu\varrho\lambda})$$

The 5×5 h_{ab} matrix and the parameters B and C have been given as input parameters for our favourite LF program. In a conventional LF treatment the h_{ab} LF matrix is constructed within the AOM specifying AOM parameters and angular geometries. The present approach allows one to circumvent such a procedure, which becomes rather complex and unsolvable without access to spectra in high-resolution or in complexes requiring consideration of a high number of AOM parameters and/or more than one ligand.

Finally, we notice that the theory developed here is not restricted to mononuclear complexes. A case study of the electronic properties of extended clusters in spinels including Mn^{IV} and mixed valence Mn^{IV}/Mn^{III} demonstrated the utility of the approach for polynuclear complexes as well [21]. In addition, introducing low symmetry and spin-orbit coupling will allow one to study the effect of fine-structure tensors in EPR and MCD thus extending the applicability of the approach to metal-sites in enzymes and bio-molecules. Such studies are in progress.

2.4 A Hybrid LFDFT Model for Cubic Symmetry (HLFDFT)

Going to the parameterization of interelectronic repulsion integrals in cubic symmetry in terms of the Griffith's parameters g_i(i=1 to 10) [12] (Table 1) we note the SD energies depend only upon 9 of them (g_{10} has no influence on the SD energies, it appears only in off-diagonal matrix element between SD). Moreover, if we consider both the electrostatic and the ligand field contributions to the SD energies, it turns out that the latter one parallels exactly the contribution inherent to g_1 (g_1=$\langle\theta\theta|\theta\theta\rangle$ parallels ε_e) and to g_7(g_7=$\langle\xi\xi|\xi\xi\rangle$ parallels ε_t), the rank of the **A** matrix (Eq. 9) being 9 instead of 11 (g_1–g_9, ε_e and ε_t). That is, the two column vectors corresponding to the ligand field (ε_e and ε_t) are simultaneously in the range of the subspace spanned by the electrostatic part (g_1 and g_7). Carrying out a rank analysis of the **A** matrix along with a singular value decomposition indicate that two additional g-parameters, g_1 and g_7 cannot be determined simply by the fitting procedure described in the two previous sections. Thus, we turn to DFT to estimate g_1 and g_7 (Eqs. 23 and 24) independently:

$$g_1 = U_{\theta\theta\theta\theta} = (\partial^2 E/dn_\theta^2)_0 = (\partial\varepsilon_e/\partial n_\theta)_0 \tag{23a}$$

$$g_1 = A_e + 4B_e + 3C_e \tag{23b}$$

$$g_7 = U_{\xi\xi\xi\xi} = (\partial^2 E/dn_\xi^2)_0 = (\partial\varepsilon_e/\partial n_\xi)_0 \tag{24a}$$

$$g_7 = A_t + 4B_t + 3C_t \tag{24b}$$

and to introduce them as constants into our least square model. The value of the parameter g_{10} which we need in order to set up the CI problem will be approximated using Eq. (25) and the B value from our LFDFT calculations:

$$g_{10} = -2\sqrt{3}B \tag{25}$$

Thus, we end up with a hybrid model (HLFDFT) which utilizes information from DFT allowing to fix the parameters g_1, g_7 and g_{10}.

Accounting for the cubic symmetry of the parameters of G we also arrive at an interpretation of 10Dq (HLFDFT) as one electron parameter, which is not the case for 10Dq (LFDFT) in the LFDFT model, where it is a measure for the energy difference between $^3T_2$ and $^3A_2$ (for cubic d^2) system and is thus to be interpreted as a many electron quantity. Calculations show that 10Dq (HLFDFT) is by 1–2% larger than 10Dq (LFDFT). It follows that the treatment of 10Dq(LFDFT) as a one-electron quantity (as is done in classical LF theory) is still a good approximation.

2.5
Computational Details

All DFT calculations have been performed using the ADF program package [22]. The approximate SCF KS one-electron equations are solved by employing an expansion of the molecular orbitals in a basis set of Slater-type orbitals (STO). All atoms were described through triple-ς STO basis sets given in the program database (basis set IV) and the core-orbitals up to 3p for the TM and up to 1 s (for O, N, C, F), 2p (Cl), 3d (Br) and 4d (I) were kept frozen. In order to study the sensitivity of our results with respect to the adopted functionals we used the local density approximation (LDA), where exchange-correlation potential and energies have been computed according to the Vosko, Wilk and Nusair's (VWN) [23] parameterization of the electron gas data. We also checked gradient corrected functionals. Within the generalized gradient approximation (GGA) we decided to apply the Becke-Perdew (BP) functional, which uses Becke's gradient correction to the local expression of the exchange energy [24] and Perdew's gradient correction to the local expression of the correlation energy [25].

It is known for complexes possessing a high negative charge, such as CrO_4^{4-}, that geometry optimisations using the GGA usually lead to metal-ligand distances which are too large compared to experiment [26]. In such cases we confined our analysis to LDA functionals only. For the neutral CrX_4 (X=F, Cl, Br, I) clusters, however, both LDA and GGA have been used and comparable results were obtained. SCF calculations for all d^n ions, assuming an n/5 occupancy, converged in all cases except for CrO_4^{4-} and MnO_4^{3-}. In the latter clusters a "ghost" a_1 orbital dominated by a metal s-orbital was found to be located above the ligand valence-band edge, but lower in energy than the metal d-orbitals. Convergence is only achieved in these cases by preventing electrons to populate that orbital. The population of the "ghost" a_1 orbital is directly related to the basis set superposition error (BSSE) allowing diffuse ligand orbitals to be described through a diffuse metal s function. As has been shown in [27] removing this diffuse metal s-function leads to a better description for ionic systems with highly negative charges: the ghost orbital disappears and the description of the d-d transitions is improved.

Multiplet energies in complexes of cubic (and also lower symmetry, see earlier) have been calculated utilizing the program package AOMX [28]. At the input we define the LF matrix, B and C as given by our LFDFT procedure, at the output all multiplet energies and symmetries can be obtained. In addition, ligand field parameter values from a fit to experimental LF transition have been calculated, to be compared with those from our DFT analysis.

3
Applications of the Theory

3.1
Tetrahedral d^2 Oxoanions of Cr^{IV}, Mn^{V}, Fe^{VI} and CrX_4 ($X=F^-$, Cl^-, Br^-, I^-)

Tetrahedral d^2 complexes possess a $^3A_2(e^2)$ ground state and $^3A_2 \rightarrow {}^3T_2$ and $^3A_2 \rightarrow {}^3T_1$ $e \rightarrow t_2$ singly excited states. They give rise to broad d-d transitions in the

Table 4 Electronic transition energies in CrO_4^{4-}, MnO_4^{3-} and FeO_4^{2-} oxo-anions calculated using values of B, C and 10Dq as obtained from a fit to DFT energies for LDA geometrically optimized clusters (LDA R_{opt}), for T_d geometries with metal-ligand distances from experiment (LDA R_{exp}), from an AOM fit to experimental transition energies (AOM fit) and experiment (Exp.). Values of B, C and 10Dq and mean square deviations (StDev) between DFT and fitted energies (for LDA R_{opt} and LDA R_{exp}) are listed for each entity. The values of $(10Dq)_{orb}$ as deduced from the 4 t_2-2e Kohn-Sham orbital energy difference taken from the $2e^{0.8}4\ t_2^{1.2}$ SCF Kohn-Sham energies are also listed

Term	CrO_4^{4-}				MnO_4^{3-}				FeO_4^{2-}			
	LDA R_{opt}	LDA R_{exp}	AOM fit	Exp.	LDA R_{opt}	LDA R_{exp}	AOM fit	Exp.	LDA R_{opt}	LDA R_{exp}	AOM fit	Exp.
$^3A_2(e^2)$	0	0	0	–	0	0	0		0	0	0	–
$^1E(e^2)$	7838	7844	8904	–	6560	6583	8537	8432[g]	5179	5197	5712	6215[b]
$^1A_1(e^2)$	13,136	13,412	15,276	14,730 [f]	11,546	11,698	14,633	–	9369	9446	10,605	9118[b]
$^3T_2(e^1t_2^1)$	7315	8847	8949	9087 [f]	9837	10,872	10,515	10,380[g]	11,259	11,952	12,939	12,940[b]
$^3T_1(e^1t_2^1)$	11,125	12,892	13,714	13,887 [f]	13,408	14,512	14,790	14,266[g]	13,936	14,645	16,936	17,700[b]
$^1T_2(e^1t_2^1)$	15,019	16,580	17,677	–	16,329	17,393	18,956	–	16,408	17,121	18,589	–
$^1T_1(e^1t_2^1)$	17,047	18,519	20,271	–	17,857	18,908	20,875	–	17,437	18,146	20,215	–
$^1A_1(t_2^2)$	36,567	39,265	42,471	–	37,278	39,268	44,416	–	36,109	37,491	40,514	–
$^1E(t_2^2)$	23,203	26,204	27,754	–	26,726	28,804	30,202	–	28,000	29,401	32,092	–
$^3T_1(t_2^2)$	17,359	20,053	21,459	–	21,309	23,309	23,203	23,430[g]	23,470	24,841	27,505	–
$^1T_2(t_2^2)$	23,337	26,314	27,930	–	26,794	28,866	30,298	–	28,030	29,429	32,154	–
R(M–O)	1.868	1.77[c]	–	–	1.746	1.700[d]	–	–	1.674	1.65[e]	–	–
B	436	427	555	–	347	347	430	–	242	242	375	–
C	2250	2274	2331	–	1928	1936	2600	–	1637	1645	1388	–
10Dq	7315	8847	8950	–	9831	10,872	10,515	–	11,259	11,952	12,938	–
StDev	0.036	0.039	–	–	0.025	0.027	–	–	0.016	0.016	–	–
$(10Dq)_{orb}$	7363	8831	–	–	9984	11025	–	–	11,436	12130	–	–

[a] St Dev=$\sqrt{(\Sigma\ [E_i(fit)-E_i(DFT)]^2)/(N-1)}$, N=45.
[b] Brunold TC,Hauser A, Guedel HU (1994) J.Lumin 59:321.
[c] [31].
[d] [30].
[e] Estimated as a sum of ionic radii of Fe^{VI} (0.25 Å)and O^{-II} (1.40 Å), Shannon RD (1976) Acta Cryst. A32:751.
[f] [29].
[g] [30].

Table 5 Electronic transition energies of CrX_4, X=F^-, Cl^-, Br^- and I^- ions with geometries optimized using LDA and GGA functionals calculated using values of B, C and 10Dq from least square fit to DFT energies of the Slater determinants. The values of $(10Dq)_{orb}$ as deduced from the 4 t_2-2e Kohn-Sham orbital energy difference taken from the $2e^{0.8}4\,t_2^{1.2}$ SCF Kohn-Sham energies are also listed. Experimental transition energies for $CrCl_4$ and $CrBr_4$ as well as values of B, C and 10Dq deduced from a fit to experiment for $CrCl_4$ are also included

Term	CrF_4		$CrCl_4$				$CrBr_4$			CrI_4	
	LDA	GGA	LDA	GGA	LF–fit	Exp.[a]	LDA	GGA	Exp.[a]	LDA	GGA
$^3A_2(e^2)$	0	0	0	0	0	0	0	0	0	0	0
$^1E(e^2)$	8583	9092	6542	7101	6089	–	6373	6832	6666	5986	6514
$^1A_1(e^2)$	14,804	15,630	11,114	11,971	10,586	–	10,698	11,364	10,869	9921	10,705
$^3T_2(e^1t_2^1)$	10,259	9677	7008	6524	7010	7250	6163	5605	–	5267	4781
$^3T_1(e^1t_2^1)$	14,825	14,571	10,316	10,062	10,440	10,000	9269	8820	–	8054	7663
$^1T_2(e^1t_2^1)$	18,723	18,608	13,454	13,489	12,991	12,000	12,434	12,295	–	11,151	11,146
$^1T_1(e^1t_2^1)$	20,875	21,141	15,074	15,456	14,718	–	14,037	14,215	–	12,659	13,021
$^1A_1(t_2^2)$	43,965	44,352	32,099	32,891	30,599	–	30,120	30,531	–	27,416	28,198
$^1E(t_2^2)$	29,834	29,354	21,121	20,878	20,716	–	19,271	18,777	–	17,070	16,819
$^3T_1(t_2^2)$	23,091	22,681	16,033	15,795	16,229	16,666	14,424	14,043	13,258	12,591	12,486
$^1T_2(t_2^2)$	29,953	29,516	21,217	21,014	20,822	–	19,373	18,920	–	17,172	16,969
R(M–X)	1.710	1.735	2.104	2.144	–	–	2.264	2.318	–	2.489	2.547
B	476	548	355	419	376	–	347	403	–	323	387
C	2452	2444	1903	1952	1579	–	1855	1887	–	1758	1798
10Dq	10,259	9678	7008	6524	7250	–	6162	5605	–	5266	4782
StDev	0.034	0.043	0.030	0.039	–	–	0.030	0.038	–	0.032	0.033
$(10Dq)_{orb}$	10,549	9928	7258	6686	–	–	6371	5726	–	5605	4984

LDA and GGA optimized geometries correspond to stable minima in the ground state potential surface with harmonic (GGA) frequencies of the α_1, ε, $\tau_2(1)$ and $\tau_2(2)$ vibrational modes of 678, 180, 186 and 758 cm^{-1} (for CrF_4); 359, 113,126 and 464 cm^{-1} (for $CrCl_4$); 207, 63, 82 and 350 cm^{-1} (for $CrBr_4$); 141, 49, 61 and 295 cm^{-1} (for CrI_4),respectively.

[a] Studer P (1975) Thesis, University of Fribourg.

optical spectra. In addition, spin-flip transitions within the e^2 configuration lead to sharp line excitations. Multiplet energies from LDA agree within 2,000 cm^{-1} with experimental data (Table 4) supposed that use is made of experimental rather than of LDA optimised M-O bond lengths. In particular the $^3A_2 \rightarrow {}^3T_2$ transition energy and thus 10Dq nicely agrees with experiment. LDA optimised M-O bond lengths are larger than the experimental values. This becomes increasingly pronounced with increasing anionic charge from FeO_4^{2-} (0.02 Å) MnO_4^{3-} (0.05 Å) and CrO_4^{4-} (0.1 Å). This is reflected in the values of 10Dq which are distinctly smaller than 10Dq from experiment (by 1680, 680 and 1600 cm^{-1}, respectively). B and C parameters from DFT (LDA) are by 20–35% smaller than those deduced from a fit to observed LF transitions. Thus the $^3A_2 \rightarrow {}^3T_1$ and the spin-forbidden $^3A_2 \rightarrow {}^1E$, $^1A_1$ transitions, being sensitive to B and C, respectively, are underestimated by DFT (LDA) by 15–20%.

In order to study the effect of the adopted functional we calculated multiplet energies of CrX_4 ($X=F^-, Cl^-, Br^-, I^-$) (Table 5). On going from the LDA to the gradient corrected GGA we get a lengthening of the geometry optimised Cr-X bond distances accompanied with a decrease of the value of 10Dq. On the other hand the value of B increases by 15–20% going from the LDA to the GGA functional.

In order to study the effect of the $R_3 \rightarrow T_d$ symmetry lowering on U_{abcd}, we plotted in Fig. 2 transition energies for CrO_4^{4-} resulting from the LFDFT and HLFDFT models. An inspection of Table 2 shows that the $^3A_2 \rightarrow {}^3T_2$ energy depends on g_i in the HLFDFT model as different to LFDFT where it is identical to 10Dq. It is seen from Fig. 2 that upon symmetry lowering from R_3 to T_d interelectronic repulsion (IR) terms lead to a positive contributions to the $^3A_2 \rightarrow {}^3T_2$ energy. As expected, based on the 20Dq dependence of the $^3A_2(e^2) \rightarrow {}^3T_1(t_2^2)$ transition its energy is affected even stronger by this effect. Accounting for the symmetry lowering of the

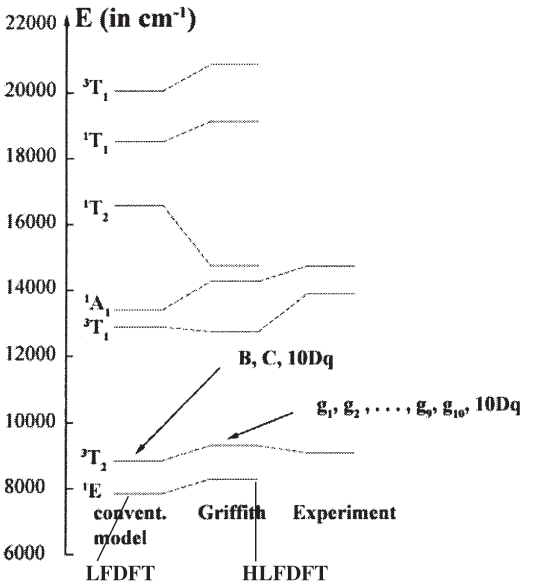

Fig. 2 Transition energies of CrO_4^{4-} (d^2) calculated using LFDFT, HLFDFT and taken from experiment-averaging over the split components

IR terms also leads to an increase of the $^3A_2 \rightarrow {}^1E$ and $^3A_2 \rightarrow {}^1A_1$ energies. This improves the agreement between theory and experiment for the latter transition. Similar observations have been made also for the MnO_4^{3-} and FeO_4^{2-} ions.

3.2
Low-Symmetry Distortions: CrO_4^{4-} (C_s) and MnO_4^{3-}(D_{2d})

As follows from reported spectra, CrO_4^{4-} and MnO_4^{3-} chromophores in Cr^{IV} and Mn^{V} doped Ca_2GeO_4 (olivine) [29] and Sr_2VO_4Cl (spodiosite) [30] host lattices deviate significantly from the cubic geometry. The CrO_4^{4-} spectra are consistent with a trigonal distortion superimposed by a symmetry lowering to C_s, while MnO_4^{3-} presents a D_{2d} compressed tetrahedron. In the analysis of spectra in high resolution it was assumed that Cr^{IV} [29] and Mn^{V} [30] adopt the geometries of the host sites which is expected for the $^3A_2$ orbitally non-degenerate ground state. The GeO_4^{4-} host site possesses a trigonal distortion with O_{eq}-Ge-O_{ax} angles which are by 6.2° larger and O_{eq}-Ge-O_{eq} bond angles which are by 6.8° smaller than the tetrahedral angle (109.47°). A C_s distortion finally leads to O_{eq}-Ge-O_{ax} angles of 115.9×2, 115.3×1 and O_{eq}-Ge-O_{eq} of 101.8×2, 104.3°. Ge-O bond distances are not altered much (Ge-O_{ax} 1.748 Å Ge-O_{eq} 1.785×2, 1.777×1 Å). The VO_4^{3-} tetrahedra in Sr_2VO_4Cl shows a tetragonal compression by 3.7° [30].

LDA energies of electronic transitions calculated adopting these geometries are plotted in Figs. 3 and 4 for CrO_4^{4-} and MnO_4^{3-}, respectively. In these figures we compare our results with calculations where we approximated the geometry as tetrahedral and with calculations where we use the AOM with LF parameters fitted to the experimental spectra [29]. Concerning CrO_4^{4-} both the DFT and the

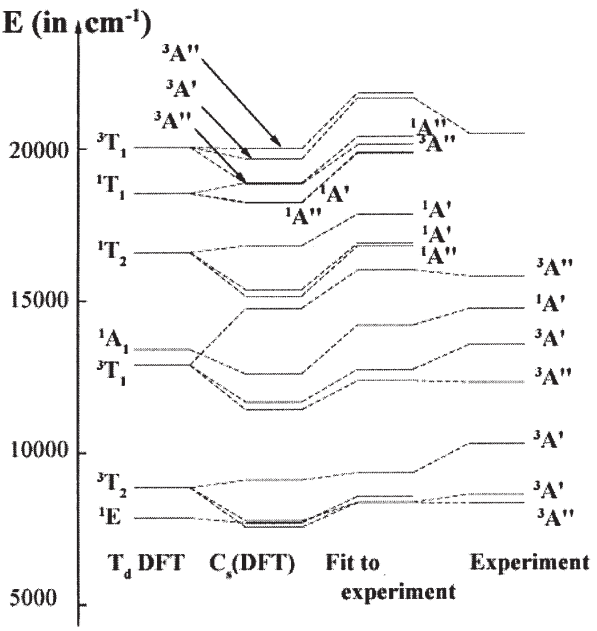

Fig. 3 DFT treatment of low-symmetry splitting for the CrO_4^{4-}, effect of angular distortion C_{3v} + C_s (host lattice in $CaGeO_4$: Cr^{4+}). The experimental data come from the work of Güdel et al. [29]

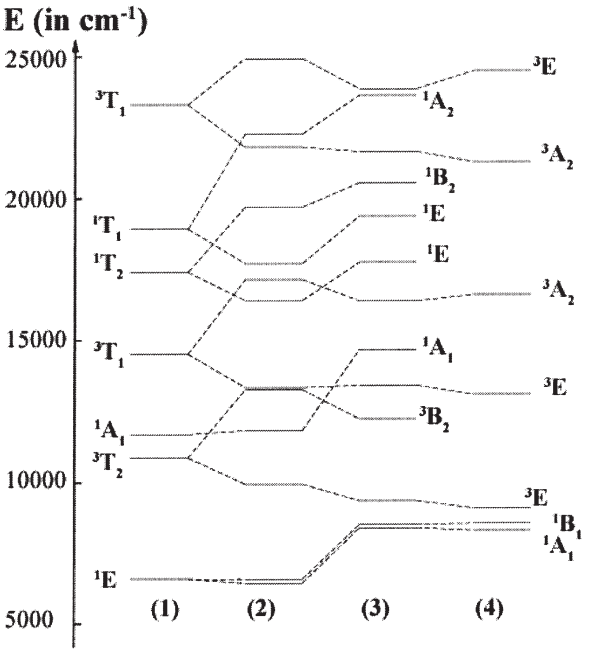

Fig. 4 DFT treatment of low-symmetry splitting, example MnO_4^{3-} (d^2): **1** geometry T_d, LDA, experimental R_{ML}; **2** D_{2d} distorted experimental geometry LDA (Sr_2VO_4Cl host lattice: MnO_4^{3-}); **3** AOM fit of B, C, e_σ and e_π to the experiment, Atanasov M, Adamsky H, Reinen D (1996) Chem Phys 202, 155; **4** experimental spectrum: Milstein JB, Holt SL (1969) Inorg Chem 8:1021; Milstein JB, Ackerman J, Holt SL, McGarvey BR (1972) Inorg Chem 11:1178; Oetliker U, Herren M, Güdel HU, Kesper U, Albrecht C, Reinen D (1994) J Chem Phys 100:8656

AOM treatments lead to splitting pattern which are very similar and compare reasonable with experiment. The C_s splitting manifested in the spectrum is somewhat larger compared to that calculated using LFDFT and the fit of the transition energies from experiment using the AOM yields a similar result. Possibly, when entering the Ca_2GeO_4 host, Cr^{4+} leads to slight modification of the host site geometry. A good agreement between calculated and experimental transition energies is also obtained for MnO_4^{3-} (Fig. 4). We can conclude that the LFDFT model supplemented with a low-symmetric LF-Hamiltonian constructed following the recipes given earlier can properly account for the low-symmetric spectral patterns.

3.3 Octahedral Cr^{III} d^3 and Co^{II} d^7 Complexes

In Tables 6 and 7 we list multiplet energies for the CrX_6^{3-} (X=F^-, Cl^-, Br^-, CN^-) and d^7 CoX_6^{4-} (X=F^-, Cl^-, Br^-) complexes. We use a LDA functional and optimised Cr^{III}-X and Co^{II}-X bond lengths and compare these results with energies from an LF calculation utilizing values of B, C and 10Dq obtained from a best fit to the spectra. In lines with our results from earlier, LDA bonds lengths are too long while values of 10Dq are too small compared to experiment. The situation improves again (see above) if instead of optimised, experimental bond lengths are taken for the calculation (see $CoCl_6^{4-}$ in Table 7). Even in this case, spin-forbidden transitions come out by 3000–4000 cm^{-1} too low in energy compared to experiment. For the $Cr(CN)_6^{3-}$ we note an LDA value of 10Dq which is by 4000 cm^{-1}

Table 6 Electronic transition energies of CrX_6^{3-}, X=F^-,Cl^-,Br^- and CN^- complexes with geometries optimized using LDA functionals calculated using values of B, C and 10Dq from least square fit to DFT energies (LDA) of the Slater determinants and to experiment (LFT fit to exp.). The values of $(10Dq)_{orb}$ as deduced from the e_g-t_{2g} Kohn-Sham orbital energy difference taken from the $t_{2g}^{1.8}e_g^{1.2}$ SCF Kohn-Sham energies are also listed. Experimental transition energies are also listed

Term	CrF_6^{3-}			$CrCl_6^{3-}$			$CrBr_6^{3-}$			$Cr(CN)_6^{3-}$		
	LDA	LFT fit to exp.	Exp.	LDA	LFT fit to exp.	Exp.	LDA	LFT fit to exp.	Exp.	LDA	LFT fit to exp.	Exp.
$^4A_{2g}(t_{2g}^3)$	0	0	0	0	0	0	0	0	0	0	0	0
$^2E_g(t_{2g}^3)$	12,497	15,802	16,300[a]	10,756	14,426	14,430[b]	10,333	13,900	13,900[b]	9413	12,034	12,460[f]
$^2T_{1g}(t_{2g}^3)$	13,044	16,461	16,300[a]	11,180	14,873	–	10,694	14,348	–	9682	12,425	13,070[f]
$^2T_{2g}(t_{2g}^3)$	18,628	23,260	23,000[a]	15,918	21,037	–	15,185	20,281	–	15,234	19,084	18,370[f]
$^4T_{2g}(t_{2g}^1e_g^1)$	13,569	15,298	15,200[a]	10,911	12,800	12,800[b]	9816	12,400	12,400[b]	30,760	26,595	26,700[f]
$^4T_{1g}(t_{2g}^1e_g^1)$	19,443	22,262	21,800[a]	15,618	18,198	18,200[b]	13,992	17,700	17,700[b]	35,910	32,743	32,680[f]
$^2A_{1g}(t_{2g}^1e_g^1)$	24,071	28,709	–	20,056	25,351	–	18,709	24,459	–	38,324	36,488	–
$^2T_{1g}(t_{2g}^1e_g^1)$	26,348	31,473	–	21,878	27,421	–	20,316	26,503	–	40,022	38,569	–
$^2T_{2g}(t_{2g}^1e_g^1)$	25,959	30,970	–	21,568	27,079	–	20,047	26,159	–	39,983	38,438	–
$^2E_g(t_{2g}^1e_g^1)$	27,819	33,341	–	23,147	29,098	–	21,530	28,126	–	41,084	39,952	–
$^4T_{1g}(t_{2g}^1e_g^1)$	30,339	34,636	35,000[a]	24,375	28,455	–	21,861	27,643	–	63,147	55,352	–
R(M–X)	1.957	–	1.933[c]	2.419	–	2.335[d]	2.588	–	2.47[e]	2.071	–	2.077[g]
B	605	734	–	484	550	–	427	543	–	452	554	–
C	2694	3492	–	2403	3450	–	2395	3296	–	1919	2559	–
10Dq	13,598	15,297	–	10,911	12,800	–	9816	12,400	–	30,760	26,595	–
StDev	0.113	–	–	0.105	–	–	0.113	–	–	0.105	–	–
$(10Dq)_{orb}$	13,928	–	–	10,775	–	–	9622	–	–	30,953	–	–

[a] K_3CrF_6: Allen GC, El-Sharkawy AM, Warren KD (1971) Inorg Chem 10:2538.
[b] $Cs_2NaYCl[Br]_6$: Cr^{3+}, Schwartz RW(1976) Inorg Chem 15:2817.
[c] Knox K, Mitchell DW (1961) J Inorg Nucl Chem 21:253.
[d,e] Estimated for $Cs_2NaCrCl_6$ and $Cs_2NaCrBr_6$ [9].
[f] Witzke H(1971) Theoret Chim Acta 20:171(1974).
[g] Jagner S, Ljungstroem E, Vannerberg N-G (1974) Acta Chem. Scand A28:623.

Table 7 Theoretical and experimental electronic transition energies of high-spin CoX_6^{4-}, X=F, Cl, Br octahedral d^7 complexes. Theoretical values are obtained using geometries from a LDA geometry optimization utilizing values of B, C and 10Dq resulting from least square fit to the energies of Slater determinants constructed from 2 $t_{2g}^{4.2}4e_g^{2.8}$ SCF Kohn-Sham orbitals. Best fit B, C and 10Dq parameters from experimental transition energies are also included as are LDA results utilizing experimental bond lengths for the Cl and Br complexes

Term	CoF_6^{4-}			$CoCl_6^{4-}$				$CoBr_6^{4-}$			
	Fit to LDA R_{opt}	LF–fit to Exp.	Exp.	Fit to LDA R_{opt}	LDA R_{exp}	LF–fit to Exp.	Exp.	Fit to LDA–R_{opt}	LDA R_{exp}	LF–fit to Exp.	Exp.
$^4T_1$	0	0	–	0	0	0	–	0	0	0	–
$^4T_2$	4192	7086	7150[a]	3384	6613	6261	6600[a]	3258	5687	5506	5700[b]
^2E	8686	8430	–	7772	3980	7794	–	7171	4307	8817	–
$^4A_2$	9097	15,231	15,200[a]	7335	14,050	13,467	13,300[a]	7041	12,074	11,890	11,800[b]
$^2T_1$	12,395	14,952	–	10,688	10,134	13,542	–	9960	9481	13,789	–
$^2T_2$	12,473	15,230	–	10,804	10,479	13,783	–	10,124	9836	13,969	–
$^4T_1$	14,610	19,197	19,200[a]	11,412	14,008	17,241	17,250[a]	10,113	11,886	16,748	16,750[b]
R	2.235	–	–	2.684	2.414	2.414	–	2.821	2.589	–	–
B	742	878	–	573	548	795	–	492	460	808	–
C	2807	3433	–	2540	2436	3108	–	2444	2371	3159	–
10Dq	4904	8145	–	3952	7436	7206	–	3782	6387	6384	–
StDev	0.086	–	–	0.108	0.110	–	–	0.122	0.124	–	–

[a] Ferguson J, Wood DL, Knox K (1963) J Chem Phys 39:881.
[b] Ludi A, Feitknecht W (1963) Helv Chim Acta 46:2226.

higher than the experimental one. This is unusual and not expected: calculated and experimental Cr-C bond distances are indeed very close. LDA and GGA functionals fail to describe multiplet energies in CoX_4^{2-} (X=Cl^-, Br^- and I^-), however. For these complexes with a $^4A_2$ ground state spin-forbidden transitions deviate from reported experimental energies by about 6000 cm^{-1}, a result due to a drastic lowering of the B and C energies. We can conclude that for the latter systems existing DFT functionals do not perform properly. In addition standard deviations comparing DFT and LFDFT numerical values are too high. We stimulate more work to improve this.

3.4 Octahedral Mn^{III} d^4 and Co^{III} and Fe^{II} d^6 Complexes

$Mn(CN)_6^{3-}$ is a low-spin complex with a $^3T_{1\,g}$ ground state. The LDA optimised bond distance (1.99 Å) matches perfectly the experimental one (1.98 Å [32]) and calculated multiplet energies agree reasonably with the experimental spectrum (Table 8) – the highest deviation (2400 cm^{-1}) being met for the $^3T_{1g} \rightarrow {}^1A_{1g}$ transition. Multiplet energies of the low-spin d^6 complexes $Fe(CN)_6^{4-}$ and $Co(CN)_6^{3-}$ possessing a $^1A_{1g}$ ground state calculated using LDA optimised bond lengths (Fe-C 1.930 Å and Co-C 1.899 Å) are listed in Table 9. Owing to the overestimate of the 10Dq value by 1740 and 2230 for the Fe and Co complex respectively, DFT energies of $^1A_{1g} \rightarrow {}^1T_{1g}$, $^1T_{2g}$ transition are higher in energy than the experimental values, values of B from DFT and experiment being very close in these complexes. Differences in the C parameter are just the opposite – they would lead to

Table 8 Theoretical and experimental electronic transition energies of the low-spin $Mn(CN)_6^{3-}$ octahedral d^4 complex.Theoretical values are obtained using geometries from a LDA geometry optimization utilizing values of B, C and 10Dq resulting from least square fit to the energies of Slater determinants constructed from 2 $t_{2\,g}^{2.4}4e_g^{1.6}$ SCF Kohn-Sham orbitals. Best fit B, C and 10Dq parameters from experimental transition energies are also included

Electronic state	LDA	LF-fit	Exp.
$^3T_{1\,g}$	0	0	
$^1T_{2\,g}$	6796	7948	7984[a]
^1E_g	7242	8710	8710[a]
$^1A_{1\,g}$	16,028	18,519	18,470[a]
^5E_g	20,013	20,699	20,700[a]
^3E_g	31,746	34,326	
$^3T_{1\,g}$	32,354	34,966	
$^3T_{2\,g}$	32,935	35,713	
$^3A_{1\,g}$	33,453	36,761	
$^3A_{2\,g}$	34,591	38,130	
^3E_g	35,499	39,630	
B	444	630	
C	2361	2598	
10Dq	34,085	36,900	
StDev	0.082		

[a] Mukherjee RK, Chowdhury M (1975) Chem Phys Lett 34:178.

Table 9 Theoretical and experimental electronic transition energies of low-spin $Fe(CN)_6^{4-}$ and $Co(CN)_6^{3-}$ octahedral d^6 complexes. Theoretical values are obtained using geometries from a LDA geometry optimization utilizing values of B, C and 10Dq resulting from least square fit to the energies of Slater determinants constructed from $2\,t_{2g}^{3.6}4e_g^{2.4}$ SCF Kohn-Sham orbitals. Best fit B, C and 10Dq parameters from experimental transition energies are also included

Electronic state	$Fe(CN)_6^{4-}$			$Co(CN)_6^{3-}$		
	LDA	LF–fit	Exp.	LDA	LF–fit	Exp.
$^1A_{1g}$	0	0		0	0	
$^3T_{1g}$	28,516	23,698	23,700[a]	29,845	25,969	25,969[a]
$^3T_{2g}$	31,669	26,664	–	32,721	29276	–
$^1T_{1g}$	33,499	30,969	30,970[a]	35,107	32,500	32,500[a]
$^1T_{2g}$	39,842	37,001	37,000[a]	40,900	39,194	39,200[a]
$^5T_{2g}$	50,080	38,067		52,577	43,240	
$^3T_{1g}$	62,079	54,723		65,030	58,538	
$^3T_{2g}$	62,543	55,010		65,391	58,948	
^3E_g	63,939	56,352		66,667	60,430	
B	427	411		387	456	
C	2420	3566		2573	3184	
10Dq	35,421	33,678		37,180	34,944	
StDev	0.082			0.112	–	

[a] Alexander JJ, Gray HB (1968) J Am Chem Soc 90:4260.

lowering of energies of spin-forbidden transition. However this is overcompensated by the larger DFT value of the parameter 10Dq.

In Fig. 5 we compare our results for $Co(CN)_6^{3-}$ with transition energies using a time-depending DFT (TDDFT) calculation performed using the same basis functions and a LDA functional. The comparison with experimental transition energies show the better performance of our approach: thus while $^3T_{2g}$ and $^3T_{1g}$ are nearly accidentally degenerate at the TDDFT level, they are split in our treatment and the $^3T_{1g}$ approaches closer to the energy of the $^1A_{1g} \rightarrow {}^3T_{1g}$ transition in the spectrum. The difference in the two treatments is possibly due to the neglect of double excitation in TDDFT, as different to our approach which takes full account of them.

3.5 Applications to Tetrahedral d^5 $MnCl_4^{2-}$ and $FeCl_4^{1-}$ Complexes

In the discussions thus far we have noted, that because B and C deduced using DFT data are smaller than parameters from a direct fit to experiment, electronic transitions with change of the spin are calculated at lower energies than experiment. In this respect high-spin d^5 complexes with tetrahedral geometry and a $^6A_1$ ground state, such as $MnCl_4^{2-}$ and $FeCl_4^{-}$, provide a stringent test of the ability of the up-to-date functionals to calculate multiplet structures for such cases. In Table 10 we list such energies and compare them with experiment and with energies using a direct fit of B, C and 10Dq to experiment. We base our treatment on LDA optimised Mn-Cl (2.385 Å) and Fe-Cl (2.207 Å) bond distances. For both

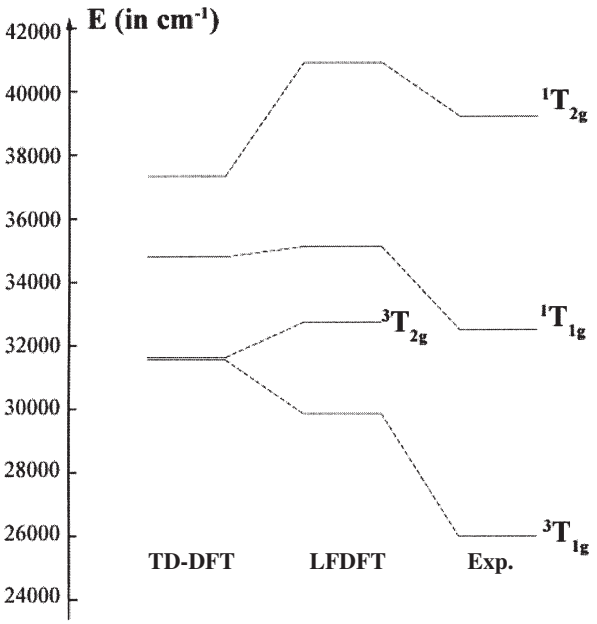

Fig. 5 Comparison between transition energies calculated using TD-DFT with our LFDFT method and experiment values for low spin $^1A_1$ $Co(CN)_6^{3-}$ (taken from Alexander JJ, Gray HB (1968) J Am Chem Soc 90:4260)

Table 10 Theoretical and experimental electronic transition energies of high-spin tetrahedral ($MnCl_4^{2-}$ and $FeCl_4^{1-}$) d^5 complexes. Theoretical values are obtained using geometries from a LDA geometry optimization utilizing values of B, C and 10Dq resulting from least square fit to the energies of Slater determinants constructed from 2 $t_2^3 4e^2$ SCF Kohn-Sham orbitals. Best fit B, C and 10Dq parameters from experimental transition energies are also included

Electronic state	$MnCl_4^{2-}$			$FeCl_4^{1-}$		
	LDA	LF–fit	Exp.	LDA	LF–fit	Exp.
$^6A_1$	0	0		0	0	
$^4T_1$	15,253	20,954	21,250[b]	8875	14,835	15,600[b]
$^4T_2$	16,720	21,720	22,235[b]	11,060	16,836	16,300[b]
$^4A_1$, ^4E	17,175	21,975	23,020[b]	12,940	18,230	18,800[b]
$^4T_2$	20,359	25,198	26,080[b]	14,554	20,271	20,100[b]
^4E	21,011	25,587	26,710[b]	15,705	21,366	22,400[b]
$^4T_1$	21,922	28,051	27,770[b]	18,436	25,114	
$^4A_2$	28,429	34,883	33,300[b]	21,276	29,106	
$^4T_1$	28,638	34,998	34,500[b]	22,255	29,774	
$^4T_2$	29,536	35,514	36,650[b]	24,307	32,917	
B	548	516		395	448	
C	2339	3363		1798	[a]	
10Dq	3298	2661		5395	5320	
StDev	0.061	–		0.051		

[a] Calculated using a C/B ratio of 6.14.
[b] Taken from Lever ABP (1984) Inorganic electronic spectroscopy 2nd edn. Elsevier, p 450.

systems we obtain the remarkable result that all transitions match nicely the observed transition energies provided a shift of about 6000 cm^{-1} to higher energies is taken into account. The origin of this correction is possibly due to the fact that DFT leads to lower values in particular of the parameter C (see above).

3.6 Performance of the Existing Functionals Interpreting and Predicting LF Spectra of TM Complexes

We can state that, with the exception of CN complexes where 10Dq (LFDFT) values are higher than experimental, up-to-date LDA and GGA functionals are accurate enough in calculating ligand field matrix elements (h_{ab}) not only for cubic but also for complexes with lower symmetries. This is not the case for B and C. In Table 11 we collected DFT (LDA) values of B and C of different complexes. For the sake of comparison we also list values of B and C deduced using a fit to LF transitions from experiment. When comparing the two sets of data one should be cautious, because experimental uncertainties prevent an accurate fit of B and C in many cases. In spite of this, we note that the DFT B and C values are systematically lower that experimental ones. Thus in tetra-oxo anions of Cr^{IV}, Mn^{V} and Fe^{VI} experimental values of B exceed DFT ones by a factor of 1.24 to 1.50 for B and by a smaller but mostly larger than 1 factor for C. A drastic deterioration

Table 11 Values of B and C for various tetrahedral and octahedral complexes, deduced from a fit to DFT energies of all SD and from a fit to experimental ligand field spectra. Recommended scaling factors, needed to adjust the values of B and C from DFT calculations to the ones deduced from experiment are also included

Complex			Fit to DFT[a]		Fit to well documented LF spectra		Scaling factor	
$NiCl_4^{2-}$ d^8	B	C	452	2315	825	3032	1.825	1.310
CrO_4^{2-} d^2	B	C	436	2250	555	2331	1.300	1.025
MnO_4^{3-} d^2	B	C	347	1928	430	2600	1.239	1.343
FeO_4^{2-} d^2	B	C	242	1637	375	1388	1.550	0.844
$CrCl_4$ d^2	B	C	355	1903	376	1579	1.059	0.830
CrF_6^{3-} d^3	B	C	605	2694	734	3492	1.213	1.296
$CrCl_6^{3-}$ d^3	B	C	484	2403	550	3450	1.136	1.436
$CrBr_6^{3-}$ d^3	B	C	427	2395	543	3296	1.272	1.376
$Cr(CN)_6^{3-}$ d^3	B	C	452	1919	554	2559	1.226	1.334
$Mn(CN)_6^{3-}$ d^4	B	C	444	2361	630	2598	1.419	1.100
$Co(CN)_6^{3-}$ d^6	B	C	387	2573	456	3184	1.178	1.237
$CoCl_4^{2-}$ d^7	B	C	460	2339	710	2776	1.543	1.187
$CoBr_4^{2-}$ d^7	B	C	427	2218	695	2717	1.628	1.225
CoI_4^{2-} d^7	B	C	379	2113	665	2600	1.755	1.230
$CoCl_6^{4-}$ d^7	B	C	548	2436	795	3108	1.45	1.276
$CoBr_6^{4-}$ d^7	B	C	460	2371	808	3159	1.756	1.332
$MnCl_4^{-}$ d^5	B	C	548	2339	516	3363	0.942	1.438

[a] Calculations are based on LDA optimized DFT geometries for complexes.

of this comparison appears for $NiCl_4^{2-}$, CoX_4^{2-}, CoX_6^{4-} ($X=Cl^-, Br^-, I^-$) complexes, showing, for complexes of the late TM ions, that both LDA and also GGA do not perform well.

One can propose further work introducing elaborate functionals, which are better suited for LF spectroscopic purposes. Alternatively, one can propose a recipe within the existing functionals introducing scaling factors – those listed in Table 11, which improve the agreement between the DFT theory and experiment.

Finally, our LFDFT allows to calculate multiplet energies in TM complexes, similar to the empirical CI-DFT procedure described by Grimme [2]. In this approach, KS potential and energies have been used to approximate the exact CI Hamiltonian by introducing scaling factors, thus avoiding double counting of electron correlation in the off-diagonal CI matrix elements. Though principally able to treat open-shell TM complexes as well, the method has been applied thus far only to closed shell ground state systems.

4 Conclusions and Outlook

We have developed a DFT based LF model which utilizes SD energies in order to determine ligand field parameters from first principles. The formalism has been implemented using the following recipe:

1. Make a geometry choice; for neutral complexes we recommend a GGA geometry optimisation. For complexes with negative charges use of experimental bond lengths or LDA geometry optimisation is preferable.
2. Construct KS-LF orbitals with the average of configuration (AOC) providing n/5 occupancy of each d-MO for a TM with a d^n configuration.
3. Calculate the set of *all* SD energies using these orbitals without allowing for orbital relaxation (no SCF iteration).
4. Determine B,C and the 5×5 LF matrix h_{ab} from these data.
5. Introduce these parameters into a favourite LF-program which allows full CI and use of symmetry to get all multiplet energies.

The rather consistent fit for cubic symmetry reproducing the total manifold of symmetry independent SD shows that DFT and LF theory are compatible. A theoretical justification (analysis) of this result is still lacking (but see the discussion in [15]). Comparing LF parameters deduced from DFT calculations with those resulting from fit to experimental spectra in high resolution, we can conclude that existing functionals are able to describe properly not only cubic but also low-symmetric ligand fields. In contrast parameters of interelectronic repulsion are calculated systematically smaller than values from spectral data. Similar observations have been reported by Solomon et al. [33]. We can use these results in order to motivate further work aimed at developing functionals and/or basis sets for spectroscopic purposes. Alternatively, scaling factors have been proposed for B and C to improve the agreement between DFT and experiment.

The formalism is equally suited to extend the treatment to TM complexes including more than one TM and spin-orbit coupling. Thus fine structure tensors

in EPR and data from MCD can become good candidates for further applications using this approach. Work in this direction is in progress.

Acknowledgements This study was supported by the Swiss National Science Foundation. We owe thanks Dr T. Mineva and Prof. Dr. N. Neshev Bulgarian Academy of Sciences (Sofia, Bulgaria) for valuable discussions.

5 Appendix

Two-electron integrals $\iint a(1)b(2)(1/r_{12})c(1)d(2)d\tau_1 d\tau_2$ of Coulomb interactions for d-electrons in the spherical (A,B,C) and cubic approximation are of interest. The relationship between the notations of Griffith for cubic symmetry (a to j) and g_1 to g_{10} (this work) are included:

a(1)	b(2)	c(1)	d(1)	A, B, C	i to j	g_1 to g_{10}
ζ	ζ	ζ	ζ	A+4B+3C	A	g_7
ζ	ζ	ξ	ξ	3B+C	J	g_8
ζ	η	ζ	η	A–2B+C	B	g_9
ζ	ξ	ζ	ξ	A–2B+C	B	g_9
ζ	ε	ζ	ε	A+4B+C	d+√3c	$g_5+g_6/\sqrt{3}$
ζ	ε	ξ	η	3B	i√3	$-(\sqrt{3}/2)g_{10}$
ζ	θ	ζ	θ	A–4B+C	d–(1/√3)c	$g_5-\sqrt{3}g_6$
ζ	θ	ξ	η	√3B	I	$-g_{10}/2$
η	η	ζ	ζ	3B+C	J	g_8
η	η	η	η	A+4B+3C	A	g_7
η	ξ	η	ξ	A–2B+C	B	g_9
η	ε	ζ	ξ	–3B	–i√3	$(\sqrt{3}/2)g_{10}$
η	ε	η	ε	A–2B+C	D	$g_5-2g_6/\sqrt{3}$
η	θ	ζ	ξ	√3B	I	$-g_{10}/2$
η	θ	η	ε	–2√3B	–c	$-g_6$
η	θ	η	θ	A+2B+C	d+2c/√3	g_5
ξ	ξ	η	η	3B+C	J	g_8
ξ	ξ	ξ	ξ	A+4B+3C	A	g_7
ξ	ε	ξ	ε	A–2B+C	d	$g_5-2g_6/\sqrt{3}$
ξ	θ	η	ζ	–2√3B	–2i	g_{10}
ξ	θ	ξ	ε	2√3B	c	g_6
ξ	θ	ξ	θ	A+2B+C	d+2c/√3	g_5
ε	ε	ζ	ζ	C	g–h/√3	$g_3+g_4/\sqrt{3}$
ε	ε	η	η	3B+C	d+2 h/√3	$g_3-2g_4/\sqrt{3}$
ε	ε	ξ	ξ	3B+C	g+2 h/√3	$g_3-2g_4/\sqrt{3}$
ε	ε	ε	ε	A+4B+3C	e	g_1
ε	θ	η	η	√3B	h	$-g_4$
ε	θ	ξ	ξ	–√3B	–h	g_4
ε	θ	ε	θ	A–4B+C	e–2f	g_1-2g_2
θ	θ	ζ	ζ	4B+C	g+√3 h	$g_3-\sqrt{3}g_4$
θ	θ	η	η	B+C	g	g_3
θ	θ	ξ	ξ	B+C	g	g_3
θ	θ	ε	ε	4B+C	f	g_2
θ	θ	θ	θ	A+4B+3C	e	g_1

For calculation of low-symmetric LF matrices we take the ion CrO_4^{4-} as given in the Cr^{IV} doped into the C_s distorted tetrahedral site of the Ca_2GeO_4 host lattice [31]. With the xy plane coinciding the C_s plane, the d_{z2}, d_{x2-y2},d_{xy} and d_{xz},d_{yz} transforming as the A′ and A″ representations, respectively we get from the DFT output the following **U** and **Λ**(in eV) matrices written in the specified order of atomic 3d basis functions:

				U		A	
		e	t_2	t_2	e	t_2	t_2
	d_{z2}	−0.570	0.374	0.616	20.116	0	0
A′	d_{x2-y2}	−0.354	−0.713	0.244	0	21.032	0
	d_{xy}	−0.661	0.082	−0.667	0	0	21.304

(A1)

		e	t_2	e	t_2
	d_{xz}	0.622	0.712	20.125	0
A″	d_{yz}	0.710	−0.619	0	21.265

In Eq. (A1) we list the relation of the C_s split a′ and a″ KS-orbitals with the corresponding parent e and t_2 ones. Applying Eqs. (15–17) we obtain the following off-diagonal LF **h**(A′) and **h**(A″) matrices:

$$h(A') = \begin{array}{c|ccc} & d_{z2} & d_{x2-y2} & d_{xy} \\ & 20.817 & -0.166 & -0.512 \\ & -0.166 & 20.915 & -0.297 \\ & -0.512 & -0.297 & 20.720 \end{array} \qquad \text{(A2)}$$

$$h(A'') = \begin{array}{c|cc} & d_{xz} & d_{yz} \\ & 20.772 & -0.565 \\ & -0.565 & 20.617 \end{array}$$

6 References

1. Casida ME In: DP Chong (ed) Recent advances in density functional methods. Part 1. World Scientific, Singapore, p 155
2. Grimme S (1996) Chem Phys Lett 259:128; Grimme S, Waletzke M (1999) J Chem Phys 111:5645
3. Bethe H (1929) Ann Phys 3:133; Hartmann H, Schlaefer HL (1951) Z Phys 197:115; Ilse FE, Hartmann H (1951) Z Phys 197:239; Hartmann H, Schlaefer HL (1951) Z Naturforsch 6a:751, 760
4. Jørgensen CK, Pappalardo R, Schmidtke H-H (1963) J Chem Phys 39:1422; Schaeffer, CE, Jørgensen CK (1965) Mol Phys 9:401
5. Solomon EI, Hodgson KO (eds) (1998) Spectroscopic methods in bioinorganic chemistry. Oxford
6. Bertini I, Gray HB, Lippard SJ, Valentine JS Bioinorganic chemistry. University Science Books Herndon, VA 20172
7. Slater JC (1972) Adv Quantum Chem 6:1; Messmer RP, Salahub DR (1976) J Chem Phys 65:779; Ziegler T, Rauk A, Baerends EJ (1977) Theor Chim Acta 43:261
8. Daul CA (1994) Int J Quantum Chemistry 52:867
9. Gilardoni F, Weber J, Bellafrough K, Daul CA, Guedel HU (1996) J Chem Phys 104:7624

10. Aramburu JA, Moreno M, Doclo K, Daul CA, Barriuso MT (1999) J Chem Phys 110:1497
11. Deghoul F, Chermette H, Rogemond F, Moncorge R, Stueckl C, Daul C (1999) Phys Rev 60: 2404
12. Griffith JS (1971) The theory of transition-metal ions. University Press, Cambridge
13. Sugano S, Tanabe Y, Kamimura H (1970) Multiplets of transition-metal ions in crystals. Academic Press, New York London
14. Mineva T, Goursot A, Daul C (2001) Chem Phys Lett 350:147
15. Bridgeman AJ, Gerloch M (1997) Prog Inorg Chem 45:179
16. MATLAB 6.1 scripts and programs written for each system can be obtained from the authors on request
17. Slater JC (1974) The self-consistent field for molecules and solids. McGraw-Hill Book Company
18. Janak JF (1978) Phys Rev 18:7165
19. Durand PH, Malrieu JP (1987) Advances in Chem Phys 67, page 321, Wiley, New York
20. des Cloizeaux J (1960) Nucl Phys 20:321
21. Atanasov M, Barras J-L, Benco L, Daul CA (2000) J Am Chem Soc 122:4718
22. Baerends EJ, Ellis DE, Ros P (1993) Chem Phys 2:42; Boerrigter PM, te Velde G, Baerends EJ (1988) Int J Quantum Chem 33:87; te Velde G, Baerends EJ (1992) Comput Phys 99:84
23. Vosko SH, Wilk L, Nusair M (1980) 58:1200
24. Becke AD (1988) J Phys C 88:2547
25. Perdew JP (1986) Phys Rev B 33:8822; Perdew JP (1986) Phys Rev B 34:7406 (Erratum)
26. Ziegler T (1991) Chem Rev 91:651
27. Michel-Calendini FM, Bellafrouh K, Chermette H (1994) Phys Rev B 50:12,326
28. Adamsky H (1995) Thesis, University of Düsseldorf. For beginners a traditional LF program AOMX is available through the Internet at the address http://www.aomx.de. This site provides selected examples and an AOM parameter database, and will be further developed into a forum for scientific exchange about Angular Overlap Model applications to TM complexes. For the sake of our purposes the conventional modules constructing the LF matrix from geometries and AOM parameters have been substituted by the data given by the LFDFT model. In using model HLFDFT the matrix of interelectronic repulsion integrals has been replaced with expressions in terms of the parameters g_i(i=1 to 10)
29. Hazenkamp MF, Guedel HU, Atanasov MA, Kesper U, Reinen D (1996) Phys Rev B 53:2367
30. Cohen S, Mayer I, Reinen D (1993) J Solid State Chem 107:218
31. Shigekazu U, Kazuyori U, Keiichi K (1975) Semento Gijetsu Nenpo 29:32
32. Gupta MP, Milledge HJ, McCarthy AE (1974) Acta Crystallogr B 30:656
33. Solomon EL, Chen P, Metz M, Lee S-K, Palmer AE (2001) Angew Chem (Int Ed) 40:4570

Structure and Bonding, Vol. 106 (2004): 127–152
DOI 10.1007/b11309

Electronic Properties and Bonding in Transition Metal Complexes: Influence of Pressure

M. Moreno[1] · J. A. Aramburu[1] · M. T. Barriuso[2]

[1] Universidad de Cantabria, Departamento de Ciencias de la Tierra y Física de la Materia Condensada, Facultad de Ciencias, 39005 Santander, Spain
E-mail: morenom@unican.es
[2] Universidad de Cantabria, Departamento de Física Moderna, Facultad de Ciencias, 39005 Santander, Spain

Abstract Changes undergone by optical and magnetic properties of O_h, T_d and D_{4h} Transition metal (TM) complexes induced by variations of the metal-ligand distance, R, are explored in this work. In parallel, the corresponding variations experienced by the chemical bonding in the complex are analysed in detail. Particular attention is addressed to TM complexes associated with impurities in insulating lattices with halides or oxygen as ligands. Experimental and theoretical results show that charge transfer (CT) transitions experience a blue shift when R decreases. This fact, which allows one to detect R variations down to ~0.1 pm, is shown to come mainly from the increase of electrostatic repulsion between metal electrons and anions. By means of this technique it is pointed out that the equatorial distance of an elongated D_{4h} $CuCl_6^{4-}$ unit can increase when a hydrostatic pressure is applied. Electronic relaxation in the excited state is shown to play a key role for explaining the energy of CT transitions. Particular attention is also paid to the admixture of *p* and *s* ligand valence orbitals into antibonding $e_g^*(\sim 3z^2{-}r^2; x^2{-}y^2)$ and $t_{2g}^*(\sim xy; xz; yz)$ orbitals of octahedral complexes. Although the *s*-admixture in e_g^* is much smaller than the *p*-admixture the former is shown to be much more sensitive to R variations than the latter. As a salient feature it is stressed that the small *s*-admixture in e_g^* is mainly responsible for the strong sensitivity of the cubic field splitting parameter,10Dq, to changes of R.

Keywords Transition metal complexes · Metal-ligand distance variations · Charge transfer transitions · Bonding variations · Changes of 10Dq · Microscopic origin

List of Abbreviations

ADF	Amsterdam density functional code
CF	Crystal-field
CT	Charge transfer
CASPT2	Complete active space perturbation theory order 2
DFT	Density functional theory
E_{CT}	Energy of the first dipole allowed charge transfer transition
ENDOR	Electron nuclear double resonance
EPR	Electron paramagnetic resonance
EXAFS	Extended X-ray absorption fine structure
HOMO	Highest occupied molecular orbital
LUMO	Lowest unoccupied molecular orbital
MSXα	Multiple scattering Xα
SCCEH	Self-consistent charge extended Hückel
TM	Transition metal
VUV	Visible ultraviolet

1 Introduction

Since the work by Alfred Werner [1] the properties of an ML_N complex, formed by a transition metal (TM) cation, M, and N ligands, L, are known to depend not only on the metal oxidation state but also on the number N and geometrical arrangement of ligands. As these molecules usually exhibit an open shell electronic structure they are of interest not only in chemistry but also in other do-

mains like biology, condensed matter physics or material sciences. In fact, TM complexes are involved in some active sites of proteins or enzymes [2, 3] while devices like solid state lasers are often based on TM impurities doped insulating materials [4, 5]. The attractive *electronic* properties associated with substitutional TM impurities in insulators can often be understood to a great extent *only* on the basis of a ML_N *molecule* (formed by the TM impurity M and the N nearest anions) which is however not isolated but *embedded* in a host lattice [6, 7]. This situation is no longer true when vibrational properties are involved [8].

The advent in 1926 of fundamental laws governing the microscopic world made possible to improve our understanding of optical and magnetic properties due to TM complexes and their relation to the nature and geometry displayed by ligands. In a first step, ligands were taken as punctual charges leading to the so-called Crystal-Field (CF) model [1, 7, 9]. Through this crude approximation it was however possible to explain, at least qualitatively, relevant facts such as: 1) the blue colour of $Cu(H_2O)_6^{2+}$ units [1, 9] as a result of the cubic field splitting, 10Dq, between $e_g^*(\sim 3z^2-r^2; x^2-y^2)$ and $t_{2g}^*(\sim xy; xz; yz)$ antibonding orbitals; 2) the shift with respect to $g_0=2.0023$ (corresponding to a free electron) of the gyromagnetic factor, g, measured [10] for TM complexes through Electron Paramagnetic Resonance (EPR).

Despite these facts it was recognised early on that CF model was unable to account for other relevant experimental facts. For instance, in optical absorption spectra of TM complexes, apart from to the *d-d* or CF transitions, intense Charge Transfer (CT) transitions are often observed in the visible-ultraviolet region [1, 9, 11–14]. On the other hand, the observation of hyperfine interaction with ligands (called superhyperfine) in EPR spectra of TM complexes [10, 15] cannot be accounted for through the simple CF description. Moreover, the CF model was shown to be *quantitatively* wrong as, for instance, it leads to 10Dq values much smaller than experimental ones [1, 6, 7]. This situation was shown to be largely improved considering a TM complex as a molecule and thus treating the ligands on the same footing as the central cation. Within a Molecular Orbital (MO) description of a TM complex it was possible to relate the superhyperfine constants measured by EPR to the covalency in the MX_N complex [10, 15], and this quantity to the energy of the first CT transition, E_{CT}. Moreover, Jørgensen demonstrated [11, 12] that, for a given geometry and cation, E_{CT} is basically governed by the electronegativity of ligand atoms. This simple rule has played a key role in the identification of CT transitions due to TM impurities and also to less common impurities such as Ag^0 or Tl^{2+} [16].

It was also noted by Jørgensen [1, 11] that the reduction experienced by Racah parameters, B and C, on passing from free M species to the ML_N complex basically reflects the partial transfer of electronic charge from d-orbitals of central cation to ligands. These ideas have been corroborated by subsequent theoretical calculations [17–32], which started in the pioneering work, by Sugano and Shulman [6].

In the present work, focused on electronic properties of TM complexes, particular attention is paid to explore the variations undergone by optical and magnetic parameters when the metal-ligand distances, termed as R_i (i=1,2,...,N), are varied. Such distances can be modified through an external applied pressure.

When the complex is embedded in a host lattice such distances can also be modified by placing the complex in another lattice which, though similar, can exert a different *chemical pressure* upon the complex. So, the metal ligand distance and electronic properties of the MnF_6^{4-} complex placed in two different cubic lattices like $KMgF_3$ and $CsCaF_3$ are not the same [8].

The main reasons for the present research are the following:

1. If metal-ligand distances of a given ML_N complex are changed by a hydrostatic or chemical pressure their optical and magnetic *properties do also change* as they depend on the equilibrium R_i values.
2. Variations of impurity-ligand distances can be well monitored through optical, magnetic or vibrational parameters, which are strongly dependent upon metal-ligand distances [33–40]. This crucial task cannot be carried out by means of standard diffraction methods when impurities are involved. In the case of EXAFs technique impurity concentrations higher than ~1% are often required and thus *truly diluted* solutions cannot be explored. Moreover, the uncertainty on distances obtained in EXAFS is higher than 1 pm and then effects of pressure lower than about 5 GPa can hardly be detected through this technique [41].
3. The present work helps one to gain a better insight into the relation between macroscopic properties and *fine details* of chemical bonding between metal and ligands.
4. Let us denote by $E(R_i)$ the energy of an electronic transition keeping frozen the nuclei at R_i. Once this $E(R_i)$ dependence is known it is also possible to get an additional information on coupling constants with local vibrational modes of the complex and thus on *dynamic quantities* like the associated bandwidth observed in absorption or emission, Stokes shift or Huang-Rhys factors [42, 43].

In addition to compare reliable theoretical results to experimental ones particular attention will be paid to clarify the *main cause* responsible for a given phenomenon. For achieving this goal examples given in this work will involve *model systems* where the symmetry of the complex is preferentially high (O_h, T_d or D_{4h}) and ligands are *simple* anions like F^-, Cl^- or O^{2-}.

Along this work emphasis is put on the sensitivity of CF and CT transitions of octahedral complexes to variations of the metal-ligand distance, R. As a salient feature the actual origin of the strong dependence of 10Dq upon R [33, 35–40] is analysed showing that it is the result of a subtle phenomenon related to chemical bonding.

2 Transition Metal Impurities in Insulators: Do They Actually Form a Complex?

Due to the lack of translational symmetry a basic understanding of properties due to a TM impurity embedded in a crystalline lattice is, in principle, more difficult to achieve than in the case of a pure compound. Despite this fact the *electronic* properties of a TM impurity, M, in an insulating lattice (where electrons are

localised in the ground state [44]) can often (but not always) be accounted for *only* through the ML_N *molecule* involving the N nearest anions around M. This important simplification is favoured by the following conditions.

2.1 Electron Localisation

Active electrons coming from the m impurity should be *localised* in the volume corresponding to the ML_N *molecule*, its presence in further domains of crystal lattice being fully negligible. This condition is favoured by increasing the host lattice band gap and the separation between the HOMO level, associated with the impurity, and the bottom of the conduction band. These requirements are fulfilled, for instance, in the case of divalent TM impurities (Ni^{2+}, Mn^{2+}, V^{2+}) in cubic fluoroperovskites. By contrast, for substitutional silver atoms ($5s^1$ configuration) at cationic positions (Ag_c^0) in KCl the stability is due to a huge (~20%) outwards relaxation of first Cl^- anions which locates the a_{1g}* level (mainly 5s character) just below the conduction band [45]. According to this fact it has also been detected [46] unpaired electron density onto K^+ ions belonging to the second and fourth shell of Ag_c^0:KCl. Along this line an electron centre detected in the less ionic AgCl has a radius of ~15 Å [47] and thus a character more comparable to the highly delocalised shallow impurities in semiconductors whose band gap is smaller than about 1 eV [48].

In some cases the electron localisation in the complex region is helped by a decoupling of the complex from the rest of the host lattice. This can arise in a lattice like NaCl when an M^{2+} impurity replaces the monovalent Na^+ ion and the charge compensation is remote. If the ionic radius of M^{2+} is smaller than ~1 Å the $Na^+ \rightarrow M^{2+}$ substitution would lead to an inwards relaxation of ligand shell, while the electric field created by the positive charge excess avoids the approaching of close Na^+ ions. This effect has recently been found in the study of NaCl doped with a divalent impurity [49].

2.2 Electrostatic Field Due to the Rest of Lattice Ions on the Complex

If we want to interpret the optical transitions arising from an *M* impurity in a host lattice in terms of the ML_N *molecule* it is also necessary that the *electric field* created by the host lattice *ions lying outside the complex* upon the electrons in the complex is zero. Let us consider (Fig. 1) the case of the cubic fluoroperovskite $KMgF_3$ where a few Mg^{2+} ions have been *substituted* by a divalent TM impurity, like Ni^{2+} or Mn^{2+}, leading to the formation of MF_6^{4-} complexes (M: divalent cation) embedded in the host lattice. The rest of the lattice thus possesses a total charge equal to 4*e* displaying cubic symmetry. If the density associated with this charge is assumed, in a first step, to display spherical instead of cubic symmetry the electrostatic potential, V_R, coming from the rest of the lattice ions should be perfectly flat in the complex region. It was firstly remarked by Sugano and Shulman [6] (Fig. 1) that the actual V_R potential on a MF_6^{4-} complex formed in the cubic $KMgF_3$ lattice is very flat indeed.

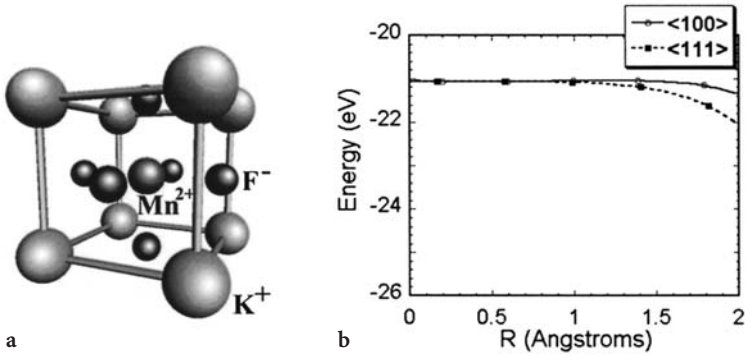

Fig. 1 **a** The substitutional Mn^{2+} impurity in $KMgF_3$. **b** Representation of the electrostatic potential due to the rest of the lattice, $V_R(\mathbf{r})$, for the MnF_6^{4-} complex embedded in $KMgF_3$. Results are shown for **r** along <100> and <111> type directions

In some cases this potential is far from being flat inside the complex and then it is necessary to consider it for a satisfactory explanation of optical transitions associated with the impurity [23, 50]. A good example of this situation concerns the $CuX_4(NH_3)_2^{2-}$ complex (X=Cl, Br) formed [51] in lattices like NH_4Cl, CsCl or NH_4Br (Fig. 2). In these cases Cu^{2+} is not located replacing the host cation but *interstitially* in the middle of a <100> face and thus the local symmetry around Cu^{2+} is markedly tetragonal. The associated V_R potential (Fig. 2) reduces the separation between the n_Lp levels of the halide (n_L=3 for Cl and n_L=4 for Br) and the 2p levels of nitrogen in NH_3 [50]. This fact allows one to explain the CT spectrum [51] of $CuBr_4(NH_3)_2^{2-}$ where the energy of the first $Br^- \rightarrow Cu^{2+}$ transition is measured to be *only* 6000 cm^{-1} higher than the corresponding to the NH_3 ligand. If V_R were fully flat in the complex region one would expect [50] that such a difference is about 15,000 cm^{-1} in view of the different optical electronegativity, χ_L, displayed [11, 12] by bromine (χ_L=2.8) and NH_3 (χ_L=3.3).

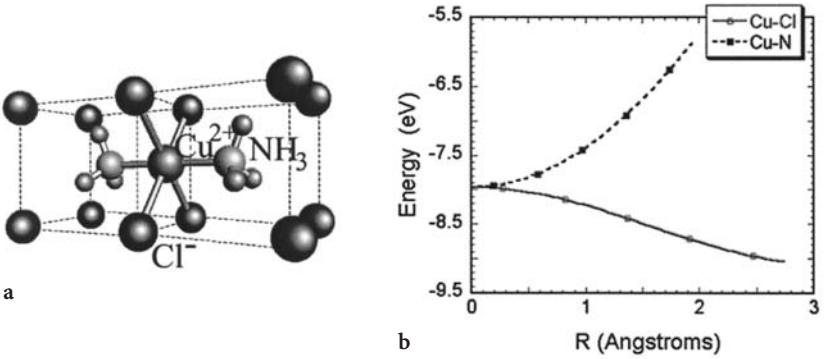

Fig. 2 **a** The substitutional $CuCl_4(NH_3)^{2-}$ complex formed inside a CsCl-type lattice. Cu^{2+} does not replace the host lattice cation but it is located interstitially. **b** Picture of $V_R(\mathbf{r})$ for the $CuCl_4(NH_3)^{2-}$ complex embedded in NH_4Cl. The origin is taken at Cu^{2+} ion. Results are shown for **r** along Cu-Cl and Cu-N directions

3
Energy of the One Electron Levels of Octahedral Transition Metal Complexes

3.1
Simple Analysis

Valence one-electron levels of a ML_N complex can be described to a good extent on the basis of valence levels of involved M and L species. If M is a 3d ion and L a simple ligand like a halide or O^{2-} the relevant levels are 3d, 4s and 4p of central ion and $n_L p$ and $n_L s$ of ligand ions, where n_L denotes the ligand valence shell. It is worth noting that the separation between $n_L p$ and $n_L s$ levels of species like F^- is much higher [52–54] than that for monovalent or tetravalent atoms like Li or C (Table 1). For instance the energy difference between 2p and 2s levels is equal to 1.85 eV and 4.5 eV for Li and C, respectively, while it amounts to about 23 eV for fluorine. The last figure already suggests that the admixture of 2s(F) orbitals in valence orbitals of a complex like NiF_6^{4-} will be much smaller than that coming from 2p(F) orbitals.

In an octahedral MX_6 complex the wavefunctions associated with the antibonding e_g^* levels can shortly be described by

$$\begin{aligned} |e_g^*; \theta\rangle &= \alpha_e |3z^2 - r^2\rangle - \beta_{ep} |\chi_{p\theta}\rangle - \beta_{es} |\chi_{s\theta}\rangle \\ |e_g^*; \varepsilon\rangle &= \alpha_e |x^2 - y^2\rangle - \beta_{ep} |\chi_{p\varepsilon}\rangle - \beta_{es} |\chi_{s\varepsilon}\rangle \end{aligned} \tag{1}$$

where $|\chi_{p\theta}\rangle$ or $|\chi_{s\theta}\rangle$ mean symmetry adapted linear combination of $n_L p$ and $n_L s$ ligand orbitals respectively [7, 9]. The $n_L s$ admixture into the antibonding t_{2g}^* level is however symmetry forbidden and thus a 3d electron can spend some time only on the $n_L p$ ligand orbitals. The wavefunction associated with the $|t^*_{2g}; xy\rangle$ orbital can shortly be written as

$$|t_{2g}^*; xy\rangle = \alpha_t |xy\rangle - \beta_t |\chi_{pxy}\rangle \tag{2}$$

It is worth noting that the admixture of the metal 4s orbital into e_g^* and t_{2g}^* wavefunctions is also not permitted by symmetry if the complex is perfectly octahedral. Under a perturbation of D_{4h} symmetry an octahedral e_g level is however

Table 1 Energy difference, $\varepsilon(n_L p) - \varepsilon(n_L s)$, between the valence $n_L p$ and $n_L s$ levels for several *free* atoms and ions derived from experimental data [52] and theoretical calculations [53]. Results are given in eV

Species	$\varepsilon(n_L p) - \varepsilon(n_L s)$	Species	$\varepsilon(n_L p) - \varepsilon(n_L s)$
Li	1.85	F	22.9
Be	2.75	F^-	24.3
C	4.5	Cl	15.4
N	10.3	Cl^-	15.9
O	16.7	Br	14.6
S	12.0	Br^-	14.9

split into b_{1g}~x^2–y^2 and a_{1g}~$3z^2$–r^2 and thus the 4s hybridisation becomes allowed in the latter orbital. This hybridisation plays a key role for understanding hyperfine constants of distorted ML_6 complexes containing unpaired electrons in a_{1g} orbitals [49].

Due to the covalency reflected in Eq. (1) unpaired electrons coming from the metal M spend some time on ligand orbitals. At the same time the opposite situation happens in bonding counterpart orbitals leading to a net flow of electronic charge from ligands to central cation. This fact ultimately reflects the closed shell structure of *simple* ligands like F^-, Cl^- or I^- and makes that the total charge, q_M, on central ion is smaller than its nominal charge, z_M.

In the *ground state* of a ML_6 complex let us consider a mainly d-orbital transforming like the γ irreducible representation of O_h. The associated one electron energy, $\varepsilon_d(\gamma)$, can be accounted for in a simple view through the three following steps [24], described in Fig. 3.

In a first step a free M ion, but with a fractional charge q_M is considered. The properties of this entity, though artificial can be obtained in the framework of DFT and also through interpolation of experimental results reached for free ions with different z_M values. By both procedures it is thus possible to get the one electron energy, $\varepsilon_d(q_M)$, as a function of q_M. In the same way $\varepsilon_p(q_L)$ can be obtained, where $\varepsilon_p(q_L)$ means the energy of a valence p electron of a ligand with a total charge q_L. If the complex is highly ionic then $q_M=z_M$. As an example, for MnF_6^{4-} $q_M=1.75$ (taking the *proton charge* as *unity*) leading to $\varepsilon_d(q_M)=-27.5$ eV and $\varepsilon_p(q_L)=-4$ eV. Thus in this first step d-orbitals lie well below n_Lp orbitals of ligands.

In a second step the electrons on the central cation with charge q_M are considered to undergo *only* the influence of the *electrostatic field* created by ligands taken as punctual charges. Thus in this step an admixture like that of Eq. (1) is not yet allowed. Calling U_M the associated potential energy, $\varepsilon_d(\gamma)$ can be approximated by

$$\varepsilon_d(\gamma) = \varepsilon_d^0(q_M) + U_M \tag{3}$$

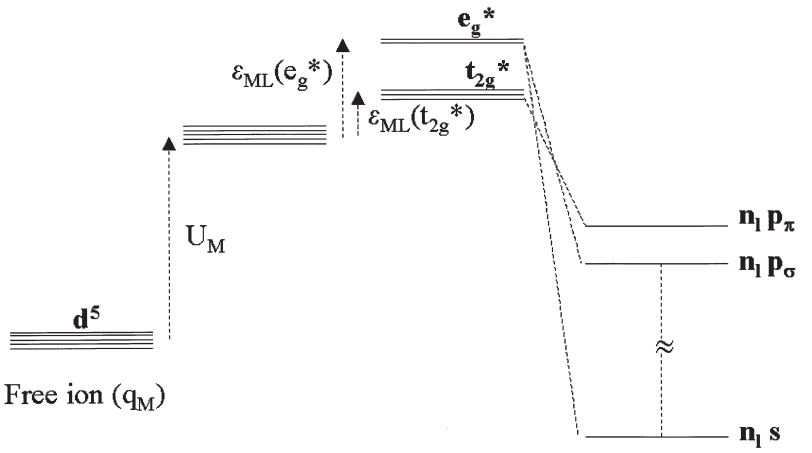

Fig. 3 Pictorial description of three steps described in Sect. 3.1

where U_M, for an octahedral complex, is given by [7, 9]

$$U_M = U_0 + U_4 \tag{4}$$

with

$$U_0 = -6q_L e^2/R \tag{5}$$

$$U_4 = -\frac{\frac{7}{6}\sqrt{4\pi}}{R^5} q_L e^2 \langle \gamma | O_4 | \gamma \rangle$$
$$O_4 = r^4 \{Y_4^0 + \sqrt{\tfrac{5}{14}} [Y_4^4 + Y_4^{-4}]\} \tag{6}$$

U_0 is the main term and U_4 comes out because of the non-punctual character of the d-electron. If q_L=–1 and R=2.12 Å then U_0=40.7 eV, thus leading to an important energy raising of d-electrons with respect to the free ion situation. As to the energy of an n_Lp ligand electron under the electrostatic field created by the metal M and the rest of ligands, it can be approximated by

$$\varepsilon_p(\gamma_L) = \varepsilon_p^0(q_L) + U_L \tag{7}$$

$$U_L = -(q_M + 3.33q_L)\, e^2/R \tag{8}$$

For q_M=2 and q_L=–1, R=2.12 Å then U_L=9 eV. Thus, at this level of approximation, the 3d levels of MnF_6^{4-} are already placed above the 2p levels of F^-.

The U_4 contribution in Eq. (3) is sensitive to cubic symmetry and thus it differs between γ=e_g and γ=t_{2g}. The corresponding splitting, called 10Dq, obtained through the present approximation is given by [7, 9]

$$10Dq = \frac{5}{3}\frac{|q_L|\, e^2 \langle r^4 \rangle_d}{R^5} \tag{9}$$

This expression is just obtained in CF framework but *fails to explain* experimental 10Dq values. For instance, for the $CrCl_6^{3-}$ complex Eq. (8) leads to a value 10Dq=650 cm^{-1} using R=2.4 Å and $\langle r^4 \rangle$=3.4 au for free Cr^{3+} [55]. The comparison with the experimental value for $CrCl_6^{3-}$ (10Dq=13,000 cm^{-1} [56]) clearly indicates that Eq. (8) is unable to explain the separation between the energies of e_g^* and t_{2g}^* orbitals. It also suggests that 10Dq does reflect the different chemical bonding in e_g^* and t_{2g}^* orbitals as first pointed out by Sugano and Shulman [6].

In a third step the admixture of central cation d-orbitals with n_Lp and n_Ls ligand orbitals is finally allowed. This leads to the formation of antibonding orbitals (where unpaired electrons coming from *free* metal ion are located) described by Eq. (1) as well as of bonding counterparts. In the case of an antibonding level the 3d-n_Lp hybridisation leads to a *supplementary increase* of the one electron energy (termed $\varepsilon_{ML}(\gamma)$) which is strongly dependent upon the character (σ or π) of the level. An additional contribution coming from the 3d-n_Ls hybridisation has to be considered for antibonding σ orbitals. Therefore $\varepsilon_d(\gamma)$ can be written as a sum of three contributions:

$$\varepsilon_d(\gamma) = \varepsilon_d^0(q_M) + U_M + \varepsilon_{ML}(\gamma) \tag{10}$$

In a calculation of an ML_6 complex in vacuo, carried out at a metal-ligand distance R, $\varepsilon_d(\gamma)$ and the q_M and q_L charges are determined. Then the $\varepsilon_{ML}(\gamma)$ contribution, which directly reflects chemical bonding, can be estimated by means of Eqs. (3), (4), (5) and (10). For MnF_6^{4-} in vacuo at R=2.12 Å it is found that q_M=1.75, $\varepsilon_d^0(q_M)$=–27.5 eV and U_0=38.3 eV while the obtained values of $\varepsilon_{ML}(e_g^*)$ and $\varepsilon_{ML}(t_{2g}^*)$ are equal to 1.14 and 0.29 eV, respectively.

3.2 Dependence on the Metal-Ligand Distance

The analysis carried out in the preceding section is useful for explaining the variations undergone by the energy of one-electron levels of MX_6 units when R is changed. Theoretical results for significant one-electron levels of the ground state of MnF_6^{4-} are collected in Fig. 4, where R is varied in the 2.0–2.2 pm range. Three different methods have been employed for this purpose. In addition to the R dependence exhibited by antibonding e_g^* and t_{2g}^* orbitals, results obtained for the $t_{1u}(\pi)$ ligand level are also given in that figure. The $t_{1u}(\pi)$ level has a higher energy than the other t_{1u} level, denoted as $t_{1u}(\sigma)$, mainly built from $n_L p_\sigma$ ligand orbitals. Looking at Fig. 4 it can be noted that the energy of e_g^* and t_{2g}^* orbitals is much more sensitive to R variations than that for the $t_{1u}(\pi)$ level. The energy of both e_g^* and t_{2g}^* antibonding orbitals as well as the separation between them, 10Dq, is found to increase when R decreases. These trends are qualitatively reproduced by the three employed methods.

Searching to explain the R dependence of $\varepsilon_d(e_g^*)$ we have first explored the *variations* undergone by the three contributions $\varepsilon_d(q_M)$, U_M and $\varepsilon_{ML}(e_g^*)$ described in Sect. 3.1. Results obtained for the SCCEH calculations on MnF_6^{4-} when R varies in the 2.0–2.2 Å range are collected in Fig. 5. In this range the Mulliken charge on metal is found to vary slightly from q_M=1.75 to q_M=1.65. Accordingly $\varepsilon_d(q_M)$ varies from –27.5 eV to –26.7 eV. By contrast the electrostatic contribution, U_M, undergoes a much bigger variation of about 4 eV. This variation is certainly higher than that experienced by the $\varepsilon_{ML}(e_g^*)$ contribution in the same range

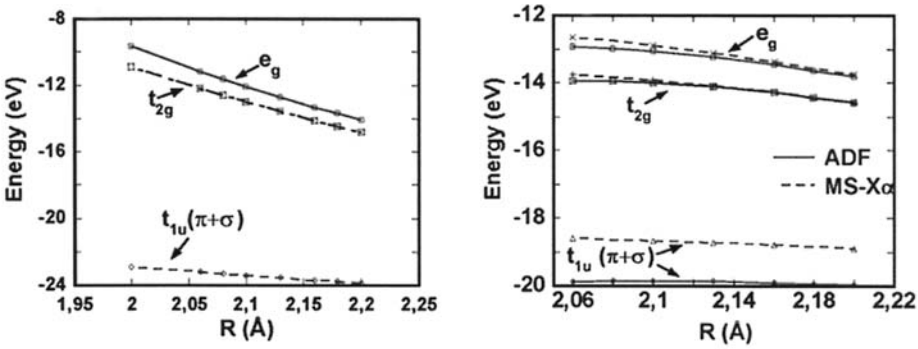

Fig. 4a,b Dependence of the one-electron energy of three valence orbitals of the octahedral MnF_6^{4-} complex upon the metal-ligand distance, R: **a** results have been derived by means of SCCEH calculations; **b** results have been obtained using MSXα and the ADF code [57] in the framework of DFT

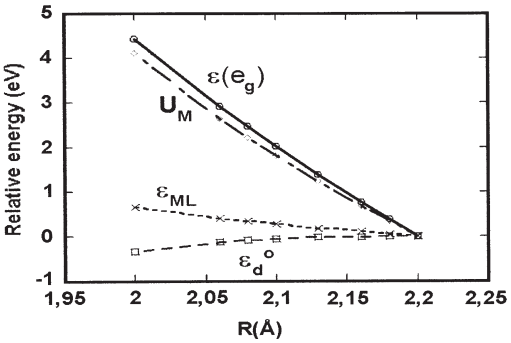

Fig. 5 Relative variation of the one-electron energy of the e_g^* level, $\varepsilon(e_g^*)$, for the octahedral MnF_6^{4-} complex calculated using the SCCEH method when R varies in the 2.0–2.2 Å range. These variations are compared to those undergone by U_M, ε_d^o and ε_{ML} quantities defined in Sect. 3.1

(0.6 eV) and thus it is the *main responsible* for the increase of both $\varepsilon_d(e_g^*)$ and $\varepsilon_d(t_{2g}^*)$ quantities when the metal ligand distance is reduced. Similar trends are found for $MnCl_6^{4-}$ when R varies in the 2.52–2.68 Å range. At R=2.52 Å SCCEH calculations give q_M=1.50 while q_M=1.52 at R=2.68 Å. On passing from R=2.68 Å to R=2.52 Å $\varepsilon_d(e_g^*)$ and U_M are found to increase 2.03 eV and 1.78 eV respectively while $\varepsilon_{ML}(e_g^*)$ increases only 0.22 eV.

4
Pressure Influence on Charge Transfer Transitions

Electric dipole allowed CT transitions are mainly responsible for the polarisability and Raman response of simple complexes [29]. Moreover, they play a key role for explaining the gyromagnetic factor of complexes with high covalency [58–60]. Despite these facts CT transitions have received less attention than the *d-d* transitions. In particular few studies on the sensitivity of CT transitions to changes of R have been performed. Results obtained in this domain show however that CT transitions could be more sensitive than *d-d* transitions to changes of metal ligand distances. In this sense variations of metal ligand distances down to ~0.1 pm can be detected through the corresponding variation of maxima of a CT band [20, 50, 51].

4.1
Systems with Equivalent Ligands

4.1.1
Results for O_h, T_d and Square Planar Complexes

Let us first discuss available experimental results on complexes where all ligands are equivalent and thus only one metal-ligand distance, R, is involved. In Table 2 are gathered experimental CT maxima for two compounds [61] containing

Table 2 Experimental values (in cm^{-1}) of allowed CT transitions [61] corresponding to $(creat)_2CuCl_4$ (first row) and $(N\text{-}mpH)_2CuCl_4$ (second row) compounds containing the square-planar $CuCl_4^{2-}$ unit. The metal ligand distance, R, of the $CuCl_4^{2-}$ complex is however different in both compounds being equal to 225 pm for $(creat)_2CuCl_4$ and 226.5 for $(N\text{-}mpH)_2CuCl_4$. As both systems display a small orthorhombicity the reported R value (in pm) corresponds to an average distance. Calculated MSXα values of transitions for a $CuCl_4^{2-}$ unit in vacuo [20] are given for comparison

R	$e_u(\pi)\rightarrow b_{1g}^*$		$e_u(\sigma)\rightarrow b_{1g}^*$	
	Experimental	Xα	Experimental	Xα
225	27,150	28,870	38,100	40,250
226.5	26,050	28,870	37,700	39,040

$CuCl_4^{2-}$ units which are practically square planar and where the unpaired electron is placed in the $b_{1g}^*\sim x^2-y^2$ level in the ground state. The experimental R distance for $CuCl_4^{2-}$ in $(N\text{-}mpH)_2CuCl_4$ and $(creat)_2CuCl_4$ compounds is however not the same but there is a difference of 1.5 pm [61]. On passing from the former system to the latter one allowed CT maxima experience a blue shift close to 1000 cm^{-1}. This important variation was ascribed simply to the change undergone by R of the $CuCl_4^{2-}$ unit and is supported [20] by theoretical MSXα results on $CuCl_4^{2-}$ in vacuo performed at different R values. From this analysis it turns out that $\partial E_{CT}/\partial R\approx -600$ cm^{-1}/pm for this complex.

Information on the R dependence of CT bands can also be extracted from experimental results on Tl^{2+} in different alkali halides [62] leading to the formation of octahedral TlL_6^{4-} units (L=Cl, Br, I). In the ground state of these complexes there is an unpaired electron placed in the antibonding a_{1g}^* level coming from the atomic 6s level of free Tl^{2+}. Experimental data [62] for the E_{CT} value corresponding to KL:Tl^{2+} and RbL:Tl^{2+} (L=Cl, Br, I) are shown in Table 3. It can be noted that there is a blue shift of E_{CT} on passing from RbCl:Tl^{2+} to KCl:Tl^{2+}. A similar situation holds for the bromine complex. This blue shift can also be interpreted [63] as being due to a reduction of R, which is expected to happen when RbCl is replaced as host lattice by KCl with a smaller lattice parameter. Calculations based on the Density Functional Theory (DFT) performed on RbCl:Tl^{2+} and KCl:Tl^{2+} lead in fact to a small variation $\Delta R\approx -2$ pm on passing from the former to the latter system [64]. Therefore the 1350 cm^{-1} blue shift of E_{CT} observed when RbCl is replaced by KCl can be understood through $\partial E_{CT}/\partial R\approx -650$ cm^{-1}/pm for $TlCl_6^{4-}$. MSXα calculations for this complex (Table 4) lead to $\partial E_{CT}/\partial R=-530$ cm^{-1}/pm. Though $\partial E_{CT}/\partial R$ for Tl^{2+} complexes is found to be always negative $|\partial E_{CT}/\partial R|$ decreases along the ligand series Cl→Br→I. As shown in Table 4 the calculated $\partial E_{CT}/\partial R\approx -300$ cm^{-1}/pm for TlI_6^{4-} by means of MSXα method is substantially smaller than the figure $\partial E_{CT}/\partial R=-530$ cm^{-1}/pm derived for $TlCl_6^{4-}$. This result thus explains why on passing from RbX:Tl^{2+} to KX:Tl^{2+} (X:Cl; I) the increase experienced by E_{CT} is smaller when iodine is involved as ligand than when it is chlorine (Table 3).

Representative values of $\partial E_{CT}/\partial R$ calculated for a variety of TM complexes displaying octahedral or tetrahedral symmetry are also shown in Table 4. As a salient

Table 3 Experimental energy, E_{CT}, corresponding to the first CT transition, $t_{1u}(\pi) \rightarrow a_{1g}^*(6s)$, of octahedral TlX_6^{4-} units (X=Cl, Br and I) placed in KX and RbX hostlattices. As effects due to spinorbit splitting are seen in experiments the figures reported in this Table refer to the centre of the gravity. Experimental values of E_{CT} (in cm^{-1} units) are taken from [62]

Host lattice	$TlCl_6^{4-}$	$TlBr_6^{4-}$	TlI_6^{4-}
KX	27,700	21,910	14,170
RbX	26,350	21,267	13,900

Table 4 Calculated values of the energy, E_{CT}, (corresponding to the first CT transition) and $\partial E_{CT}/\partial R$ for representative octahedral and tetrahedral complexes. E_{CT} is given in cm^{-1} and $\partial E_{CT}/\partial R$ in cm^{-1}/pm. Typical equilibrium distances, R_e, are in pm. E_{CT} usually corresponds to the lowest allowed CT transition with the exception of the FeO_4^{4-} complex where the lowest is the $t_1 \rightarrow e^*$ transition. In this case however $t_1 \rightarrow t_2^*$ is found to lie only 3000 cm^{-1} above

Complex	Method	R_e	Transition	E_{CT}	$\partial E_{CT}/\partial R$	Reference
$TlCl_6^{4-}$	MSXα	2.8	$t_{1u}(\pi) \rightarrow a_{1g}^*$	26,300	–530	[63]
$TlBr_6^{4-}$	MSXα	3.0	$t_{1u}(\pi) \rightarrow a_{1g}^*$	16,500	–400	[63]
TlI_6^{4-}	MSXα	3.25	$t_{1u}(\pi) \rightarrow a_{1g}^*$	11,700	–300	[63]
CrF_6^{3-}	ADF	1.90	$t_{1u}(\pi) \rightarrow e_g^*$	62,000	–1200	[29]
CrF_6^{3-}	MSXα	1.90	$t_{1u}(\pi) \rightarrow e_g^*$	68,000	–1600	[65]
$CrCl_6^{3-}$	MSXα	2.40	$t_{1u}(\pi) \rightarrow e_g^*$	34,000	–720	Present work
$CrBr_6^{3-}$	MSXα	2.55	$t_{1u}(\pi) \rightarrow e_g^*$	27,100	–520	Present work
CrO_4^{4-}	ADF	1.76	$t_1 \rightarrow t_2^*$	39,500	–900	[31]
FeO_4^{2-}	ADF	1.65	$t_1 \rightarrow t_2^*$	24,400	–700	[31]

feature, the sign of $\partial E_{CT}/\partial R$ is found to be *always negative*. This result implies that for O_h and T_d complexes E_{CT} should experience a *blue shift* under an applied pressure. In fact, as a consequence of the second principle of thermodynamics [66] an applied pressure always leads to the reduction of the molecule volume. For O_h and T_d complexes this implies necessarily a diminution of the R value.

Similar to the results reached for Tl^{2+}complexes, those on Cr^{3+} reveal that $|\partial E_{CT}/\partial R|$ decreases along the ligand series F→Cl→Br. Table 4 also offers the comparison between two T_d complexes with oxygen as ligand and d^2 central cations (Cr^{4+} and Fe^{6+}) displaying a different nominal charge. It can be noted that $|\partial E_{CT}/\partial R|$ is calculated to be smaller for the FeO_4^{2-} complex where covalency is expected to be higher. The higher covalency in FeO_4^{2-} is well confirmed [31, 67] by the diminution of E_{CT} on passing from CrO_4^{4-} to FeO_4^{2-} (cf. Table 4).

4.1.2 *Simple Explanation of Trends*

Let us consider a basically *ionic* complex and assume in a crude step that in a $\gamma_L \rightarrow \gamma$ CT jump E_{CT} can be approximated as follows:

$$E_{CT} \approx \varepsilon_d(\gamma) - \varepsilon_p(\gamma_L) \approx \varepsilon_d^0(q_M) - \varepsilon_p^0(q_L) + U_M - U_L + \varepsilon_{ML}(\gamma) \tag{11}$$

where $q_M \approx z_M$. Bearing in mind the analysis carried out in Sect. 3.2, one is tempted to attribute the R dependence of E_{CT} basically to the $(U_M - U_L)$ contribution in Eq. (11). The calculation of $\partial(U_M - U_L)/\partial R$ is simple leading to

$$\partial (U_M - U_L)/\partial R = -(e^2/R^2)\,[q_M - \mu q_L] \tag{12}$$

where μ=2.67, 2.16 and 2.086 for octahedral, tetrahedral and square-planar complexes, respectively. As for TM complexes with halides or oxygen as ligands $q_L<0$ and $q_M>0$ then $\partial(U_M - U_L)/\partial R$ should always be negative in agreement with results gathered in Table 4. Taking q_M=3, q_L=–1 and R=1.9 Å it is found that $\partial(U_M - U_L)/\partial R$=–1,820 cm^{-1}/pm. Therefore, this result is not far from the calculated $\partial E_{CT}/\partial R$ value for CrF_6^{3-} (Table 4) despite the approximation involved in Eq. (11). When the electron in the γ orbital spends a significant part of the time on ligands, Eqs. (11) and (12) have to be modified [31] in order to include only the electron fraction that has been moved from ligands to the central cation in a $\gamma_L \rightarrow \gamma$ CT jump. Therefore, in this situation $\partial E_{CT}/\partial R$ can be approximated by

$$\partial E_{CT}/\partial R \approx -\alpha^2 (e^2/R^2)\,[q_M - \mu q_L] \tag{13}$$

where α^2, as shown in Eq. (1), is the electron fraction residing on metal in the γ orbital. Thus, in comparison with what is expected for an ionic complex, Eq. (13) indicates that covalency reduces the value of $\partial E_{CT}/\partial R$. As an example $\partial E_{CT}/\partial R$ for FeO_4^{2-} would be equal to –4400 cm^{-1}/pm if that complex were ionic. Due to strong covalency q_M is reduced from 6 to 1.5 and α_t^2=0.5 [31]. By means of these values and Eq. (13) the computed $\partial E_{CT}/\partial R$=–700 cm^{-1}/pm value (Table 4) can be understood. Also the higher value of $\partial E_{CT}/\partial R$ for CrO_4^{4-} in comparison with that for FeO_4^{2-} can be explained as being due to the smaller covalency of the former complex where α_t^2=0.8 [31]. Moreover, the diminution of $\partial E_{CT}/\partial R$ for a given TM cation and symmetry along the ligand series F→Cl→Br (Table 4) can qualitatively be explained through the increase of covalency and the parallel increase of R.

4.1.3
Electronic Relaxation in Charge Transfer States

Let us consider a mainly ionic complex. The simple expression at Eq. (11) gives E_{CT} as the difference $\varepsilon_d(\gamma) - \varepsilon_p(\gamma_L)$ where *the two* involved orbitals correspond to the *ground state* of the complex. This is certainly a crude approximation as in an ionic complex a $\gamma_L \rightarrow \gamma$ jump would in principle lead to a total charge on the metal which is not z_M but $(z_M - 1)$. If there is some covalency q_M should be replaced by $[q_M - (\alpha_i)^2]$ (where α_i (i=e, t) is defined in Eq. 1) assuming that all orbitals are kept frozen in the $\gamma_L \rightarrow \gamma$ jump. It should be mentioned that γ_L orbitals involved in allowed CT transitions usually display a *non bonding* character [11–14] and thus the electron is localised on ligands to a good extent.

Once the electron flows from ligands to central cation however, *a hole is left* on the γ_L ligand orbital lying below mainly *d*-orbitals. Thus, the energy of the CT state induced by the $\gamma_L \rightarrow \gamma$ jump can decrease through a *relaxation of electronic orbitals* favouring a transfer of electronic charge from metal to ligands. This process cannot occur in the ground state of complexes with ligands such as F^- or Cl^- as they have a closed shell structure and are not able to accept additional elec-

tronic charge from central cation. Back bonding effects can however appear in the ground state of complexes where ligands are molecules and whose LUMO orbital lies close to the HOMO orbital.

Electronic relaxation in CT excited states was firstly investigated by Ziegler et al. [18] and subsequently by other workers [28, 29, 31, 68]. As a salient feature it is found that the charge on central cation is often close to that of the ground state of the complex once relaxation of electronic orbitals comes out.

Let us take as a guide the case of the FeO_4^{2-} complex whose ground state belongs to the $(e^*\uparrow)^2$ configuration and has a spin S=1. DFT calculations lead to q_M=1.35 for the ground state. After an electric dipole allowed $t_1\uparrow \rightarrow t_2^*\uparrow$ jump a CT state is formed characterised by a $(t_1\downarrow)^3\ (t_1\uparrow)^2\ (e^*\uparrow)^2\ (t_2^*\uparrow)^1$ configuration and S=1. If the energy and q_M for this excited state are calculated *keeping frozen* the orbitals of the ground state it is found q_M=0.88 and E_{CT}=43,000 cm^{-1}. When *relaxation* of electronic orbitals is allowed to come it is however found that q_M is equal to the ground state value and E_{CT} *decreases* down to 24,000 cm^{-1}.

The flow of 0.5*e* from metal to ligands in the electronic relaxation process however involves *small changes* in the e^* and t_2^* antibonding orbitals as well as in the e and t_2 bonding counterparts. Let us take for simplicity $\beta_t \approx \beta_e = \beta$. The meaning of β_t and β_e symbols is the same as described in Eqs. (1) and (2) for O_h complexes. For the present discussion the small 2s(O) admixture in the t_2^* orbital of FeO_4^{2-} can be discarded. Let us neglect in a first approximation overlap integrals like $\langle xy|\chi_{pxy}|\rangle$ involved in the $|t^*_{2g};xy\rangle$ orbital defined in Eq. (2). In the ground state the electronic charge lying on metal coming from e^* and e orbitals is equal to $-2(1-\beta^2)$ and $-4\beta^2$ respectively, while that arising from t_2 amounts to $-6\beta^2$. Thus the total electronic charge on iron due to electrons in valence orbitals is $-(2+8\beta^2)$ and the total charge on metal is $q_M = 8-(2+8\beta^2) = 6-8\beta^2$. In the $(t_1\downarrow)^3\ (t_1\uparrow)^2\ (e^*\uparrow)^2\ (t_2^*\uparrow)^1$ CT state the total charge on metal, $q_M(ex)$, is however equal to $5-7(\beta_{ex})^2$. In the unrelaxed excited state $\beta_{ex}=\beta$ and thus a flow of 0.5*e* is consistent with $\beta^2 \approx 0.6$ underlining the big covalency in the FeO_4^2 complex. When electronic relaxation comes out $q_M(ex)$ can be equal to the ground state charge, q_M, if only $\beta^2-(\beta_{ex})^2 \approx 0.06$. DFT calculations [31] for FeO_4^{2-} give $(\beta_{ex})^2=0.45$ while $\beta^2=0.53$. It is worth noting that the present mechanism needs of some ground state covalency as it requires $(\beta_{ex})^2<\beta^2$ and $(\beta_{ex})^2>0$. In the case of the more ionic CrF_6^{3-} complex the recovery of electronic charge in the first CT state is found to be not so perfect [29] as in the more covalent FeO_4^{2-} unit. DFT calculations indicate that after electronic relaxation in CT state is allowed $q_M - q_M(ex) = 0.2$. Calculations carried out on MnF_6^{4-} and $MnCl_6^{4-}$ also lead to $q_M - q_M(ex) = 0.2$ for *both* complexes.

4.1.4
Ligand Substitution: Jørgensen Rule

A central question in the realm of TM complexes is the effect of ligand substitution upon E_{CT}. The empirical but quite useful rule established by Jørgensen [11, 12, 69] says that when in an ML_N complex the ligand L is substituted by another one L′ the variation undergone by E_{CT}, called ΔE_{CT}, can simply be approximated by

$$\Delta E_{CT} = K\{\chi(L) - \chi(L')\} \tag{14}$$

Table 5 Estimated reductions of the U_M–U_L contribution, $\Delta(U_M–U_L)$, with respect to the MF_6 complex, induced by the $F^-\rightarrow L'$ (L′=Cl,Br, I) substitution if M is a divalent d ion and all involved complexes are assumed to be ionic. The results, given in 10^3 cm^{-1} units, are compared to the corresponding variations, ΔE_{CT}, undergone by E_{CT} given by Eq. (14). R=2.15 Å has been taken as typical value for a MF_6 complex of a divalent cation. The typical variations, ΔR, with respect to this value producedby the $F^-\rightarrow L'$ substitution arealso given in Å

L′	Cl^-	Br^-	I^-
ΔR	0.48	0.63	0.87
$\Delta(U_M–U_L)$	–45	–57	–73
ΔE_{CT}	–30	–36	–45

Here K=30,000 cm^{-1} and χ(L) and χ(L′) are the optical electronegativities of L and L′ species. In the case of ligands such as F^- or Cl^- optical electronegativities coincide with Pauling electronegativities for fluorine or chlorine *atoms*. Therefore, if an MCl_6 complex has an optical absorption band whose maximum is red shifted by about 6000 cm^{-1} upon $Cl^-\rightarrow Br^-$ substitution that band can be due to a CT transition. Equation (14) has been used for identifying CT bands associated with impurities such as Cu^{2+}, Ni^{2+}, V^{2+} [13, 14] and also with less common ions [16, 69, 70] such as Tl^{2+}, or Ag^0.

Some microscopic insight about Eq. (14) can be gained from the analysis carried out in Sects. 4.1.2 and 4.1.3. The $F^-\rightarrow L'$ substitution (L′=Cl, Br, I) in an MF_6 complex keeping the same cation leads to a change of R according to the ionic radius of L′. This leads to a decrement of the U_M–U_L contribution in Eq. (11) and thus to a red shift of E_{CT}. If in a crude approximation all complexes are taken as ionic, the variation experienced by the U_M-U_L contribution as a result of the $F^-\rightarrow L'$ substitution can easily be calculated. Results obtained for a divalent TM cation are given in Table 5. It can be noted that the variations of U_M–U_L along the series, termed $\Delta(U_M–U_L)$, follow the *same trend* that ΔE_{CT} although $|\Delta(U_M\text{-}U_L)|>|\Delta E_{CT}|$. The last result can qualitatively be understood. In fact, a substitution like $F^-\rightarrow Cl^-$ leads to a diminution of the U_M–U_L contribution and thus to a smaller separation among d-orbitals of central cation and n_Lp ligand orbitals. This enhances covalency and thus transfer of electronic charge from ligands to metal which reduces q_M and thus increases $\varepsilon_d^0(q_M)$. For instance calculations give $\varepsilon_d^0(q_M)$=–27.5 and –26.0 eV for MnF_6^{4-} and $MnCl_6^{4-}$, respectively. It is worth noting that in CT states q_M–q_M(ex)=0.2 for *both* MnF_6^{4-} and $MnCl_6^{4-}$ complexes, so implying that the small reduction of metal charge on passing from the ground to the relaxed CT state is the *same for both* systems.

4.2
Systems with Inequivalent Ligands

4.2.1
Tetragonal Cu^{2+} Complexes

Let us first consider the $CuCl_6^{4-}$ complex involved in pure compounds like $(C_2H_5NH_3)_2CuCl_4$ or as impurity in lattices like $CdCl_2$, NaCl or $(C_2h_5NH_3)_2CdCl_4$. In these cases the six Cl^- ligands of $CuCl_6^{4-}$ are not equivalent. In fact, even in NaCl:Cu^{2+} where the host lattice is cubic $CuCl_6^{4-}$ complexes display at low temperatures a static tetragonal symmetry whose C_4 axis is one of the three <100> directions of NaCl. This static distortion comes from a strong Jahn-Teller effect and *random strains*, which favour at a given region of the lattice one of the three possible distortions [71]. Due to this fact the local symmetry around Cu^{2+} in $CuCl_6^{4-}$ units corresponds to an *elongated* octahedron with four *equatorial* Cl^- at a distance R_{eq} and two axial Cl^- at $R_{ax}>R_{eq}$. A compressed geometry with $R_{ax}<R_{eq}$ is less favourable than the elongated one once the anharmonic terms involved in the distortion are taken into account [71, 72].

For an elongated $CuCl_6^{4-}$ unit the unpaired electron lies in the $b_{1g}^*\sim x^2-y^2$ level. Typical equilibrium values are R_{eq}=2.30 Å and R_{ax}=3.0 Å [73]. As to observed CT transitions they involve electron jumps from *equatorial* 3p(Cl) levels to b_{1g}^*. Transitions coming from axial ligands are calculated to have smaller oscillator strength [73]. An explanation of this relevant fact is given in [29, 73].

The first allowed CT transition from *equatorial* ligands, E_{CT}, involves the $e_u(\pi)$ level of $CuCl_6^{4-}$ and appears around 26,500 cm^{-1} [13, 14, 75]. In principle the energy, $E_{CT,}$ of the $e_u(\pi)\rightarrow b_{1g}^*$ jump depends on R_{eq} and also on R_{ax}. This dependence has recently been explored by means of *four* different *methods* [76.] Main results are gathered in Table 6. It can be noticed that: i) the sign of *both* $\partial E_{CT}/\partial R_{eq}$ and $\partial E_{CT}/\partial R_{ax}$ around R_{eq}=228 pm and R_{ax}=297 pm is *again negative* although $|\partial E_{CT}/\partial R_{eq}|$ is found to be much higher than $|\partial E_{CT}/\partial R_{ax}|$; ii) both trends are qualitatively reproduced by all methods employed; iii) the most powerful methods indicate that $|\partial E_{CT}/\partial R_{eq}|$ is *practically ten times* higher than $|\partial E_{CT}/\partial R_{ax}|$. A similar situation is encountered in the case of the $e_u(\sigma)\rightarrow b_{1g}$ transition which is observed at 36,000 cm^{-1}.

Table 6 Calculated values of derivatives $\partial E_{CT}/\partial R_i$ (i=eq, ax) for the first CT transition $e_u(\pi)\rightarrow b_{1g}^*$ ($\sim x^2-y^2$) observed for elongated $CuCl_6^{2-}$ units, using four different theoretical methods[76]: Self-consistent Charge Extended Hückel (SCCEH), Complete Active Space Self Consistent Field (CASPT2), DFT (ADF code) and Multiple Scattering Xα (MSXα). Calculations have been performed around R_{eq}=228 pm and R_{ax}=297 pm. Results obtained for $e_u(\sigma)\rightarrow b_{1g}^*$ ($\sim x^2-y^2$) CT transition (whose energy is called $E_u(\sigma)$) are also reported. Values of $\partial E_{CT}/\partial R_i$ and $\partial E_u(\sigma)/\partial R_i$ are all given in cm^{-1}/pm

	SCCEH	MSXα	CASPT2	ADF
$\partial E_{CT}/\partial R_{eq}$	−435	−374	−256	−252
$\partial E_{CT}/\partial R_{ax}$	−131	−52	−29	−15
$\partial E_u(\sigma)/\partial R_{eq}$	−470	−543	−425	−409
$\partial E_u(\sigma)/\partial R_{ax}$	−150	−67	−39	−20

The big difference between $|\partial E_{CT}/\partial R_{eq}|$ and $|\partial E_{CT}/\partial R_{ax}|$ reflects that R_{ax}=1.4 R_{eq} and the electron density *in both* $b_{1g}{}^{*}\sim x^2-y^2$ and $e_u(\pi)$ orbitals is lying in the *equatorial plane*. Thus E_{CT} is found to be more sensitive to R_{eq} variations than to changes of R_{ax}.

4.2.2
Applications: Can a Metal-Ligand Distance of a CuX_4Y_2 Complex Increase Under Pressure?

Theoretical results collected in Tables 2, 3, 4 and 6 point out that *CT transitions* due to a complex embedded in a lattice can be used for *detecting variations of metal-ligand distances* caused by hydrostatic and chemical pressures. For a typical bandwidth of ~1000 cm^{-1} variations of the band maximum down to ~100 cm^{-1} can be detected experimentally. This means that ΔR_i changes down to typically ~0.1 pm can be measured through E_{CT} once $\partial E_{CT}/\partial R_i$ quantities are known.

As a first application of these ideas let us first comment on optical absorption data from $(C_2H_5NH_3)_2CdCl_4$:Cu^{2+} under hydrostatic pressures [76]. Surprisingly such experimental results show that the first CT transition $e_u(\pi)\rightarrow b_{1g}{}^{*}$ associated with the D_{4h} $CuCl_6{}^{4-}$ complex experiences a *red shift* when pressure increases. In particular E_{CT}=25,000 cm^{-1} at ambient pressure while E_{CT}=23,400 cm^{-1} at P=3.5 GPa. As discussed in Sect. 4.1, a red shift of E_{CT} under pressure can hardly be expected for an octahedral TM complex. In the present case results given in the preceding section for $CuCl_6{}^{4-}$ indicate that a red shift of E_{CT} requires that one of the two R_{eq} and R_{ax} distances increases when pressure increases. At the same time the volume of the $CuCl_6{}^{4-}$ unit must decrease upon pressure. Bearing in mind that $|\partial E_{CT}/\partial R_{eq}|>>|\partial E_{CT}/\partial R_{ax}|$ (Table 6) both conditions can however be fulfilled and the 1400 cm^{-1} red shift explained assuming that $\Delta R_{ax}\approx$–25 pm while $\Delta R_{eq}\approx$7 pm [76]. In other words, pressure in $(C_2H_5NH_3)_2CdCl_4$:Cu^{2+} favours a decrement of the tetragonality. It is worth noting that this relevant conclusion has been derived *simply* from an analysis of changes undergone by the first CT transition upon pressure. For this goal small crystals of size ~100 μm with a Cu^{2+} concentration of ~1000 ppm were employed in view of the high oscillator strength (f~0.1) of allowed CT bands in comparison with that for CF transitions (f~10^{-4}). A similar conclusion has recently been derived for $LaMnO_3$ under pressure [77].

CT transitions have been used for extracting valuable information on lattice relaxation around an impurity in other systems [51, 78]. As an example let us now mention the case of NH_4Cl containing the $CuCl_4(NH_3)_2{}^{2-}$ complex (Fig. 2). The first CT transition of this complex involves an $e_u(\pi)$ level mainly built from 3p orbitals of equatorial Cl^- ligands. In comparison with the room temperature situation the lattice parameter of NH_4Cl experiences at T=243 K an abrupt decrement of 0.4 pm as a result of a structural phase transition. Nevertheless optical absorption data reveal [78] that when this happens E_{CT} of the $CuCl_4(NH_3)_2{}^{2-}$ complex undergoes a 600 cm^{-1} *red shift*. According to the present discussion such a red shift was related to an *increase* of ~2 pm of the equatorial Cu-Cl distance. Additional Raman spectra support this interpretation [78]. In fact when the structural phase transition comes out the frequency of the symmetric $\overrightarrow{Cu}-\overleftarrow{Cl}$ vibration is shown to *decrease* 11 cm^{-1} while that associated with NH_3 ligands *increases* 7 cm^{-1}.

5
Transferred Electronic Charge: Pressure Dependence

Let us come back to three steps described in Sect. 3 which help to understand the electronic structure of TM complexes. In the third step the admixture between d-orbitals of central cation and n_Lp and n_Ls ligand orbitals is finally allowed. Due to this admixture unpaired electrons also spend some time on n_Lp and n_Ls orbitals of ligands. This electron sharing is experimentally well observed through the superhyperfine interaction in EPR and ENDOR spectra of TM complexes placed in diamagnetic host lattices [10, 15]. From the analysis of the experimental superhyperfine tensor reliable information on quantities like β_{ep}, β_{es} or β_t defined in Eqs. (1) and (2) can be obtained. For the sake of clarity let us consider O_h complexes with unpaired e_g electrons in the ground state such as MnF_6^{4-}, NiF_6^{4-} or FeF_6^{3-}. In these cases [34, 79, 80] the isotropic superhyperfine constant, A_s, is essentially proportional to $(\beta_{es})^2$. The anisotropic one, A_p, for the two d^5 complexes depends on both $(\beta_{ep})^2$ and $(\beta_t)^2$ while only on $(\beta_{ep})^2$ for NiF_6^{4-} complex which does not have unpaired t_{2g}^* electrons in the ground state [10].

Therefore, in the case of paramagnetic TM complexes the theoretically calculated covalency can be checked with data coming from the analysis of EPR parameters [10, 24, 59, 80]. A relevant question in this domain is to know the variations undergone by $(\beta_{ep})^2$, $(\beta_t)^2$ and $(\beta_{es})^2$ in an O_h complex when R is changed. Results on this subject for a model complex like MnF_6^{4-} are given in the next section.

5.1
Unpaired Charge Transferred to Valence n_Lp and n_Ls Orbitals of Ligands

In Fig. 6 the calculated R dependences of $(\beta_{ep})^2$ and $(\beta_{es})^2$ are depicted for the ground state of a MnF_6^{4-} complex in the 2 Å<R<2.2 Å range using two different theoretical methods. It can first been noticed that the *main trends* obtained through both methods are quite similar. As expected $(\beta_{ep})^2$ is found to be higher than $(\beta_{es})^2$ basically as a result of the ~23 eV separation between 2p and 2s levels in both free F^- ion and F atom (Table 1). In particular at R=2.15 Å $(\beta_{ep})^2/(\beta_{es})^2$

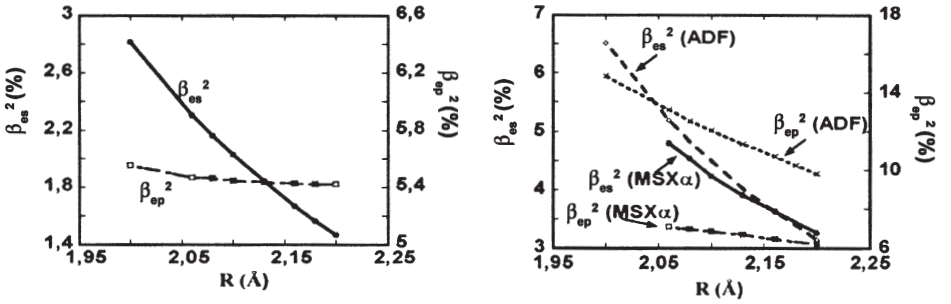

Fig. 6 Dependence of covalency parameters β_{ep}^2 and β_{es}^2, associated with the e_g^* orbital of the octahedral MnF_6^{4-} complex, on the metal-ligand distance. Results derived using the SCCEH method (*left*) and those obtained by means of MSXα and ADF calculations (*right*) are shown

is found to be equal to ~3 for SCCEH and ADF calculations while equal to 1.6 in the case of the MSXα. Usually the *tiny* $(\beta_{es})^2$ quantity (whose experimental value [81] is only around 1.5%) is overestimated in MSXα and DFT calculations [80].

Despite $(\beta_{ep})^2>>(\beta_{es})^2$ results collected in Fig. 6 reveal that $(\beta_{ep})^2$ is much less R dependent than $(\beta_{es})^2$. The slight R dependence of $(\beta_{ep})^2$ can appear in principle as a bit surprising. In fact, intuitively one can imagine that a reduction of R increases significantly the overlap, S_σ, between a metal wavefunction like $|3z^2-r^2>$ and the associated combination of 2p ligand orbitals, $|\chi_{p\theta}>$, in Eq. (1). As $(\beta_{ep})^2$ depends on S_σ^2 one then would expect a much stronger R dependence of $(\beta_{ep})^2$ than that portrayed in Fig. 6. Nevertheless $(\beta_{ep})^2$ *not only* depends on S_σ^2 *but also* on the difference $\varepsilon_d-\varepsilon_p$ obtained after the two first steps. In second order [82] β_{ep} can simply be written as

$$\beta_{ep} \cong \frac{\langle 3z^2 - r^2 | h - \varepsilon_d | \chi_{p\theta} \rangle}{\varepsilon_d - \varepsilon_p} \tag{15}$$

Using now the Wolfsberg-Helmholz guess [83] the R dependence of β_{ep} is just controlled by the ratio $S_\sigma/(\varepsilon_d-\varepsilon_p)$ where $\varepsilon_d-\varepsilon_p$ determines E_{CT}. As discussed in Sect. 4, E_{CT} *also increases* when R decreases and thus cancels to a good extent the effects due to S_σ alone. Writing $S_\sigma \backsim R^{-t_\sigma}$ and $E_{CT} \backsim R^{-t_{CT}}$ it is found that $t_\sigma \approx t_{CT} \approx 2$. A further discussion on this subject is given in [24, 80].

The great sensitivity to R variations experienced by $(\beta_{es})^2$ comes essentially from the big separation between n_Lp and n_Ls orbitals of simple ligands like F^-,Cl^- or O^2 (Table 1). Qualitatively, one can expect a more internal character of the n_Ls orbital in comparison with the n_Lp orbital. Thus if $S_s=<3z^2-r^2|\chi_{s\theta}>$ and it is written $S_s \backsim R^{-t_s}$ one expects that $t_\sigma<t_s$. Theoretical values of t_s for MnF_6^{4-} are around 4. Similar to Eq. (15), β_{es} can be approximated by

$$\beta_{es} \cong \frac{\langle 3z^2 - r^2 | h - \varepsilon_d | \chi_{s\theta} \rangle}{\varepsilon_d - \varepsilon_s} \tag{16}$$

and thus the R dependence of β_{es} is determined by the ratio $S_s/(\varepsilon_d-\varepsilon_s)$. When R is moved the *relative* variation of $\varepsilon_d-\varepsilon_s$ will be much smaller than that of $\varepsilon_d-\varepsilon_p$, because $\varepsilon_d-\varepsilon_p<<\varepsilon_d-\varepsilon_s$ and the change of both quantities is governed (Fig. 4) by the variation undergone by ε_d. This explains basically [24] the big sensitivity of $(\beta_{es})^2$ to R variations displayed in Fig. 6.

The trends collected in Fig. 6 basically account for the quite different R dependence displayed by the superhyperfine constants, A_s and A_p, coming from complexes like MnF_6^{4-} [34, 81], NiF_6^{4-} [79], FeF_6^{3-} [81] or the square planar NiF_4^{3-} unit [24, 84, 85]. For instance when the NiF_4^{3-} complex is formed in the $RbCaF_3$ lattice a value A_s=150 MHz is measured through EPR while A_p=42 MHz [85]. If the same complex is formed in the K_2MgF_4 it turns out that A_s=198 MHz [84] implying a significant 32% increase with respect to the value measured in $RbCaF_3$. By contrast the A_p value for NiF_4^{3-} in both lattices is found to be *the same* within experimental uncertainties. This fact stresses that for NiF_4^{3-} $(\beta_{ep})^2$ is nearly independent of R while $(\beta_{es})^2$ is proportional to R^{-7}. Moreover as $(\beta_{ep})^2>>(\beta_{es})^2$ for TM complexes with halides as ligands results in Fig. 6 explain that the total charge on metal depends only slightly upon R.

6
Dependence of 10Dq on the Metal-Ligand Distance

The separation between antibonding e^* and t_2^* orbitals in octahedral and tetrahedral TM complexes, called 10Dq, plays a key role for explaining the experimental *d-d* transitions lying in the VUV range. A central question concerns the sensitivity of 10Dq to variations of the metal-ligand distance, R, and its microscopic origin.

6.1
Experimental Data and Theoretical Calculations

Early experiments on the optical absorption of NiO under pressure by Drickamer [33, 86] already showed a strong R dependence of 10Dq upon R. Quantitatively, experimental data were fitted to a law:

$$10Dq = K\,R^{-n} \tag{17}$$

where the exponent was found to be n=5. Subsequent experimental work on other TM complexes showed that 10Dq is quite sensitive to R variations [35–40, 87]. For instance from absorption data under hydrostatic pressure on $K_2NaGaF_6:Cr^{3+}$ a value n=4.5 was estimated for the CrF_6^{3-} complex [37]. Similar experiments carried out on ruby, $K_2NaGaCl_6:Cr^{3+}$ and NH_4MnCl_3 gave estimated values of the exponent n in the range 5–6 [36, 38, 87]. The analysis of experimental 10Dq values in $RbMnF_3$ and $KMnF_3$ as well as in cubic perovskites like $KMgF_3$ or $CsCaF_3$ doped with Mn^{2+} lead to n=4.7 for the MnF_6^{4-} complex [35]. At the same time it was also shown that 10Dq can be used for detecting R variations down to ~0.2 pm produced by chemical or hydrostatic pressures [35, 39].

Although CF model predicts an exponent n=5 it was also pointed out in Sect. 3 that such a model fails to explain the 10Dq value itself and thus the present agreement has to be viewed as a fortuitous coincidence. Despite this big discrepancy some workers are still using the CF model for explaining the variations of CF transitions measured under pressure [56].

First SCCEH calculations by Axe and Burns on NiF_6^{4-} and VF_6^{4-} [88] revealed that an exponent n≈5 is also obtained within a reliable MO framework where 10Dq values are found to be comparable to experimental ones. Subsequent theoretical calculations on TM complexes at different R values using several methods (Hartree-Fock, MSXα, DFT, etc.) also lead to values of the exponent n in Eq. (17) in the range 3.5–6 [22, 29, 31, 43, 80, 89–91]. Therefore, theoretical calculations of TM complexes in the MO scheme appear to reproduce the strong R dependence of 10Dq observed experimentally. Despite this overall agreement however it cannot be concluded that the main cause responsible for the great sensitivity of 10Dq to R variations is well understood.

6.2 Microscopic Explanation: Role of Valence $n_L s$ Orbitals of Ligands

According to the analysis carried out in Sect. 3, the separation between antibonding e^* and t_2^* orbitals essentially appears in the third step. In other words

$$10Dq \approx \varepsilon_{ML}\,(\varepsilon_g^*) - \varepsilon_{ML}\,(t_{2g}^*) \tag{18}$$

for an octahedral complex. Bearing in mind the partition scheme by Löwdin [82, 92] $\varepsilon_{ML}(e_g^*)$ and $\varepsilon_{ML}(t_{2g}^*)$ come from off-diagonal matrix elements of the one-electron Hamiltonian like $\langle 3z^2 - r^2 | h | \chi_{s\theta} \rangle$, $\langle 3z^2 - r^2 | h | \chi_{p\theta} \rangle$ or $\langle xy | h | \chi_{pxy} \rangle$, respectively. The same origin have quantities like β_{ep}, β_{es} or β_t as pointed out in Eqs. (15) and (16). In a second order perturbation $\varepsilon_{ML}(e_g^*)$ and $\varepsilon_{ML}(t_{2g}^*)$ can simply be written as

$$\begin{aligned} \varepsilon_{ML}\,(e_g^*) &\cong \frac{\langle 3z^2 - r^2 | h - \varepsilon_d | \chi_{p\theta} \rangle^2}{\varepsilon_d - \varepsilon_p} + \frac{\langle 3z^2 - r^2 | h - \varepsilon_d | \chi_{s\theta} \rangle^2}{\varepsilon_d - \varepsilon_s} \\ \varepsilon_{ML}\,(t_{2g}^*) &\cong \frac{\langle xy | h - \varepsilon_d | \chi_{pxy} \rangle^2}{\varepsilon_d - \varepsilon_p} \end{aligned} \tag{19}$$

Therefore, once the admixture between d-orbitals of metal and valence ligand orbitals is switched on the energy of t_{2g}^* is raised due *only* to the interaction with ligand wavefunctions like $|\chi_{pxy}\rangle$ made of $n_L p$ orbitals. Nevertheless, as shown in Fig. 3, the e_g^* orbitals of the metal can interact with *both* $n_L p$ and $n_L s$ ligand orbitals. It would be quite interesting to elucidate the importance of each one of two contributions to $\varepsilon_{ML}(e_g^*)$ involved in Eq. (19). This task is not easily done experimentally but can be achieved through theoretical calculations where ligand $n_L s$ orbitals can easily be removed from the basis set [93, 94]. Representative results for MnF_6^{4-} are collected in Table 7.

It can be seen that the suppression of $n_L s$ ligand orbitals from the basis set has very little influence upon quantities like $(\beta_{ep})^2$ or $(\beta_t)^2$. Nevertheless the removal of $n_L s$ ligand orbitals has an important effect on the 10Dq value and a dramatic influence upon the exponent n in Eq. (17). A similar behaviour has been encountered for other complexes like CrL_6^{3-} (L=F, Cl), FeF_6^{3-} [80] or FeO_4^{2-} [31]. The surprising changes induced by the lack of a small bonding with $n_L s$ ligand orbitals can however be simply explained [93, 94] through Eqs. (15), (16), (18) and (19), and the results on the R dependence of $(\beta_{ep})^2$, $(\beta_{es})^2$ and $(\beta_t)^2$ given in Fig. 6 and Table 7. The 10Dq value can be expressed as

$$10Dq \cong (\varepsilon_d - \varepsilon_p)\,\{\beta_{ep}^2 - \beta_t^2\} + (\varepsilon_d - \varepsilon_s)\,\beta_{es}^2 \tag{20}$$

Therefore, though $(\beta_{ep})^2 >> (\beta_{es})^2$ both contributions in Eq. (20) can be comparable because $\varepsilon_d - \varepsilon_p << \varepsilon_d - \varepsilon_s$. For MnF_6^{4-} $\varepsilon_d - \varepsilon_p \approx 9$ eV while $\varepsilon_d - \varepsilon_s \approx 30$ eV. Moreover, Eq. (20), Fig. 6 and Table 7 reveal that the strong sensitivity to R variations comes from the small $n_L s$ admixture in Eq. (1). In other words, the strong R dependence of 10Dq and the EPR parameter, A_s, are both related microscopically to the great sensitivity to R variations displayed by $(\beta_{es})^2$ in Fig. 6. This analysis thus stresses that *fine details* in the wavefunctions can play a key role for understanding rele-

Table 7 Calculated values of 10Dq (in cm^{-1}), β_{ep}^2, β_{es}^2 and β_t^2 (in %) for MnF_6^{4-} at R=2.13 Å using both MSXα (first row) and SCCEH (second row) methods [93]. In addition to results of a normal calculation, those obtained removing the 2s(F)orbitals from the basis set ("restricted" calculation) are also shown. Writing $10Dq \propto R^{-n}$, $\beta_{ep}^2 \propto R^{-n_{ep}}$, $\beta_{es}^2 \propto R^{-n_{es}}$ and $\beta_t^2 \propto R^{-n_t}$, the calculated exponents are also given

	10Dq	β_{es}^2	β_{ep}^2	β_t^2	n	n_{es}	n_{ep}	n_t
Normal	7950	4.56	6.63	3.36	4.6	7.3	1.6	5.1
	7140	1.86	7.47	4.16	6.1	7.7	0.2	2.2
Restricted	5060	–	8.49	3.08	0.3	–	2.8	5.7
	2380	–	7.83	4.08	1.2	–	0.2	2.2

vant macroscopic properties. Moreover the present reasoning indicates that the angular overlap model [9, 69, 95] is, in principle, not suitable for explaining the R dependence of 10Dq or the covalency parameter $(\beta_{ep})^2$. As pointed out in Sect. 5, the variation of $(\beta_{ep})^2$ due to R changes is controlled not only by the R dependence of S_σ^2 *but also* by that of $(E_{CT})^{-2}$ which *cannot* be taken as a *constant*.

6.3 Consequences and Final Remarks

The small n_Ls admixture, β_{es}, in Eq. (1) also plays a role in explaining optical parameters like the bandwidth or the Stokes shift of transitions depending on 10Dq [94]. A good example is the lowest CF transition of CrL_6^{3-} complexes (L=F, Cl, Br) involving a simple $t_{2g}^* \rightarrow e_g^*$ jump. In general, the equilibrium metal-ligand distance in an excited state, R_{ex}, is different from that for the ground state, R_g. When an electron jumps from a π-orbital (like t_{2g}^*) to a σ-orbital (like e_g^*) where antibonding effects are stronger, the energy is lowered if $R_{ex} > R_g$. The $R_{ex} - R_g$ difference is controlled by the Huang-Rhys parameter, S_A, corresponding to the symmetric mode, A_1. In the case of a CrL_6^{3-} complex the relation between S_A and $R_{ex} - R_g$ for the first excited state is simply given by [42]

$$S_A \hbar \omega_A = 3 M_L \omega_A^2 (R_{ex} - R_g)^2 \tag{21}$$

where M_L denotes the ligand mass and ω_A is the angular frequency of the A_1 mode. The value of S_A for this transition is governed by $(d10Dq/dR)^2$, the expression for S_A being the following [37, 43]:

$$S_A \hbar \omega_A = n^2 (10Dq)^2 / (12 M_L R_g^2 \omega_A^2) \tag{22}$$

Considering only the coupling of an excited state to the symmetric mode it turns out [42] that the bandwidth is proportional to $\sqrt{S_A}$ while the Stokes shift is given by $S_A \hbar \omega_A$. Bearing in mind the analysis carried out in Sect. 6.2 and the relation $S_A \propto n^2 (10Dq)^2$ it is clear that S_A, the bandwidth and the Stokes shift depend *significantly* on the small 3d-n_Ls hybridisation in the e_g^* orbital [94].

The present work has been devoted to discuss the changes undergone by electronic properties of TM complexes when metal-ligand distances are varied. Particular attention has been paid to explain the main features on simple grounds.

Accurate quantum mechanical calculations are certainly necessary to improve our knowledge on properties due to TM complexes. Despite this fact chemists and physicists should not forget imagination and simple models which allow our mind to understand truly the main reason for a given phenomenon. L. Pauling, E. Wigner [96] and C.K. Jørgensen are good examples of this attitude.

7 References

1. Jørgensen CK (1962) Absorption spectra and chemical bonding in complexes. Pergamon Press, Oxford
2. Solomon EI, Penfield K, Wilcox D (1983) Struct Bond 53:1
3. Solomon EI (2001) Inorg Chem 40:3656
4. Di Bartolo B (ed) (1987) Spectroscopy of solid-state laser-type materials. Plenum, New York
5. Blasse G, Grabmaier BC (1994) Luminescent materials. Springer, Berlin Heidelberg New York
6. Sugano S, Shulman RG (1963) Phys Rev B 130:517
7. Sugano S, Tanabe Y, Kamimura H (1970) Multiplets of transition-metal ions in crystals. Academic Press, New York
8. Barriuso MT, Aramburu JA, Moreno M (2002) Phys Rev B 56:604
9. Lever AP (1984) Inorganic electronic spectroscopy, 2nd edn. Elsevier, Amsterdam
10. Abragam A, Bleaney B (1970) Electron paramagnetic resonance of transition metal ions. Oxford University Press, London
11. Jørgensen CK (1962) Solid State Phys 13:375
12. Jørgensen CK (1970) Prog Inorg Chem 12:101
13. Simonetti J, McClure DS (1979) J Chem Phys 71:793
14. Hirako S, Onaka R (1982) J Phys Soc Jpn 51:1255
15. Spaeth JM, Niklas JR, Bartram RH (1992) Structural analysis of point defects in solids. Springer, Berlin Heidelberg New York
16. Moreno M (1979) J Phys C Solid State Phys 12:L921
17. Larsson S, Connolly WD (1974) J Chem Phys 60:1514
18. Ziegler T, Rauk A, Baerends EJ (1976) Chem Phys 16:209
19. Pueyo L, Richardson JW (1977) J Chem Phys 67:3583
20. Aramburu JA, Moreno M, Bencini A (1987) Chem Phys Lett 140:462
21. Winter NW, Pitzer RM (1988) J Chem Phys 89:446
22. Luaña V, Bermejo M, Florez M, Recio J, Pueyo L (1989) J Chem Phys 90:6409
23. Pierloot K, van Praet E, Vanquickenborne LG (1992) J Chem Phys 96:4163
24. Aramburu JA, Moreno M, Barriuso MT (1992) J Phys Condens Matter 4:9089
25. Woods AM, Sinkovits S, Charpie J, Huang WL, Bartram RH, Rossi AR (1993) J Phys Chem Solids 54:543
26. Pascual JL, Seijo L, Barandiaran Z (1996) Phys Rev B 53:1
27. Pollak C, Rosa A, Baerends EJ (1997) J Am Chem Soc 119:7324
28. Stuckl AC, Daul C, Güdel HU (1997) J Chem Phys 107:4606
29. Aramburu JA, Moreno M, Doclo K, Daul C, Barriuso MT (1999) J Chem Phys 110:1497
30. Dong-Ping Ma, Ellis DE (1997) J Lumin 71:329
31. Wissing K, Aramburu JA, Barriuso MT, Moreno M (1999) J Chem Phys 111:10,217
32. Grochala W, Hoffmann R (2001) Angew Chem Int Ed 40:2743
33. Drickamer H (1967) J Chem Phys 47:1880
34. Barriuso MT, Moreno M (1984) Phys Rev B 29:3623
35. Rodríguez F, Moreno M (1986) J Chem Phys 84:692
36. Duclos SJ, Vohra YK, Ruoff AL (1990) Phys Rev B 41:5372
37. Dolan JF, Rinzler AG, Kappers LA, Bartram RH (1992) J Phys Chem Solids 53:905
38. Rinzler AG, Dolan JF, Kappers LA, Hamilton DS, Bartram RH (1993) J Phys Chem Solids 54:89

39. Marco de Lucas C, Rodríguez F, Dance JM, Moreno M, Tressaud A (1991) J Lumin 57:1
40. Bray KL (2001) Top Curr Chem 213:1
41. Barkyoumb JH, Mansour AN (1992) Phys Rev B 46:8768
42. Bourgoin J, Lannoo M (1983) Point defects in semiconductors II. Springer, Berlin Heidelberg New York
43. Moreno M, Aramburu JA, Barriuso MT (1992) J Phys Condens Matter 4:9481
44. Resta R (2002) J Phys Condens Matter 14:R625
45. Aramburu J A, Moreno M, Cabria I, Barriuso MT, Sousa C, de Graaf C, Illas F (2000) Phys Rev B 62:13356
46. Holmberg GE, Unruh WP, Friauf RJ (1976) Phys Rev B 13:983
47. Bennebroek MT, Poluektov OG, Zakrzewski AJ, Baranov PG, Schmidt J (1995) Phys Rev Lett 74:442
48. Kohn W (1957) Solid State Phys 5:257
49. Barriuso MT, Aramburu JA, Moreno M (2002) J Phys Condens Matter 14:6521
50. Aramburu JA, Moreno M (1997) Phys Rev B 56:604
51. Breñosa A, Rodríguez F, Moreno M (1988) J Phys C Solid State Phys 21:L623
52. Moore CE (1971) Nat Stand Ref Pat Ser Nat Bur Stand 35
53. Clementi E, Roetti C (1974) At Data Nucl Data Tables 14:177
54. Pollini I, Mosser A, Parlebas JC (2001) Phys Rep 355:1
55. Fraga S, Karwowski J, Saxena KMS (1976) Handbook of atomic data. Elsevier, Amsterdam
56. Wenger O, Valiente R, Güdel HU (2001) J Chem Phys 115:3819
57. Te Velde G, Baerends EJ (1992) J Comput Phys 99:84
58. Lacroix R, Emch G (1962) Helv Phys Acta 35:592
59. Aramburu JA, Moreno M (1985) J Chem Phys 83:6071
60. Aramburu JA, Moreno M (1986) Solid State Commun 62:305
61. Desjardins SR, Penfield K, Cohen S, Musselman R, Solomon EI (1983) J Am Chem Soc 105:4590
62. Rogulis U, Spaeth JM, Cabria I, Moreno M, Aramburu JA, Barriuso MT (1998) J Phys Condens Matter 10:6473
63. Cabria I, Moreno M, Aramburu JA, Barriuso MT, Rogulis U, Spaeth JM (1998) J Phys Condens Matter 10:6481
64. Cabria I, Moreno M, Aramburu JA, Barriuso MT (1999) Radiat Eff Defects Solids 151:281
65. Aramburu JA, Barriuso MT, Moreno M (1996) J Phys Condens Matter 8:6901
66. Landau L, Lifschitz E (1958) Statistical mechanics. Pergamon, Oxford
67. Hazenkamp MF, Güdel HU, Atanasov M, Kesper U, Reinen D (1996) Phys Rev B 53:2367
68. Johansen H (1989) Chem Phys Lett 156:592
69. Jørgensen CK (1971) Modern aspects of ligand field theory. North Holland, Amsterdam
70. Nistor SV, Schoemaker D, Ursu I (1994) Phys Status Solidi B 185:9
71. Ham FS (1972) Electron paramagnetic resonance (Geschwind S, ed). Plenum Press, New York
72. Barriuso MT, García-Fernández P, Aramburu JA, Moreno M (2001) Solid State Commun 120:1
73. Valiente R, Rodríguez F (1999) Phys Rev B 60:9423
74. Barriuso MT, Aramburu JA, Daul C, Moreno M (1997) Int J Quantum Chem 61:563
75. Kan'no K, Naoe S, Mukai S, Nakai Y (1973) Solid State Commun 13:1325
76. Valiente R, Rodríguez F, Aramburu JA, Moreno M, Barriuso MT, Sousa C, de Graaf C (2002) Int J Quantum Chem 86:239
77. Loa I, Adler P, Grezchnik A, Syassen K, Schwarz U, Hanfland M, Rozenberg G, Gorrodetsky P, Pasternak M (2001) Phys Rev Lett 87:125,501
78. Breñosa A, Rodríguez F, Moreno M, Couzi M (1991) Phys Rev B 44:9859
79. Villacampa B, Cases R, Orera VM, Alcalá R (1994) J Phys Chem Solids 55:263
80. Aramburu JA, Paredes JI, Barriuso MT, Moreno M (2000) Phys Rev B 61:6525
81. Rousseau JJ, Leble A, Fayet JC (1978) J Phys 39:1215
82. McWeeny R, Sutcliffe BT (1976) Methods of molecular quantum mechanics. Academic Press, London

83. Ballhausen CJ, Gray HB (1965) Molecular orbital theory. Benjamin, New York
84. Alcalá R, Zorita E, Alonso PJ (1988) J Phys C Solid State Phys 21:461
85. Villacampa B, Alcalá R, Alonso PJ, Moreno M, Aramburu JA, Barriuso MT (1994) Phys Rev B 49:1039
86. Drickamer HG, Frank CW (1973) Electronic transitions and the high pressure chemistry and physics of solids. Chapman and Hall, London
87. Hernández D, Rodríguez F, Moreno M, Güdel HU(1999) Physica B 265:186
88. Burns G, Axe J (1966) J Chem Phys 45:4362
89. Bermejo M, Pueyo L (1982) J Chem Phys 78:854
90. Adachi H, Shiokawa S, Tsukada M, Sugano S (1979) J Phys Soc Jpn 47:1528
91. Richardson JW, Janssen G (1989) Phys Rev B 39:4958
92. Löwdin PO (1951) J Chem Phys 19:1396
93. Moreno M, Barriuso MT, Aramburu JA (1994) Int J Quantum Chem 52:829
94. Moreno M, Aramburu JA, Barriuso MT (1997) Phys Rev B 56:14,423
95. Schönherr T (1997) Top Curr Chem 191:88
96. Wigner EP, Seitz F (1956) Solid State Phys 1:97

Structure and Bonding, Vol. 106 (2004): 153–172
DOI 10.1007/b11310

Structure, Spectroscopy and Photochemistry of the $[M(\eta^5\text{-}C_5H_5)(CO)_2]_2$ Complexes (M=Fe, Ru)

Maria Jaworska[1] · Wojciech Macyk[2] · Zofia Stasicka[3]

[1] Silesian University, Department of Theoretical Chemistry, Szkolna 9, 40-006 Katowice, Poland
[2] University of Erlangen-Nürnberg, Institute of Inorganic Chemistry, Egerlandstrasse 1, 91058 Erlangen, Germany
[3] Jagiellonian University, Faculty of Chemistry, Ingardena 3, 30-060 Kraków, Poland
E-mail: stasicka@chemia.uj.edu.pl

Abstract The structures of all possible isomeric forms of the $[M(\eta^5\text{-}C_5H_5)(CO)_2]_2$ complexes (M=Fe, Ru) are calculated with the use of the DFT method. The results indicate that both dimers can occur in three stable forms: bridged *trans* and *cis* and non-bridged *trans*. Contrary to the previous reports, the *cis* non-bridged form turns out to be an unstable transition state. Instead, an additional stable structure, a *gauche* non-bridged one, is found but only in the case of the Ru compound. Without any outer-sphere interaction the *trans*-bridged form is of the lowest energy for both dimers. The results are compared with the experimental data. Strong impact of the medium on the stability of the individual structures in solution is emphasized. The electronic spectra of all stable forms, calculated using TDDFT method, reproduce well spectral properties of both complexes. Moreover, they are useful in interpreting the medium effect and photochemical behaviour. The photoreactivity is briefly reviewed pointing at analogies and differences between the Fe and Ru complexes.

Keywords Cyclopentadienyl metal carbonyl compounds · DFT calculation · Structure · Electronic spectrum · Photochemistry

This paper is respectfully dedicated to the memory of Professor Christian Klixbull Jorgensen

1 Introduction

For about 50 years $[M(\eta^5\text{-}C_5H_5)(CO)_2]_2$ complexes (M=Fe, Ru, Os) have been at the centre of interest from both theoretical and application aspects. The latter prospect is connected with the development in activation of the C-H bond, which is believed to involve an oxidative addition as the C-H breaking step, and may be either thermal or photochemical. Moreover, the dimers may be considered as cluster prototypes and their chemistry may provide insights into reactions occurring at metal surfaces.

The theoretical interest in the $[M(\eta^5\text{-}C_5H_5)(CO)_2]_2$ dimers concerns mostly their versatile structures which entail varied thermal and photochemical behaviour [1, 2]. The versatility is reflected by the structural changes accompanying crystal dissolution or a change of solvent [2]. The behaviour is dependent on the central atom nature: the iron and ruthenium dimers crystallize mostly in the bridged forms, $[M(\eta^5\text{-}C_5H_5)(\mu\text{-}CO)(CO)]_2$, distinct from the osmium compound, which forms only the non-bridged dimer. In solution, the Fe-dimer is present predominantly as the bridged form (>99%), whereas in the case of Ru-dimer both bridged and non-bridged forms are in equilibrium, which is strongly affected by many parameters, such as solvent polarity, temperature and pressure [3].

2 Molecular Structure

2.1 Experimental Data

The synthesis and infrared spectrum of $[CpFe(CO)_2]_2$ (Cp=η^5-C_5H_5) (**I**) were reported for the first time in 1955 [4]; analogous $[CpRu(CO)_2]_2$ (**II**) and $[CpOs(CO)_2]_2$ complexes were described in 1962 [5, 6]. The X-ray and neutron diffraction studies [7–9] showed that **I** has a centrosymmetric structure in the solid phase with two bridging and two terminal carbonyl groups (*trans*-bridged form). Low-temperature crystallization made possible isolation of the *cis* form [10]. However, only the *trans*-bridged structure of crystalline **II** was detected by the X-ray and neutron diffraction methods [11, 12].

IR investigations of **I** and **II** in solutions showed that not only bridged but also non-bridged forms are present [13–15]. Three forms of **I** in equilibrium were detected in various solvents: *trans*-bridged, *cis*-bridged and non-bridged; the last form in small amount. The ratio between the bridged forms depended on the solvent polarity with the *trans* form predominating in non-polar and *cis* in polar solvents [13]. The relative intensities of *cis* and *trans* forms were found to be temperature independent, which led to the conclusion of equal formation enthalpy for both forms.

IR spectra of the dissolved **II** were interpreted in terms of existence of four forms: bridged and non-bridged, each of them in *cis* and *trans* conformations [16]. Alternatively, the non-bridged form was considered as a conformational intermediate between the *cis* and *trans* isomers. In solutions of **II** the non-bridged

form appeared to be favoured by non-polar solvents, increased temperature and decreased pressure [3]. From the temperature dependence of the UV/vis and IR spectra the enthalpy ΔH of the bridged-$[CpM(CO)_2]_2$↔non-bridged-$[CpM(CO)_2]_2$ equilibrium was assessed to 6.3 kJ/mol for **II** and 16.7 kJ/mol in the case of **I** [3, 17].

Many attempts have been made to compare the stability of two conformers of the bridged form both in the solid phase and in solution. X-ray study of **I** together with sublimation experiments and low-temperature crystallization led to conclusion that the *cis* form is thermodynamically less stable [7, 10]. ^{1}H-NMR spectra of **I** dissolved in C_6D_6-CS_2 showed, however, that the *cis*-bridged isomer is by 4.2 kJ/mol more stable than the *trans* one, with the energy barrier of *trans*-bridged-**I**↔non-bridged-**I** interconversion of about 54.3 kJ/mol [18]. The energy barrier for *cis*-bridged-**I**↔*trans*-bridged-**I** isomerization in dichloromethane was determined from temperature dependent ^{13}C-NMR spectra to be 48.9 kJ/mol [19]. In $CFCl_3$-CS_2 the relative stabilities of *cis*-bridged, *trans*-bridged and non-bridged isomers and respective energy barriers were determined for both **I** and **II** [20]. The *cis*-bridged form turned out to be more stable than the *trans*-bridged one by 5.4 kJ/mol for **I** and 4.2 kJ/mol for **II**. The enthalpy of non-bridged forms appeared to be about 21 kJ/mol higher than *cis*-bridged for **I** and ca. 12 kJ/mol lower for **II**.

Investigation of the temperature-dependent ^{13}C-NMR spectra of **I** led to the conclusion that the exchange of bridge carbonyl ligands is much easier in the *trans* isomer than in the *cis* one [21]. This phenomenon was explained by Adams and Cotton [22] who showed that carbonyl exchange in the *cis*-bridged isomer needs the rotation around the Fe-Fe bond in the non-bridged intermediate, while in the *trans* form opening and consecutive closing of the carbonyl bridges is sufficient to activate the carbonyl exchange.

2.2 Theoretical Calculations

All possible forms, i.e. bridged *cis* and *trans*, and non-bridged *cis* and *trans* were optimised with the use of the DFT method [23]. Two density functionals were used, namely B3LYP [24] and BP86 [25]. The results of the optimisation for both functionals are generally the same (apart from the specific geometry parameters). LANL2 basis set with additional *d* and *f* functions was used for the metal atoms with the exponents 0.1214 and 2.3 for iron and 0.081 and 1.533 for ruthenium, for *d* and *f* functions, respectively. DZV(*d*) basis for the carbon and oxygen atoms was employed, and DZV basis for the hydrogen atoms. Frequencies were calculated for all forms under investigation, to check if they are stable minima or transition states on the potential energy surfaces. The full details of calculations are described elsewhere [26].

The optimised structures are shown in Fig. 1 and optimised structural parameters are presented in Table 1. Three stable forms of **I** were found: *trans*-bridged (**trans-b**), *cis*-bridged (**cis-b**) and *trans*-non-bridged (**trans-nb**). The frequencies calculated for all mentioned forms are real, confirming that these are true minima of the energy surface. The *cis*-non-bridged (**cis-nb**) form was also optimised;

Table 1 Calculated geometry parameters for the stable forms of $[CpFe(CO)_2]_2$ and $[CpRu(CO)_2]_2$ (distances in Å)

$[CpFe(CO)_2]_2$									
	methods	trans-b			cis-b			trans-nb	
M-M	B3LYP/BP86/Exp.	2.545	2.514	2.539[c]	2.545	2.516	2.531[d]	2.687	2.665
M-C(Cp)[a]	B3LYP/BP86/Exp.	2.163	2.158	2.127[c]	2.160	2.153	2.114[d]	2.151	2.140
$M\text{-}C(CO)_b$[a]	B3LYP/BP86/Exp.	1.907	1.902	1.924[c]	1.911	1.906	1.917[d]		
$M\text{-}C(CO)_t$[a]	B3LYP/BP86/Exp.	1.752	1.729	1.761[c]	1.757	1.736	1.745[d]	1.748	1.730
$C\text{-}O_b$[a]	B3LYP/BP86/Exp.	1.184	1.199	1.180[c]	1.184	1.199	1.180[d]		
$C\text{-}O_t$[a]	B3LYP/BP86/Exp.	1.161	1.179	1.150[c]	1.158	1.176	1.153[d]	1.166	1.181
$CO_b\text{-}M\text{-}CO_b$[a], $CO_t\text{-}M\text{-}CO_t$[b]	B3LYP/BP86/Exp.	96.3	97.3	97.4[c]	95.2	96.0	96.0[d]	95.1	93.9
$M\text{-}CO_b\text{-}M$[a]	B3LYP/BP86/Exp.	83.7	82.7	82.6[c]	83.5	82.6	82.8[d]		
$CO_t\text{-}M\text{-}CO_b$[a], $CO_t\text{-}M\text{-}M$[b]	B3LYP/BP86/Exp.	93.0	92.9	93.8[c]	90.2	90.1	89.0[d]	80.2	80.5
Cp-M-M-Cp	B3LYP/BP86	180.0	180.0		0.0	0.0		180.0	180.0
$[CpRu(CO)_2]_2$									
	methods	trans-b			cis-b		trans-nb		gauche-nb	
M-M	B3LYP/BP86/Exp.	2.781	2.759	2.738[e]	2.778	2.760	2.876	2.852	2.857	2.844
M-C(Cp)[a]	B3LYP/BP86/Exp.	2.343	2.339	2.258[e]	2.340	2.333	2.333	2.324	2.333	2.322
$M\text{-}C(CO)_b$[a]	B3LYP/BP86/Exp.	2.052	2.048	2.035[e]	2.056	2.052				
$M\text{-}C(CO)_t$[a]	B3LYP/BP86/Exp.	1.874	1.862	1.850[e]	1.877	1.867	1.870	1.861	1.875	1.864
$C\text{-}O_b$[a]	B3LYP/BP86/Exp.	1.185	1.199	1.247[f]	1.184	1.199				
$C\text{-}O_t$[a]	B3LYP/BP86/Exp.	1.163	1.179	1.132[f]	1.161	1.176	1.165	1.180	1.162	1.177
$CO_b\text{-}M\text{-}CO_b$[a], $CO_t\text{-}M\text{-}CO_t$[b]	B3LYP/BP86/Exp.	94.7	95.3	93.0[f]	93.6	94.1	91.8	91.5	91.2	91.2
$M\text{-}CO_b\text{-}M$[a]	B3LYP/BP86/Exp.	85.3	84.6	87.0[f]	85.0	84.5				
$CO_t\text{-}M\text{-}CO_b$[a], $CO_t\text{-}M\text{-}M$[b]	B3LYP/BP86/Exp.	92.3	92.4	92.1[e]	90.0	89.8	82.8	93.2	86.7	86.8
Cp-M-M-Cp	B3LYP/BP86	180.0	180.0		0.0	0.0	180.0	180.0	71.0	72.5

[a] Average values
[b] For non-bridged form
[c] [9]
[d] [10]
[e] [12]
[f] [7]

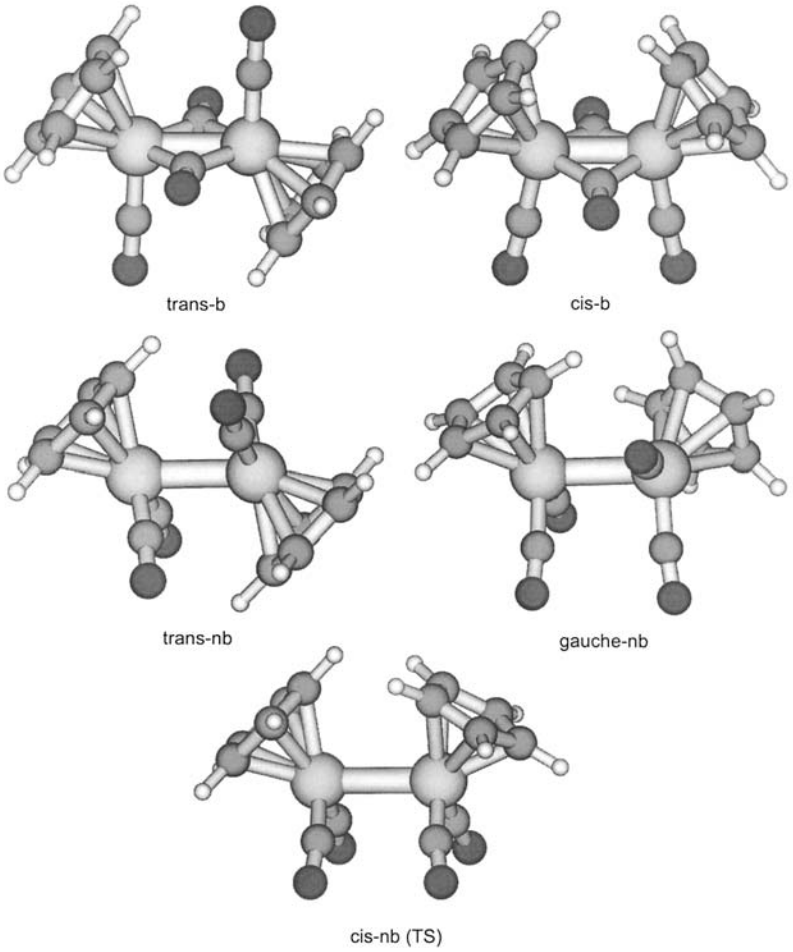

Fig. 1 The DFT optimised structures for different conformers of $[CpM(CO)_2]_2$. TS denotes transition state

this form, however, revealed one imaginary frequency for both **I** and **II**, which indicated its transition state character. The **cis-nb** form was examined because it was postulated earlier as one of the possible isomers of **I** and **II**. After releasing the symmetry constraints, however, it converts to one of the stable forms. This transition state should correspond to a rotational barrier around the metal-metal bond. There are other possible transition states between different isomers, but they were not sought in the calculations.

An additional stable form was detected for **II**, i.e. *gauche*-non-bridged isomer (**gauche-nb**). The dihedral angle Cp-Ru-Ru-Cp in this conformer is 71.0°. Two carbonyl groups at different Ru atoms are nearly in the *trans* position (dihedral angle 165°) whereas two others are placed at approximately *cis* positions (dihedral angle 15.0°). This form does not exist in the case of the iron compound; it con-

verts during optimisation into the *cis*-bridged form. This phenomenon can be explained by relatively short Fe-Fe bond, which enables terminal-CO to transform easily into a bridged-CO.

The **trans-b** and **trans-nb** forms have C_{2h} symmetry, the symmetry of **cis-b** form is C_2 due to modest rotation of the cyclopentadienyl rings (about 10°), **gauche-nb** is of C_2 symmetry, and **cis-b** transition state has C_s symmetry. The comparison of the calculated geometry parameters with the experimental ones (Table 1) shows that the B3LYP method gives better agreement for **I**. The calculated Fe-Fe bond length agrees very well, especially for the **trans-b** form. Geometry of the **trans-b** form of **II** is better reproduced by the BP86 method.

Energies of different forms of **I** and **II** calculated using the B3LYP and BP86 methods are collected in Table 2 together with the experimental data [20]. The energies are calculated relatively to the **trans-b** form. The BP86 method points to **trans-b** as the form of lowest energy, in contrast to the B3LYP method**,** which indicates **trans-nb** as a somewhat lower energy form. In both methods the **cis-b** form is close in energy to the **trans-b** one, the largest difference being 8.0 kJ/mol for **II**. The BP86 places **trans-nb** form 28.2 and 24.7 kJ/mol higher than **trans-b** for **I** and **II**, respectively, but **gauche-nb** 35.0 kJ/mol higher than **trans-b** of **II**.

Different ordering of bridged and non-bridged forms shown by the B3LYP and BP86 methods is typical for dimeric transition metal carbonyl compounds. A similar effect was obtained for $[Co_2(CO)_8]$ [27]. It is caused by various estimations of the relative metal-metal bond and metal-carbonyl bond energies in both methods. The B3LYP method as compared to BP86 overestimates the strength of the metal-metal bond. For this class of compounds, the ordering of conformers is better reproduced by BP86.

The energetics of interconversion between different forms of **I** and **II**, presented in Table 2, differs considerably from that concluded from NMR spectra of their $CFCl_3$-CS_2 solutions [20]. The calculated energy, however, concerns molecular entities without any outer-sphere interaction and does not account for the solvent effects that strongly influence the equilibrium between the isomers [3, 13–17].

Table 2 Calculated energies of different forms of $[CpFe(CO)_2]_2$ and $[CpRu(CO)_2]_2$

	Relative energy (kJ/mol)[a]					
	$[FeCp(CO)_2]_2$			$[RuCp(CO)_2]_2$		
	B3LYP	BP86	Exp.[b]	B3LYP	BP86	Exp[b].
trans-b	0.0	0.0	0.0	0.0	0.0	0.0
cis-b	1.6	5.8	–5.4	4.1	8.0	–4.2
trans-nb	–1.4	28.2	15.9	–0.4	24.7	7.5
gauche-nb			15.0	11.4	35.0	6.7
cis-b(TS)	60.7	92.3	46.4	41.0	68.1	31.7

[a] Relative to the *trans*-bridged form.
[b] [20].

3
Electronic Spectroscopy

3.1
Molecular Orbitals

The results are exemplified in Fig. 2, where six HOMO and six LUMO orbitals of the **trans-b** form of **I** obtained from the B3LYP calculations are presented. The HOMO orbital is a four-centre σ-type orbital describing bonding formed by two metal d_π orbitals and the π^* orbitals of the bridging carbonyls. This orbital is placed in the plane formed by two metal atoms and the bridging carbonyl groups and is denoted further as $\sigma_{d\text{-}CO(b)}$. The LUMO orbital is a σ^* metal-metal orbital. Calculations using other theoretical models like extended Hückel [9, 28, 29], Hartree-Fock [30, 31], Fenske-Hall [32, 33] and DFT [2] show similar pattern of the HOMO-LUMO orbitals. The σ metal-metal orbital (HOMO-5, denoted further as σ) is placed low and the orbital contour between two metal atoms is rather small, which indicates that direct metal-metal bond in the bridged Fe-complex is quite weak. This is in accord with the experimentally determined electron density distribution in the **trans-b** form of **I** [9], showing that the electron density gradient between the metal atoms is small. The LUMO+1 orbital is the antibonding counterpart of $\sigma_{d\text{-}CO(b)}$. Other HOMO and LUMO orbitals are bonding and antibonding combinations of metal *d* orbitals and π^*_{CO}, respectively, with the prevailing *d* metal character in HOMO orbitals and π^*_{CO} in LUMO orbitals. They are denoted further as *d* and π^*_{CO}.

3.2
Calculated Spectra

The widely used assignments of transitions in dinuclear complexes [34–40] follow the designation suggested by Levenson et al. [35] for $[Mn_2(CO)_{10}]$ which exists in the non-bridged form. The intense, near-UV band (around 340 nm) was ascribed to $\sigma\rightarrow\sigma^*$ transition (where σ denotes metal-metal bond) based on the intensity, polarization and energy criteria. The weaker, low energy band was assigned to $d\rightarrow\sigma^*$ transition and the higher energy bands to $d\rightarrow\pi^*_{CO}$ and $\sigma\rightarrow\pi^*_{CO}$ transitions [36]. The first low energy band of $[Re_2(CO)_{10}]$ was suggested to overlap with the intense near-UV band [37]. For $[Co_2(CO)_8]$ two low energy bands at about 430 and 410 nm were ascribed to $d\rightarrow\sigma^*$ transitions in the non-bridged and bridged isomers, respectively, and two higher energy bands at about 350 and 280 nm were ascribed to $\sigma\rightarrow\sigma^*$ transitions in non-bridged and bridged isomers, respectively [39].

The electronic spectra of $[CpFe(CO)_2]_2$ and $[CpRu(CO)_2]_2$ were calculated using the TDDFT method [41] with the B3LYP and BP86 functionals, for geometries optimised with the same functionals for all stable forms of **I** and **II**. The spin allowed singlet states were taken into account and the calculated wavelengths and energies of the transitions that are characterized by the highest oscillator strengths for **I** and **II** are shown in Tables 3 and 4, respectively. Some less intensive transitions relevant to the comparison with the experimental data are also

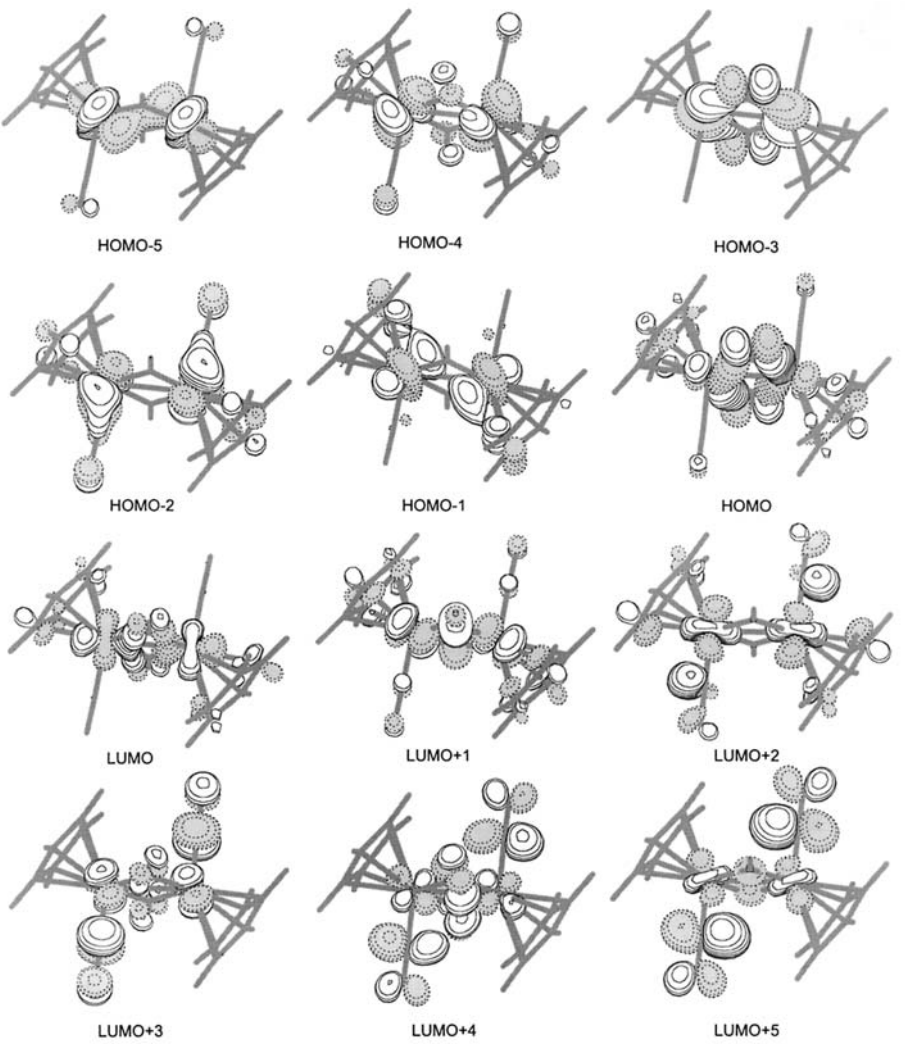

Fig. 2 Six HOMO orbitals and six LUMO orbitals for **trans-b** form of **I** (B3LYP)

included. The previous calculation of the electronic spectrum of **I** was performed with the INDO method by Li et al. [42].

3.2.1 *[CpFe(CO)$_2$]$_2$*

Three solvent sensitive bands characterize the experimental spectrum of **I**: at 514 (710), 410 (1870) and 346 nm (9190) in benzene solution [34, 43], at 520 (770), 407 (2070) and 348 nm (8320) in methylocyclohexane [44] and at 505 (620), 398 (1930) and 343 nm (8350) in 2-MeTHF [44] (molar absorption coefficients,

Table 3 Calculated wavelengths (λ), transition energies (E) and oscillator strengths (f) for the transitions of $[CpFe(CO)_2]_2$ (H denotes HOMO, L=LUMO)

State	λ(nm)	E(eV)	f	The most important orbital excitations
B3LYP				
trans-b				
B_u	508.9	2.43	0.004	0.613 H-1→L($d\rightarrow\sigma^*$)
B_u	435.5	2.85	0.017	0.567 H-5→L($\sigma\rightarrow\sigma^*$) +0.348 H→L+1($\sigma_{d\text{-}CO(b)}\rightarrow\sigma^*_{d\text{-}CO(b)}$)
B_u	359.0	3.45	0.099	−0.265 H-3→L+2($d\rightarrow\pi^*_{CO}$) +0.494 H→L+1($\sigma_{d\text{-}CO(b)}\rightarrow\sigma^*_{d\text{-}CO(b)}$)
cis-b				
A	482.6	2.57	0.004	−0.325 H-5→L($d\rightarrow\sigma^*$) +0.514 H-1→L($d\rightarrow\sigma^*$)
B	369.6	3.35	0.057	0.280 H-1→L+2($d\rightarrow\pi^*_{CO}$) +0.498 H→L+1($\sigma_{d\text{-}CO(b)}\rightarrow\sigma^*_{d\text{-}CO(b)}$)
B	311.7	3.97	0.032	0.325 H-2→L+1($d\rightarrow\sigma^*_{d\text{-}CO(b)}$) −0.259 H-1→L+3($d\rightarrow\pi^*_{CO}$) +0.352 H→L+5($\sigma_{d\text{-}CO(b)}\rightarrow\pi^*_{CO}$)
B	308.2	4.02	0.015	0.249 H-5→L+1($d\rightarrow\sigma^*_{d\text{-}CO(b)}$) +0.431 H-4→L+1($d\rightarrow\sigma^*_{d\text{-}CO(b)}$) −0.228 H-3→L+2($\sigma\rightarrow\pi^*_{CO}$)
B	278.7	4.45	0.041	−0.239 H-2→L+5($d\rightarrow\pi^*_{CO}$) +0.515 H-1→L+3($d\rightarrow\pi^*_{CO}$)
trans-nb				
B_u	530.7	2.33	0.019	0.593 H-2→L($d\rightarrow\sigma^*$) −0.235 H→L($\sigma\rightarrow\sigma^*$)
B_u	423.3	2.92	0.011	0.540 H-1→L+1($d\rightarrow\pi^*_{CO}$) +0.242 H→L($\sigma\rightarrow\sigma^*$)
B_u	369.9	3.35	0.162	0.306 H-2→ L($d\rightarrow\sigma^*$) +0.453 H→L($\sigma\rightarrow\sigma^*$)
B_u	321.9	3.85	0.025	0.534 H-5→L($d\rightarrow\sigma^*$)
B_u	301.6	4.11	0.023	0.638 H→L+4($\sigma\rightarrow\pi^*_{CO}$)
B_u	268.6	4.61	0.094	0.421 H-2→L+4($d\rightarrow\pi^*_{CO}$) −0.286 H-3→L+5($d\rightarrow\pi^*_{CO}$) +0.289 H→L+6($\sigma\rightarrow\pi^*_{CO}$)

Table 3 (continued)

State	λ(nm)	E(eV)	f	The most important orbital excitations
BP86				
trans-b				
B_u	488.0	2.54	0.008	0.650 H-1→L($d\rightarrow\sigma^*$)
B_u	425.1	2.92	0.022	0.517 H-4→L($\sigma\rightarrow\sigma^*$) +0.449 H→L+1($\sigma_{d\text{-}CO(b)}\rightarrow\sigma^*_{d\text{-}CO(b)}$)
B_u	356.7	3.47	0.111	0.401 H-4→L($\sigma\rightarrow\sigma^*$) −0.347 H→L+1($\sigma_{d\text{-}CO(b)}\rightarrow\sigma^*_{d\text{-}CO(b)}$)
A_u	338.6	3.66	0.011	0.656 H-2→L+2($d\rightarrow\pi^*_{CO}$)
cis-b				
A	477.3	2.60	0.004	0.656 H-1→L($d\rightarrow\sigma^*$)
B	368.1	3.37	0.014	0.343 H-2→L+1($d\rightarrow\sigma^*_{d\text{-}CO(b)}$) −0.367 H-1→L+1($d\rightarrow\sigma^*_{d\text{-}CO(b)}$)
B	342.3	3.62	0.057	0.234 H-4→L+2($\sigma\rightarrow\pi^*_{CO}$) −0.262 H-3→L+2($d\rightarrow\pi^*_{CO}$) −0.430 H-2→L+1($d\rightarrow\sigma^*_{d\text{-}CO(b)}$)
B	340.9	3.64	0.024	0.414 H-4→L+2($\sigma\rightarrow\pi^*_{CO}$) +0.352 H-3→L+2($d\rightarrow\pi^*_{CO}$) +0.210 H-2→L+1($d\rightarrow\sigma^*_{d\text{-}CO(b)}$)
A	331.8	3.74	0.011	0.515 H-4→L+1($\sigma\rightarrow\sigma^*_{d\text{-}CO(b)}$) +0.365 H→L+4($\sigma_{d\text{-}CO(b)}\rightarrow\pi^*_{CO}$)
B	314.7	3.94	0.026	0.243 H-3→L+2($d\rightarrow\pi^*_{CO}$) −0.258 H-1→L+3($d\rightarrow\pi^*_{CO}$) +0.424 H→L+5($\sigma_{d\text{-}CO(b)}\rightarrow\pi^*_{CO}$)
trans-nb				
B_u	493.7	2.51	0.009	0.396 H-2→L($d\rightarrow\sigma^*$) +0.556 H-1→L($\sigma\rightarrow\sigma^*$)
B_u	381.3	3.25	0.143	−0.308 H-5→L($d\rightarrow\sigma^*$) +0.419 H-2→L($d\rightarrow\sigma^*$) +0.241 H-1→L($\sigma\rightarrow\sigma^*$) +0.234 H→L+1($d\rightarrow\pi^*_{CO}$)
B_u	327.9	3.78	0.032	0.549 H-5→L($d\rightarrow\sigma^*$) +0.257 H-1→L+4($\sigma\rightarrow\pi^*_{CO}$)

Table 4 Calculated wavelengths (λ), transition energies (E) and oscillator strengths (f) for the transitions of $[CpRu(CO)_2]_2$

State	λ (nm)	E (eV)	f	The most important orbital excitations
B3LYP				
trans-b				
B_u	349.1	3.55	0.094	-0.454 H-4→L($\sigma\rightarrow\sigma^*$) +0.475 H→L+1($\sigma_{d\text{-}CO(b)}\rightarrow\sigma^*_{d\text{-}CO(b)}$)
B_u	301.7	4.11	0.160	0.405 H-4→L($\sigma\rightarrow\sigma^*$) +0.329 H-3→L+2($d\rightarrow\pi^*_{CO}$)+0.270 H→L+1 ($\sigma_{d\text{-}CO(b)}\rightarrow\sigma^*_{d\text{-}CO(b)}$)
cis-b				
B	361.2	3.43	0.034	-0.350 H-4→L($\sigma\rightarrow\sigma^*$) +0.585 H→L+2($\sigma_{d\text{-}CO(b)}\rightarrow\pi^*_{CO}$)
B	313.7	3.95	0.016	0.369 H-4→L($\sigma\rightarrow\sigma^*$) +0.453 H-2→L+1($d\rightarrow\sigma^*_{d\text{-}CO(b)}$)
B	309.8	4.00	0.054	0.588 H-1→L+1($d\rightarrow\sigma^*_{d\text{-}CO(b)}$)
trans-nb				
B_u	407.4	3.04	0.009	0.589 H-2→L($d\rightarrow\sigma^*$) +0.349 H→L($\sigma\rightarrow\sigma^*$)
B_u	348.4	3.56	0.108	0.268 H-2→L($d\rightarrow\sigma^*$) +0.469 H-1→L+1($d\rightarrow\pi^*_{CO}$) -0.378 H→L($\sigma\rightarrow\sigma^*$)
B_u	324.0	3.83	0.282	0.451 H-1→L+1($d\rightarrow\pi^*_{CO}$) +0.349 H→L($\sigma\rightarrow\sigma^*$)
B_u	279.4	4.44	0.080	0.606 H-5→L($d\rightarrow\sigma^*$)
gauche-nb				
B	362.3	3.42	0.177	-0.279 H-4→L($d\rightarrow\sigma^*$) +0.557 H→L($\sigma\rightarrow\sigma^*$)
B	318.7	3.89	0.039	0.391 H-4→L($d\rightarrow\sigma^*$) +0.417 H-2→L+2($d\rightarrow\pi^*_{CO}$)
B	309.9	4.00	0.057	0.572 H-1→L+1($d\rightarrow\pi^*_{CO}$)
B	301.8	4.10	0.136	-0.273 H-4→L($d\rightarrow\sigma^*$) +0.448 H-2→L+2($d\rightarrow\pi^*_{CO}$)+0.232 H-1→L+3($d\rightarrow\pi^*_{CO}$)
B	283.5	4.37	0.031	0.533 H-6→L($d\rightarrow\sigma^*$)

Table 4 (continued)

State	λ (nm)	E (eV)	f	The most important orbital excitations
BP86				
trans-b				
B_u	362.4	3.42	0.091	−0.390 H-4→L($\sigma\rightarrow\sigma^*$) +0.340 H-1→L(d→$\sigma^*$) +0.418 H→L+1($\sigma_{d\text{-}CO(b)}\rightarrow\sigma^*_{d\text{-}CO(b)}$)
B_u	306.9	4.04	0.087	0.427 H-4→L($\sigma\rightarrow\sigma^*$) −0.425 H-2→L+2(d→$\pi^*_{CO}$)
B_u	303.3	4.09	0.115	0.242 H-4→L($\sigma\rightarrow\sigma^*$)+0.508 H-2→L+2(d→$\pi^*_{CO}$)
B_u	284.4	4.36	0.032	0.634 H-1→L+3(d→π^*_{CO})
cis-b				
B	382.9	3.24	0.029	−0.251 H-4→L($\sigma\rightarrow\sigma^*$) +0.615 H→L+2($\sigma_{d\text{-}CO(b)}\rightarrow\pi^*_{CO}$)
B	297.0	4.17	0.126	−0.329 H-5→L+2(d→π^*_{CO})+0.323 H-4→L($\sigma\rightarrow\sigma^*$) +0.235 H→L+5($\sigma_{d\text{-}CO(b)}\rightarrow\pi^*_{CO}$)
B	271.0	4.57	0.042	0.430 H-5→L+2(d→π^*_{CO})+0.378 H→L+10
B	270.2	4.59	0.023	−0.306 H-5→L+2(d→π^*_{CO})+0.537 H→L+10
trans-nb				
B_u	415.9	2.98	0.018	0.413 H-2→L(d→σ^*) +0.548 H-1→L($\sigma\rightarrow\sigma^*$)
B_u	335.6	3.69	0.271	0.266 H-5→L(d→σ^*) +0.422 H-2→L(d→σ^*) −0.310 H-1→L($\sigma\rightarrow\sigma^*$)
B_u	287.7	4.31	0.036	0.507 H-5→L(d→σ^*) +0.376 H→L+7(d→π^*_{CO})
B_u	281.0	4.41	0.026	−0.266 H-5→L(d→σ^*) +0.579 H→L+7(d→π^*_{CO})
gauche-nb				
B	377.4	3.28	0.119	−0.280 H-4→L(d→σ^*) −0.394 H-1→L(d→σ^*) +0.404 H→L($\sigma\rightarrow\sigma^*$)
B	339.2	3.65	0.015	0.620 H-2→L+2(d→π^*_{CO})
B	303.0	4.09	0.043	0.276 H-4→L(d→σ^*) +0.585 H-2→L+3(d→π^*_{CO})
B	297.8	4.16	0.119	0.424 H-4→L(d→σ^*) −0.270 H-2→L+3(d→π^*_{CO}) +0.311 H-2→L+4(d→π^*_{CO})
B	288.5	4.30	0.012	0.596 H-3→L+2(d→π^*_{CO})

$dm^3\ mol^{-1}\ cm^{-1}$, are given in parentheses). The bands at about 500 and 400 nm were assigned to $d \rightarrow \sigma^*$ transitions and the band at about 345 nm to the $\sigma \rightarrow \sigma^*$ transition in the bridged form [34, 40]. The wavelength of the $\sigma \rightarrow \sigma^*$ transition of the non-bridged form was estimated from the respective band energies in non-bridged heteronuclear M-Fe complexes to be 430 nm. The changes of ca. 400-nm band intensity with solvent polarity were explained as a possible result of the presence of small amount of the non-bridged form [40].

In the calculated spectrum of **I** long-wave transitions are observed (at 508.9 and 530.7 nm in B3LYP, 488.0 and 493.7 nm in BP86, for **trans-b** and **trans-nb**, respectively). The energy difference in comparison to the experiment is between 0.03 and 0.16 eV. All these transitions are characterized by small oscillator strengths, consistent with the lowest intensity band at about 500 nm in the experimental spectrum. The calculated transitions arise from $d \rightarrow \sigma^*$ excitations with the admixture of $\sigma \rightarrow \sigma^*$ excitation in the **trans-nb** form.

A transition that can be assigned to the experimental band at about 400 nm is found only in the **trans-b** form of **I**. It occurs at 435.5 nm in B3LYP and at 425.1 nm in BP86. This transition has a medium oscillator strength and is composed of two excitations $\sigma \rightarrow \sigma^*$ and $\sigma_{d\text{-}CO(b)} \rightarrow \sigma^*_{d\text{-}CO(b)}$. The energy difference between experimental and calculated transitions is 0.11–0.36 eV.

Transitions that can be assigned to the experimental band of the highest intensity, at about 345 nm, are found in calculated spectra of all forms of **I**. In B3LYP these are transitions at 359.0 nm for **trans-b**, 369.9 nm for **cis-b** and 369.9 nm for **trans-nb** forms. In BP86 they occur at 356.7 nm, 342.3 nm and 381.3 nm, respectively. These transitions have the largest oscillator strengths, especially large for **trans-b** and **trans-nb** forms, although the latter**,** due to its sparsity, should not contribute really to the spectrum of **I**. The energy differences between calculated and experimental transitions are 0.01–0.36 eV. The orbitals involved in these transitions for **cis-b** and **trans-b** forms are $d \rightarrow \pi^*_{CO}$ and $\sigma_{d\text{-}CO(b)} \rightarrow \sigma^*_{d\text{-}CO(b)}$. In BP86 other excitations also play a role, namely $\sigma \rightarrow \sigma^*$ for **trans-b** and $\sigma \rightarrow \sigma^*_{d\text{-}CO(b)}$ and $d \rightarrow \sigma^*_{d\text{-}CO(b)}$ for **cis-b**.

3.2.2 *$[CpRu(CO)_2]_2$*

The experimental spectrum of **II** in CCl_4 consists of three bands at 435, 330 and 265 nm [34]. The energy of the bands depends moderately on the solvent nature varying within 263–271 nm and 330–345 nm in *n*-heptane, isooctane, toluene, isopropanol and acetonitrile. However, the relative intensities of the bands depend strongly on temperature, pressure and solvent polarity, with that at ~330 nm prevailing at high temperature, low pressure and non-polar solvent. The position of the band at ~330 nm in polar solvents becomes more sensitive to temperature changes [3]. Abrahamson et al. [34] ascribed the bands at about 330 and 260 nm to $\sigma \rightarrow \sigma^*$ transition in the non-bridged and bridged forms, respectively. The long-wave band at about 430 nm was assigned to $d \rightarrow \sigma^*$ transition.

The transition that can be compared to the experimental one at about 435 nm is found in the calculated spectrum of **trans-nb** form, at 407.4 nm in B3LYP and 415.9 nm in BP86. This transition is characterized by a small oscillator strength

and consists of the $d \rightarrow \sigma^*$ and $\sigma \rightarrow \sigma^*$ excitations. The energy differences between calculated and experimental transitions are in the range of 0.13–0.19 eV.

The second experimental band at about 330 nm has its equivalents in all conformers of **II**. In B3LYP they are at 349.1 (**trans-b**), 361.2 (**cis-b**), 348.4 and 324.0 (**trans-nb**) and 362.3 nm (**gauche-nb**); in BP86 these transitions are at 362.4 (**trans-b**), 382.9 (**cis-b**), 335.6 (**trans-nb**) and 377.4 nm (**gauche-nb**). The highest oscillator strength characterizes the transitions in **trans-nb** form. The energy difference between the experimental and calculated transitions is between 0.03 and 0.5 eV, the largest difference being for the **gauche-nb** and **cis-b** isomers in BP86. The orbital excitations involved in these transitions with the highest oscillator strengths in **trans-nb** are $d \rightarrow \sigma^*$, $d \rightarrow \pi^*_{CO}$ and $\sigma \rightarrow \sigma^*$ in B3LYP, while in BP86 these are $d \rightarrow \sigma^*$ and $\sigma \rightarrow \sigma^*$.

The calculated transitions, which can be attributed to the experimental band at about 265 nm, appear in all forms of **II**, but the wavelengths are longer than expected. In B3LYP these are transitions at 301.7 (**trans-b**), 309.8 (**cis-b**), 279.4 (**trans-nb**) and 301.8 nm (**gauche-nb**). In BP86 these are transitions at 303.3, 297.0, 287.7 (and 281.0) and 297.8 nm, respectively. In both methods the highest oscillator strengths characterize the **trans-b** and **gauche-nb** forms. The energy difference between calculated and experimental energy is within 0.24–0.68 eV. The following orbital excitations contribute to the transitions: $\sigma \rightarrow \sigma^*$, $d \rightarrow \pi^*_{CO}$ and $\sigma_{d\text{-}CO(b)} \rightarrow \sigma^*_{d\text{-}CO(b)}$ for **trans-b** and $d \rightarrow \sigma^*$ and $d \rightarrow \pi^*_{CO}$ for **gauche-nb** isomer.

In conclusion, it may be stated that the DFT methods reproduce well the spectral properties of **I** and **II**. The transition energies are calculated with the average error of about 0.2 eV for most transitions, except the shortest wavelength band of **II** for which it is ca. 0.5 eV. The transitions are characterized usually by more than one orbital excitation, and some orbital excitations are different in B3LYP and BP86 methods.

According to the presented calculations the transition at about 500 nm can be attributed to the *trans* conformers of **I** (both bridged and non-bridged). The transition at about 400 nm has its counterpart only in the **trans-b** form. The band at ~345 nm can be ascribed to all forms, although the oscillator strength values suggest the *trans* isomer domination in the spectrum.

The transition at about 435 nm can be attributed to the **trans-nb** form of **II** basing on the DFT calculations. The increasing intensity of the band at about 330 nm with increasing temperature is connected with the growing concentration of the **trans-nb** form, due to the high oscillator strength of this transition. The band at about 265 nm can be mostly ascribed to the **trans-b** and **gauche-nb** forms.

The assignment based on the DFT calculations agrees with the commonly accepted interpretation of the spectra of **I** and **II**, in which the most intense band of **I** at ~345 nm is attributed to the bridged form, and the two intense bands of **II**, at ~330 and 265 nm are assigned to the non-bridged and bridged forms, respectively [3, 34].

4
Photochemical Reactivity

The variety of structures of the $[CpM(CO)_2]_2$ complexes reflects in various chemical and photochemical pathways reported for these moieties. Since **I** occurs in solution mostly in the bridged structures only the *cis-trans* equilibrium can be considered [14–17]. As distinct from **I**, in solutions of **II** the CO-bridged (**II-b**) and non-bridged (**II-nb**) forms coexist [3, 15, 16, 34]:

$$\underset{\textbf{II-b}}{[Cp(CO)Ru(\mu - CO)_2 - Ru(CO)Cp]} \leftrightarrows \underset{\textbf{II-nb}}{[Cp(CO)_2Ru - Ru(CO)_2Cp]} \quad (1)$$

Recently photochemistry of **I** was reviewed in details by Bitterwolf [2], whereas behaviour of its ruthenium analogue was described to a lesser extent. At the same time the possibility of using $[CpM(CO)_2]_2$ complexes as versatile systems was considered with the ligand and medium controlled photochemistry [1]. Here we intend to emphasize some points of **I** and **II** photochemistry, which are closely associated with their structures.

4.1
$[CpFe(CO)_2]_2$

Two main photochemical modes of **I** were observed:

1. Radical pathway consisting in the metal-metal bond splitting with generation of the $17e^-$ $[CpFe(CO)_2]^\cdot$ radicals. The radicals produce mononuclear $[CpFe(CO)_2X]$ complexes in the presence of radical precursors RX (X=Cl, Br, I) [34, 45, 46]. Phosphites, however, can substitute one of the carbonyl groups in $[CpFe(CO)_2]^\cdot$ yielding $[CpFe(CO)P(OR)_3]^\cdot$ radicals [47]. In the presence of a ligand L highly reductive $19e^-$ adducts $[CpFe(CO)_2L]^\cdot$ are formed [48]. Finally, the $[CpFe(CO)_2]^\cdot$ radicals can dimerize or couple with $[CpFe(CO)P(OR)_3]^\cdot$ [47]. Recently Amatore et al. found that $[CpFe(CO)_2]^-$ anion can be formed in reaction of **I** with photoexcited 1-benzyl-1,4-dihydronicotinamide dimer [49].
2. Non-radical pathway consisting in the cleavage of one of the CO groups. The formed unsaturated complex can coordinate a ligand like PR_3, $P(OR)_3$ [45, 50] or a molecule of coordinating solvent, e.g. THF [47] or acetonitrile [50]. The alkyne coordination, leading to formation of a transient $[Cp_2Fe_2(CO)_3(RC{\equiv}CR)]$ species, followed by intramolecular transformations, was also reported [51]. The nature of the $[Cp_2Fe_2(CO)_3]$ intermediate has been discussed in the literature and was postulated to be triply [52–58], doubly [59] or singly CO-bridged [59]. Recently the photogenerated CO-loss intermediate was studied by time-resolved IR spectroscopy and its triply bridged structure was proved [60]. Extended irradiation of the solution leads to the loss of further CO ligand and formation of $[Cp_2Fe_2(CO)_2]$ with a triple Fe-Fe bond [58, 61].

The non-radical pathway was reported to proceed only from the **trans-b** form upon long wavelength (λ_{irr}>475 nm) irradiation [52]. This is consistent with the

domination of the absorption of the **trans-b** and **trans-nb** isomers within this radiation range (cf. Table 3). However, the same irradiation range was also found to induce the Fe-Fe bond cleavage leading to $[CpFe(CO)_2]^{\cdot}$ formation [47, 57, 62].

Secondary thermal and/or photochemical reactions make the photochemistry of **I** even more interesting. An example can be formation of ferrocene upon prolonged irradiation of $[CpFe(CO)_2X]$ (X=Cl, Br) [46]. Alternatively, the ligated halogen can be photochemically substituted by an N-donor ligand, generating, e.g. $[CpFe(CO)_2NR_2]$ [63–65].

$[CpFe(CO)_2X]$ complexes can also be formed in the thermal reaction of **I** with strong acids HX (X=$O_3SC_6H_4Me$-4, Cl) in acetonitrile solutions [66]. In addition $[CpFe(CO)_2(NCMe)]X$ is formed. The bridging CO groups can undergo reduction, e.g. by calcium tetrakis(isopropoxy)alanate yielding the μ-CH_2 analogues of **I** [67].

4.2
$[CpRu(CO)_2]_2$

Structural differences of **II** entail changes in the excited state energy and character: the $\sigma_{bridge} \rightarrow \sigma^*_{bridge}$ excitation needs higher energy (λ_{max}=265 nm) than the $\sigma_{nonbridge} \rightarrow \sigma^*_{nonbridge}$ one (λ_{max}=330 nm) (see above). In consequence, the two isomeric forms **II-b** and **II-nb**, are characterized by different photochemical modes (Scheme 1) [68].

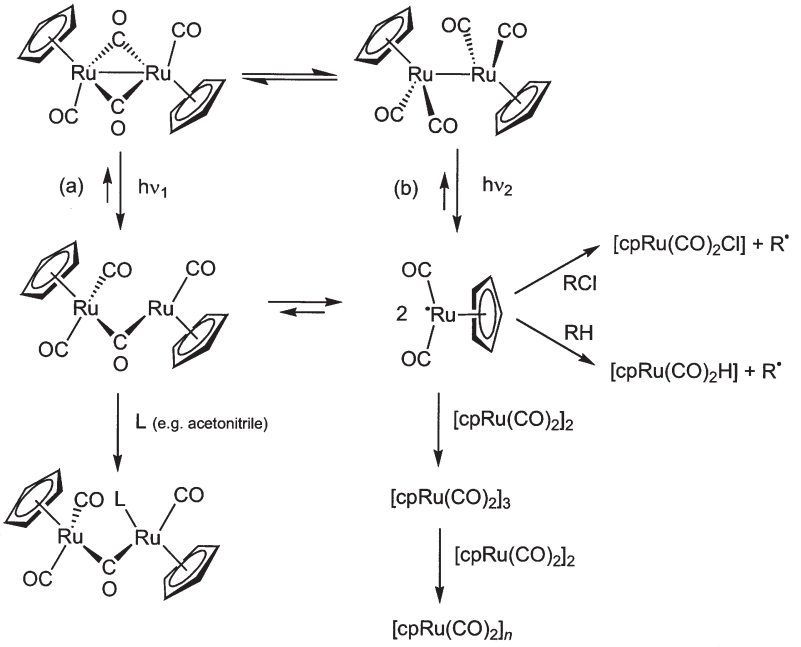

Scheme 1 Photochemical channels for $[CpRu(CO)_2]_2$ ($h\nu_1$ denotes that λ_{irr}≈250 nm; $h\nu_2$: λ_{irr}≈330 nm). Adapted from [1]

Contrary to the previous reports [34, 52, 69], in recent studies no photochemical dissociation of the terminal CO ligand was identified. Instead the cleavage of Ru-$CO_{bridged}$ and Ru-Ru bonds was recognized to follow the excitations at 265 and 330 nm of **II-b** and **II-nb**, respectively (paths **a** and **b** in Scheme 1) [3, 68, 69]. In the former case, the monobridged dimeric radical species is formed, whereas in the latter the monomeric $[CpRu(CO)_2]^{\cdot}$ radicals are generated photochemically. The radicals are interconvertible and undergo back and secondary processes, which can finally transform the dimer into a monomeric or polymeric form. The course of these pathways strongly depends on the nature of solvent and the presence of a ligand or radical precursor in the system.

The effect of irradiation energy on the photochemical mode can be easily recognized using flash technique with a microsecond resolution. In continuous photolysis, however, the final products of the pathway **a** are observed only under specific conditions. First, the isomerization reactions of **II** are fast enough [20, 70] to convert the whole substrate into the photoproducts by irradiation either of the isomers. Second, due to the radicals evolving into each other with different kinetics (cf. Scheme 1), the yield of the monobridged radicals generated from recombination of $[CpRu(CO)_2]^{\cdot}$ can be neglected in continuous photolysis, and in a ligating solvent its coordination product, e.g. $[CpRu(CO)_2CH_3CN]$ or $[CpRu(CO)_2][CpRu(CO)_2CH_3CN]$, may be regarded as selectively produced by irradiation within the 265 nm band of **II-b** (path **a** in Scheme 1) [68]. In contrast, the $[CpRu(CO)_2]^{\cdot}$ radicals and, in consequence, their addition products, e.g. $[CpRu(CO)_2Cl]$, are generated easily in both pathways. Light energy can thus be used for steering the reaction pathways, but only to a limited extent. It has also some quantitative effect: somewhat increased quantum yields of the dimer decay were observed at shorter wavelength [34, 68].

The influence of solvent nature on the photoproducts formed from **II** can be described in a general way. In non-polar and poor radical precursor solvents (e.g. heptane, octane) polymerisation is the only reactive pathway of the photochemically generated radicals, irrespective of their origin from the bridged or non-bridged isomer [68]. In non-polar, but good radical precursors (e.g. toluene, carbon tetrachloride) all photochemically generated radicals are transformed into the monomeric Ru(II) complexes, e.g. $[CpRu(CO)_2Cl]$ [3, 34, 68, 69]. In the presence of the ligating solvents (e.g. acetonitrile, DMSO) the Ru-radicals can undergo complexation and/or disproportionation, similar to that observed in the case of **I** [68].

It is known that dimers **I** and **II** can activate C-H bond. As an example a catalytic hydroformylation of 1-octene (thermal process) may be mentioned [71]. Alternatively the photocatalytic activation of the C-H bond can be considered according to the pathway **b** in Scheme 1. The system was tested using toluene as a radical precursor. EPR spectroscopy was applied to detect the radical products: generation of the hydride Ru transient complex, $[CpRu(CO)_2H]$, and $C_6H_5CH_2^{\cdot}$ radicals were determined [3, 69]. Formation of the ruthenium hydride species was recently reported also by Bitterwolf et al. in the reaction of photoexcited **II-nb** with H_2 [72]. $[CpRu(CO)_2H]$ can be oxidised in air to the original dimer **II** [73].

5 Conclusions

The photochemical behaviour of the $[M(\eta^5\text{-}C_5H_5)(CO)_2]_2$ (M=Fe or Ru) dimers is complicated because in solution the compounds occur in equilibria between their two or more isomeric forms. To interpret the photochemistry of such systems the equilibrium controlling parameters and characteristics of the individual forms should be known. The former was recognized earlier, whereas the structure and spectral properties of all possible forms of **I** and **II** are calculated in this work. The DFT calculations point to three stable forms (**trans-b**, **cis-b** and **trans-nb**) in the case of the Fe-dimer, whereas for the Ru species an additional stable form (**gauche-nb**) is found. Its **cis-nb** conformer suggested in earlier studies turned out to be an unstable transition state.

Analysis of the calculated transitions of all the isomeric forms shows that the most essential contribution of both dimers to the UV/vis spectra comes from the *trans* isomers. These are especially responsible for the low energy bands in the Fe and Ru compounds, which is consistent with the photoreactivity of the *trans* form of **I** within the long wavelength region.

Almost all excitations responsible for the transitions contribute to population of the σ^* and/or $\sigma^*_{\text{d-CO(b)}}$ orbitals which should lead to weakening of both M–M and M–CO_{bridge} bonds. In consequence, cleavage of both bonds seems probable. The differences between the photochemical behaviour of the Fe and Ru compounds derive mostly from the difference in the central atom radii. In particular, the cleavage of the Fe–CO_{bridge} bond should be followed by the immediate conversion of two terminal CO groups into the bridged CO, leading to formation of the triply bridged $[CpFe(\mu\text{-}CO)_3FeCp]$ intermediate and release of one of the CO ligands. In contrast, the Ru-Ru distance is too long to form such intermediate and therefore CO ligand is not released. Instead, the monobridged species either decomposes to two $[CpRu(CO)_2]^{\cdot}$ radicals or, in presence of a ligating species, becomes stabilized (Scheme 1).

6 References

1. Szacilowski K, Macyk W, Stochel G, Stasicka Z, Sostero S, Traverso O (2000) Coord Chem Rev 208:277
2. Bitterwolf TE (2000) Coord Chem Rev 206/7:419
3. Macyk W, Herdegen A, Stochel G, Stasicka Z, Sostero S, Traverso O (1997) Polyhedron 16:3339
4. Piper TS, Cotton FA, Wilkinson C (1955) J Inorg Nucl Chem 1:165
5. Fischer EO, Vogler A (1962) Z Naturforsch Teil B 17:421
6. Fischer EO, Bittler K (1962) Z Naturforsch Teil B 17:274
7. Mills SO (1958) Acta Cryst 11:620
8. Bryan RF, Greene PT (1970) J Chem Soc A 3064
9. Mitschler A, Rees B, Lehmann MS (1978) J Am Chem Soc 100:3390
10. Bryan RF, Greene PT, Newlands MJ, Field DS (1970) J Chem Soc A 3068
11. Mills SO, Nice JP (1967) J Organomet Chem 9:339
12. Mague JT (1995) Acta Cryst C 51:831
13. Manning AR (1968) J Chem Soc A 1319

14. Fischer RD, Vogler A, Noack K (1967) J Organomet Chem 7:135
15. Cotton FA, Yagupsky G (1967) Inorg Chem 6:15
16. McArdle P, Manning AR (1970) J Chem Soc A 2128
17. Noack K (1967) J Organomet Chem 7:151
18. Bullit JG, Cotton FA, Marks TJ (1970) J Am Chem Soc 92:2155
19. Harris DC, Rosenberg E, Roberts JD (1974) J Chem Soc Dalton Trans 2398
20. Gansow OA, Burke AR, Vernon WD (1976) J Am Chem Soc 98:5817
21. Gansow OA, Burke AR, Vernon WD (1972) J Am Chem Soc 94:2550
22. Adams RD, Cotton FA (1973) J Am Chem Soc 95:6589
23. Becke AD (1993) J Phys Chem 98:5648
24. Lee C, Yang W, Parr RG (1988) Phys Rev B 37:785
25. Perdew JP (1986) Phys Rev B 38:3098
26. Jaworska M (to be published)
27. Kenny JP, King RB, Schaefer IHF (2001) Inorg Chem 40:900
28. Jemmis ED, Pinhas AR, Hoffman R (1980) J Am Chem Soc 102:2576
29. Granozzi G, Tondello E, Benard M, Fragala I (1980) J Organomet Chem 194:83
30. Benard M (1979) Inorg Chem 18:2782
31. Benard M (1978) J Am Chem Soc 100:7740
32. Bursten BE, Cayton RH, Gatter MG (1988) Organometallics 7:1342
33. Bursten BE, Cayton RH (1986) J Am Chem Soc 108:8241
34. Abrahamson HB, Palazzotto MC, Reichel CL, Wrighton MS (1979) J Am Chem Soc 101:4123
35. Levenson RA, Gray HB, Ceasar GP (1970) J Am Chem Soc 92:3653
36. Levenson RA, Gray HB (1975) J Am Chem Soc 97:6042
37. Wrighton MS, Ginley DS (1975) J Am Chem Soc 97:2065
38. Ginley DS, Wrighton MS (1975) J Am Chem Soc 97:4908
39. Abrahamson HB, Frazier CF, Ginley DS, Gray HB, Lilienthal J, Tyler DR, Wrighton MS (1977) Inorg Chem 16:1554
40. Abrahamson HB, Wrighton MS (1978) Inorg Chem 17:1003
41. Casida ME, Jamorski C, Casida KC, Salahub DR (1998) J Chem Phys 108:4439
42. Li Z, Wang H, Li Q, Li J, Feng J, Zheng Z (1991) Gaodeng Xuexiao Huaxue Xuebao 12:1640
43. Wrighton MS (1978) J Am Chem Soc 101:4123
44. Hepp AF, Blaha JP, Lewis C, Wrighton MS (1984) Organometallics 3:174
45. Caspar JV, Meyer TJ (1980) J Am Chem Soc 102:7794
46. Giannotti C, Merle G (1976) J Organomet Chem 105:97
47. Dixon AJ, George MW, Hughes C, Poliakoff M, Turner JJ (1992) J Am Chem Soc 114:1719
48. Goldman AS, Tyler DR (1987) Inorg Chem 26:253
49. Fukuzumi S, Ohkubo K, Fujitsuka M, Ito O, Teichmann MC, Maisonhaute E, Amatore C (2001) Inorg Chem 40:1213
50. Dixon AJ, Healy MA, Poliakoff M, Turner JJ (1986) J Chem Soc Chem Commun 994
51. Bursten BE, McKee SD, Platz MS (1989) J Am Chem Soc 111:3428
52. Bloyce PE, Campen AK, Hooker RH, Rest AJ, Thomas NR, Bitterwolf TE, Shade JE (1990) J Chem Soc Dalton Trans 2833
53. Meyer TJ, Caspar J (1985) Chem Rev 85:187
54. Hooker RH, Mahmoud KA, Rest AJ (1983) J Chem Soc Chem Commun 1022
55. Moore BD, Simpson MB, Poliakoff M, Turner JJ (1984) J Chem Soc Chem Commun 972
56. Blaha JP, Bursten BE, Dewan JC, Frankel RB, Randolf CW, Wilson BA, Wrighton MS (1985) J Am Chem Soc 107:4561
57. Moore JN, Hansen PA, Hochstrasser RM (1989) J Am Chem Soc 111:4563
58. Kvietok FA, Bursten BE (1994) J Am Chem Soc 116:9807
59. George MW, Dougherty TP, Heilweil EJ (1996) J Phys Chem 100:201
60. Bradley PM, Drommond ML, Turro C, Bursten BE (2002) Inorg Chim Acta 334:371
61. Vitale M, Archer ME, Bursten BE (1998) J Chem Soc Chem Commun 179
62. Anfinrud PA, Han C-H, Lian T, Hochstrasser RM (1991) J Phys Chem 95:574
63. Zakrzewski J (1987) J Organomet Chem 327:C41
64. Zakrzewski J (1989) J Organomet Chem 359:215

65. Zakrzewski J, Tosik A, Bukowska-Strzyzewska M (1995) J Organomet Chem 495:83
66. Callan B, Manning AR (1983) J Organomet Chem 252:C81
67. Ortaggi G, Paolesse R (1988) J Organomet Chem 346:219
68. Macyk W, Herdegen A, Karocki A, Stochel G, Stasicka Z, Sostero S, Traverso O (1997) J Photochem Photobiol A Chem 103:221
69. Sostero S, Rehorek D, Polo E, Traverso O (1993) Inorg Chim Acta 209:171
70. Dalton EF, Ching S, Murray RW (1991) Inorg Chem 30:2642
71. Cesarotti E, Fusi A, Ugo R, Zanderighi GM (1978) J Mol Catal 4:205
72. Bitterwolf TE (2000) Organometallics 19:4915
73. Doherty NM, Knox SAR, Morris MJ (1990) Inorg Synth 28:189

Structure and Bonding, Vol. 106 (2004): 173–180
DOI 10.1007/b11311

Average One-Center Two-Electron Exchange Integrals and Exchange Interactions

Susanne Mossin · Høgni Weihe

University of Copenhagen, Department of Chemistry, Universitetsparken 5, 2100 Copenhagen, Denmark
E-mail: mossin@kiku.dk or weihe@kiku.dk

Abstract We show how the introduction of the average one-center two-electron exchange integral, which is closely related to Jørgensens spin-pairing energy parameter, facilitates comparison of the Heisenberg-Dirac-van Vleck exchange parameter for different transition metal dimers. The formalism is illustrated on μ-oxo-dimanganese(III) and μ-oxo-dichromium(III) complexes in which the oxo bridge is the important exchange pathway.

Keywords Exchange interactions · Spin-pairing energy

1 Introduction

The conceptual framework to understand the exchange interaction between nearest-neighbor paramagnetic ions in three-dimensional lattices was put forward by Andersson in the late 1950s [1]. Simultaneously, and independently, Jørgensen [2] used similar ideas to interpret the antiferromagnetic interaction between the two copper(II) ions in copper(II) acetate. Based on the Anderson theory are the so-called Goodenough-Kanamori rules [3] – a set of rules expressing the nature and magnitude of the interaction depending on the electronic occupancy of the relevant interacting orbitals.

In recent works we demonstrated how the correct quantitative expressions for the Goodenough-Kanamori rules [1, 3, 4] successfully accounted for the magnetic properties in linear and bent oxo-bridged iron(III) dimers. Here we treat the analogous manganese(III) and chromium(III) dimers and focus on the fact that the average one-center two-electron exchange integral K_{av} provides the means to compare magnetic properties of dimers containing differ-

ent metal ions. K_{av} is closely related to Jørgensens spin-pairing energy parameter D [5]:

$$D = \frac{2l + 3}{2l + 2} K_{av} \tag{1}$$

K_{av} is the average value of the $2l(2l+1)$ possibly different exchange integral pertinent to the l shell, D expresses the energy difference between the center of gravity of all terms with spin quantum number S–1 and the center of gravity of all terms having spin quantum number S as

$$\bar{E}(S - 1) - \bar{E}(S) = 2SD \tag{2}$$

The relevant structural and magnetic properties of all oxo-bridged Mn(III) and Cr(III) dimers, which have been both structurally and magnetically characterized, are collected in Tables 1 and 2, respectively. The magnetic properties are given in terms of J being the parameter in the effective Hamiltonian

$$\mathbf{H} = J\,\mathbf{S}_1 \cdot \mathbf{S}_2 \tag{3}$$

All the complexes are octahedrally coordinate and have one compositional feature in common, namely one oxo bridge. Some of the complexes have one or two supporting carboxylato bridging ligands. These are considered to be of less importance as interaction pathways compared to the oxo bridge [4]. The com-

Table 1 Structural and magnetic parameters for oxo-bridged manganese(III) dimers

Compound	φ/degrees	r/Å	J/cm^{-1}	Ref.
$[Mn_2OL_2]^{2+}$	180	1.758	216	[6]
$[Mn_2O(5\text{-}NO_2saldien)_2]$	168.4	1.754	240	[7]
$[\{(BispicMe_2en)Mn\}_2(O)(CH_3COO)]^{3+}$	133	1.79	13.5	[8]
$[\{(Bispicen)Mn\}_2(O)(CH_3COO)]^{3+}$	130.8	1.801	19.5	[8]
$[\{HB(pz)_3Mn\}_2(O)(CH_3COO)_2]$	125.1	1.78	0.4–1.4	[9]
$[\{(TMIP)Mn\}_2(O)(CH_3COO)_2]^{2+}$	124.4	1.789	0.4	[10]
$[\{(bpy)ClMn\}_2(O)(CH_3COO)_2]$	124.3	1.783	8.2	[11]
$[(bpy)(OH)Mn(O)(PhCOO)_2Mn(NO_3)(bpy)]$	124.1	1.777	–2.0	[12]
$[\{bpy(H_2O)Mn\}_2(O)(CH_3COO)_2]^{2+}$	122.9	1.783	6.8	[13]
$[(bpy)(H_2O)Mn(O)(mpdp)(bpy)(MeCN)Mn]^{2+}$	122.9	1.787	0.6	[14]
$[\{(TP\text{-}TACN)Mn\}_2(O)(CH_3COO)_2]^{2+}$	122.3	1.802	9.2	[15]
$[\{(bpy)(N_3)Mn\}_2(O)(PhCOO)_2]$	122.0	1.802	–17.6	[11]
$[\{(Me_3TACN)Mn\}_2(O)(CH_3COO)_2]^{2+}$	120.9	1.810	–18	[16]

Ligandabbreviations:
L^-=*N*,*N*-bis(2-pyridylmethyl)-*N*′-salicyliden-1,2-diaminoethane
(5-NO_2saldien)=*N*,*N*′-bis(5-nitrosalicylidene)-1,7-diamino-3-azapentane
BispicMe_2en=*N*,*N*′-bis(2-pyridylmethyl)-*N*,*N*′-dimethylethane-1,2-diamine
Bispicen=*N*,*N*′-bis(2-pyridylmethyl)ethane-1,2-diamine
$HB(pz)_3^-$=hydrotris(1-pyrazolyl)borate
TMIP=tris-(*N*-methylimidazol-2-yl)phosphine
bpy=2,2′-bipyridine; $PhCOO^-$=benzoate
$mpdp^{2-}$=*m*-phenylenedipropionate
Me_3TACN=*N*,*N*′,*N*″-trimethyl-1,4,7-triazacyclononane

Table 2 Structural and magnetic parameters for oxo-bridged chromium(III) dimers

Compound	φ/degrees	r/Å	J/cm^{-1}	Ref.
$[\{(tmpa)(NCS)Cr\}_2(O)]^{2+}$	180	1.800	510	[17, 18]
$[\{(NH_3)_5Cr\}_2(O)]^{4+}$	180	1.821	450	[19]
$[\{(tmpa)Cr\}_2(O)(CH_3COO)]^{3+}$	131.9	1.832	100.6	[18]
$[\{(tmpa)Cr\}_2(O)(CO_3)]^{2+}$	128.3	1.828	60.8	[20]
$[\{(Me_3tacn)Cr\}_2(O)(CH_3COO)_2]^{2+}$	121.0	1.850	56	[21]

Ligand abbreviations: tmpa=tris(2-pyridylmethyl)amine
Me_3tacn=*N*,*N*′,*N*″-trimethyl-1,4,7-triazacyclononane

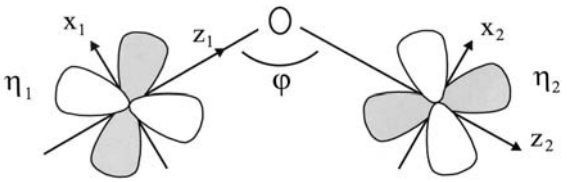

Fig. 1 Definition of the coordinate systems and the angle φ

plexes having only the oxo bridge exhibit M-O-M angles, see Fig. 1, φ in the range 180° to 168°. The complexes having one and two supporting bridging ligands exhibit φ in the range 133–131° and 124–120°, respectively.

2 Theory

We consider a dimer AB composed of the metal ions A and B. The ground state of A which is designated $S_A\Gamma_A$ arises from the electron configuration $(a)^{NA,nA}$. (a) is a set of orbitals centered on A. N_A and n_A is the total number of electrons and the number of unpaired electrons, respectively. Similar designations apply to center B. Hence, the ground state manifold of functions can be symbolized as

$$|S\Gamma M_S\gamma\rangle = [(a)^{N_A,\,n_A}\,S_A\Gamma_A] \otimes [(b)^{N_B,\,n_B}\,S_B\Gamma_B] \tag{4}$$

In the theory originally developed by Anderson [1] the splitting of this manifold of states arises due to an interaction of these functions with functions arising from charge-transfer states (CT). Such a CT function, in which an electron has been removed from center A and restored on center B is designated as

$$|S\Gamma M'_S\gamma\rangle = [(a)^{N_A-1,\,n'_A}\,S'_A\Gamma'_A] \otimes [(b)^{N_B+1,\,n'_B}\,S'_B\Gamma'_B] \tag{5}$$

where n_A' and n_B' may differ from n_A and n_B by ±1 depending on the number of electrons in the orbitals losing and receiving the electron.

The key matrix elements to be calculated are hence of the type

$$\langle S\Gamma M_S\gamma\,|\,V_{AB}\,|S\Gamma M'_S\gamma\rangle \tag{6}$$

V_{AB} is the one-electron operator and it is specified by its one-electron matrix elements h_{ab}. To second order in perturbation theory it is found that the energies

of the ground state (GR) manifold are proportional to $S(S+1)$. Basically the CT function can be generated from the GR function in four distinct ways: the electron can be removed from a half-filled or a full orbital, and it may be restored in an empty or a half-full orbital. Only two types of electron transfers are needed here: half-full to half-full and half-full to empty, and the expressions follow below. Similar expressions for the two remaining types of CT can be found in [22].

For the half-full to half-full electron transfer we find the following antiferromagnetic contribution to J:

$$J = \frac{2}{n_A n_B} \frac{h_{ab}^2}{U_{eff}} \tag{7}$$

where U_{eff} is the energy of the CT manifold of states (Eq. 5), and h_{ab} is the matrix element of V_{AB} connecting the relevant orbitals on A and B. For the half-full to empty electron transfer we find the following ferromagnetic contribution to J:

$$J = \frac{-2}{n_A (n_B + 1)} h_{ab}^2 \left[\frac{1}{U_{eff}} - \frac{1}{U'_{eff}} \right] \cong \frac{-2}{n_A (n_B + 1)} \frac{h_{ab}^2}{U_{eff}} \frac{U'_{eff} - U_{eff}}{U_{eff}} \tag{8}$$

Two CT energies appear in Eq. (8), because the GR functions interact with two different manifolds of the CT functions. The reason for this is that S_{B}' in Eq. (5) can take the values $S'_B = S_B \otimes {}^1/_2 = S_B + {}^1/_2$ and $S_B - {}^1/_2$, and $U'_{eff} - U_{eff} = E(S_B - {}^1/_2) - E(S_B + {}^1/_2)$. In all cases relevant to the calculation of ground state J values of these systems, the two S'_{B} values represent the highest and next-highest spin value of the configuration $(b)^{N_B+1, n_B+1}$.

3 Model Parameters

Equations (7) and (8) express the contribution to J in terms of the number of unpaired electrons on the interacting centers, one-electron matrix elements and the energies of metal-metal CT states.

Although U_{eff} appears as a metal-metal charge transfer energy, it inherently contains some ligand-metal CT character as well. It can be shown that on explicitly including the relevant ligand-metal CT states; $1/U_{\mathrm{eff}}$ and $1/(U_{\mathrm{eff}})^2$ in Eqs. (7) and (8) should be replaced by

$$\frac{1}{U_{eff}} = \frac{1}{U} + \frac{1}{E_{CT}} \tag{9}$$

and

$$\frac{1}{U_{eff}^2} = \frac{2U + E_{CT}}{E_{CT} U^2} + \frac{3}{E_{CT}^2} \tag{10}$$

respectively, where E_{CT} is the energy of the bridging ligand-metal CT state, and U is a true metal-metal CT energy. For the complexes in Table 1 and 2 we have [23, 25] $35{,}000 < E_{\mathrm{CT}} < 40{,}000\ \mathrm{cm}^{-1}$. The U values are typically 2–3 times larger [24, 26]. Hence, we conclude from Eqs. (9) and (10) that U_{eff} in Eqs. (7) and (9) are slightly higher and slightly lower than E_{CT}, respectively.

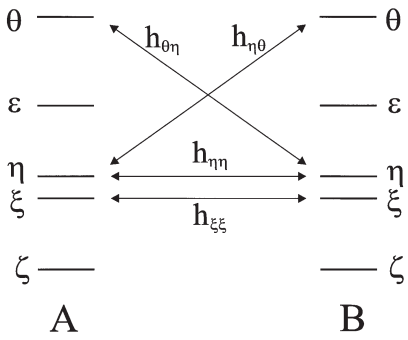

Fig. 2 Schematic illustration of the d orbital energies. The non-zero one-electron interaction parameters are indicated with *double arrows*. We have written θ, ε, ξ, η and ζ for d_{z2}, d_{x2-y2}, d_{yz}, d_{zx} and d_{xy}, respectively

The metal-oxo distance – see Tables 1 and 2 – is significantly shorter than the other metal-ligand distances which are found in the range 2.03–2.21 Å [6–21].

This in conjunction with the oxide ligand being a good σ as well as π donor results in the d orbitals having the energy order as indicated in Fig. 2. Hence the chromium and manganese centers have the ground state electron configurations $(a)^{3,3}=(b)^{3,3}=\zeta^1\eta^1\xi^1$ and $(a)^{4,4}=(b)^{4,4}=\zeta^1\eta^1\xi^1\varepsilon^1$, respectively. The non-zero interaction matrix elements h_{ab} are those which involve orbitals overlapping with the oxo 2s and 2p orbitals. These interaction elements are indicated with arrows in Fig. 2. The parameters $h_{\eta\eta}$ and $h_{\eta\theta}=h_{\theta\eta}$ depend on φ and $h_{\xi\xi}$ does not. They can be expressed in angular overlap model (AOM) parameters as follows [25, 26].

$$\begin{aligned} h_{\xi\xi} &= -e_{p\pi} \\ h_{\eta\eta} &= -e_{p\pi}\cos\varphi \\ h_{\theta\eta} &= h_{\eta\theta} = \sqrt{e_{p\pi}e_{p\sigma}}\sin\varphi \end{aligned} \tag{11}$$

All parameters involving the ε and ζ orbitals are much smaller, due to the fact that these have δ symmetry with respect to the metal-oxo bond, and the oxide ligand has no low-energy δ orbitals.

In principle, it is always possible to calculate the energy difference $U'_{eff} - U_{eff} = E(S_B - {}^1/_2) - E(S_B + {}^1/_2)$ of Eq. (8), and express it in, e.g., the Racah repulsion parameters. In practice, however, it is profitable to recognize that for any given electron configuration, having n unpaired electrons, the lowest energy difference between the terms having the highest and the next-highest spin multiplicity is given approximately as

$$E(S_{\max} - 1) - E(S_{\max}) \cong 2S_{\max}K_{av} = nK_{av} \tag{12}$$

For d electrons in spherical symmetry

$$K_{av} = C + \frac{5}{2}\,\mathrm{B} \tag{13}$$

At first sight this might seem a rather crude approximation. This is however not the case as we now show. In Table 3 we have collected the experimentally determined first spin-forbidden excitation energies for several di- and trivalent metal ions in octahedral and tetrahedral environments. It is clearly evident that the ex-

Table 3 Energies ofthe first spin forbidden transitions in some first-row di- and trivalent-transition metal complexes. The first three columns give the electron configuration, the spin-forbidden transition of lowest energy, and the first-order energy expressed in Racah *B* and *C* parameters. The fourth column gives the energy range observed for this transition in complexes containing the metal ion in the fifth column

$t_2^r e^s$ (n)	$^{2S+1}\Gamma \rightarrow {}^{2S}\Gamma'$	E_{theory}	E_{exp}/cm^{-1}	M^{q+}	RRef.
t_2^2 (2)	$^3T_1 \rightarrow {}^1E, {}^1T_2$	2C+6B	9,000–10,000	V^{3+}	[27]
$t_2^6 e^2$ (2)	$^3A_2 \rightarrow {}^1E$	2C+8B	11,000–15,000	$Ni^{2+}(O_h)$	[27]
t_2^3 (3)	$^4A_2 \rightarrow {}^2E, {}^2T_1$	3C+9B	14,000–15,000	Cr^{3+}	[27]
$t_2^3 e^1$ (4)	$^5E \rightarrow {}^3E$	4C+8B	≈21,000	Mn^{3+}	[28]
$t_2^3 e^2$ (5)	$^6A_1 \rightarrow {}^4A_1$	5C+10B	23,000–25,000	Fe^{3+}, Mn^{2+}	[27]
$e^4 t_2^4$ (2)	$^3T_1 \rightarrow {}^1E$	2C+6B	10,600–12,000	$Ni^{2+}(T_d)$	[27]

perimentally determined energies scale linearly with the number of unpaired electrons *n*; by comparing the first and fourth column of Table 3 and using Eq. (12), we immediately see that $4500 < K_{av} < 5000\ cm^{-1}$. Table 3 only lists ground state electron configurations. Inspection of the d^q ($2 \le q \le 8$) repulsion matrices [29] reveals that this simple relationship also holds for excited electron configurations. We note in passing, that the approximation Eq. (12) also holds for the rare earth elements with K_{av} in the range given above.

The above discussion allows us to rewrite Eq. (8) using $U'_{eff} - U_{eff} \cong (n_B + 1)\, K_{av}$ and we therefore have

$$J \cong -\frac{2}{n_A} \frac{h_{ab}^2}{U_{eff}} \frac{K_{av}}{U_{eff}} \tag{14}$$

Using Eq. (10), and the CT energies mentioned above we estimate $K_{av}/U_{eff} \cong 0.25$.

Using Eqs. (7), (11) and (14) the expressions for the *J* values for the chromium(III) and the manganese(III) dimers in Tables 1 and 2 are given as

$$J_{CrCr} = \frac{4}{9} e'_{p\pi} e'_{p\pi} (1 + \cos^2 \varphi) - \frac{4}{3} e'_{p\pi} e'_{p\sigma} K'_{av} \sin^2 \varphi \tag{15}$$

and

$$J_{MnMn} = \frac{1}{4} e'_{p\pi} e'_{p\pi} (1 + \cos^2 \varphi) - e'_{p\pi} e'_{p\sigma} K'_{av} \sin^2 \varphi \tag{16}$$

respectively, where we have written $e_{p\pi}'$, $e_{p\sigma}'$ and K_{av}' for $e_{p\pi}/\sqrt{U_{eff}}$, $e_{p\sigma}/\sqrt{U_{eff}}$ and K_{av}/U_{eff}, respectively.

4 Results and Discussion

The expressions for J_{calc}, Eqs. (15) and (16) are fitted to the J_{exp} values in Tables 1 and 2, with $e_{p\pi}'$ and $e_{p\sigma}'$ as adjustable parameters, and $K_{av}'=0.25$. The parameter values obtained are $e'_{p\pi} = 22.4\ cm^{-1/2}$ and $e'_{p\sigma} = 47\ cm^{-1/2}$. The calculated angular variation of *J* for the manganese(III) and chromium(III) complexes is shown in

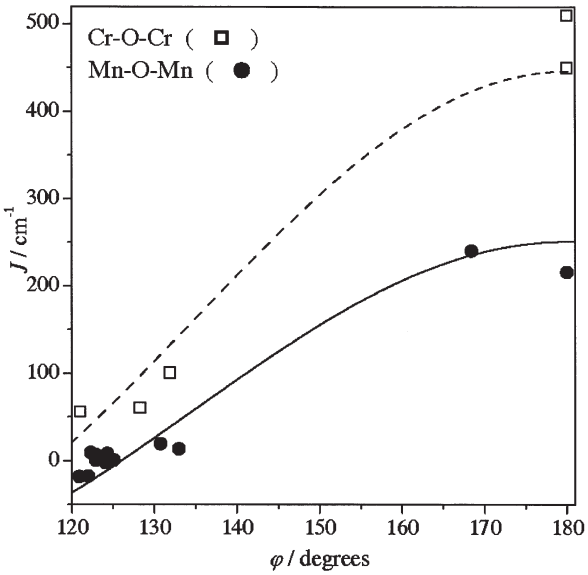

Fig. 3 Experimental and calculated angular variation of J for the dimers listed in Tables 1 and 2. The curves were calculated from Eqs. (15) and (16) with the parameters given in the text

Fig. 3. For both systems, the agreement of experimental and calculated J values is excellent, and we must conclude that it is justified to use the same parameter values for both systems.

The model parameters e_π' and e_σ' are related to AOM parameters, and with U_{eff} values in the range of ligand-metal CT energies, as discussed above, we get the values for the corresponding AOM parameters $e_{p\pi} \cong 4300\ \text{cm}^{-1}$ and $e_{p\sigma} \cong 8300\ \text{cm}^{-1}$, corresponding to oxide being a strong σ and π donor. The contribution to the $e_\sigma = e_{p\sigma} + e_{s\sigma}$ AOM parameter from the oxide 2s orbital cannot be obtained from the dimers in Tables 1 and 2. The reason for this is the θ orbital (Fig. 1) being unoccupied in the ground state of both the chromium(III) and the manganese(III) dimers. From a similar analysis of oxo-bridged iron(III) dimers we estimated $e_{s\sigma} \cong e_{p\pi}$, which makes $e_\sigma \cong 12{,}000\ \text{cm}^{-1}$. In comparison, the donor properties of OH^- have been parameterized with $e_\pi = 2300\ \text{cm}^{-1}$ and $e_\sigma = 9000\ \text{cm}^{-1}$ [30], and we conclude that the higher values for oxide can be attributed to the higher negative charge as compared to hydroxide.

From Fig. 3 we see that the dimers exhibit strong antiferromagnetic coupling in the linear configuration. For the chromium(III) and the manganese(III) dimers the J value vanishes at ≈115° and ≈125°, respectively. Using Eqs. (15) or (16) we calculate the ferromagnetic contribution to J as large as $\approx -230\ \text{cm}^{-1}$.

In his latest book [5] Jørgensen stated "It is much more difficult to explain ferromagnetism which must be connected with a rather uncommon side effect of strong spin-pairing energy in partly filled shells." From the above discussion we have seen that the spin-pairing energy, or equivalently the average exchange integral, determines the size of the ferromagnetic contribution to J in these dimers, and Eqs. (15) and (16) provide a quantitative measure of this statement.

5 References

1. Anderson PW (1959) Phys Rev 115:2
2. Jørgensen CK (1962) Absorption spectra and chemical bonding. Pergamon Press, Oxford
3. Goodenough JB (1963) Magnetism and the chemical bond. Interscience, New York
4. Weihe H, Güdel HU (1997) J Am Chem Soc 119:6539
5. Jørgensen CK (1971) Modern aspects of ligand field theory. North Holland Publishing, Amsterdam
6. Horner O, Anxolabéhère-Mallart E, Charlot M-F, Tchertanov L, Guilhem J, Mattioli TA, Boussac A, Girerd J-J (1999) Inorg Chem 38:1222
7. Kipke CA, Scott MJ, Gohdes JW, Armstrong WH (1990) Inorg Chem 29:2193
8. Arulsamy N, Glerup J, Hazell A, Hodgson DJ, McKenzie CJ, Toftlund H (1994) Inorg Chem 33:3023
9. Sheats JE, Czernuszewicz RS, Dismukes GC, Rheingold AL, Petrouleas V, Stubbe J, Armstrong WH, Beer RH, Lippard SJ (1987) J Am Chem Soc 109:1435
10. Wu F-J, Kurtz DM, Hagen KS, Nyman PD, Debrunner PG, Vankai VA (1990) Inorg Chem 29:5174
11. Vincent JB, Tsai H-L, Blackman AG, Wang S, Poyd PDW, Folting K, Huffman JC, Lobkovsky EB, Hendrickson DN, Christou G (1993) J Am Chem Soc 115:12,353
12. Corbella M, Costa R, Ribas J, Fries PH, Latour J-M, Öhrström L, Solans X, Rodríguez V (1996) Inorg Chem 35:1857
13. Ménage S, Girerd J, Gleizes A (1988) J Chem Soc Chem Commun 431
14. Cañada-Vilalta C, Huffman JC, Streib WE, Davidson ER, Christou G (2001) Polyhedron 20:1375
15. Bolm C, Meyer N, Raabe G, Weyhermüller T, Bothe E (2000) J Chem Soc Chem Commun 2435
16. Wieghardt K, Bossek U, Nuber B, Weiss J, Bonvoisin J, Corbella M, Vitols SE, Girerd JJ (1988) J Am Chem Soc 110:7398; Wieghardt K, Bossek U, Ventur D, Weiss J (1985) J Chem Soc Chem Commun 347
17. Gafford BG, Holwerda RA, Schugar HJ, Potenza JA (1988) Inorg Chem 27:1126
18. Gafford BG, Marsh RE, Schaefer WP, Zhang JH, O'Connor CJ, Holwerda RA (1990) Inorg Chem 29:4652
19. Pedersen E (1972) Acta Chem Scand 26:333; Yevitz M, Stanko JA (1971) J Am Chem Soc 93:1512
20. Dalley NK, Kou X, O'Connor CJ, Holwerda RA (1996) Inorg Chem 35:2196
21. Martin LL, Wieghardt K, Blondin G, Girerd J-J, Nuber B, Weiss J (1985) J Chem Soc Chem Commun 347
22. Weihe H, Güdel HU (1997) Inorg Chem 36:3632
23. Güdel HU, Dubicki L (1974) Chem Phys 6:272; Brunold TC, Gamelin DR, Solomon EI (2000) 122:8511
24. Didziulis SV, Cohen SL, Gewirth AA, Solomon EI (1988) J Am Chem Soc 110:250
25. Glerup J (1972) Acta Chem Scand 26:3775
26. Atanasov M, Angelov S (1991) Chem Phys 150:383
27. Lever ABP (1984) Inorganic electronic spectroscopy, 2nd edn. Elsevier, Amsterdam
28. Mossin S, Weihe H (unpublished results)
29. Griffith JS (1961) The theory of transition metal ions. Cambridge University Press, Cambridge
30. Glerup J, Mønsted O, Schäffer CE (1976) Inorg Chem 15:1399

Structure and Bonding, Vol. 106 (2004): 181–191
DOI 10.1007/b11312

Christian Klixbull Jørgensen and the Nature of the Chemical Bond in HArF*

Matthias Lein · Jan Frunzke · Gernot Frenking

[1] Philipps-Universität Marburg, Fachbereich Chemie, Hans-Meerwein-Strasse 3, 5032 Marburg, Germany
E-mail: frenking@chemie.uni-marburg.de

Abstract The chemical bond in HArF is investigated with the help of the topological analysis of the electron density distribution and with an energy partitioning analysis. The results give quantitative insight into the nature of the interatomic interactions. The H-ArF bond is mainly covalent while the most important contributions to the argon-fluorine bond come from the electrostatic attraction between HAr^+ and F^-. The strong interatomic attractions in HArF arise from the concerted hydrogen-argon and argon-fluorine interactions. It is the concert of the two forces which leads to chemically bonded argon. The diatomic species ArH and ArF are only weakly bonded van der Waals complexes.

Keywords Noble gas compounds · Bonding analysis · Interatomic interactions

List of Abbreviations

IE Ionization Energy
NG Noble Gas

* Lein M, Frunzke J, Frenking G (2003) Theoretical studies of inorganic compounds XXIV, part XXIII: Lein M, Frunzke J, Frenking G (2003) Angew Chem 115:1341, Angew Chem Int Ed Engl 42:1303.

1 Prologue

It was in the year 1987, when I (GF) was working at the Stanford Research Institute (SRI International) at Menlo Park, California, that a letter by Christian Klixbull Jørgensen was delivered to my office. The name was familiar to me since my introductory courses in inorganic chemistry in the early 1970s but I had never met him personally, nor did I have any previous contact with him. It was one of those letters whose style is well known to anyone who has ever communicated with him. A neatly handwritten document which was clearly focusing on a scientific topic and yet it was full of humour and irony. I had never received such a letter from a scientist, and I learned only later that the invention of the typewriter had passed him by like many other novelties which he considered unimportant.

In his letter he asked me about some recent publications of mine which reported on quantum chemical calculations of the light noble gas elements helium, neon and argon. My interest in doubly charged organic cations [1] had led to me calculating the structure of $HeCCHe^{2+}$, which according to the calculations has a very short carbon-helium bond length of 1.085 Å [2]. The analysis of the bonding situation suggested that the short bond is not simply caused by strong electrostatic attraction but rather by low-lying empty orbitals of CC^{2+}. Systematic calculations of isoelectronic analogues of $HeCCHe^{2+}$ which are less highly charged guided me first to singly charged $HeCCH^{+}$ and then to neutral HeBeO [3]. The calculations predicted that the neutral species HeBeO has a remarkably short He-Be bond (1.54 Å) and that the He-BeO bond dissociation energy (3 kcal/mol) is much larger than that of any theoretically or experimentally studied neutral helium compound. The theoretical prediction that neutral helium compounds may become synthesized was surprising and I felt flattered when renowned newspapers and research journals reported the scientific news [4]. My enthusiasm was a bit dampened, however, by the disappointing finding that the bonding between He and BeO is caused by unusually strong van der Waals forces and not by genuine covalent interactions [3c]. The summary of our theoretical research in light noble gas chemistry has been published in a review with Dieter Cremer [5].

Back to Christian Klixbull Jørgensen (CKJ). He wrote to me because he realized that the peculiar bonding in He-BeO should become manifest in other donor-acceptor complexes D-BeO where D is a heavier and thus more polarizable element. His letter was full of data and ideas about other possibly stable molecules which I had never thought about because I clearly lacked the enormous chemical knowledge of CKJ. By training, I was a theoretical organic chemist and my chemical perspective was much more limited at that time than his. The periodic system of the elements was his playground where he knew every corner and every grain of sand. I remember when I visited him few years later in Geneva in order to give a seminar, that he told me my reimbursement for travel costs would be the atomic number of a certain lanthanide element multiplied by the oxidation number of another lanthanide. I was perplexed but I knew that the sum would be correct!

In the same letter CKJ informed me that he would soon be coming to California to give seminars at several universities. I was living with my wife in San

Francisco at that time, and since this was the departure port for his return flight I invited him to come to our place and to spend the last night in our apartment. Everyone who ever met CKJ knows what this means! It became an extremely entertaining evening full of jokes and fun with witty conversation where science and life mix in an ingenious way. And while we joked about many things we continued to have serious discussions about science, particularly about noble gas chemistry. He opened my eyes and enabled me to see my theoretical discovery about the chemical bonding of light noble gases in the context of other fields. In particular, he taught me about the history of the chemistry of the noble gases. We continued our discussion on the topic after he returned to Geneva by written communication which made me the proud owner of a large collection of handwritten CKJ letters. The result of our communication was the decision to coauthor a review article entitled "Historical, spectroscopic and chemical comparison of noble gases" [6]. We believed at that time that the final chapter about neutral compounds of the light noble gas elements had been written and that no further breakthrough could be expected. The recent synthesis of the first chemically bonded neutral argon compound HArF by Khriatchev et al. proved us wrong! [7].

2 Chemical Bonding in Noble Gas Compounds

In order to understand the difference between earlier attempts to synthesize a neutral argon compound and the approach which led to the first isolation of a neutral argon compound in a condensed phase it is helpful to consider the nature of the bond in the previously synthesized compounds of the heavier noble gases. This shall not be done in great detail but only in the context of the bonding in HArF which will be analysed below. For the history of noble gas chemistry and a detailed discussion of the chemical bonding of noble gases we refer to the previously mentioned review [6] and to the account by Laszlo and Schrobilgen about the experimental studies which finally led to the first noble gas compound [8].

All attempts to synthesize a neutral noble gas (NG) compound focussed in the beginning on trying to react NG with the most electronegative elements, particularly fluorine. The idea was that it takes strong electron attracting forces to bring the valence electrons of NG, which has a filled valence shell with eight electrons, to engage into chemical bonding with other elements. The most electronegative element fluorine seemed to be the best choice, and xenon should be the most accessible noble gas element because it has the lowest ionisation energy (IE) of all NG elements. It is ironic that just at the time when this idea turned out to be true, leading to the synthesis of XeF_2 [9], a different approach which was based on the same principle was successful and led to the first publication of a stable neutral noble gas compound. Neil Bartlett found in 1961 that PtF_6 is such a strongly oxidising agent that it even oxidizes oxygen yielding the salt $O_2^+(PtF_6)^-$ [10]. According to his values [11, 12], the first IE of O_2 (12.2 eV) is even slightly higher than the IE of Xe (12.03 eV), and thus it seemed conceivable that PtF_6 could also oxidize xenon. This was indeed the case. Although the compound

which is immediately formed when the gases Xe and PtF_6 react is not $Xe^+(PtF_6)^-$ as was originally formulated [13] but rather a mixture of which the most important molecule has the formula $(XeF)^+(PtF_6)^-$ [14] the basic idea of bringing a noble gas to forming a chemical bond was proven to be correct by the synthesis of XeF_2 and by the latter salt compound. There are elements and molecules like PtF_6 whose electron attracting strength is so strong that the valence electrons of NG engage in chemical bonding.

In the following years it turned out that the strength of the electron attraction of an atom or molecule X and the ionisation energy of NG are the main factors which determine the strength of the NG-X bond. Xenon compounds are much more stable than krypton compounds and the stability of the molecules with NG-X bonds follows the order of the electronegativity of X=F>O>N>C. It is only recently that compounds with xenon-carbon bonds could be made [15]. Stable neutral compounds of argon have not been synthesized prior to the work of Khriatchev et al. [7]. A theoretical study showed that salt compounds of ArF^+ should be accessible because the bond dissociation energy of ArF^+ is very high (49 kcal/mol) [16]. The first IE of fluorine (17.422 eV) is higher than that of argon (15.759 eV) which means that ArF^+ dissociates into Ar^+ and F. It is probably the choice of a very weakly coordinating anion and the difficult experimental conditions which until now frustrated the synthesis of stable salt compounds with the cation ArF^+ which therefore remains a challenge to experiment.

Because the experimental approaches to synthesize a noble gas compound which were finally successful for xenon and krypton failed for argon, it was believed for a long time that the lighter noble gas elements neon and particularly helium would be the eternal guardian of the nobility of the group eight elements. In 1988 we published our work on NGBeO (NG=He, Ne, Ar) which showed that the light noble gases form unprecedentedly strong donor-acceptor bonds with the Lewis acid BeO [3c]. As mentioned above, after careful analysis of the nature of the chemical bonding we had to recognize that the NG-BeO bond is not a true chemical bond but rather a strong van der Waals interaction. It seemed at that time that both approaches, i.e. electron attraction by a very electronegative element such as fluorine and donor-acceptor interactions with a strong Lewis acid, would not become successful in experimental attempts to isolate stable compounds of He, Ne, Ar. The only possible way might be salt compounds of ArF^+. Quantum chemical calculations of ArF_2 predicted that the molecule is a very weakly bonded van der Waals complex [17]. What else could be expected? Light noble gas chemistry appeared to be a dead area for inorganic chemists.

3 The Electronic Structure of HArF

The nature of the chemical bonding in a molecule can either be analysed by inspecting the electronic structure in the interatomic region, or by an energy decomposition analysis of the interatomic interaction energy. Numerous partitioning techniques have been suggested with the aim to provide information about the strength of the two principle components of chemical bonding, i.e. electrostatic and covalent interactions, and to elucidate the degree of multiple bond-

ing in molecules which have π or δ bonds. It should be kept in mind that the results of such an analysis are no observable quantities and they cannot be verified or falsified by experimental methods. The value of the methods can only be judged by the finding that they are useful to classify different chemical bonds in a consistent way. All methods have their strengths and pitfalls which shall not be discussed here. We have chosen one method for analysing the electronic structure and one for the interaction energy of HArF which we consider to be very useful for the purpose. In the following we will first discuss the electronic structure followed by the energy analysis which will be given in the next section.

The method which we considered most useful for analysing the electronic structure is the topological analysis of the electron density distribution It was developed by Bader [18] and therefore it is also called Bader analysis. An important quantity in the Bader analysis is the second derivative of the electron density distribution $\nabla^2\rho(r)$ which is called Laplacian distribution. The Laplacian distribution is a much more sensitive probe for changes in the valence shell of an atom which are caused by interatomic electronic interactions than the electron density distribution $\rho(r)$. This can be nicely shown in graphical displays of contour line diagrams of $\nabla^2\rho(r)$.

Figure 1 shows the contour line diagrams $\nabla^2\rho(r)$ of the molecules ArF, ArH and HArF. Solid lines indicate areas of charge concentration ($\nabla^2\rho(r)<0$) while dashed lines show areas of charge depletion ($\nabla^2\rho(r)<0$). We begin the discussion with ArF. Figure 1a shows that the argon atom has a circular shaped area of charge concentration which is practically undisturbed by the fluorine atom. The latter atom has an area of charge concentration which shows maxima in the direction that is perpendicular to the bonding line. The maxima come from the lone electron pairs of the doubly occupied p(π) AOs of F which has a singly occupied p(σ) AO. The shape of the atomic Laplacian distributions of Ar and F in ArF is essentially the same as in the free atoms. Thus, the contour line diagram of $\nabla^2\rho(r)$ of ArF suggests that there are only very weak interatomic interactions. This is in agreement with the very long calculated bond length (4.468 Å) and with the theoretically predicted low bond dissociation energy (D_e=0.14 kcal/mol). There is no doubt that ArF is a weak van der Waals complex and not a chemically bonded molecule. It should be noted, however, that neither the bond length nor the bond dissociation energy are reliable probes for addressing the question if the interatomic interactions should be classified as chemical bonding or as van der Waals forces.

A similar situation is found for ArH. Figure 1b shows that the argon and hydrogen atoms have circular shaped areas of electron concentration in the valence shell. Like ArF, ArH is a van der Waals complex which has a long (3.564 Å) and weak (D_e=0.03 kcal/mol) bond. The picture is completely different when the Laplacian distribution of HArF is considered. Figure 1c shows that there is a continuous area of charge concentration ($\nabla^2\rho(r)<0$, solid lines) between the hydrogen and argon atom. The valence shell region of both atoms is strongly distorted towards accumulated charge concentration in the bonding region. There is a dramatic difference between the Laplacian distributions of the Ar-H bonds of ArH (Fig. 1b) and HArF (Fig. 1c). However, the Laplacian distribution of the Ar-F bonding in the latter molecule also exhibits significant differences when it is

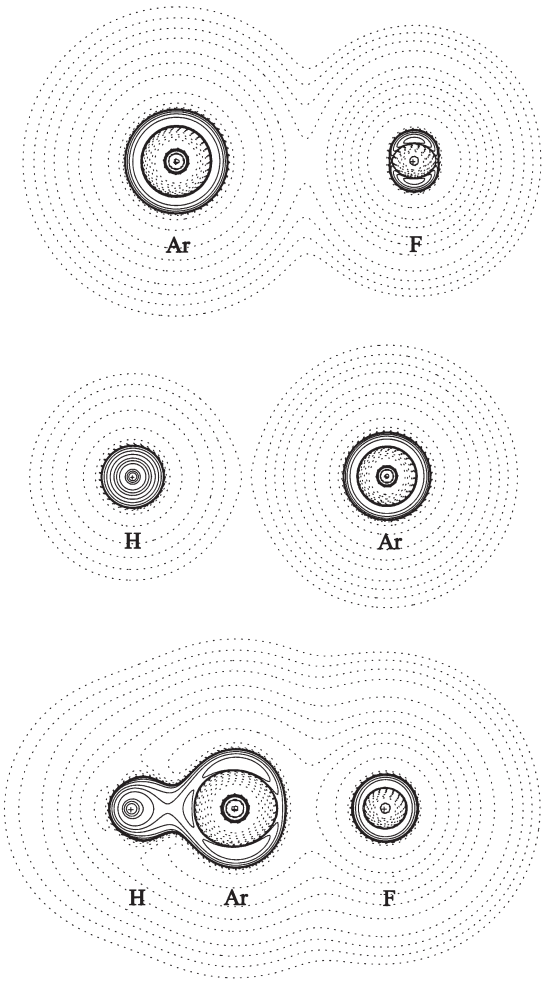

Fig. 1 Contour line diagrams $\nabla^2\rho(r)$ of the molecules ArF, ArH and HArF. *Solid lines* indicate areas of charge concentration ($\nabla^2\rho(r)<0$) while *dashed lines* show areas of charge depletion ($\nabla^2\rho(r)>0$)

compared with ArF (Fig. 1a). The fluorine atom in HArF has a circular shaped area of charge concentration which does not have those local maxima that are clearly exhibited by the fluorine atom of ArF. The isotropic charge concentration of the fluorine atom in HArF suggests that additional electronic charge has been donated yielding an F^- anion. The conclusion is supported by the calculation of the atomic partial charges of HArF which gives a value q(F)=–0.76. The atomic partial charges of the other atoms are q(H)=+0.22 and q(Ar)=+0.54. The Laplacian distribution and the calculated charges indicate that the HAr-F bond is mainly electrostatic which can be written as HAr^+-F^- and that the H-ArF bond is mainly covalent. Is it possible to quantify the results about the nature of the

bonding in HArF more accurately? In the next section we will show that this is indeed the case.

4 Energy Partitioning Analysis of HArF

The method which we employed for analysing the bonding energy in HArF has been developed by Morokuma [19] and independently by Ziegler [20]. The central quantity of the bonding analysis is the instantaneous interaction energy ΔE_{int} between the bonding fragments. It is calculated as the energy difference between the optimised molecule and the fragments with the frozen geometries of the complex. The choice of the fragments is given in the discussion of the results. The interaction energy ΔE_{int} can be divided into three main components:

$$\Delta E_{\text{int}} = \Delta E_{elstat} + \Delta E_{Pauli} + \Delta E_{orb} \quad (1)$$

The three terms ΔE_{elstat}, ΔE_{Pauli} and ΔE_{orb} can be interpreted in a physically meaningful way. ΔE_{elstat} gives the electrostatic interaction energy between the fragments which are calculated with the frozen electron density distribution of A and B in the geometry of the complex AB. The second term in the equation, ΔE_{Pauli}, refers to the repulsive interactions between the fragments which are caused by the fact, that two electrons with the same spin cannot occupy the same region in space. The term comprises the four-electron destabilizing interactions between occupied orbitals. ΔE_{Pauli} is calculated by forcing the Kohn-Sham determinant of AB, which results from superimposing fragments A and B, to obey the Pauli principle by antisymmetrization and renormalization. The stabilizing orbital interaction term, ΔE_{orb}, is calculated in the final step of the ETS analysis when the Kohn-Sham orbitals relax to their optimal form. This term can be further partitioned into contributions by the orbitals which belong to different irreducible representations of the interacting system. It is thus possible to estimate the stabilizing contributions which come from orbitals having σ, π or δ symmetry. The method has been used in a systematic investigation of different types of chemical bonds between atoms across the periodic system [21]. The results have recently been summarized in a review [22]. Details about the method are found in these publications.

Table 1 shows the results of the energy partitioning analysis of HArF. First we discuss the energy components of the interactions between H and ArF. The calculated total interaction energy is ΔE_{int}=–33.6 kcal/mol. The largest component is the repulsive Pauli term ΔE_{Pauli}=136.5 kcal/mol. The two stabilizing forces are the electrostatic attraction whose strength is ΔE_{elstat}=–62.1 kcal/mol and the covalent orbital term ΔE_{orb}=–107.9 kcal/mol. Thus, the energy decomposition analysis suggests that the H-ArF bond is 36.5% electrostatic and 63.4% covalent. The larger energy contribution of the covalent term is in accord with the conclusion that was drawn from the analysis of the electron density distribution.

The HAr-F interaction energy has been analysed in two different ways. First we considered the fragments HAr^+ and F^- because the above results of the electronic structure suggests that the fragments are highly charged and that the fluorine moiety has a closed-shell configuration. Table 1 shows that the total inter-

Table 1 Results of the energy decomposition analysis of HArF. The energy values are given in kcal/mol

Term	H+ArF	HAr^++F^-	HAr+F
ΔE_{int}	−33.6	−172.7	−75.2
ΔE_{Pauli}	136.5	88.5	65.2
ΔE_{elstat} [a]	−62.1 (36.5%)	−183.1 (70.1%)	−24.7 (17.6%)
ΔE_{orb} [a]	−107.9 (63.4%)	−78.1 (29.9%)	−115.7 (82.4%)
A_1	−103.6 (96.0%)[b]	−69.6 (89.1%)[b]	−111.4 (96.3%)[b]
A_2	0.0	0.0	0.0
B_1	−2.2 (2.0%)[b]	0.0	−2.2 (1.9%)
B_2	−2.2 (2.0%)[b]	−8.4 (10.9%)[b]	−2.2 (1.9%)[b]

[a] The value in parentheses gives the percentage contribution to the total attractive interactions.
[b] The value in parentheses gives the percentage contribution to the total orbital interactions.

action energy ΔE_{int}=−172.7 kcal/mol is very large. The largest component of ΔE_{int} is the electrostatic attraction ΔE_{elstat}=−183.1 kcal/mol which is significantly larger than the attractive orbital interaction term ΔE_{orb}=−78.1 kcal/mol. Thus, the energy partitioning analysis suggests that the chemical bonding between HAr^+ and F^- is 70.0% electrostatic and 30.0% covalent. The covalent bonding comes mainly from σ orbitals (89.2%) while the π interactions are much less important (10.8%).

We also analysed the argon-fluorine bonding in HArF using the neutral fragments HAr and F as interacting moieties. Table 1 shows that the energy partitioning analysis of the latter gives a significantly different picture of the nature of the chemical bonding. The value of the interaction energy ΔE_{int}=−75.2 kcal/mol is clearly lower than for the charged fragments. More important than this are the values for the attractive components. The bonding analysis in terms of neutral fragments gives a much larger value for the covalent bonding ΔE_{orb}=−115.7 kcal/mol than for the electrostatic attraction ΔE_{elstat}=−24.7 kcal/mol. The conclusion is that the bonding between neutral fluorine atom and HAr in HArF is largely covalent. The results demonstrate that the choice of the fragments is crucially important for the results of the energy partitioning analysis, which is not very surprising. The topological analysis of the electron density distribution shows clearly that the interacting fragments of HArF are HAr^+ and F^-. The energy partitioning analysis shows that the latter interactions are mainly electrostatic. This is not a trivial result! It has been shown before that the choice of charged fragments does not necessarily lead to higher degree of electrostatic bonding. The charges have a strong influence on the energy levels of the orbitals which may enhance the orbital interactions more than the electrostatic interactions [21a].

Finally we want to point out that the strong electronic interactions in HArF which are revealed by the charge and energy analyses do not become obvious by the calculated bond dissociation energies (BDEs). Note that the calculated interaction energies ΔE_{int} which are given in Table 1 have been calculated using the frozen geometries of the diatomic fragments. The theoretically predicted BDEs which are calculated using the optimised geometries of the fragments are much lower. The calculated value of the H-ArF bond is only D_e=2.2 kcal/mol and

the BDE of the HAr-F bond is D_e=2.3 kcal/mol. The dissociation reaction HArF→Ar+HF is even exoenergetic with D_e=–137.6 kcal/mol. The barrier for the latter dissociation reaction is sufficiently high, however, to stabilize the molecule that it can be isolated in a low-temperature matrix. High-level calculations by Wong predict that the activation energy is ΔE^{+}=28.0 kcal/mol [23].

5 Epilogue

Christian Klixbull Jørgensen had the unusual ability to combine physical insights into the structure of atoms and molecules with chemical models that are useful for a qualitative ordering scheme of heavy atom molecules. He had a profound knowledge of physics and physical chemistry which enabled him to explain chemical observations with physically sound models. The theoretical research which is described above would be approved by him, because the results consist not only of numbers but the data are part of a bonding analysis which strives at giving insight into the mechanism which leads to a chemical bond. The trick which was used by Khriatchev et al. [7] to force argon into a chemical bonding was to combine two different interatomic interactions, i.e. Ar-H and Ar-F interactions, which only together lead to the desired goal. This can be recognized by the topological analysis of the electron density distribution. The energy partitioning analysis makes it possible to give a quantitative estimate of those important contributions to the interatomic interactions which had previously been discussed only qualitatively. CKJ would have been pleased.

6 Methods

The geometries of the molecules have been optimised at the MP2/6–311G(d,p) level using Gaussian 98 [24]. The nature of the stationary points on the potential energy surface was investigated by calculation of the Hessian matrices. All reported structures are energy minima. Bond dissociation energies have been calculated at the CCSD(T)/cc-pVQZ level using MP2/6–311G(d,p) optimised geometries.

The energy decomposition analysis was performed at the non-local DFT level of theory using the exchange functional of Becke [25] and the correlation functional of Perdew [26] (BP86). Scalar relativistic effects have been considered using the zero-order regular approximation (ZORA) [27, 28]. Uncontracted Slater-type orbitals (STOs) were used as basis functions for the SCF calculations [29]. The basis sets for all atoms have triple-zeta quality augmented with one set of d-type and one set of f-type polarization functions for carbon and one set of p polarization functions for hydrogen. This is denoted TZ2P. The $(1s2s2p)^{10}$ core electrons of argon and the $1s^2$ core electrons of carbon were treated by the frozen core approximation [30]. An auxiliary set of s, p, d, f and g STOs was used to fit the molecular densities and to represent the Coulomb and exchange potentials accurately in each SCF cycle [31]. The energy decomposition analysis was carried out using optimised geometries at the BP86/TZ2P level of theory. The calculated

bond lengths at BP86/TZ2P and MP2/6-311G(d,p) are very similar. The BP86/TZ2P calculations were carried out with the program package ADF(2000.02) [32, 33].

Acknowledgments This work has been financially supported by the Deutsche Forschungsgemeinschaft and the Fonds der Chemischen Industrie.

7 References

1. Frenking G, Koch W, Gauss J, Cremer D (1986) J Am Chem Soc 108:5808
2. Koch W, Frenking G (1986) Int J Mass Spectrom Ion Proc 74:133
3. (a) Koch W, Collins JR, Frenking G (1986) Chem Phys Lett 132:330; (b) Koch W, Frenking G, Gauss J, Cremer D, Collins JB (1987) J Am Chem Soc 109:5917; (c) Frenking G, Koch W, Gauss J, Cremer D (1988) J Am Chem Soc 110:8007
4. (a) New York Times (1988) March 22, p C4; (b) Frankfurter Allgemeine Zeitung (1988) March 30, p II of 'Natur und Wissenschaft'; (c) Nature (1988) 331:487; (d) C&N News (1987) 65:16; (e) Sci News (1987) 132:334
5. Frenking G, Cremer D (1990) Struct Bond, vol 73. Springer, Berlin Heidelberg New York, p 17
6. Jørgensen CK, Frenking G (1990) Struct Bond, vol 73. Springer, Berlin Heidelberg New York, p 1
7. Khriatchev L, Pettersson M, Runeberg N, Lundell J, Räsanen M (2000) Nature 40:874
8. Laszlo P, Schrobilgen G (1988) Angew Chem 100:495; Laszlo P, Schrobilgen G (1988) Angew Chem Int Ed Engl 27:479
9. Hoppe R, Dähne W, Mattauch H, Rödder KM (1988) Angew Chem 100:495; Hoppe R, Dähne W, Mattauch H, Rödder KM (1988) Angew Chem Int Ed Engl 27:479
10. Bartlett N, Lohmann DH (1962) Proc Chem Soc 115
11. See the copy of the relevant page of Bartlett's laboratory notebook which is given as Fig. 6 in [8]
12. Another ironic twist in the history of noble gas chemistry is that the more accurate values for the ionisation energies which are available now show that the first IE of O_2 (12.0697 eV) is actually slightly lower than the IE of Xe (12.1298 eV): (a) Moore CE (1970) Ionization potentials and ionization limits derive from the analysis of optical spectra, Natl Stand Ref Data Ser-Nat Bur Stand (US), no 34; (b) Lias SG, Bartmess JE, Liebman JF, Holmes JL, Levin RD, Mallard WG (1988) J Phys Chem Ref Data 17, Suppl 1
13. Bartlett N (1962) Proc Chem Soc 218
14. Graham L, Graudejus O, Jha NK, Bartlett N (2000) Coord Chem Rev 197:321
15. Frohn HJ, Jakobs S, Henkel G (1989) Angew Chem 101:1534; Frohn HJ, Jakobs S, Henkel G (1989) Angew Chem, Int Ed Engl 28:1506
16. Frenking G, Koch W, Deakyne CA, Liebman JF, Bartlett N (1989) J Am Chem Soc 111:31
17. Chan KW, Power TD, Jai-Nhuknan J, Cybulski SM (1999) J Chem Phys 110:860
18. (a) Bader RFW (1990) Atoms in molecules. A quantum theory. Oxford University Press, Oxford. Other methods which use the total electron density distribution for analysing the electronic structure and bonding situation have been suggested by: (b) Becke AD, Edgecomb KE (1990) J Chem Phys 92:5397; (c) Savin A, Silvi B (1994) Nature 371:683
19. (a) Morokuma K (1971) J Chem Phys 55:1236; (b) Kitaura K, Morokuma K (1976) Int J Quantum Chem 10:325
20. Ziegler T, Rauk A (1977) Theor Chim Acta 46:1
21. (a) Diefenbach A, Bickelhaupt FM, Frenking G (2000) J Am Chem Soc 122:6449; (b) Uddin J, Frenking G (2001) J Am Chem Soc 123:1683; (c) Chen Y, Frenking G (2001) J Chem Soc Dalton Trans 434; (d) Doerr M, Frenking G (2002) Z Allg Anorg Chem 628:843; (e) Loschen C, Voigt K, Frunzke J, Diefenbach A, Diedenhofen M, Frenking G (2002) Z Allg Anorg Chem 628:1294; (f) Frenking G, Wichmann K, Fröhlich N, Grobe J, Golla W, Le Van D, Krebs B, Läge M (2001) Organometallics 21:2921; (g) Rayón VM, Frenking G (2002) Chem Eur J 8:4693;

(g) Lein M, Frunzke J, Timoshkin AY, Frenking G (2001) Chem Eur J 7:4155; (h) Frunzke J, Lein M, Frenking G (2002) Organometallics 21:3351
22. Frenking G, Wichmann K, Fröhlich N, Loschen C, Lein M, Frunzke J, Rayón VM (2003) Coord Chem Rev 55:238–239
23. Wong MW (2000) J Am Chem Soc 122:6289
24. Frisch MJ, Trucks GW, Schlegel HB, Scuseria GE, Robb MA, Cheeseman JR, Zakrzewski VG, Montgomery JA Jr, Stratmann RE, Burant JC, Dapprich S, Millam JM, Daniels AD, Kudin KN, Strain MC, Farkas O, Tomasi J, Barone V, Cossi M, Cammi R, Mennucci B, Pomelli C, Adamo C, Clifford S, Ochterski J, Petersson GA, Ayala PY, Cui Q, Morokuma K, Malick DK, Rabuck AD, Raghavachari K, Foresman JB, Cioslowski J, Ortiz JV, Stefanov BB, Liu G, Liashenko A, Piskorz P, Komaromi I, Gomperts R, Martin RL, Fox DJ, Keith T, Al-Laham MA, Peng CY, Nanayakkara A, Gonzalez C, Challacombe M, Gill PMW, Johnson B, Chen W, Wong MW, Andres JL, Gonzalez C, Head-Gordon M, Replogle ES, Pople JA (1998) Gaussian 98, Revision A3. Gaussian Inc., Pittsburgh PA
25. Becke AD (1988) Phys Rev A 38:3098
26. Perdew JP(1986) Phys Rev B 33:8822
27. Snijders JG (1989) Mol Phys 36:1789
28. Snijders JG, Ros P (1979) Mol Phys 38:1909
29. Snijders JG, Baerends EJ, Vernooijs P (1982) At Nucl Data Tables 26:483
30. Baerends EJ, Ellis DE, Ros P (1973) Chem Phys 2:41
31. Krijn J, Baerends EJ (1984) Fit functions in the HFS-method. Internal Report, Vrije Universiteit Amsterdam, The Netherlands (in Dutch)
32. Bickelhaupt FM, Baerends EJ (2000) Rev Comput Chem 15:1
33. te Velde G, Bickelhaupt FM, Baerends EJ, van Gisbergen SJA, Fonseca Guerra C, Snijders JG, Ziegler T (2001) J Comput Chem 22:931

Structure and Bonding, Vol. 106 (2004): 193–208
DOI 10.1007/b11313

Spectroscopy of Trivalent Praseodymium in Barium Yttrium Fluoride

B. E. Bowlby[1,2] · B. Di Bartolo[1]

[1] Boston College, Department of Physics, Chestnut Hill, MA 0246, USA
E-mail: bowlby@bu.edu; dibartob@bc.edu
[2] Boston University, Department of Cognitive and Neural Systems, Boston MA, USA

Abstract This work reports the results of an investigation of the spectroscopic properties of trivalent praseodymium (Pr^{3+}) in barium yttrium fluoride (BaY_2F_8). Two doping concentrations were used: BaY_2F_8:Pr^{3+} (0.3%) and BaY_2F_8:Pr^{3+} (1%). Absorption spectra, taken at 77 and 300 K, allowed the placement of the energy levels of the $4f^2$ electronic configuration of Pr^{3+}. Luminescence spectra were obtained with transitions originating mainly in the metastable levels $^3P_0$, $^1D_2$, and $^3F_3$. Time-resolved spectroscopy was used to clarify the assignment of several spectral lines.

The lifetimes of both $^3P_0$ and $^1D_2$ were found to be essentially independent of concentration and temperature with values of 55 and ~250 μs respectively, in the temperature range 77 to 500 K. In the same temperature range, the lifetime of the $^3F_3$ level was found to vary from 23 ms at 77 K to 5 ms at 500 K. The effects of temperature on the widths and positions of several spectral lines originating in the $^3P_0$ and $^1D_2$ levels were studied. The mechanism of Raman scattering of phonons fitted the observed results with an effective Debye temperature of 500 K.

Keywords Luminescence · Praseodymium in fluorides · Lifetimes · Line-broadening · Line-shift

List of Abbreviations

IR Infrared
UV Ultraviolet

1 Introduction

The praseodymium ion in its trivalent state is a very good representative of the entire class of rare earth ions and of the complex spectroscopic properties that they exhibit when placed in a host lattice. As a system, it presents an intricate energy level scheme, energy gaps of various sizes that foster a competition between radiative and nonradiative transitions, several metastable states emitting multicolored light, and host dependence of its spectroscopic parameters. Its spectral properties include laser emission [1], infrared quantum counting [2], upconversion [3], avalanche effect [2, 3], and photon splitting [4].

The present work deals with trivalent praseodymium (Pr^{3+}) in barium yttrium fluoride (BaY_2F_8). This crystal is monoclinic, and, as such, should completely split all of the energy levels of Pr^{3+}. BaY_2F_8:Pr^{3+} has lased as reported in [5]. The

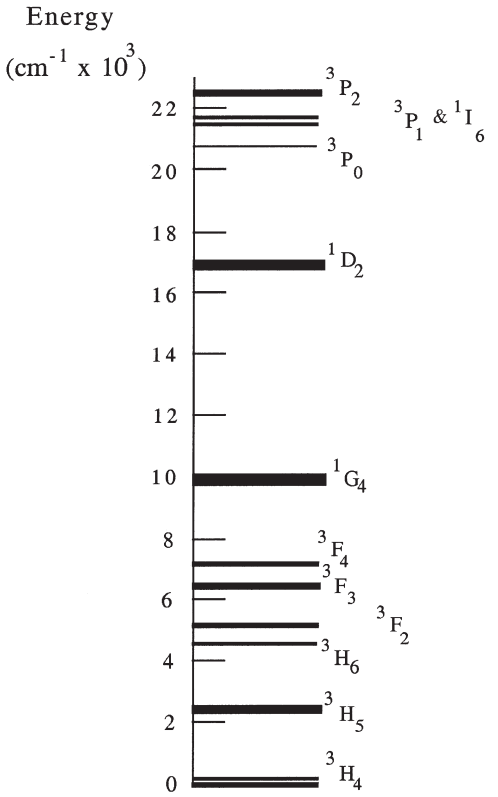

Fig. 1 Energy level scheme of Pr^{3+} in BaY_2F_8

motivation for this investigation is to characterize spectroscopically this laser system.

The treatment of the electronic configurations of rare earth ions in spherical symmetry is presented in great detail in the book by Reisfeld and Jørgensen [6]. The electronic configuration of the ion Pr^{3+} is [(closed shells)+$4f^2$]. The total number of $4f^2$ quantum states is 91. The electron-electron interaction creates the LS terms ^3H, ^3F, ^1G, ^1D, ^1I, ^3P, and ^1S. The spin-orbit interaction splits the LS terms into J sublevels, but mixes states with the same J and different L and S. Because of this term mixing, there are departures from the Landé interval rule. The crystalline field splits the J levels. An energy level scheme of the Pr^{3+} ion is presented in Fig. 1.

2 Experimental

2.1 Samples Studied

The samples investigated in this work were barium yttrium fluoride (BaY_2F_8) crystals doped with praseodymium (Pr^{3+}). Two doping concentrations were studied: 1% and 0.3%. These crystals were grown using the Bridgman-Stockbarger method at the Institute of Crystallography of the Russian Academy of Sciences.

BaY_2F_8 belongs to the space group C^3_{2h} and has β-BaY_2F_8 structure. Praseodymium substitutes for yttrium with no charge compensation and sits in a site with symmetry C_2. This site is non-centrosymmetric, which means that the Judd-Ofelt theory may be applied to this system. The concentration of Y is $1.28\times10^{22}/cm^3$. The unit cell parameters are a=0.6972 nm, b=1.0505 nm, c=0.4260 nm, and β=99.4 °. The phonon spectrum extends up to 415 cm^{-1}.

The samples were both cubic in shape, with edges approximately 5 mm long. One of the physical axes of the cube was aligned with the c-axis of the crystal, but unfortunately the other axis did not correspond to either of the other crystallographic axis. This, however, did not present any difficulties in the spectroscopy of the crystals because all excitation, and all detection, were unpolarized.

2.2 Absorption Measurements

The absorption spectra were obtained using a Perkin-Elmer Lambda 9 spectrophotometer. This apparatus uses a tungsten-halogen light source for the visible and infrared regions, a photomultiplier tube for detection of the visible spectra, and an uncooled lead-sulfide detector for the infrared spectra. The spectrophotometer was controlled with an IBM AT personal computer, which also served to record the data. The sample was placed in a Dewar. Absorption spectra were obtained in the ranges 400–500 nm, 560–610 nm, 950–1050 nm, 1,350–1650 nm and 1850–2450 nm at both room temperature (300 K) and at liquid nitrogen temperature (77 K). These ranges correspond to transitions from the $^3H_4$ ground state to the levels $^3P_2$, $^3P_1$, $^1I_6$ and $^3P_0$ (400–500 nm), $^1D_2$ (565–615 nm),

$^1G_4$ (950–1050 nm), $^3F_4$ and $^3F_3$ (1350–1650 nm), and $^3F_2$ and $^3H_6$ (1850–2450 nm). Due to its limitations, the spectrophotometer would not allow the absorption to the $^3H_5$ level (at approximately 5 μm) to be measured.

2.3 Continuous Luminescence Measurements

Three different light sources were used to excite the samples. The source most used was an Omnichrome model 532 argon-ion laser powered by an Omnichrome model 150 power supply. Also used were an ILC model LX300F xenon lamp and a Sylvania DVY 650 Watt sun gun. The output of the source was generally filtered so that a specific energy level of the sample could be populated, and then focused onto the sample. The sample was housed in either a Janis Research model ST-4 cryostat for measurements in the temperature range 77–300 K, or a quartz furnace wound with a Ni-Cr ribbon for temperatures above 300 K. For low temperature measurements, the air in the cryostat was evacuated, and liquid nitrogen was forced into a chamber around the sample holder. The temperature of the sample was monitored and controlled with a Lake Shore Cryogenics model 805 temperature control unit.

The resulting luminescence, which was observed at 90° from the exciting axis, was then chopped at 250 Hz with a Bulova L-40-C tuning fork and focused onto the entrance slit of a McPherson model 2051 1-m monochromator. The monochromator has a 600 groove per millimeter grating blazed at 1.25 μ. Most of the linewidth data were taken with slit sizes of 50 μ which gave a resolution of ≤5 Å. The monochromator was controlled via a McPherson model 789A-3 scan control unit which allows scan speeds from 0.1 Å/min to 1000 Å/min. The signal emerging from the monochromator was detected with either a Mitsubishi 4667 photomultiplier tube (400–800 nm), a Mitsubishi 7102 photomultiplier tube (600–1000 nm) or an Optoelectronics model OTC-22-5 PbS infrared detector. The IR detector, which comes packaged in a T0-5 canister, contains a thermoelectric cooler. The TO-5 canister was placed on a copper heat sink in order to prevent small temperature fluctuations. Its temperature was controlled by an Optoelectronics model PN-11454 temperature control unit. The output of the IR detector was then sent to an Optoelectronics model PN-11598 IR preamplifier. After detection, the signal was amplified with a Princeton Applied Research model 122 lock-in amplifier that used the chopping frequency as a reference. The output of the lock-in amplifier was sent to a Data Translation DT2811-PGL analog to digital converter board that is installed in a Thinkmate 386SX personal computer.

For this work, a Hoffman Engineering Corporation model S80-17 standard black body lamp was used as the standard reference source. This lamp was calibrated so as to emit radiation which followed the Planck formula for a black body of T=2856 K when supplied with an electric potential of 16.03 V and a current of 4.75 A. The observed spectra could then be compared with the theoretical spectra for this black body, and a "correction" curve could be calculated. This "correction" curve could then be used to calculate the "true" spectra of a sample from the observed data. This also allowed the relative intensities and integrated intensities

of various transitions to be calculated and compared, even when they were taken with different detectors.

2.4 Lifetime Measurements

Responses to pulsed excitation and time-resolved spectra were obtained by using the same excitation source, a Molectron model DL-II Tunable Dye Laser which was pumped with a Molectron model UV12 Pulsed Nitrogen Laser. The nitrogen laser provided pulse widths of 10 ns with a repetition rate of up to 30 Hz. Dyes used included Coumarin 480 and Coumarin 600. These dyes lase in the ranges 430–500 nm and 560–640, with maximum output at 480 and 600 nm, respectively.

The sample was housed in the Janis cryostat and its temperature was monitored and controlled as before. The luminescence was passed through a filter in order to observe a specific transition, and then focused onto the appropriate detector for the transition being monitored. The output of the detector was sent to a Tektronix model 2232 Digital Storage Oscilloscope which was triggered via a reference pulse sent from the nitrogen laser. The decay of the fluorescence was averaged over several hundred pulses and the result is stored in the oscilloscope's memory. The contents of the memory were then downloaded to the computer via Tektronix's Wavesaver software.

In the time-resolved spectroscopy the resulting luminescence was passed through a monochromator and detected with one of the previously mentioned detectors. The output of the detector was sent to a PAR model 105 Boxcar Integrator which uses a signal from the nitrogen laser as a reference. The boxcar integrator allows the signal from the detector to be monitored at a set amount of time after the reference pulse. Then, by adjusting the time delay on the boxcar integrator, spectra at different times after the excitation can be taken. Spectra taken in this way can show how the various lines develop over time. The output of the boxcar is then sent to the A/D board and digitized.

3 Results and Discussion

3.1 Absorption Data

The absorption spectra of $BaY_2F_8:Pr^{3+}$ were obtained at two temperatures: 300 and 77 K. The spectral region covered was 430–2400 nm. All the J levels were identified. Figure 2 gives a part of the entire spectrum covering the manifolds $^3P_0$, $^3P_1$, $^3P_2$, and $^1I_6$.

There was no difference between the spectra of the two samples used, apart from the fact that the spectra of the sample with the higher concentration of Pr^{3+} were more intense. It is worth commenting on the usefulness of the level $^3P_0$, a singlet. Some weak lines on the low energy side of the main sharp line are due to transitions from the excited sublevels of the ground $^3H_4$ multiplet. The higher energy side of $^3P_0$ is clear of any absorption line for ~10 nm that in this spectral

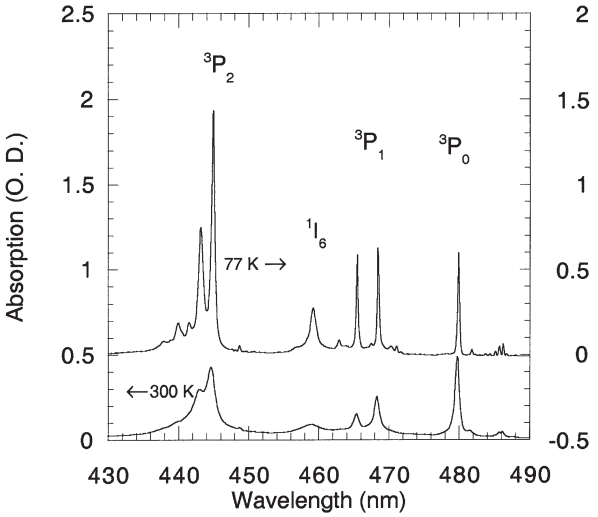

Fig. 2 Absorption spectra of $BaY_2F_8:Pr^{3+}$(1%) at 300 K and 77 K in the spectral region 430 to 490 nm

region correspond to ~450 cm^{-1}. This may lend itself to the observation of vibronic lines in the excitation spectrum of a transition from, say, $^3P_0$ to $^3H_6$. This method has actually been used by Moune et al. [7] to investigate the phonon spectrum of YPO_4 (doped with Pr^{3+}).

The absorption spectra that we have obtained contain a lot of detailed information that we have reported in another paper on the applications of the Judd-Ofelt theory to the praseodymium ion in solids [8]. In this regard it is worth noting the usage of the Judd-Ofelt theory made by Antipenko in a system of $BaYb_2F_8$ doped with rare earth ions [9]. In particular, he reports that the predictions of this theory regarding electric dipole transitions of the praseodymium ion are rather poor on account of the low energy position of the levels of the $4f^5d$ configuration.

3.2 Luminescence Data

The emission spectra of $BaY_2F_8:Pr^{3+}$ were found to originate mainly from the $^3P_0$, $^1D_2$, and $^3F_3$ levels. The excitation of the $^3P_0$ level did not pose any problem because several of the argon laser lines matched the absorption peaks of the manifolds $^3P_2$, $^1I_6$, and $^3P_1$. We chose to excite the $^3P_0$ level by using the argon laser output filtered to allow only the 457.9 nm emission to reach the sample, resulting in the excitation of a sublevel of $^3P_1$.

The emission spectra originating from the $^3P_0$ level can be associated with transitions from $^3P_0$ to the multiplet levels $^3H_4$, $^3H_5$, $^3H_6$, $^3F_2$, $^3F_3$, and $^3F_4$. The emission related to the $^3P_0 \rightarrow {}^3H_4$ transition is reported in Fig. 3.

Emission from the $^1D_2$ level was more difficult to obtain. Because of the very low radiative or nonradiative $^3P_0 \rightarrow {}^1D_2$ transition rates, excitation by the argon laser was not suitable. Other sources were tried, including a Sylvania sungun and a xenon lamp. However, we found that the best excitation for observing the emis-

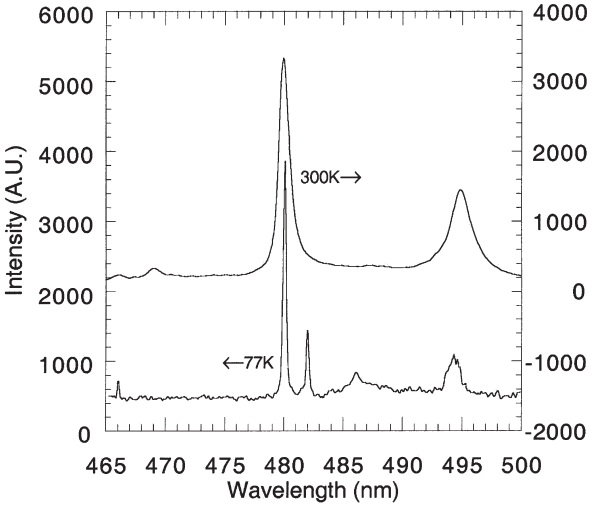

Fig. 3 Emission spectra of $BaY_2F_8:Pr^{3+}$(1%) at 300 K and 77 K in the spectral region 465 to 500 nm. λ_{exc}=457.9 nm (argon laser)

sion from the $^1D_2$ level was provided by the dye laser using the dye Coumarin 600. The reference signal from the (pulsed) dye laser was sent to the boxcar integrator that provided the relevant electronic output.

The emission spectra originating from the $^1D_2$ level can be associated with transitions from $^1D_2$ to $^3H_4$, $^3H_5$, $^3H_6$, $^3F_2$, $^3F_3$, and $^3F_4$. The emission related to the $^1D_2 \rightarrow {}^3H_4$ transition is reported in Fig. 4.

No luminescence originating in the $^1G_4$ level was observed under the excitation conditions that allowed the observation of the emission from levels $^3P_0$ and $^1D_2$. As pointed out by Antipenko [9], on account of the large energy gap between $^1G_4$ and the level above it, radiationless transitions terminating on $^1G_4$ are highly

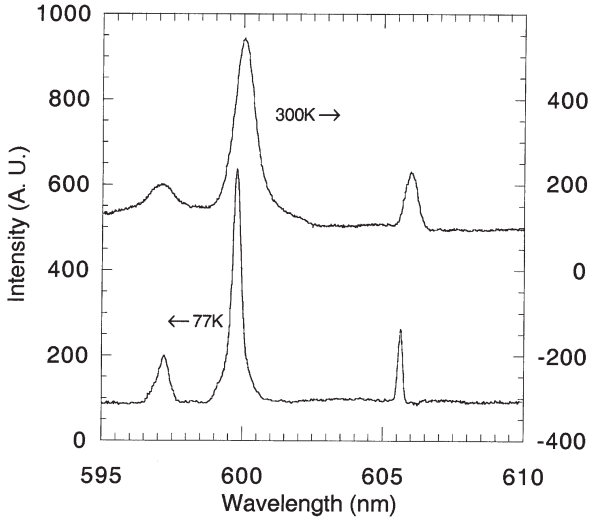

Fig. 4 Emission spectra of $BaY_2F_8:Pr^{3+}$(1%) at 300 K and 77 K in the spectral region 595 to 610 nm. λ_{exc}=589 nm (dye laser)

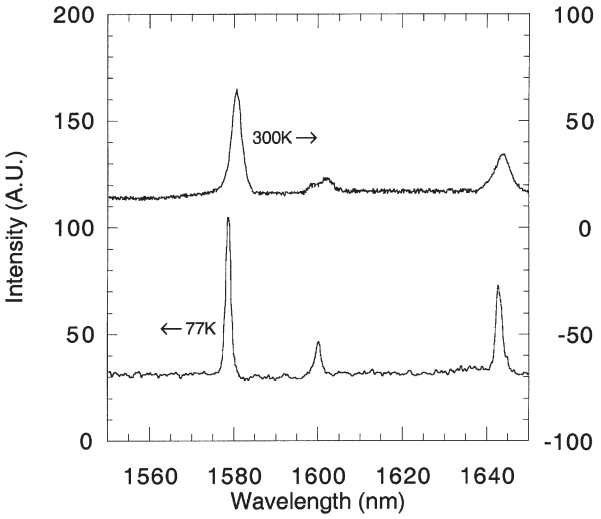

Fig. 5 Emission spectra of $BaY_2F_8:Pr^{3+}$(1%) at 300 K and 77 K in the spectral region 1550 to 1650 nm. λ_{exc}=unfiltered argon laser output

improbable and, as such, do not represent an effective mechanism for pumping $^1G_4$. On the other hand, it is possible to observe emission from $^1G_4$ in the 1.3–1.5 μm spectral region by exciting this level directly, as proven by Garapon et al. [10], who made this observation in a variety of systems. The experimental conditions of our apparatus did not allow us the direct excitation of the level $^1G_4$.

The only other manifold that displayed luminescence was $^3F_3$ and obtaining the emission spectra was relatively easy. Because of the radiative and nonradiative pathways available, it was possible to excite the $^3F_3$ manifold by using the argon laser. This time, however, the unfiltered output of the laser was used to excite the sample. As the upper levels relaxed, the $^3F_3$ level was excited and then, in turn, relaxed to the lower levels in a cascade-type of sequential transitions.

Table 1 Energy levelsof $BaY_2F_8:Pr^{3+}$

(S, L, J)	Energy levels (cm^{-1})	Sub-levels (theor)	Sub-levels (exp)	ΔE (cm^{-1})
$^3P_2$	22836, 22727, 22650, 22563, 22472	5	5	364
$^3P_1+^1I_6$	21906, 21777, 21603, 21482, 21349	16	5	557
$^3P_0$	20838	1	1	
$^1D_2$	17337, 17271, 16975, 16750	5	4	587
$^1G_4$	10485, 10425, 10359, 10335, 9978, 9747, 9725	9	7	760
$^3F_4$	7254, 7181, 7144, 7112, 7053, 6975, 6949, 6929, 6861	9	9	393
$^3F_3$	6704, 6672, 6629, 6543, 6512, 6427, 6336	7	7	368
$^3F_2$	5344, 5285, 5186, 5159, 5049	5	5	295
$^3H_6$	4471, 4413, 4388, 4363, 4327, 4319, 4220	13	6	251
$^3H_5$	2748, 2415, 2255, 2224, 2110	11	5	638
$^3H_4$	638, 249, 84, 0	9	4	638

The emission spectra originating from the $^3F_3$ level can be associated with transitions from $^3F_3$ to $^3H_4$ (see Fig. 5). Combining the absorption data with the emission data led us to the energy levels for Pr^{3+} in BaY_2F_8 reported in Table 1.

3.3 Response to Pulsed Excitation Data

Next we examine the response of the $^3P_0$ level to pulsed excitation. Two types of measurements were performed – lifetime measurements and time resolved spectroscopy. The lifetime vs temperature graph of the $^3P_0$ level for both samples is given in Fig. 6. The samples were excited with the dye laser using Coumarin 480. The lasing wavelength was 480 nm and the emission was monitored at 609 nm (the $^3P_0 \rightarrow {}^3H_6$ transition). All decay patterns were exponential. The lifetime of the $^3P_0$ level appears to be temperature independent in the temperature range measured, and to have a value of approximately 55 μs for both samples. The fact that the lifetime is independent of the temperature in this regime is not unexpected. The energy difference between the $^3P_0$ and the next lower lying level, the $^1D_2$, is over 4000 cm^{-1}. Since the phonon spectrum extends to only about 415 cm^{-1}, at least ten phonons would be needed to bridge this energy gap, a very unlikely event. $^3P_0$ lifetime measurements were also performed on emissions from the $^3P_1$ level (at 465.9 nm), but the lifetime of this level was found to be identical to that of the $^3P_0$ level, leading us to believe that thermalization is occurring between these two manifolds.

Time resolved spectra of the $^3P_0 \rightarrow {}^3H_4$ transition in BaY_2F_8:Pr^{3+} (0.3%) at 300 K are shown in Fig. 7. The delay after the excitation ranged from 20 μs (top spectrum) to 140 μs (bottom spectrum) with a step size of 20 μs. Excitation was with the dye laser using Coumarin 480 and a lasing wavelength of 480 nm. Other transitions that were studied were those from the $^3P_0$ level to the $^3H_6$, $^3F_2$, and $^3F_4$ man-

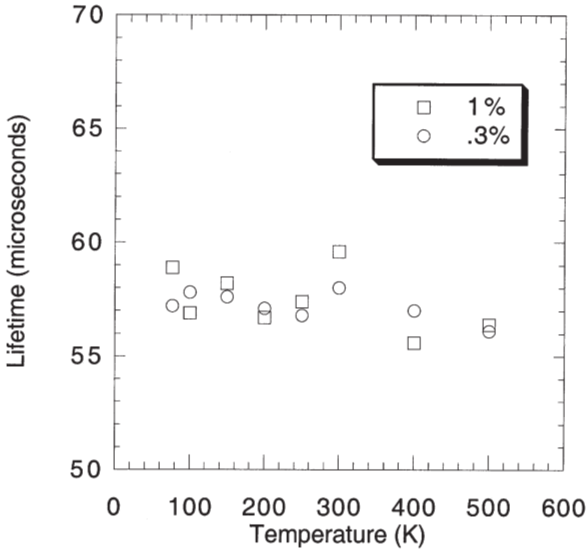

Fig. 6 Lifetime of the $^3P_0$ level of BaY_2F_8:Pr^{3+} vs temperature. λ_{exc}=480 nm (dye laser), λ_{em}=609 nm

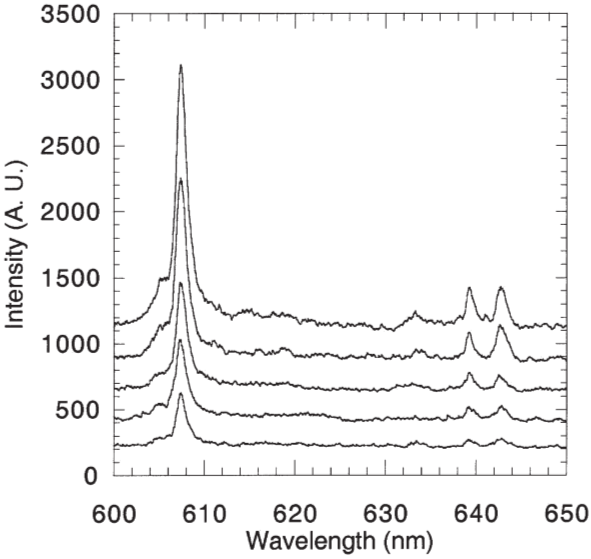

Fig. 7 Time-resolved emission spectra of $BaY_2F_8:Pr^{3+}$ in the spectral region 600 to 650 nm. λ_{exc}=480 nm (dye laser)

ifolds. Once again, these were taken at room temperature with excitation at 480 nm. In all these spectra we see the intensity of fluorescence decrease with time with no sign of any energy transfer mechanisms.

Moving on to the response of the $^1D_2$ manifold to pulsed excitation we find that, similar to the $^3P_0$ level, the lifetime of the $^1D_2$ manifold appears to be essentially temperature independent for both samples. The measured lifetime was approximately 250 μs. The lifetime vs temperature graph for both samples is shown in Fig. 8. The samples were once again excited with the dye laser, this time using

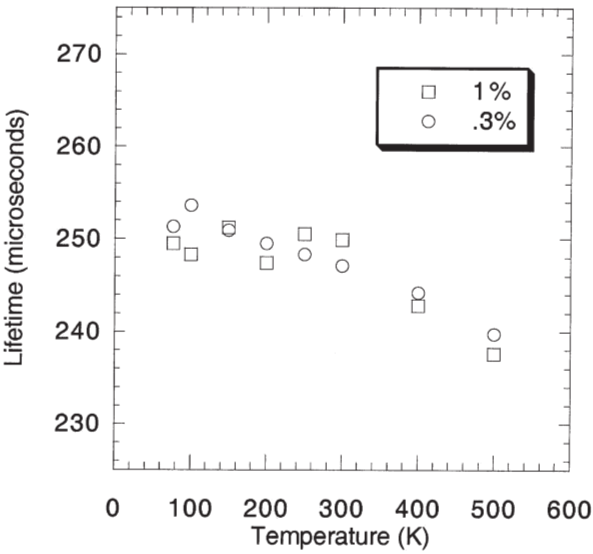

Fig. 8 Lifetime of the $^1D_2$ level of $BaY_2F_8:Pr^{3+}$ vs temperature. λ_{exc}=589 nm (dye laser), λ_{em}=597 nm

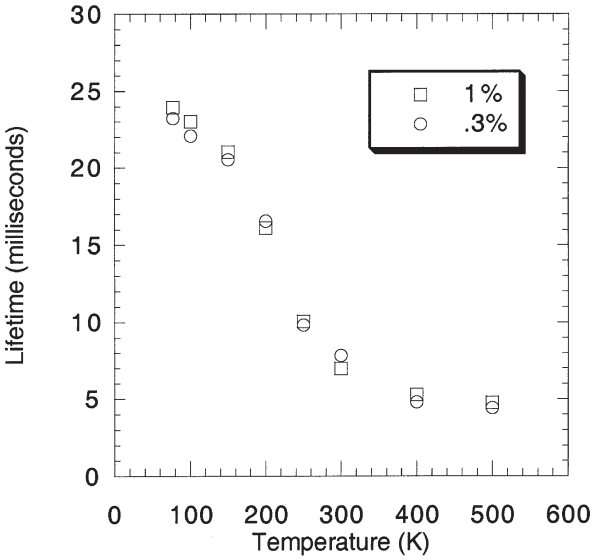

Fig. 9 Lifetime of the $^3F_3$ level of $BaY_2F_8:Pr^{3+}$ vs temperature. λ_{exc}=480 nm (dye laser), λ_{em}=1,580 nm

Coumarin 600 and a lasing wavelength of 589 nm. Emission was monitored at 597 nm. Again, the fact that the lifetime of the $^1D_2$ level is independent of temperature is not surprising. Here, the energy difference between this level (the $^1D_2$) and the next lower level (the $^1G_4$) is 6000 cm^{-1}, even greater than the previous case. Again, multiphonon processes bridging this gap are very improbable.

The other level to decay radiatively is the $^3F_3$ level. Emission was seen originating from this level and terminating on the $^3H_4$ ground state. Unlike the previous cases, the lifetime of the $^3F_3$ level shows a strong temperature dependence. Excitation in this case was again at 480 nm using the dye laser and Coumarin 480. This excited the $^3P_0$ level, which then decayed through various channels to the $^3F_3$ level. Emission was monitored at 1580 nm. The lifetime vs temperature graph for both samples is given in Fig. 9. We see that the lifetime varies from 23 ms at 77 K to about 5 ms at 500 K.

3.4 Thermal Effects on Spectral Lines

We investigated the temperature dependence of the linewidth and position of several radiative transitions. For these studies we chose the most intense lines in the $^3P_0 \rightarrow {}^3H_4$, $^3H_6$, $^3F_4$, and $^1D_2 \rightarrow {}^3H_4$ transitions. We report in Figs. 10 and 11 on the temperature dependence of width and position of a $^3P_0 \rightarrow {}^3H_6$ line and in Figs. 12 and 13 on the temperature dependence of similar parameters of a $^1D_2 \rightarrow {}^3H_4$ line.

We fitted the experimental data for all the lines by assuming that the thermal width is mainly determined by the Raman scattering of phonons [11]. In such a model, two adjustable parameters are used: α, a coefficient that gives a measure of the coupling of the ion with the phonon spectrum, and T_D, the Debye temperature. These parameters for all the lines examined are reported in Table 2.

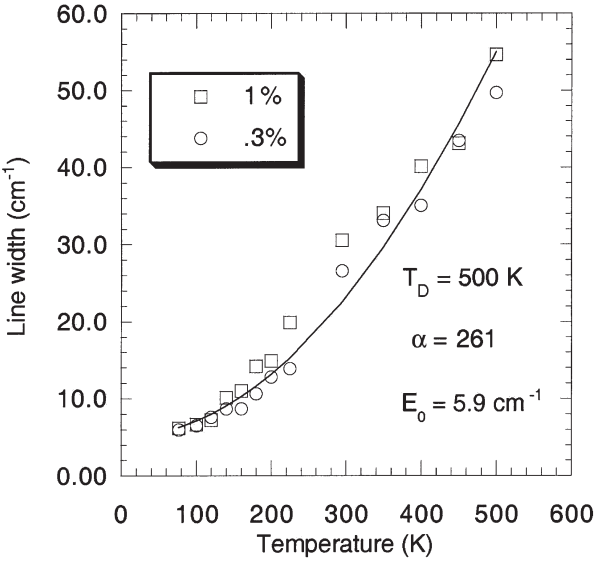

Fig. 10 Width of a $^3P_0 \rightarrow {}^3H_6$ line of $BaY_2F_8:Pr^{3+}$ in the temperature range 77 to 600 K. λ_{exc}=457.9 nm (argon laser)

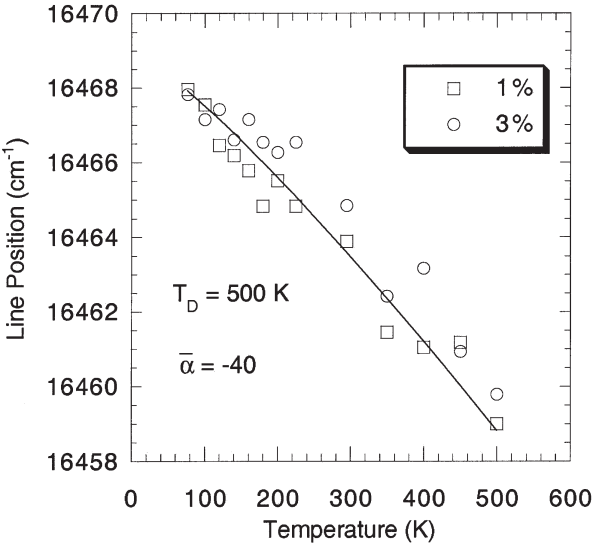

Fig. 11 Position of a $^3P_0 \rightarrow {}^3H_6$ line of $BaY_2F_8:Pr^{3+}$ in the temperature range 77 to 600 K. λ_{exc}=457.9 nm (argon laser)

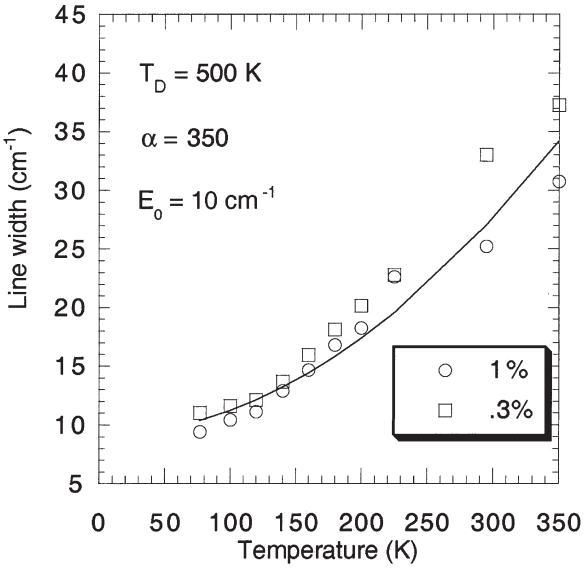

Fig. 12 Width of a $^1D_2 \rightarrow {}^3H_4$ line of $BaY_2F_8:Pr^{3+}$ in the temperature range 77 to 600 K. λ_{exc}=580 nm (dye laser)

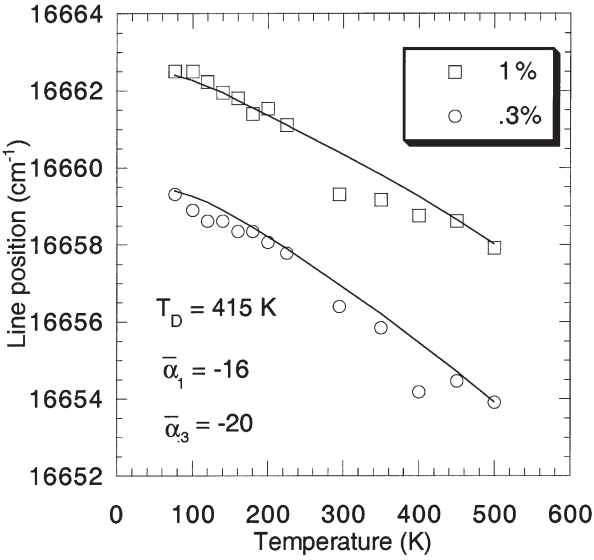

Fig. 13 Position of a $^1D_2 \rightarrow {}^3H_4$ line of $BaY_2F_8:Pr^{3+}$ in the temperature range 77 to 600 K. λ_{exc}=580 nm (dye laser)

Table 2 Linewidth parameters

Transition	E_0 (cm^{-1})	α (cm^{-1})	T_D (K)
$^3P_0 \rightarrow {}^3H_4$	13.5	195	500
$^3P_0 \rightarrow {}^3H_6$	5.9	261	500
$^3P_0 \rightarrow {}^3F_4$	10.5	150	500
$^1D_2 \rightarrow {}^3H_4$	10	350	500

Table 3 Lineshift parameters

Transition	$\bar{\alpha}$ (cm^{-1})	T_D (K)
$^3P_0 \rightarrow {}^3H_4$	45	500
$^3P_0 \rightarrow {}^3H_6$	–40	500
$^3P_0 \rightarrow {}^3F_4$	–11	415
$^1D_2 \rightarrow {}^3H_4$	–16, –20	415

We also fitted the thermal change of the position of each line by assuming a mechanism by which the ion emits and re-absorbs virtual phonons [11]. In such a model, again two adjustable parameters are used: $\bar{\alpha}$, different from α above, a coefficient that depends on the coupling of the ion with the phonon system, and T_D, the Debye temperature. We should note that, while α is intrinsically positive, $\bar{\alpha}$ may be positive or negative, as shown in Table 3 where we report on the thermal shifts of all the lines examined.

Examining first the line width vs temperature data, we found that a Debye temperature of 500 K characterizes all four transitions. This is very close to the reported cutoff of the phonon spectra of barium yttrium fluoride (415 cm^{-1} or about 600 K). Values for α ranged from 150 to 350. All transitions had a residual line width of about 10 cm^{-1} (5.9 cm^{-1} to 13.5 cm^{-1}). Also, the agreement between theory and experiment is very good, as can be seen from the figures.

Looking next at the position vs temperature data, we found that there is a thermal "blue shift" for the transition $^3P_0 \rightarrow {}^3H_4$ in both samples. This phenomenon has been reported previously for praseodymium in other hosts [12]. The emissions from the $^3P_0$ level to the $^3H_6$ and $^3F_4$ levels, on the other hand, show a thermal red shift. Similarly, the $^1D_2 \rightarrow {}^3H_4$ emission line shows a red shift with increasing temperatures, with the 1% sample showing a somewhat greater shift.

Numerically, we find that a Debye temperature of 500 K gives the best fit for the $^3P_0 \rightarrow {}^3H_4$ line position vs temperature data. Here, as noted previously, we have a "blue shift" with increasing temperature and a value of 45 for $\bar{\alpha}$. Likewise, the line position vs temperature data for the $^3P_0 \rightarrow {}^3H_6$ transition is best represented by a Debye temperature of 500 K, but with an $\bar{\alpha}$ value of –40. The line position vs temperature data for the other two transitions, $^3P_0 \rightarrow {}^3F_4$ and $^1D_2 \rightarrow {}^3H_4$, are best characterized by a Debye temperature of 415 K, much less than the 415 cm^{-1} (approximately 600 K) given as the phonon cutoff energy. The amount of shift, affected by $\bar{\alpha}$ is also smaller for these transitions, with values ranging from –11 to

–20. Also, the line position of the $^1D_2 \rightarrow {}^3H_4$ transition shows a difference with concentration of about 3 cm^{-1} at all temperatures with the 1% sample having the higher energy.

4 Conclusions

We have conducted a detailed investigation of the absorption and emission properties of the Pr^{3+} ion in BaY_2F_8. We now list our conclusions:

1. We have identified the levels responsible for the spectroscopic properties of this system with the three levels $^3P_0$, $^1D_2$, and $^3F_3$ mainly responsible for the emission properties.
2. The lifetimes of the levels $^3P_0$ and $^1D_2$ were found to be essentially independent of temperature and not affected by the variation of Pr^{3+} concentration (0.3% or 1%).
3. In accordance with point 2 above, nonradiative decay processes do not affect the lifetimes of $^3P_0$ and $^1D_2$, and their values should be considered due entirely to radiative processes.
4. The lifetime of the $^3F_3$ level was found to be dependent on temperature, on account of the smaller energy gap between the $^3F_3$ level and the next lower level, $^3F_2$.
5. In order to observe the luminescence originating in the $^3P_0$ level, the system had to be excited in the spectral region above $^3P_0$ where the $^3P_1$, $^1I_6$, and $^3P_2$ levels reside. From these levels the excitation quickly reached $^3P_0$. Under these conditions of excitation, no luminescence originating from the $^1D_2$ level is observed.
6. Luminescence originating from the $^3P_1$ level was observed at 300 K, but not at 77 K, giving additional proof of the thermalization of the levels above $^3P_0$ with the $^3P_0$ level.
7. In order to observe the luminescence originating in the $^1D_2$ level, the system had to be excited in the same level. Under these conditions of excitation, no luminescence originating in the $^3F_3$ level was observed.
8. For the excitation of the $^3F_3$ level, we had to rely on the radiative transitions $^3P_0 \rightarrow {}^3F_4$ and $^3P_0 \rightarrow {}^3F_3$, which populate the $^3F_3$ level, following the laser excitation of level $^3P_0$.
9. The thermal dependence of the widths and positions of the most prominent spectral lines were adequately explained by using a simple model which postulates nonlinear interaction between the optically active ion and the phonons distributed according to a Debye law.
10. The Debye temperature used to fit the thermal dependence of the spectral line parameters was 500 K, corresponding to a phonon cutoff at ~330 cm^{-1}. It should be interesting to investigate the effective phonon spectrum by using the method outlined in Sect. 2.2.
11. The investigation of BaY_2F_8:Pr^{3+} has brought to our attention the interesting spectral features of the Pr^{3+} ion in this system, and may contribute to validate the renewed interest in this laser ion.

Acknowledgements The authors feel honored to contribute this work to the book dedicated to the memory of Professor Christian Jørgensen. In particular, they are very pleased by the fact that this work illustrates a representative example of the spectroscopy of rare earth ions, a subject to which Jørgensen made many important and learned contributions. They would also like to acknowledge the benefit of discussions about the spectral characteristics of the praseodymium ion with Dr. Norman Barnes of NASA Langley Research Center and Dr. Brian Walsh and Mr. Yueli Chen of Boston College, and the partial sponsorship of this research by the National Aeronautics and Space Administration under Research Grant NAG-01–019. They would also like to thank Prof. A. Kaminskii for providing them with the crystals used in this spectroscopic investigation.

7 References

1. Kaminskii AA (1996) Crystalline lasers. CRC Press, Boca Raton
2. Chivian JS, Case WE, Eden, DD (1979) Appl Phys Lett 35:124
3. Koch ME, Kueny AW, Case WE (1990) Appl Phys Lett 56:1083
4. Piper WW, deLuca JA, Ham FS (1974) J Lumin 8:344
5. Kaminskii AA, Sarkisov SE (1986) Phys Stat Sol A97:K163
6. Reisfeld R, Jørgensen C K (1977) Lasers and excited states of rare earths. Springer, Berlin Heidelberg New York
7. Moune OK, Faucher MD, Edelstein N (2002) J Lumin 96:51
8. Bowlby BE, Di Bartolo B (2002) J Lumin 100:131
9. Antipenko BM (1984) Opt Spectrosc (USSR) 56:72
10. Garapon C, Malinowski M, Joubert MF, Kaminskii AA, Jacquier B (1994) J Phys IV 4:C4–349
11. Di Bartolo B (1968) Optical interactions in solids. Wiley, New York
12. Raspa N (1992) PhD Thesis, Concordia University, Montreal, Quebec, Canada

Supplementary Material

Christian Klixbüll Jørgensen

1931-2001

PUBLICATION LIST [1]

Books

1. "Energy Levels of Complexes and Gaseous Ions" – *Copenhagen, Gjellerup* (1957) 56 p.
2. "Absorption Spectra and Chemical Bonding in Complexes" – *Oxford, Pergamon Press* (1962) 355 p. (Second edition 1964)
3. "Orbitals in Atoms and Molecules" – *London, Academic Press* (1962) 162 p.
4. "Inorganic Complexes" – *London, Academic Press* (1963) 220 p.
5. "Inorganic Complexes" *translated into Japanese* – *Tokyo, Shuppan Kyoritsu* (1970) 261 p.
6. "Oxidation Numbers and Oxidation States" – *Berlin, Springer Verlag* (1969) 291 p.
7. "Modern Aspects of Ligand Field Theory" – *Amsterdam, North-Holland* (1971) 538 p.
8. "Lasers and Excited States of Rare Earths" (with R. Reisfeld) – *Springer, Berlin* (1977) 226 p.

Articles

9. *Consecutive Formation of Aquo Metallic Ions in Alcoholic Solution (with J. Bjerrum).*
   Acta Chem. Scand., Copenhagen, 7 (1953) p. 951-955.
10. *Aquo Ion Formation II. The First Transition Group in Ethanol.*
    Acta Chem. Scand., Copenhagen, 8 (1954) p. 175-191.
11. *Studies of Absorption Spectra I. Results of Calculations on the Spectra and Configuration of Copper(II) Ions (with J. Bjerrum and C.J. Ballhausen).*
    Acta Chem. Scand., Copenhagen, 8 (1954) p. 1275-1289.
12. *Studies of Absorption Spectra III. Absorption Bands as Gaussian Error Curves.*
    Acta Chem. Scand., Copenhagen, 8 (1954) p. 1495-1501.
13. *Studies of Absorption Spectra IV. Some New Transition Group Bands of Low Intensity.*
    Acta Chem. Scand., Copenhagen, 8 (1954) p. 1502-1512.
14. *Studies of Absorption Spectra VI. Actinide Ions with two 5f-Electrons.*
    Mat. fys. Medd. Dan. Vid. Selskab, Copenhagen, 29, No 7 (1955) 21 p.
15. *Studies of Absorption Spectra VII. Systems with Three and more f-Electrons.*
    Mat. fys. Medd. Dan. Vid. Selskab, Copenhagen, 29, No 11 (1955) 29 p.
16. *Studies of Absorption Spectra VIII. Three and more d-Electrons in Cubic Crystal Fields.*
    Acta Chem. Scand., Copenhagen, 9 (1955) p. 116-121.
17. *Crystal Field Stabilization of First Transition Group Complexes (with J. Bjerrum).*
    Acta Chem. Scand., Copenhagen, 9 (1955) p. 180-182.
18. *Studies of Absorption Spectra IX. The Spectra of Cobalt(II) Complexes (with C.J. Ballhausen).*
    Acta Chem. Scand., Copenhagen, 9 (1955) p. 397-404.
19. *Studies of Absorption Spectra X. d-Electrons in Crystal Fields of Different Symmetries (with C.J. Ballhausen).*
    Mat. fys. Medd. Dan. Vid. Selskab., Copenhagen, 29, No 14 (1955) p 32.

[1] *The references were provided by Alan F. Williams, Geneva.*

20. *Some Problems of Intensity of Absorption Bands and Chemical Bonding.*
    Acta Chem. Scand., Copenhagen, 9 (1955) p. 405-411.
21. *Absorption Spectra of Lanthanide and Actinide Ions.*
    J. Chem. Phys., New York, 23 (1955) p. 399-400.
22. *Formation of Aquo Ions (with J. Bjerrum).*
    Nature, London, 175 (1955) p. 426-427.
23. *The States ^1I Trivalent Praseodymium and Thulium.*
    Acta Chem. Scand., Copenhagen, 9 (1955) p. 540-541.
24. *Vibrational Structure of a Spin-forbidden Band of Hexachlororhenate(IV).*
    Acta Chem. Scand., Copenhagen, 9 (1955) p. 710-712.
25. *4s-Electrons in the First Transition Group Complexes.*
    Acta Chem. Scand., Copenhagen, 9 (1955) p. 717-719.
26. *Effective Quantum Numbers in d- and f-Shells.*
    J. Inorg. Nucl. Chem., Oxford, 1 (1955) p. 301-308.
27. *Comparative Crystal Field Studies of some Ligands and the Lowest Singlet State of Paramagnetic Nickel(II) Complexes.*
    Acta Chem. Scand., Copenhagen, 9 (1955) p. 1362-1377.
28. *Crystal Field Stabilization and Tendency towards Complex Formation of First Transition Group Elements (with J. Bjerrum).*
    Rec. trav. chim. Pays-Bas, La Haye, 75 (1956) p. 658-664.
29. *Complexes of the 4d- and 5d-Groups I. Crystal Field Spectra of Rhodium(III) and Iridium(III).*
    Acta Chem. Scand., Copenhagen, 10 (1956) p. 500-517.
30. *Complexes of the 4d- and 5d-Groups 11. Crystal Field and Electron Transfer Spectra of Ruthenium(II) and (III), Iridium(IV) and Platinum(IV).*
    Acta Chem. Scand., Copenhagen, 10 (1956) p. 518-534.
31. *Absorption Spectra of Complexes with Unfilled d-Shells.*
    Institut International de Chimie Solvay, Bruxelles (1956) p. 355-385.
32. *Variation of the Parameters of Electrostatic Interaction F^k derived from Absorption Spectra of Lanthanide Complexes.*
    Mat. fys. Medd. Dan. Vid. Selskab, Copenhagen, 30, No 22 (1956) p. 38.
33. *Comparative Crystal Field Studies 11. Nickel(II) and Copper(II) Complexes with Polydentate Ligands and the Behaviour of the Residual Places for Coordination.*
    Acta Chem. Scand., Copenhagen, 10 (1956) p. 887-910.
34. *The Electrostatic Model for Calculation of the Ligand Field Parameter of Octahedral Complexes (with O. Bostrup).*
    Acta Chem. Scand., Copenhagen, 10 (1956) p. 1501-1503.
35. *Absorption Spectra of Red Uranium(III) Chloro Complexes in Strong Hydrochloric Acid.*
    Acta Chem. Scand., Copenhagen, 10 (1956) p. 1503-1505.
36. *The Hump of Ionization Potentials at Half-filled Shells and the Influence of Spinpairing Energy on Standard Oxidation Potentials.*
    Acta Chem. Scand., Copenhagen, 10 (1956) p. 1505-1507.
37. *Comparative Ligand Field Studies III. The Decrease of the Integrals F^k for Manganese(II) Complexes as Evidence for Partly Covalent Bonding.*
    Acta Chem. Scand., Copenhagen, 11 (1957) p. 53-72.
38. *Comparative Ligand Field Studies IV. Vanadium(IV), Titanium(III), Molybdenum(V) and other Systems with one d-Electron.*
    Acta Chem. Scand., Copenhagen, 11 (1957) p. 73-85.
39. *Complexes of the 4d- and 5d- Groups III. Absorption Spectra of Marcel Delepine's Rhodium(III) and Iridium(III) Complexes.*
    Acta Chem. Scand., Copenhagen, 11 (1957) p. 151-165.
40. *Complexes of the 4d and 5d-Groups IV. Electron Transfer Bands with Special Application to M. Delepine's Complexes and a Transition from Iridium(III) to Pyridine, with some Remarks about Intermediate Coupling in Halide Complexes and the Uranyl Ion.*
    Acta Chem. Scand., Copenhagen, 11 (1957) p. 166-178.
41. *Elektronskaller og Molekylorbitaler.*
    Kemisk Manedsblad, Copenhagen, 38 (1957) p. 35-40.

42. *The Equilibrium Between Yellow and Blue Nickel(II) Triethylenetetramine Ions in Strong Salt Solutions.*
    Acta Chem. Scand., Copenhagen, 11 (1957) p. 399-400.
43. *Screening Constants Derived from Atomic Term Distances as Function of the Ionic Charge.*
    J. Inorg. Nucl. Chem., Oxford, 4 (1957) p. 369-371.
44. *Absorption Spectra of Dysprosium(III), Holmium(III), and Erbium(III) Aquo Ions.*
    Acta Chem. Scand., Copenhagen, 11 (1957) p. 981-989.
45. *The Decrease of F^k Integrals, Tetragonal Perturbations and Effects of Average Environment in the Reflection Spectra of Nickel(II) Complexes (with O. Bostrup).*
    Acta Chem. Scand., Copenhagen, 11 (1957) p. 1223-1231.
46. *5f-and 6d-Orbitals in Actinide Compounds.*
    16. International Congress of Pure and Applied Chemistry in Paris 1957. London, Buttersworth (1957) p. 313-318.
47. *The Nephelauxetic Series of Ligands Corresponding to Increasing Tendency of Partly Covalent Bonding (with C.E. Schäffer).*
    J. Inorg. Nucl. Chem., Oxford, 8 (1958) p.143-148.
48. *The Interelectronic Repulsion Integrals and the Purity of Molecular Orbital Configurations, as Derived from the Absorption Spectra of Transition Group Complexes.*
    Acta Chem. Scand., Copenhagen, 12 (1958) p. 903-918.
49. *Ligand Field Bands of Four-coordinated Paramagnetic Nickel(II) Complexes.*
    Mol. Phys., London, 1 (1958) p. 410-412.
50. *Ligand Field Spectrum of Vanadium(II) Hexaquo Ions.*
    Acta Chem. Scand., Copenhagen, 12 (1958) p. 1537-1538.
51. *Ligand Field Bands of Hexafluoro Manganate(IV) and Predictions of Band Positions of Transition Group Fluorides.*
    Acta Chem. Scand., Copenhagen, 12 (1958) p. 1539-1541.
52. *The Interelectronic Repulsion and Partly Covalent Bonding in Transition-Group Complexes.*
    Faraday Soc. Discuss., London, 26 (1958) p. 110-115.
53. *M. Delepine's Nitrido-Iridium(III,IV) Sulphate Complexes with Nitrogen Bound to Three Iridium Atoms. Acta Chem. Scand., Copenhagen, 13 (1959) 196-198 p.*
54. *Absorption Spectra of Actinide Compounds.*
    Mol. Phys, London, 2 (1959) 96-108 p.
55. *Electron Transfer Spectra of Hexahalide Complexes.*
    Mol. Phys., London, 2 (1959) p. 309-332.
56. *Les électrons d et f dans les complexes des groupes de transition.*
    J. Chimie physique, Paris, 56 (1959) p. 889-896.
57. *New Interpretations of the Orbital Energy Differences in Hexafluorides.*
    Mol. Phys., London, 3 (1960) p. 201-202.
58. *Parameters α and β in the Spectra of the Iron Group (with R.E. Trees).*
    Phys. Rev., New York, 123 (1961) p. 1278-1280.
59. *Energy Levels and n Bonding in Polynuclear Complexes (with L.E. Orgel).*
    Mol. Phys., London, 4 (1961) p. 215-218.
60. *Electron Transfer Spectrum of Caesium Rhodium(IV) Hexachloride at Relatively Low Wavenumber.*
    Mol. Phys., London, 4 (1961) p. 231-233.
61. *Reflection Spectra of Alkali Metal, Thallium(I), Silver(I), Iridium(IV) Hexachlorides.*
    Mol. Phys., London, 4 (1961) p. 235-239.
62. *Relative Molecular Orbital Energies in Tetrahedral Complexes (with A. Carrington).*
    Mol. Phys., London, 4 (1961) p. 395-400.
63. *Chemical Bonding Inferred from Visible and Ultraviolet Absorption Spectra.*
    Solid State Phys., New York, 13 (1962) p. 375-462.
64. *Vibrational Structure and Solvent Effects on an Intra-subshell Transition of Osmium(IV) Hexachloro Ions.*
    Acta Chem. Scand., Copenhagen, 16 (1962) p. 793-798.
65. *Electron Transfer Spectra of Lanthanide Complexes.*
    Mol. Phys., London, 5 (1962) p. 271-277.

66. *Absorption Spectrum of Ruthenium(III) Diethyldithiophosphate.*
Acta Chem. Scand., Copenhagen, 16 (1962) p. 1048-1049.
67. *The Absorption Spectra and the Chemistry of the 4d and 5d Groups. Proceed. 7. Int. Conf. Coord. Chem., Stockholm (1962) p. 29-31.*
68. *Absorption Spectra of Chromium(III), Rhodium(III) and Iridium(III) Diethyldiselenophosphates. Mol. Phys., London, 5 (1962) p. 485-492.*
69. *Far Ultra-violet Absorption Bands of Osmium(IV), Iridium(IV), Platinum(IV) Hexahalides (with J.S. Brinen). Mol. Phys., London, 5 (1962) p. 535-536. J&B*
70. *Reflection Spectra and M.O. Configurations of Franz Hein's Nickel(II) «Aminine» Complexes.*
Z. anorg. Chem., Leipzig, 316 (1962) p. 12-14.
71. *Relevant and Irrelevant Symmetry Components. Are the Bloch Energy Bands the Best One-Electron Functions?*
Physica status solidi, Berlin, 2 (1962) p. 1146-1150.
72. *Absorption Spectra of Cobalt (II) and Cobalt(III) Diethyldithiophosphates.*
Acta Chem. Scand., Copenhagen, 16 (1962) p. 2017-2024.
73. *New Theory for the Electron Transfer Spectra of Acetylacetonate Complexes.*
Acta Chem. Scand., Copenhagen, 16 (1962) p. 2406-2410.
74. *Absorption Spectra of Transition Group Complexes of Sulphur-containing Ligands.*
J. Inorg. Nucl. Chem., Oxford, 24 (1962) p. 1571-1585.
75. *Solvent Effects on the Absorption Bands of Iridium(IV) Hexabromide and Other 5d-hexahalides.*
J. Inorg. Nucl. Chem., Oxford, 24 (1962) p. 1587-1594.
76. *The Nephelauxetic Series.*
Progress Inorg. Chem., New York, 4 (1962) p.73-124.
77. *Optical Electronegativities of 3d Group Central Ions.*
Mol. Phys., London, 6 (1963) p. 43-47.
78. *Spectrophotometric Study of Mixed Uranium(IV) Chloro-Bromo Complexes in Nitromethane.*
Acta Chem. Scand., Copenhagen, 17 (1963) p. 251-258.
79. *Spectroscopy of Transition-Group Complexes.*
Advances Chem. Phys., New York, 5 (1963) p. 33-146.
80. *Adducts of Nickel(II) Diethyldithiophosphate with Secondary Amines and Heterocyclic Diimines. Acta Chem. Scand., Copenhagen, 17 (1963) p. 533-535.*
81. *Über ein Modell zur Beschreibung kovalenter Komplexverbindungen (with H.H. Schmidtke).*
Z. physik. Chem., Frankfurt/Main, 38 (1963) p. 118-120.
82. *Reflection Spectra of Rhenium(IV), Osmium(IV) and Iridium(IV) Hexahalides.*
Acta Chem. Scand., Copenhagen, 17 (1963) p. 1034-1042.
83. *Absorption Spectra of Osmium(III), Osmium(IV) and Platinum(IV) Mixed Halide and Hexaiodide Complexes.*
Acta Chem. Scand., Copenhagen, 17 (1963) p. 1043-1048.
84. *Far Ultra-violet Absorption Spectra of Cerium(III) and Europium(III) Aqua Ions (with J.S. Brinen).*
Mol. Phys., London, 6 (1963) p. 629-631.
85. *Do the "Ligand Field" Parameters in Lanthanides Represent Weak Covalent Bonding? (with R. Pappalardo and H.H. Schmidtke).*
J. Chem. Phys., New York, 39 (1963) p. 1422-1430.
86. *Electron Transfer and 5f $\rightarrow$ 6d Transitions in Uranium(IV), Neptunium(IV), Plutonium(IV) Hexahalides (with J.L. Ryan).*
Mol. Phys., London, 7 (1963), p. 17-29.
87. *The Configurations of Yellow and Red Trichlorotris(diethylsulfide)iridium(III) (with G.B. Kauffman, J. Hwa-San Tsai and R.C. Fay).*
Inorg. Chem., Washington, 2 (1963) p. 1233-1238.
88. *Reflection Spectra of Lanthanides in Thorium(IV) Oxide and the Large Nephelauxetic Effect of Oxide Ligands or Vacancies (with R. Pappalardo and E. Rittershaus).*
Z. Naturforsch., Tübingen, 19a (1964) p. 424-433.
89. *Fluorescence Spectra of Europium(III) Phthalate and Naphthalate and of Samarium(III), Europium(III), Terbium(III) and Dysprosium(III) Dipyridyl Complexes (with S.P. Sinha and R. Pappalardo).*

Z. Naturforsch., Tübingen, 19a (1964) p. 434-439.

90. *MoO. Description of Diatomic Molecules Containing a Transition Group Atom. Mol. Phys., London, 7 (1964) p. 417-424.*
91. *Absorption Spectra of Uranium(IV) in Octahedral Coordination (with R. Pappalardo). Helv. Phys. Acta, Bâle, 37 (1964) p. 79-103.*
92. *Inorganic Chromophores. Experientia Suppl., Bâle, 9 (1964) p. 98-111.*
93. *Absorption Spectra, Energy Levels und Chemical Bonding in Transition Group Complexes. Quaderni Chimica de Ricerca Scientifica, Rome, No 1 (1964) p. 39-45.*
94. *Influence de l'opérateur biélectronique sur les transitions 2p→3d dans l'oxyde de nickel(II) (with C. Bonnelle). J. Chimie physique, Paris, 61 (1964) p. 826-829.*
95. *«Symbiotic» Ligands, Hard and Soft Central Atoms. Inorg. Chem., Washington, 3 (1964) p. 1201 -??*
96. *Optical Electronegativities. Proceed 8. Int. Conf. Coord. Chem., Vienna, Springer Verlag (1964) p. 67-71.*
97. *Electron Transfer Spectra of Lanthanides and 5f Group Complexes - How to Distinguish Outer-sphere, Anisotropic and Normal Anion Complexes. Proceed. Symposium Tihany 1964, Budapest, Akadimia Kiadó, (1965) p. 11-21.*
98. *Optiske Elektronegativiteter. Dansk Kemi, Copenhagen, 45 (1964) p. 113-119.*
99. *An Heuristic Estimate of Correlation Energies in Many-electron Atoms. Mol. Phys., London, 8 (1964) p. 191-193.*
100. *Hypersensitive Pseudoquadrupole Transitions in Lanthanides (with B.R. Judd). Mol. Phys., London, 8 (1964) p. 281-290.*
101. *A Classification of Categorical Propositions. Logique et Analyse, Louvain, 7 (1964) p. 233-256.*
102. *A simple Molecular Orbital Model of Transition-metal Halide Complexes (with P. Day). J. Chem. Soc., London (1964) p. 6226-6234.*
103. *Reflection Spectra of Lanthanides in Cubic Oxides Containing Titanium(IV), Zirconium(IV), Indium(III), Tin(IV), Cerium(IV) and Thallium(III) (with R. Pappalardo and E. Rittershaus). Z. Naturforsch., Tübingen, 20a (1965) p. 54-64.*
104. *Comparative Interpretation of Absorption Spectra of Technetium(IV) and Rhenium(IV) Hexahalides (with K. Schwochau). Z. Naturforsch., Tübingen, 20a (1965) 65-75.*
105. *Applications of Ligand-field Theory to Complexes. Advances Chem. Phys., New York, 8 (1965) p. 47-61.*
106. *L'effet néphélauxétique dans les sulfures des terres rares (with J. Flahaut and R. Pappalardo). J. Chimie physique, Paris, 62 (1965) p. 444-448.*
107. *Oxidationstrin og Oxidationstilstand. Dansk Kemi, Copenhagen, 46 (1965) p. 67-72.*
108. *Absorption Spectra and Optical Electronegativities of Cobalt(II) and Cobalt(lll) Phosphine Complexes (with K.A. Jensen). Acta Chem. Scand., Copenhagen, 19 (1965) p. 451-454.*
109. *Chromophores, Partly Filled Shells and Positive Spin Quantum Number. Z. naturwiss.-mediz. Grundlagenforsch., Bâle, 2 (1965) p. 248-258.*
110. *The Angular Overlap Model, an Attempt to Revive the Ligand Field Approaches (with C.E. Schäffer). Mol. Phys., London, 9 (1965) p. 401-412.*
111. *Energy Levels of Orthoaxial Chromophores und the Interrelation Between Cubic Parent Configurations (with C.E. Schäffer). Mat. fys. Medd. Dan. Vid. Selskab, Copenhagen, 34, No 13 (1965) 20 p.*
112. *Molecular Orbital Treatment of Diatomic and Simple Polyatomic Molecules und Complex Ions. VIII Corso Estivo di Chimica. Fondazione Donegani, Accademia Nazionale dei Lincei, Roma (1965) p. 63-110.*

113. *Orbitales moléculaires dans les chromophores minéraux et paramètres angulaires Ξ de liaison covalente.*
J. Physique, Paris, 26 (1965) p. 825-840.

114. *Difference between the Four Halide Ligands, and Discussion Remarks about Trigonal-Bipyramidal Complexes, on Oxidation States, and on Diagonal Elements of One-Electron Energy.*
Coord. Chem. Rev., Amsterdam, 1 (1966) p. 164-178.

115. *Symmetry and Chemical Bonding in Copper-Containing Chromophores.*
Biochemistry of Copper, Academic Press, New York (1966) p. 1-14.

116. *Les elements 4f and 5f (with M. Haissinsky).*
J. Chimie physique, Paris, 63 (1966) p. 1135-1138.

117. *Recent Progress in Ligand Field Theory.*
Structure and Bonding, Berlin, 1 (1966) p. 3-31.

118. *Electric Polarizability, Innocent Ligands and Spectroscopic Oxidation States.*
Structure and Bonding, Berlin, 1 (1966) p. 234-248.

119. *The One-Electron Approximation; Epistemological, Spectroscopic and Chemical Comments.*
Quantum Theory of Atoms, Molecules and the Solid State, New York, Academic Press (1966) p. 307-318.

120. *Absorption Spectra of Octahedral Lanthanide Hexahalides (with J.I. Ryan).*
J. Phys. Chem., Washington, 70 (1966) p. 2845-2857.

121. *Fractional Charges, Integral Oxidation States und the Nephelauxetic Effect in the Five Transition Groups.*
Helv. Chim. Acta, Fasciculus extraordinarius Alfred Werner, Bâle (1967) p. 131-146.

122. *Kinetic Energy as an Essential Constituent of Non-Diagonal Elements and Spectrochemical Parameters.*
Chemical Physics Letters, Amsterdam, 1 (1967) p. 11-13.

123. *Spectrophotometric Study of Ytterbium(III) Cyclopentadienide at Liquid-Helium Temperature (with R. Pappalardo).*
J. Chem. Phys., New York, 46 (1967) p. 632-638.

124. *Ligandfeltparametre bestar mest af kinetisk energi, de diagonale elemenler indeholder Madelung-polentialer, og Kimball-modellen er urimelig.*
Dansk Kemi, Copenhagen, 48 (1967) p. 33-38.

125. *Invariance and Distortions of Octahedral Chromophores.*
Advances in Chemistry Series, Washington, 62 (1967) p. 161-177.

126. *Covalence and Ionicité.*
J. Chimie physique, Paris, 64 (1967) p. 245.

127. *Powder-Diagram and Spectroscopic Studies of Mixed Oxides of Lanthanides and Quadrivalent Metals (with E. Rittershaus).*
Mat. fys. Medd. Dan. Vid. Selskab, Copenhagen, 35, No 15 (1967) 37 p.

128. *Influence of Madelung (Interatomic Coulomb) Energy on Wolfsberg-Helmholz Calculations (with S.M. Horner, W.E. Hatfield and S.Y. Tyree). Int. J. Quantum Chem., New York, 1 (1967) p. 191-215.*

129. *Modern Developments of the Theory of Complex Compounds.*
Notas de Fisica, Rio de Janeiro, 12 (1967) p. 223-225.

130. *Interpretation of Electron Transfer Spectra of Iridium(IV) and Osmium(IV) Mixed Chloro-Bromo Complexes (with W. Preetz).*
Z. Naturforsch., Tübingen, 22a (1967) p. 945-954.

131. *The Extensional Classification of Categorical Propositions and Trivalent Logic.*
Logique et Analyse, Louvain, 10 (1967) p. 141-156.

132. *Angular Overlap Treatment of Erbium(III) in Xenotime and Yttrium Orthovanadate (with D. Kuse).*
Chemical Physics Letters, Amsterdam, 1 (1967) p. 314-316.

133. *Relations between Softness, Covalent Bonding, Ionicity and Electric Polarizability.*
Structure and Bonding, Berlin, 3 (1967) p. 106-115.

134. *Electronic Structure and Molecular Orbital Treatment of Halogen and Noble Gas Complexes in Positive, Negative and Undefined Oxidation States. Halogen Chemistry, London, Academic Press, 1 (1967) p. 265-401.*

135. *Absorption Spectra of Post-transition Group Halide Complexes (with R.A. Walton and R.W. Matthews). Inorg. Chim. Acta, Padova, 1 (1967) p. 355-359.*
136. *Might the Difference between Schrödinger and Ruedenberg's Local Contributions to the Kinetic Energy Represent Elastic Deformations of the Electron?*
Int. J. Quantum Chem., New York, 2 (1968) p. 49-54.
137. *Chemie der Komplexe von Liganden mit schweren Donoratomen II. Mössbauer-Untersuchung der Eisenkomplexe von Di-isopropyl-dithiophosphat (with L. Korecz and K. Burger).*
Helv. Chim. Acta, Bâle, 51 (1968) p. 211-213.
138. *Electron Transfer Bands of Hexachloro-Iridate(IV) at 20 K (with P. Day).*
Chemical Physics Letters, Amsterdam, 1 (1968) p. 507-508.
139. *Le tableau périodique de Mendeleeff. Point de vue mathématique, spectroscopique et chimique.*
Bull. Soc. Vaudoise Sciences Naturelles, Lausanne, 70 (1968) p. 103.
140. *Formation Constants and Absorption Spectra of Palladium(II) Complexes.*
Proceed. 11. Int. Conf. Coord. Chem., Amsterdam, Elsevier (1968) p. 547-549.
141. *Die Molrefraktion von Aquo-Ionen metallischer Elemente und die Auswertung von Lichtbrechungs-messungen in der anorganischen Chemie (with J.J. Salzmann).*
Helv. Chim. Acta, Bâle, 51 (1968) p. 1276-1293.
142. *Palladium(II) Complexes I. Spectra and Formation Constants of Ammonia and Ethylenediamine Complexes (with Lene Rasmussen).*
Acta Chem. Scand., Copenhagen, 22 (1968) p. 2313-2323.
143. *Neptunium(VII), Nobelium(II), 126 (IV) and other Unexpected Oxidation States of Trans-uranium Elements.*
Chemical Physics Letters, Amsterdam, 2 (1968) p. 549-550.
144. *La répulsion interélectronic dans la chimie.*
Bull. Soc. Chim. France, Paris (1968) p. 4745-4749.
145. *Spectra and Electronic Structure of Complexes with Sulphur-containing Ligands.*
Inorg. Chim. Acta Reviews, Padoue, 2 (1968) p. 65-88.
146. *Origine de l'additivité approximative des polarisabilités électriques en chimie minérale.*
Rev. Chimie minérale, Paris, 6 (1969) p. 183-191.
147. *Vacuo Ultraviolet Spectra of Permanganate, Pertechnetate and Perrhenate (with P. Mullen and K. Schwochau).*
Chemical Physics Letters, Amsterdam, 3 (1969) p.49-51.
148. *Les déviations de trivalence dans les groupes f et le paramètre (E-A).*
Colloques CNRS No 180 à Paris et Grenoble: Les éléments des terres rares, Paris, 1 (1969) p. 353-358.
149. *Le couplage de spin intra-atomique et l'extrême contra ire des spins distants. Colloques CNRS, Paris et Grenoble, Mai 1969, Les éléments des terres rares, Paris, 2 (1969) p. 181-186.*
150. *Stereochemistry and the Choice between Alternative Descriptions of Oxidation States.*
Chem. Phys Letters, Amsterdam, 3 (1969) p. 380-382.
151. *Valence-shell Expansion Studied by Ultra-violet Spectroscopy.*
Structure and Bonding, Berlin, 6 (1969) p. 94-115.
152. *La chimie et les spectres du palladium(II).*
J. Chimie physique, Paris, 66 (1969) p. 1007.
153. *Propriétés chimiques probables de l'élément 114 (with M. Haissinsky).*
Radiochem. Radioanal. Letters, Lausanne, 1 (1969) p. 181-184.
154. *The Connections between Electron Configuration and the Variations of the Oxidation State.*
Chimia, Aarau, 23 (1969) p. 292-298.
155. *Absorption Spectrum of Manganese(II) Diethylenetriamine Complexes.*
Inorg. Chim. Acta, Padova, 3 (1969) p. 313-314.
156. *Palladium(II) Complexes II. Diethylenetriamine and Additional Ligands, Protons and Silver(I) Ions (with Lene Rasmussen).*
Inorg. Chim. Acta, Padova, 3 (1969) p. 543-546.
157. *Palladium(II) Complexes III. Experiments with Pyridine and Phenanthroline (with Lene Rasmussen). Inorg. Chim. Acta, Padoue, 3 (1969) p. 547-551.*
158. *Les orbitales d et f adaptées à toutes les autres orbitales occupées.*

Colloque CNRS No 191 à Paris, octobre 1969: La nature et les propriétés des liaisons de coordination (1969) p. 81-88.

159. *Un nouveau type de stabilisation du «champ des ligandes» dans les complexes linéaires du cuivre(I), de l'argent(I) et de l'or(I) (with J. Pouradier).*
J. Chimie physique, Paris, 67 (1970) p. 124-127.

160. *Angular Overlap Treatment and Electron Spin Resonance of Titanium(III) in Anatase (with P. Meriaudeau and M. Che).*
Chemical Physics Letters, Amsterdam, 5 (1970) p.131-133.

161. *More or Less Quadratic Diethylenetriamine Complexes of Palladium(II) (with H.H. Schmidtke).*
Chemical Physics Letters, Amsterdam, 5 (1970) p. 202-204.

162. *Organic Selenium Compounds VIII. Electronic Spectra of Diselenocarbamate Complexes (with K.A. Jensen and V. Krishnan).*
Acta Chem. Scand., Copenhagen, 24 (1970) p. 743-745.

163. *Electron Transfer Bands of Binuclear Iron(II,III) Complexes Containing Two Cyanide Bridges (with G. Emschwiller).*
Chemical Physics Letters, Amsterdam, 5 (1970) p. 561-563.

164. *The «Tetrad Effect» of Peppard is a Variation of the Nephelauxetic Ratio in the Third Decimal.*
J. Inorg. Nucl. Chem., Oxford, 32 (1970) p. 3127-3128.

165. *Electron Transfer Spectra.*
Progress Inorg. Chem., New York, 12 (1970) p.101-158.

166. *Localized Transitions in Partly Filled Shells.*
Mem. Soc. Roy. Sciences de Liège, 20 (1970) p. 335-355.
And: Congrès et Colloques de l'Université de Liège, Vol. 57 (1971).

167. *Speculations on the Chemistry of Superheavy Elements such as Z = 164 (with R.A. Penneman and J.B. Mann).*
Chemical Physics Letters, Amsterdam, 8 (1971) p. 321-326.

168. *Breakdown of the Hybridization Theory and the Ligand Field Problem.*
Chimia, Aarau, 25 (1971) p. 109-114.

169. *High-resolution Visible Spectroscopy of Two Europium(III) Ethylenediaminetetra-acetates Differing in One Molecule of Ligated Water (with G. Geier).*
Chemical Physics Letters, Amsterdam, 9 (1971) p. 263-265.

170. *Photo-electron Spectrometry of Inorganic Solids.*
Chimia, Aarau, 25 (1971) p. 213-222.

171. *Electron Transfer Spectra of Osmium(IV) Mixed Chloro-Iodo and Bromo-Iodo Complexes (with W. Preetz and H. Homborg).*
Inorg. Chim. Acta, Padoue, 5 (1971) p. 223-230.

172. *Persistence of Atomic Orbitals in Complexes and Other Compounds.*
Accounts Chem. Res., Washington, 4 (1971) p. 307-315.

173. *A Chemical Model of the Latent Image in Silver Chloride and Bromide.*
Chemical Physics Letters, Amsterdam, 11 (1971) p. 387-388.

174. *Le déplacement chimique comme mesure du potentiel Hartree à la position du noyau.*
J. Physique, Paris, 32, colloque 4 (1971) p. 274-277.

175. *Der lose Zusammenhang zwischen Elektronenkonfiguration und chemischem Verhalten der Transurane.*
Angew. Chem., Weinheim, 83 (1971) p. 911.
Translated into English: Angew. Chem. Int. Ed., Weilheim, 10 (1971) p. 837.

176. *Photo-electron Spectra of Fluorides and the Influence of the Madelung Potential on Inner Shells (with H. Berthou and L. Balsenc).*
J. Fluorine Chem., Lausanne, 1 (1972) p. 327-336.

177. *Split Photo-electron Signals from the Unique Closed-shell Cation Lanthanum(III) (with H. Berthou).*
Chemical Physics Letters, Amsterdam, 13 (1972) p. 186-189.

178. *Chemical Effects on Inner Shells Studied by Photo-electron Spectrometry.*
Theoret. Chim. Acta, Berlin, 24 (1972) p. 241-250.

179. *Recent Developments in Photo-electron Spectra of Inorganic Compounds.*
Chimia, Aarau, 26 (1972) p. 252-254.

180. *X-ray and Photoelectron Spectroscopy for the Determination of 4f Energies in Rare Earths (with C. Bonnelle and R. Karnatak).*
Chemical Physics Letters, Amsterdam, 14 (1972) p.145-149.

181. *The Aquapentacyanoferrate(III) and its Dimerization Product Studied by Magnetic Circular Dichroism (with R. Gale and A.J. McCaffery).*
Chemical Physics Letters, Amsterdam, 15 (1972) p. 512-513.

182. *Photo-electron Spectra Induced by X-rays of Above 600 Non-metallic Compounds Containing 77 Elements (with H. Berthou).*
Mat. fys. Medd. Dan. Vid. Selskab, Copenhagen, 38, No 15 (1972) 93 p.

183. *Elektronenüberführungs-, Raman- und Photoelektronspektren sowie röntgenographische Untersuchungen von $Tl_2MO_2S_2$,Tl_2MOS_3 und Tl_2MS_4 (M=Mo,W) sowie Photoelektronenspektren zahlreicher Übergangsmetallverbindungen zum Vergleich (with A. Müller and E. Diemann).*
Z. anorg. Chem., 391 (1972) p. 38-53.

184. *Coordination Compounds with Organic Selenium-and Tellurium-containing Ligands (with K. A. Jensen). Organic Selenium Compounds (eds. D.L. Klayman and W.H.H. Günther), Wiley-Interscience, New York (1973) p.1017-1048.*

185. *The Loose Connection between Electron Configuration and the Chemical Behaviour of the Heavy Elements.*
Angew. Chem., Int. Ed., 12 (1973) p.12-19.

186. *Der lose Zusammenhang zwischen Elektronenkonfiguration und chemischem Verhalten der schweren Elemente (Transurane).*
Angew. Chem., 85 (1973) p.1-10.

187. *Measurements of Photo-electron Spectra and Charging Effects in Fluorides, Iodates and Oxides (with H. Berthou).*
J. Fluorite Chem., 2 (1973) p. 425-430.

188. *The Inner Mechanism of Rare Earths Elucidated by Photo-electron Spectra.*
Structure and Bonding, Berlin,13 (1973) p.199-253.

189. *Relative Intensities and Widths of X-ray Induced Photo-electron Signals from Different Shells in 72 Elements (with H. Berthou).*
J.C.S. Faraday Discuss., 54 (1973) p. 269-276.

190. *The Third Revolution in "Ligand Field" Theory – the Ionization Energy of the Partly Filled Shell is Sometimes Larger than of the Ligand Orbitals.*
Chimia, 27 (1973) p. 203-208.

191. *Electronic Spectra of Tetrahedral Oxo-, Thio- and Seleno-Complexes Formed by Elements of the Beginning of the Transition Groups (with A. Müller and E. Diemann).*
Structure and Bonding, Berlin, 14 (1973) p. 23-47.

192. *Photo-electron Spectra of Alkali and Ammonium Ions Adsorbed on Zirconium, Hafnium and Thorium Phosphates (with L. Balsenc and H. Berthou).*
Chimia, 27 (1973) p. 384.

193. *Les différences chimiques entre les terres rares et les trans-uraniens.*
J. Chim. Physique, 70 (1973) p. 1013-1015.

194. *Darstellung und Elektronenspektren neuer Trithiocarbonato-Komplexe; Struktur, Eigenschaften und Photoelektronenspektren von $Ni(NH_3)_3CS_3$ und $Zn(NH_3)_2CS_3$ (with A. Müller, P. Christophliemk and I. Tossidis).*
Z. anorg. Chem., 401 (1973) p. 274-294.

195. *The Coefficients of Fractional parentage for Ionization of Partly Filled f Shells Compared with Photoelectron Spectra of Lanthanide Compounds and Metals (with P. A. Cox and Y. Baer).*
Chemical Physics Letters, 22 (1973) p. 433-438.

196. *Interelectronic Repulsion as the Key to the Understanding of f Group Behaviour and 4f Ionization Energies from Photo-electron Spectra*
Recent Aspects in Actinide Chemistry, ed. G. Duykaerts, colloquium in Liege, May 1973 (1973) p. 3-17.

197. *The Importance of f-Orbitals for Chemical Bonding.*
Proceed. 13. ICCC, ed. B. Jezowska-Trzebiatowska, Nauka Press, Warszawa (1974) p.111-116.

198. *Photo-electron and Chemical Differences between Scandium, Iron, Cobalt and Gallium.*
Chimia, 28 (1974) p. 6-12.

199. *Linear Ligand Fields Influencing Auger Spectra of Fluorides, Copper(I) and Silver(I) (with H. Berthou). Chemical Physics Letters, 25 (1974) p. 21-25.*
200. *Can Hybridization Theory be Applied to Cobalt(III) Complexes - A Response to Pauling. Chemical Physics Letters, 27 (1974) p. 305-307.*
201. *Models and Paradoxes in Quantum Chemistry. Theoret. Chim. Acta, 34 (1974) p. 189-198.*
202. *Chemical Shifts and Variations of Width and Intensity of Auger Signals Obtained with a Photoelectron Spectrometer (with H. Berthou). Physica Fennica (Helsinki) 9 S (1974) p. 321-323.*
203. *Photoelectron Spectra Showing Relaxation Effects in the Continuum and Electrostatic and Chemical Influences of the Surrounding Atoms. Adv. Quantum Chem., 8 (1974) p. 137-182.*
204. *The Distinction Between Anti-bases (Electron-pair Acceptors) and Oxidizing Species (Electron Acceptors). Chimia, 28 (1974) p. 60S-608.*
205. *Photo-electron Spectra of Lanthanide Compounds. Proceed. 11. Rare Earth Research Conference, Traverse City, Michigan, ed. H. Eick, October 1974 (1974) p. 798-809.*
206. *Auger Signals Obtained with a Photoelectron Spectrometer (with H. Berthou). J. Electron Spectr., 5 (1974) p. 935-961.*
207. *Contribution à l'étude cristallographique des dérivés du ferrite bicalcique où le fer est substitué par le chrome, le Scandium ou l'yttrium (with M. Conkic). Chimia, 28 (1974) p. 732.*
208. *Chemical Effects on Photo-electron Spectra-Hopes, Deceptions and Surprises 1971-1974. Chimia, 29 (1975) p. 53-59.*
209. *Adsorption of Iodine and Halogen-containing Organic Molecules on Gold Studied by Photo-electron Spectra (with L. Balsenc and H. Berthou). Chimia, 29 (1975) p. 64-6S.*
210. *Kemikere bør väre fantasifulde og filosofiske. Dansk Kemi, Copenhagen, 56 (1975) p. 40-41.*
211. *The Separation of Hydrocarbon Photo-electron Signals as Indicator of Charging of Insulators (with H. Berthou). Chemical Physics Letters, 31 (1975) p. 416-418.*
212. *Relative Photo-electron Signal Intensities Obtained with a Magnesium X-ray Source (with H. Berthou). Analyt. Chem., 47 (1975) p. 482-488.*
213. *Continuum Effects Indicated by Hard and Soft Anti-bases (Lewis Acids) and Bases. Topics in Current Chemistry, 56 (1975) p. 1-66.*
214. *Formation Constants and Spectra of Palladium(II) Phenanthroline Complexes Containing Additional Ligands (with V. Parthasarathy). Chimia, 29 (1975) p. 210-211.*
215. *Partly Filled Shells Constituting Antibonding Orbitals with Higher Ionization Energy than their Bonding Counterparts. Structure and Bonding, Berlin,22 (1975) p. 49-81.*
216. *Photoelectron Spectra of Uranium (V) in Mixed Oxides Showing Characteristic Satellite Signals (with C. Keller). Chemical Physics Letters, 32 (1975) p. 397-400.*
217. *Narrow Band Thermoluminescence of Auer Mantles Containing Neodymium, Holmium, Erbium or Thulium in Mixed Oxides. Chemical Physics Letters, 34 (1975) p. 14-16.*
218. *Photo-electron Spectra of Non-metallic Solids and, Consequences for Quantum Chemistry. Structure and Bonding, Berlin,24 (1975) p. 1-58.*
219. *The Quantum Numbers of the Fluorescent State of the Uranyl Ion (with R. Reisfeld). Chemical Physics Letters, 35 (1975) p. 441-443.*
220. *Photoelectron and Auger Spectra of Xenon (VIII) in Solid Perxenates (with H. Berthou). Chemical Physics Letters, 36 (1975) p. 432-43S.*

221. *Hydration Energies and Specific Influence of Oxo Complexes and High Coordination Numbers on the Predicted Chemistry of Superheavy Elements (with R.A. Penneman).*
Heavy Element Properties (eds. W. Müller and H. Blank), North-Holland, Amsterdam, (1976) p. 117-121.

222. *Narrow Band Thermoluminescence (Candoluminescence) of Rare Earths in Auer Mantles.*
Structure and Bonding, Berlin,25 (1976) p. 1-21.

223. *Photo-electron-Spectra of Germanate, Tellurite and Tungstate Glasses Especially Apt to Show Lanthanide Luminescence (with R. Reisfeld and H. Berthou).*
Chimia, 30 (1976) p. 202-204.

224. *Influence of the Ligands on 3d Photoelectron Spectra of the First Four Lanthanides (with H. Berthou and C. Bonnelle).*
Chemical Physics Letters, 38 (1976) p. 199-206.

225. *New Evidence for the Existence of Orbitals in the Groundstate of Molecules.*
Naturwiss., 63 (1976) p. 191.

226. *New Understanding of Unusual Oxidation States in the Transition Groups.*
Naturwiss., 63 (1976) p. 292.

227. *Reaction of Gaseous Hydrogen Fluoride with Aluminium and its Compounds (with O. Pittion and H. Berthou).*
Chemical Physics Letters, 63 (1976) p. 357-361.

228. *ESCA appliquée à la chimie de coordination.*
J. microscopie et spectroscopie électronique, Paris, 1 (1976) p. 263-271.

229. *Photoelectron Spectra of Metallic Neodymium and Praseodymium Compared with Calculations of $3d^9 4f^3$ and $3d^9 4f^2$ in Intermediate Coupling (with N. Spector, C. Bonnelle, G. Dufour and H. Berthou).*
Chemical Physics Letters, 41 (1976) p. 199-204.

230. *Photo-electron Spectra of Germanium, Arsenic and Lead-containing Sulphide Glasses Favouring Lanthanide Luminescence (with R. Reisfeld, A. Bornstein and H. Berthou).*
Chimia, 30 (1976) p. 451-453.

231. *Sixty Years of Kossel Isoelectronic Series-Arguments Derived from Photo-electron and Atomic Spectra. Chimia, 30 (1976) p. 490-495.*

232. *Deep-lying Valence Orbitals and Problems of Degeneracy and Intensities in Photoelectron Spectra.*
Structure and Bonding, Berlin, 30 (1976) p. 141-192.

233. *Comparison of Properties of Atoms and Ions along the Lanthanide Series.*
Gmelin's Handbuch der Anorganische Chemie 39 B1 (Seltene Erden), Springer, Berlin (1976) p. 17-57.

234. *Dehydration of Various Aluminium Hydroxides Studied by Photo-electron Spectra (with O. Pitton and H. Berthou).*
Chimia, 30 (1976) p. 540-544.

235. *Photo-electron Spectra of Arsenic and Cadmium Selenides, Selenium and Germanium-Arsenic-Selenium Glasses (with R. Reisfeld, A. Bornstein and H. Berthou).*
Chimia, 31 (1977) p. 12-13.

236. *The Fluorescent State of the Uranyl Ion Assisting Solar Energy Conversion.*
Naturwiss., 64 (1977) p. 37-38.

237. *Application of the MS $X\alpha$ Method to the Understanding of Satellite Excitations in Inner Shell Photoelectron Spectra of Lanthanide Trifluorides (with J. Weber and H. Berthou).*
Chemical Physics Letters, 45 (1977) p. 1-5.

238. *Kan Filosoffer og Fysikere tale sammen?*
Gamma, Copenhagen, 30 (1977) p. 42-43.

239. *Electronic Structure, Fluorescence and Photochemistry of the Uranyl Ion, and Comparison with Octahedral Uranium(VI), Ruthenyl(VI), Rhenium(V) and Osmium(VI) Complexes.*
Revue de chimie minérale, Paris, 14 (1977) p. 127-138.

240. *Metals and Alloys Electrodeposited on a Gold Foil Studied by Means of X-ray Photoelectron Spectroscopy (with H. Berthou).*
J. microscopie et spectroscopie électronique, Paris, 2 (1977) p. 135-167.

241. *X-ray Induced Photo-electron Spectrometric Evidence for Heavy Metal Adsorption by Molybdenum Disulfide from Aqueous Solution (with P. U. Wolf, P. W. Schindler and H. Berthou).*

Chimia, 31 (1977) p. 223-225.

242. *Inadequate Models of Stereochemistry Based on Kimball Spheres and Pauli's Exclusion Principle. Chimia, 31 (1977) p. 445-446.*
243. *Photo-electron Spectra of Solid Samples. Fresenius Z. analyt. Chem., 288 (1977) p. 161-170.*
244. *Molecular Orbital Studies of the Electronic Structure of Lanthanide Complexes, II: Ionization Energies and Satellite Structure in Inner Shell Photo-electron Spectra of LaF_3, CeF_3, PrF_3, NdF_3, LaO_4^{5-} and $LaBr_3$ (with J. Weber and H. Berthou). Chem. Phys., 26 (1977) p. 69-78.*
245. *Glass Lasers. Naturwiss., 65 (1978) p. 104.*
246. *The Centenary of the Discovery of Ytterbium by Marignac in Geneva 1878. Chimia, 32 (1978) p. 89-91.*
247. *New Arguments for Atomic Character of the 4f Shell. Rare Earths in Modern Science and Technology, eds. G. J. McCarthy and J. J. Rhyne, Vol. 1, Plenum Press, New York (1978) p. 581-584..*
248. *On the Existence of Colorless Europium(IV). J. Amer. Chem. Soc., 100 (1978) p. 5968.*
249. *Kossel Isoelectronic Series and Photoelectron Spectra. Adv. Quantum Chem., 11 (1978) p. 51-91.*
250. *Predictable Quarkonium Chemistry. Structure and Bonding, Berlin, 34 (1978) p. 19-38.*
251. *Luminescence of Uranyl Ions in Phosphate Glass and Phosphoric Acid, Spontaneous Reduction to Uranium(IV) and New Description of the Electron Transfer Bands (with N. Lieblich-Sofer and R. Reisfeld). Inorg. Chim. Acta, 30 (1978) p. 259-265.*
252. *Synthèse et caractérisation du phosphate de hafnium comme échangeur d'ions (with M. G. Simona and L. R. Balsenc). Helv. Chim. Acta, 61 (1978) p. 1984-1989.*
253. *The Influence of Nitrate and Other Anions on the Absorption Spectra of Palladium(II) (with V. Parthasarathy). Acta Chem. Scand., A 32 (1978) p. 957-962.*
254. *Excited States of the Uranyl Ion. Journal of Luminescence, 18 (1979) p. 63-68.*
255. *Elektricitet fra en ny Solstralingskoncentrator og Siliciumfotoceller. Gamma, Copenhagen, 39 (1979) p. 3-13.*
256. *Theoretical Chemistry of Rare Earths. Handbook on the Physics and Chemistry of Rare Earths (eds. K. A. Gschneidner and LeRoy Eyring) Vol. 3, North-Holland, Amsterdam (1979) p. 111-169.*
257. *The Periodical Table and Induction as Basis of Chemistry. J. Chim. Physique, 76 (1979) p. 630-635.*
258. *Le Pionnier Solitaire Marignac. Centenaire de l'Ecole de Chimie 1879-1979 (ed. P. Müller) Section de Chimie, Université de Genève (1979) p. 9-16.*
259. *La Chimie Minérale, Chimie Analytique et Chimie Physique-Oscillations et Redéfinitions ä Genève. Centenaire de l'Ecole de Chimie 1879-1979 (ed. P. Müller) Section de Chimie, Université de Genève (1979) p. 27-37.*
260. *Est-ce que la Symétrie Totale Stabilise les Composés, les Atomes, les Noyaux et les Systèmes sans Couleur de Quark? Archives des Sciences, Genève, 32 (1979) p. 201-211.*
261. *Could Quarks and Leptons have Simple Constituents? Naturwiss., 67 (1980) p.35-36.*
262. *The Persistence of p, d, f and g Orbitals in Compounds. Israel J. Chem., 1, No 9 (1980) p. 174-192.*
263. *Transition Probabilities of Europium(III) in Zirconium and Beryllium Fluoride Glasses, Phosphate*

Glass and Pentaphosphate Crystals (with B. Blanzat, L. Boehm, R. Reisfeld and N. Spector). J. Solid State Chem., 32 (1980) p.185-192.

264. *Super-acids and Protonated Solvents. Naturwiss., 67 (1980) p.188-189.*
265. *Studies on Gadolinium in Geneva Since its Discovery by Marignac in 1880. Chimia, 34 (1980) p. 381-383.*
266. *Refining the Parameters of the Refined Spin-pairing Energy Description Rare Earths in Modern Science and Technology, eds. G.J. McCarthy, J.J. Rhyne and H.B. Silber, Vol. 2, Plenum Press, New York (1980) p. 425-428.*
267. *Suggestions for New Four-level Lasers. Rare Earths in Modern Science and Technology, eds. G.J. McCarthy, J.J. Rhyne and H.B. Silber, Vol. 2, Plenum Press, New York (1980) p. 607-612.*
268. *The two Luminescent Levels of Bi^{3+} in Solids (with G. Boulon and R. Reisfeld). Chemical Physics Letters, 75 (1980) p. 24-26.*
269. *Electron Transfer Spectra and Solar Energy. Chimia, 34 (1980) p. 508.*
270. *Umättede Kvarke og deres Mulige Bestanddele-Har Vi Naet Kälderetagen? Gamma, Copenhagen, 45 (1980) p. 30-40.*
271. *Quantum Harvesting and Energy Transfer. Photochemical Conversion and Storage of Solar Energy, ed. J.S. Connolly, Academic Press, New York (1981) p. 79-95.*
272. *Optimized Four-level Lasers. Proceed. Internat. Conf. on Lasers '80 in New Orleans December 1980, ed. C.B. Collins, STS Press, McLean, Virginia (1981) p. 343-348.*
273. *The Conditions for Total Symmetry Stabilizing Molecules, Atoms, Nuclei and Hadrons. Structure and Bonding, Berlin,43 (1981) p. 1-36.*
274. *Chemical Ionization Energies-Talking Points between Atomic Spectroscopists and Thermodynamicists. Comments Inorg. Chem. 1 (1981) p. 123-140.*
275. *275. Negative Exotic Particles as Low-Temperature Fusion Catalysts and Geochemical Distribution. Nature, 292 (1981) p. 41-43.*
276. *J-levels and S-values in Monatomic Entities and Condensed Matter. Int. Rev. Phys. Chem., 1 (1981) p. 225-252.*
277. *Candoluminescence of Rare Earths (with H. Bill and R. Reisfeld). Journal of Luminescence, 24 (1981) p. 91-94.*
278. *The Origin and Dissemination of the Term "Ligand" in Chemistry (W.H. Brock, K.A. Jensen and G.B. Kauffman). Ambix (Journal of the Society for the History of Alchemy and Chemistry), London, 28 (1981) p. 171-183.*
279. *Luminescent Solar Concentrators for Energy Conversion (with R. Reisfeld). Structure and Bonding, Berlin, 49 (1982) p. 1-36.*
280. *Chemistry and Spectroscopy of Rare Earths (with R. Reisfeld). Topics in Current Chemistry, 100 (1982) p. 127-167.*
281. *Uranyl Photophysics (with R. Reisfeld). Structure and Bonding, Berlin,50 (1982) p.121-171.*
282. *Possible Broken Supersymmetry Behind the Periodic Table (with J. Katriel). Chemical Physics Letters, 87 (1982) p. 315-319.*
283. *The Nephelauxetic Effect in Uranium(IV) Compounds. Chemical Physics Letters, 87 (1982) p. 320-323.*
284. *Optical Transition Probabilities of Er^{3+} in Fluoride Glasses (with R. Reisfeld, G. Katz, N. Spector, C. Jacoboni and R. DePape). J. Solid State Chem., 41 (1982) p. 253-261.*
285. *Can the Highest Occupied Molecular Orbital of the Uranyl Ion Be Essentially 5f? Chemical Physics Letters 89 (1982) p. 455-458.*
286. *Ligand: Origin and Dissemination (with W.H. Brock, K.A. Jensen and G.B. Kauffman).*

J. Coord. Chem., 11 (1982) p. 261-263.

287. *The Uranyl Ion and Solar Energy (with R. Reisfeld).*
4th International Conference on Photochemical Conversion and Storage of Solar Energy, Jerusalem, August 1982, Book of Abstracts, ed. J. Rabani (1982) p. 293-295.

288. *More News About Quarks.*
Naturwiss., 69 (1982) p. 420-427.

289. *Molecular Orbitals and X-ray Spectra.*
Advances in X-ray Spectroscopy, Contributions in Honour of Professor Y. Cauchois, eds. C. Bonnelle and C. Mandé, Pergamon Press, Oxford (1982) p. 225-239.

290. *Ligand: Origin and Dissemination (with W.H. Brock, K.A. Jensen and G.B. Kauffman).*
J. Coord.Chem., 11 (1982) p. 261-263.

291. *Atomic Sizes and Chemical Polarizability in Condensed Matter are more Important for Inorganic Chemistry than Preferred Coordination Numbers and Stoichiometry.*
Revue de Chimie minérale, Paris, 20 (1983) p. 533-548.

292. *5f Electrons in Transthorium Chemistry.*
Radiochimica Acta, 32 (1983) p.1-5.

293. *Can Quarked Niobium be a Fission Product?*
Nature, 305 (1983) p. 787-788.

294. *Fluorescence of Europium(III) in a Fluoride Glass Containing Zirconium (with R. Reisfeld, E. Greenberg, R.N. Brown and M.G. Drexhage).*
Chemical Physics Letters, 95 (1983) p. 91-94.

295. *The Comparison of Calculated Transition Probabilities with Luminescence Characteristics of Erbium(III) in Fluoride Glasses and in the Mixed Yttrium-Zirconium Oxide Crystal (with R. Reisfeld, G. Katz, C. Jacoboni, R. DePape, M.G. Drexhage and R.N. Brown).*
J. Solid State Chem., 48 (1983) p. 323-332.

296. *Judd-Ofelt Parameters and Chemical Bonding (with R. Reisfeld).*
J. Less-Common Metals, 93 (1983) p.103-112.

297. *The Uranyl Ion, Fluorescent and Fluorine-like: a Review (with R. Reisfeld).*
J. Electrochem. Soc., 130 (1983) p.681-684.

298. *F. Durville, G. Boulon, R. Reisfeld, H. Mack and C.K. Jørgensen: Site-selective Fluorescence of Europium(III) in Vitreous and Partly Crystallized Phosphotungstate Glass.*
Chemical Physics Letters, 102 (1983) p. 393-398.

299. *Ligand (with G.B. Kauffman, W.H. Brock and K.A. Jensen).*
J. Chemical Education, 60 (1983) p. 509-510.

300. *Blooming and Decline of the Two-electron Bond 1916-1984.*
Chimia, 38 (1984) p. 75-78.

301. *Consequences of the Relative Stability of Unsaturated Nuclei Containing (3A-1) Quarks.*
Naturwiss., 71 (1984) p. 151-152.

302. *Diquarks and the Instantaneous Picture of Nuclei.*
Naturwiss., 71 (1984) p. 418-419.

303. *Photo-electron Spectroscopy of Copper(II) in Spinels, and Correlation with the Jahn-Teller Effect (with A. d'Huysser, D. LeCalonnec, M. Lenglet and J.P. Bonnelle).*
Materials Research Bulletin, 19 (1984) p. 1157-1169.

304. *Cooperative Jahn-Teller Effect and Optical Spectra of the Copper(II) Ion in Chromites (with J. Arsène and M. Lenglet).*
Materials Research Bulletin, 19 (1984) p. 1281-1291.

305. *The Problems for the Two-electron Bond in Inorganic Chemistry; Analysis of the Coordination Number N.*
Topics Current Chemistry, 124 (1984) p. 1-31.

306. *Energy Transfer Between Manganese(II) and Erbium(III) in Various Fluoride Glasses (with R. Reisfeld, E. Greenberg, C. Jacoboni and R. DePape).*
J. Solid State Chem., 53 (1984) p. 236-245.

307. *Luminescence of Manganese(II) in 24 Phosphate Glasses (with R. Reisfeld and A. Kisilev).*
Chemical Physics Letters, 111 (1984) p.19-24.

308. *What has Quantum Chemistry Done for Transition-group Compounds?*

Proceedings of the Advanced Summer School on the Electronic Structure of New Materials, Loviisa, Finland, 20.-30. August 1984, ed. Henrik Stubb, Svenska Tekniska Vetenskapsakademien in Finland, Meddelande no.40, Helsinki (1985) p. 35-48.

309. *Reformed Ligand Field Theory and Oxidation States in Black and in Non-stoichiometric Materials. Proceedings of the Advanced Summer School on the Electronic Structure of New Materials, Helsinki, 3.-7.June 1985, ed. Henrik Stubb, Svenska Tekniska Vetenskapsakademien in Finland, Meddelande No 41, Helsinki (1985) p. 7-36.*
310. *The Influence of 4f Electrons on Chemistry and Various Spectrometries. J. Less-Common Metals, 112 (1985) p. 141-152.*
311. *Nonradiative Relaxation of Rare-Earths in Fluoride Glasses (with R. Reisfeld, C. Jacoboni and R. DePape). Materials Science Forum, Aedermannsdorf, 6 (1985) p. 635-640.*
312. *Access of Excited States to the Continuum. J. Physique (Colloques) 46 C 7 (1985) p. 409-412.*
313. *The Origin and Adoption of the Stock System (with G.B. Kauffman). J. Chemical Education, 62 (1985) p. 243-244.*
314. *Ewens-Bassett Notation for Inorganic Compounds (with G.B. Kauffman). J. Chemical Education, 62 (1985) p. 474-476.*
315. *Luminescence of six J-levels of Holmium(III) in Barium Zirconium Fluoride Glass at Room Temperature (with R. Reisfeld, M. Eyal and E. Greenberg). Chemical Physics Letters, 118 (1985) p. 25-28.*
316. *316. The Monazite and Xenotime Microcrystallites Formed by Lanthanides in Phosphotungstate Glasses (with H. Mack and R. Reisfeld). Inorg. Chim. Acta, 109 (1985) p. 51-53.`*
317. *Luminescence of Transition-group Ions in Fluoride Glasses and Their Laser Applications. Revue de Chimie minérale, Paris, 23 (1986) p. 614-620.*
318. *High Yield Luminescence of Lanthanide J-levels in Fluoride Glasses with Weak Multiphonon Relaxation (with R. Reisfeld and M. Eyal). J. Electrochem. Soc.,133 (1986) p. 1961-1963.*
319. *The "Ligand Field" Energy Differences Between 4f Orbitals are Mainly Provided by the Kinetic Energy Operator (with M. Faucher and D. Garcia). Chemical Physics Letters, 128 (1986) p. 250-255*
320. *Crystal Field Strength: Angular Overlap Analysis of Ligand Field Effects in Some Rare-earth Compounds (with M. Faucher and D. Garcia). Chemical Physics Letters, 129 (1986) p. 387-391.*
321. *Energy Transfer Between Manganese(II) and Neodymium(III) in Transition-metal Fluoride Glasses (with R. Reisfeld, M. Eyal and C. Jacoboni). Chemical Physics Letters, 129 (1986) p. 392-398.*
322. *Energy Transfer Between Neodymium(III) and Ytterbium(III) in Transition-metal Fluoride (TMFG) Glasses (with M. Eyal, R. Reisfeld and C. Jacoboni). Chemical Physics Letters, 129 (1986) p. 550-556.*
323. *Emission from Higher Excited States of Uranyl Salts and a Uranyl Borosilicate Glass (with M. Marcantonatos, C. Altheer and R. Reisfeld). Chemical Physics Letters, 132 (1986) p. 247-251.*
324. *Spectroscopy of Uranyl Ions in a Fluoride Glass (with R. Reisfeld and M. Eyal). Chemical Physics Letters, 132 (1986) p. 252-255.*
325. *Spectra of Zirconium Barium Fluoride Glass Containing Octahedrally Coordinated Chromium(III) and Nickel(II), or Mixtures of Manganese(II) and Neodymium(III) (with R. Reisfeld, M. Eyal, A. Guenther and B. Bendow). Chimia, 40 (1986) p. 403-405.*
326. *Conditions for Stability of Oxidation States Derived from Photo-electron Spectra and Inductive Quantum Chemistry. Z. Anorg. Allg. Chemie, 540 (1986) p. 91-105.*
327. *XANES, X-ray, Photo-electron and Optical Spectra of Divalent Nickel at the Crystallographic Transition in $NiCr_2O_4$ and the $Ni_{1-x}Cu_xCr_2O_4$ System: Correlation with the Jahn-Teller Effect (with M. Lenglet, A. d'Huysser, J. Arsène and J. P. Bonnelle).*

J. Physics C 19 (1986) p. L 363 - L 368.

328. *Fe, Ni Coordination and Oxidation States in Chromites and Cobaltites by XPS and XANES (with M. Lenglet, R. Guillamet, A. d'Huysser and J. Dürr).*
J. Physique (Colloques) 47 C 8 (1986) p. 765-769.

329. *Fluoride Glasses as Optimized Materials for Lanthanide Luminescence and Energy Storage in Manganese(II) (with R. Reisfeld and M. Eyal).*
J. Less-Common Metals, 126 (1986) p. 181-186.

330. *Comparison of Laser Properties of Rare Earths in Oxide And Fluoride Glasses (with R. Reisfeld and M. Eyal).*
J. Less-Common Metals, 126 (1986) p. 187-194.

331. *Unusual Luminescence of Titanium(III) in Aluminium Oxide (with R. Reisfeld and M. Eyal).*
Chimia, 41 (1987) p. 117-119.

332. *Nature and Notation: Ewens-Bassett Numbers and Oxidation States of Inorganic Compounds (with G. B. Kauffman).*
Chimia, 41 (1987) p. 150-151.

333. *Critical Comparison of Configuration Interaction and Oxidation State with Spectroscopic Properties of Nickel Oxide and Other Solid Oxides (with M. Lenglet and J. Arsène).*
Chemical Physics Letters, 136 (1987) p. 475-477.

334. *Analysis of X-ray Ni K/9 Emission, XANES, XPS, Ni 2p, And Optical Spectra of Nickel(II) Spinels and Structure Inference (with M. Lenglet, A. d'Huysser, J. P. Bonnelle and J. Dürr).*
Chemical Physics Letters, 136 (1987) p. 478-482.

335. *Recent Progress in Uranyl Photophysics (with R. Reisfeld).*
Photochemistry and Photophysics of Coordination Compounds, eds. H. Yersin and A. Vogler, Springer, Berlin (1987) p. 21-24.

336. *Photochemical Behaviour of Luminescent Dyes in Sol-Gel and Boric Acid Glasses (with R. Reisfeld, M. Eyal and R. Gvishi).*
Photochemistry and Photophysics of Coordination Compounds, eds. H. Yersin and A. Vogler, Springer, Berlin (1987) p. 313-316.

337. *Optical Spectra, X-ray Photoelectron Spectra and XANES of Divalent Nickel in Mixed Spinels $NiFe_{2-x}Cr_xO_4$ (with M. Lenalet and A. d'Huysser).*
Inorg. Chim. Acta, 133 (1987) p. 61-65.

338. *Laser Properties of Holmium and Erbium in Thorium-, Zinc- and Yttrium-based Fluoride Glass (with M. Eyal, R. Reisfeld and B. Bendow).*
Chemical Physics Letters, 139 (1987) p. 395-400.

339. *Energy Transfer Between Manganese(II) and Thulium(III) in Transition Metal Fluoride Glasses (with M. Eyal, R. Reisfeld, A. Schiller and C. Jacoboni).*
Chemical Physics Letters, 140 (1987) p. 592-602.

340. *Excited State Phenomena in Vitreous Materials (with R. Reisfeld).*
Handbook on the Physics and Chemistry of Rare Earths (eds. K.A. Gschneidner and LeRoy Eyring) Vol. 9, North-Holland, Amsterdam (1987) p. 1-90.

341. *Lanthanides Since 1839: From Crowded Elements to Quantum-chemical Rosetta Stone.*
Inorg. Chim. Acta, 139 (1987) p.1-5.

342. *Luminescence in Potential Fluoride Glass Lasers.*
J. Physique (Colloques) 48 C 7 (1987) p. 447-450.

343. *Energy Transfer Between Manganese(II) and Lanthanides in Fluoride Glasses (with R. Reisfeld and M. Eyal).*
Materials Science Forum, Aedermannsdorf, 21 (1987) p. 581-584.

344. *344. Local Symmetry and Optical Spectra of 3d Group Ions in Fluoride Glasses (with R. Reisfeld).*
Materials Science Forum, Aedermannsdorf, 21 (1987) p. 593-596.

345. *Closed-Shell and Chemical Bonding Effects are Almost Negligible in Two-Digit Z Elements.*
Chimia, 42 (1988) p. 21-24.

346. *Energy Levels and Luminescence of Dysprosium(III) in a Fluoride Glass With and Without Manganese(II) (with R. Reisfeld, M. Eyal and C. Jacoboni).*
Chimia, 42 (1988) p. 145-146.

347. *Excited States of Chromium(III) in Translucent Glass-Ceramics as Prospective Laser Materials (with R. Reisfeld).*

Structure and Bonding, Berlin, 69 (1988) p. 63-96.

348. *Influence of Rare Earths on Chemical Understanding and Classification. Handbook on the Physics and Chemistry of Rare Earths, eds. K.A. Gschneidner and LeRoy Eyring, North-Holland, Amsterdam, 11, (1988) p. 197-292.*
349. *Electronic Structure of $CuCr_2S_4$ by XPS, XANES and EXAFS (with M. Lenglet, P. Foulatier, A. d'Huysser and J. Dürr). Chemical Physics Letters, 145 (1988) p. 139-142.*
350. *Differential Ionization Energies and Non-Classical Aspects of Quantum Electrostatics. Quimica Nova, Sao Paulo, 11 (1988) p.10-19.*
351. *Ligand Field of Noble Gases and Closed-Shell Molecules Coordinated to Chromium(0) Pentacarbonyl. Chemical Physics Letters, 153 (1988) p.185-190.*
352. *Are Atoms Significantly Modified by Chemical Bonding? Topics Current Chemistry, 150 (1989) p.1-45.*
353. *Green Copper(II) Chloride Dihydrate Is NOT Autoionized (with G.B. Kauffman). J. Chemical Education 66 (1989) p.76.*
354. *New Paradoxes of Spin-pairing Energy in Gadolinium(III). J. Less-Common Metals 148 (1989) p.147-150.*
355. *Radiative Transitions and Lifetimes of Pr(III) in Tellurite Glasses (with M. Eyal, R. Reisfeld and C. Nyman). J. Less-Common Metals 148 (1989) p. 223-226.*
356. *Scenarios for Nuclear Fusion in Palladium-Deuterium Alloys at Ambient Temperature. Chimia 43 (1989) p.*
357. *Chemistry of Systems Containing Unsaturated Quarks. Molecular Structure and Energetics, eds. J.F. Liebman and A. Greenberg, Vol.11 [From Atoms to Polymers-Isoelectronic Analogies], VCH Publ., New York (1989) p. 257-277.*
358. *Recent surprises in electronic structure, spin-pairing energy and spectroscopy of transithorium (5f) and 4f compounds. 19emes Journées des Actinides, ed. Gabriella Bombieri, Madonna di Campiglio, Trento, Italy, 29-31 mars 1989. Padova (1989) p. 129-131.*
359. *Luminescence and "ligand field" treatment of chromium(III) in glasses. Materials Science, Wroclaw, 15 (1989) p. 95-115.*
360. *Comment on: bond lengths between aluminium and different complex ions. Chemical Physics Letters, 162 (1989) p.163.*
361. *Iron-group lumophores: broken paradigms and low-symmetry thexistates. Optical Society of America Proceedings on Tunable Solid State Lasers, Washington DC, 5 (1989) p. 252-257.*
362. *Predictable chemistry of systems containing unsaturated quarks. Astronomy, Cosmology and Fundamental Physics, eds. M. Caffo & al., Dordrecht, Kluwer Academic Publishers (1989) p. 436-437.*
363. *Comments on: Missing valence states, diamagnetic insulators, and superconductors (with L. Jansen). Physical Review Letters, 63 (1989) p. 1325.*
364. *Luminescence of tris(2,2'-bipyridine) ruthenium(II) incorporated at moderate temperature in sol-gel glasses and various low-melting glasses (with R. Reisfeld, D. Brusilovsky and M. Eyal). Chimia, 43 (1989) p. 385-387*
365. *Irreversible spectral changes of cobalt(II) by moderate heating in sol-gel glasses, and their ligand field rationalization (with R. Reisfeld, V. Chernyak and M. Eyal). Chemical Physics Letters, 164 (1989) p. 307-312.*
366. *Excited states of laser-emitting ions. SPIE Proceedings of the International Society for Optical Engineering, Bellingham, WA, No 1182 (1989) p. 2-11.*
367. *Heavy elements synthesized in supernovae and detected in peculiar A-type stars. Structure and Bonding, Berlin, 73 (1990) p. 199-226.*
368. *Historical, spectroscopic and chemical comparison of noble gases (with G. Frenking). Structure and Bonding, Berlin, 73 (1990) p. 1-15.*
369. *Crookes and Marignac. A centennial of an intuitive and pragmatic appraisal of "Chemical*

Elements" and the present astrophysical status of nucleosynthesis and "Dark Matter" (with G.B. Kauffman).
Structure and Bonding, Berlin, 73 (1990) p. 227-253.

370. *Influence de la distribution cationique et de la nature des interactions magnétiques sur l'intensité des transitions de paires de l'ion Fe^3+ dans quelques spinelles mixtes (with M. Lenglet and M. Bizi).*
Journal of Solid State Chemistry, 86 (1990) p. 82-87.

371. *Quantum Background for Parametrization of J-Levels.*
European Journal of Solid State and Inorganic Chemistry, 28 (1991) p. 139-142.

372. *What are One-Electron Energies and Electronegativity-Related Parameters?*
Comments on Inorganic Chemistry, 12 (1991) p. 139-197.

373. *Angular Overlap Treatment of Multidimensional Surfaces of 3d Group Excited States.*
Optical Society of America Proceedings on Advanced Solid State Lasers, 6 (1990) p. 350-353.

374. *New Conclusion from Yellow Colour of Chromium (VI) Fluoride Decomposing Above 180K.*
European Journal of Solid State and Inorganic Chemistry, 28 (1991) p. 799-808.

375. *Optical Spectra of Ni(II) in Ni_2Ge0_4 and Germanate Spinels (with M. Lenglet).*
Chemical Physics Letters, 185 (1991) p. 111-116.

376. *Are high heats of atomization for many oxides and fluorides of Z above 37 due to enhanced correlation energy?*
Chimia, Basel, Vol 46, No 11 (1992) p. 444-446.

377. *Multi-dimensional electronic and nuclear coordinates influencing lasing action.*
Les Ulis: Ed. de physique, Vol 1, colloque C7 (1991) p. 443-446.

378. *Glasses including quantum dots of cadmium sulphide, silver and laser dyes (with R. Reisfeld, M. Eyal and V. Chernyak).*
SPIE Proceedings of the International society for optical Engineering, 1590 (1991) paper 19.

379. *Influence of the antiferromagnetic interaction associated with octahedral Fe^{3+}-Ni^{2+} on the optical spectra in oxides (with M. Lenglet).*
Chemical Physics Letters, Amsterdam, 197 (1992) p. 259-264.

380. *Optical properties of colorants or luminescent species in sol-gel glasses (with R. Reisfeld).*
Structure and Bonding, Berlin, 77 (1992) p. 207-256.

381. *Photophysical behavior of Malachite Green in solid and liquid media (with R. Reisfeld and V. Chernyak). Chimia, Basel, 46, No 4 (1992) p. 148-151.*

382. *Relations between atomic spectra, astrophysics and chemical bonding.*
Comments on astrophysics, Gordong and Breach, London, Vol. 17, No 1 (1993) p. 49-101.

383. *Fluorescent ions in glass-ceramics and glasses (with R. Reisfeld).*
In: Heavy scintillators for scientific and industrial applications, Gif-sur-Yvette, Ed. Frontières (1993) p. 155-159.

384. *Rationalization of spectra of rare earths in condensed matter (with R. Reisfeld).*
Acta physica polonica. A, Warszawa, Vol. 84, No 5 (1993) p. 1011-1019.

385. *Coordination based on known free ligands, moderate dissociation rate, weaker electron affinity of central atom than ionisation energy of ligand, and quantum paradoxes.*
Coordination chemistry, Washington D.C., American Chemical Society (1994) p. 226-239.

386. *Excited states of cerium(III) in various local symmetries by UV absorption and luminescence spectra. Journal de physique. Colloque. Les Ulis. Vol. 4, colloque C4 (1994) p. 333-336.*

387. *The inductive chemist looking at local Minkowski time, compatibility of gravity and quanta, and formation of matter having rest-mass.*
Studies in science and theology (SSTh.), Geneva, Vol. 2 (1994) p. 813.

388. *Jannik Bjerrum's later life: turning toward chemical physics: personal recollections of a grateful student. Coordination chemistry. Washington D.C.: American Chemical Society (1994) p. 117-125.*

389. *Luminescence yields, minimal photodegradation of organic and inorganic species in sol-gel glass and modalities of confinement (with R. Reisfeld).*
Sol-gel optics III. Bellingham Wash.: SPIE, cop. (1994) p. 208-215.

390. *Sophus Mads Jørgensen: organisk kemi som jordbund for koordinationsbegrebet sammenlignet med datidens "speculative kemi".*
Den komplekse kemi. (S.L): Dansk Selskab for Historisk Kemi (1994) p. 25-37.

391. *Ubiquity, Born-Oppenheimer factorisation and electron configuration representability of wave-*

functions of macroscopic samples and their incidence on laser action.
Optical materials. Amsterdam, Vol. 4 (1994) p. 81-84.

392. *The effect of magnetic interactions on X-ray photoelectron (2p shell) spectra of octahedral nickel(II) in NiO and ferrimagnetic mixed oxides (with M. Lenglet and A. D'Huysser).*
European journal of solid state and inorganic chemistry. Paris. T 3, No 4 (1994) p. 277-287.

393. *Reinvestigation of the optical properties of Co_3O_4 (with M. Lenglet).*
Chemical Physics Letters, Amsterdam, Vol. 229, No 6 (1994) p. 616-620.

394. *Coordination compounds of metal ions in sol-gel glasses. Coordination chemistry (with R. Reisfeld). American Chemical Society, Washington D.C. (1994) p. 439-443.*

395. *Photostable solar concentrators based on fluorescent glass films (with R. Reisfeld and D. Shamrakov). Solar energy materials and solar cells, Amsterdam, Vol. 33 (1994) p. 417-427.*

396. *Electronic spectrum and antiferromagnetic A-B interactions between tetrahedral $3d^5$ and $3d^5$ or $3d^3$ octahedral cations in oxidic lithium spinels (with F. Hochu and M. Lenglet).*
Journal of solid state chemistry, San Diego, Vol. 120 (1995) p. 244-253.

397. *Aedelgassernes kemi: forskelle og ligheder med andre grundstoffer.*
Dansk Kemi, Copenhagen, No 1 (1996) p. 28-29.

398. *Luminescence of cerium(III) inter-shell transitions and scintillator action.*
Structure and Bonding, Berlin, Vol. 85 (1996) p. 199-214.

399. *Optical and electronic phenomena in sol-gel glasses and modern application (with R. Reisfeld).*
Structure and Bonding, Berlin, Vol. 85, (1996) 251 p.

400. *Laser-induced luminescence of rare-earth elements in natural fluor-apatites (with R. Reisfeld, M. Gaft, G. Boulon and C. Panczer).*
Journal of Luminescence 69 (5&6) (1996) p. 343-353.

Structure and Bonding, Vol. 106 (2004): 237–253
DOI 10.1007/b13402

Personal Notes

F. Calderazzo[1] · Baldassare Di Bartolo[2] · Brian R. Judd[3] · George B. Kauffman[4] · Edwin Anthony C. Lucken[5] · Makota Morita[6] · Dirk Reinen[7] · Renata Reisfeld[8] · H.-H. Schmidtke[9] · Alan F. Williams[10]

[1] Dipartimento di Chimica e Chimica Industriale, Via Risorgimento 35, 56126 Pisa, Italy
E-mail: facal@dcci.unipi.it
[2] Boston CollegeDepartment of Physics, MA 0246, Chestnut Hill, USA
E-mail: dobartob@bc.edu
[3] The Johns Hopkins University, Henry A. Rowland Department of Physics and Astronomy, MD 21218, Baltimore, USA
[4] California State University, FresnoDepartment of Chemistry, CA 93740-8034 Fresno, USA
E-mail: georgek@csufresno.edu
[5] Sciences II, Physical Chemistry Department, 30, quai Ernest-Ansermet, 1211 Geneva 4, Switzerland
E-mail: Anthony.Lucken@chiphy.unige.ch
[6] Seikei University, Department of Applied Chemistry, Faculty of Engineering, Kitamachi 3, Kichijoji, Musashino-Shi 180–8633, Tokyo, Japan
E-mail: morita@ch.seikei.ac.jp
[7] Philipps-Universität Marburg, Fachbereich Chemie, Hans-Meerwein-Straße, 35032 Marburg, Germany
E-mail: reinen@chemie.uni-marburg.de
[8] The Hebrew University, Department of Inorganic Chemistry, 91904 Jerusalem, Israel
E-mail: renata@vms.huji.ac.il
[9] Heinrich-Heine-Universität Düsseldorf, Institut für Theoretische Chemie, Universitätsstrasse 1, 40225 Düsseldorf Germany
E-mail: schmidtke@theochem.uni-duesseldorf.de
[10] Université de Genève, Département de Chimie minérale, analytique et appliquée, 30 quai Ernest Ansermet, 1211 Genève 4, Switzerland
E-mail: Alan.Williams@chiam.unige.ch

1
A Tribute to Christian Klixbüll Jørgensen

Fausto Calderazzo

I first met Christian Klixbüll Jørgensen in January 1963 when I joined Cyanamid European Research Institute as a research associate. I enjoyed talking with him, which eventually happened quite often during the coffee breaks in the cafeteria, which was located next to the main building overlooking the lake of Geneva. The conversation was almost constantly dedicated to chemistry and although our tasks within the activity of the Institute were different (Christian was the head of the Theoretical Chemistry Group, I was a member of the Synthetic Inorganic Chemistry Group headed by Erwin Weiss), there was always the opportunity to detect interesting aspects of our work. Some years later, when Erwin Weiss left to become Professor at the University of Hamburg, in April 1965, I became director of the Group and thus the opportunities of mutual exchanges of ideas on research projects became more frequent. I believe that we became friends and our fami-

lies got acquainted. On the other hand, the atmosphere within the Institute was excellent; the scientific activity was very intensive and, at least in the beginning, there was no pressure on the side of the US headquarters to direct our research towards some specific subjects, relevant from the point of view of possible applications. The idea was that collecting some capable people in the same place and letting them work on some specific areas of their interest, some results within the areas of commercial interest for American Cyanamid could come out. In this operation Christian had a relevant position. His scientific contacts have been very useful in letting the scientific community recognise the quality of the work which was being carried out in Geneva. Before writing this personal memory, I felt it necessary to read again his book "Inorganic Complexes", published in 1963 for Academic Press. This is the book in which presumably Christian has been closer to chemical problems of interest to an inorganic chemist mainly interested in the discovery of new classes of compounds, as I have been in the course of my work.

The book was written in a period of important new discoveries, especially in Inorganic Chemistry. For example, organo-transition metal chemistry underwent a tremendous advancement thanks to G. Wilkinson and E. O. Fischer who were due to receive the Nobel Prize for their new scientifically relevant and revolutionary findings within transition metal chemistry some years later. Jørgensen's book contains important items, often connected to the scientific work by himself, discussed in the context of the current literature. Those days, chemistry used to develop rapidly, and new areas of research used to be introduced or interesting new compounds would appear in the literature. For example, this book, which, at least in part, was compiled during the year 1963, contains a reference to the synthesis of XeF_2 [1], substantially simultaneous to the discovery of XeF_4 [2], and to the solution of its crystal structure [3]. In spite of these rapid developments, Christian was not surprised by them and in a sense he was able to categorise them readily, due to the vast knowledge of chemistry he possessed. He was attracted by the unusual features of the experimental facts and by the new theoretical treatments required to interpret them. He was himself a systematic type of scientist, with a vivid intelligence, an enormous curiosity and a lot of fantasy. He had a knowledge and an understanding of spectroscopic features of metal complexes, which, I believe, has never been reached by any other scientist of our time. As he points out in the preface to the above mentioned book, Christian felt about forty years ago that "without some qualitative understanding of spectroscopy and quantum chemistry, a chemist may frequently miss the really interesting part of new developments in his field". This sentence is completely true, as it has been shown by the later developments of chemistry and science in general since those days. Spectroscopy, and especially NMR, has made tremendous progress since then, and has become an indispensable tool for research. However, Christian also felt that chemistry should not be reduced to a subdivision of physics, and in this respect he pointed out that a fundamental knowledge of natural history is essential in order to be able to progress in the understanding of chemical bonding. Thus, theoreticians and experimental chemists should try to work in combination, sometimes theory coming before the experiment, more often theory being essential to understand the nature of the phenomena observed by the experimentalist in the first place.

Beside many other contributions, Christian used UV-VIS spectra as a diagnostic tool for the identification of chemical substances, and his contributions to this field are first class. His memory in terms of recollecting shape and wavenumber values of visible and near ultraviolet spectra was amazing. However, Christian had no limits in his interests for chemistry. He could span from non-transitional to transition elements and their compounds with equal competence. He had a well-defined interest in derivatives of 4*f* and 5*f* elements. For example, in his book he anticipated that the aquo complexes of the lanthanides (Ln) in the oxidation state III should contain nine H_2O ligands. It is interesting to notice that it has now been established that the lanthanide aquo cations, with the poorly coordinating triflato $CF_3SO_3^-$ and $EtOSO_3^-$ anions, of formula $[Ln(H_2O)_9]^{3+}$ form a series of isotypical compounds, in which the central metal has in fact a CN of nine, with a tricapped trigonal prismatic geometry [4]. Thus, the anticipation by Christian that the trivalent aquo cation "probably occurs as trigonally prismatic (with a central triangle rotated 60°) $M(H_2O)_9^{3+}$" could not be more exact. Of course, now we know that also the plutonium derivative $[Ln(H_2O)_9]^{3+}$ as the triflato derivative is isostructural with the corresponding samarium(III) complex, the metal-OH_2 distances differing by only a few hundreths of an Å on going from samarium(III) (2.548 and 2.418 Å) to plutonium(III) (2.574 and 2.476 Å) [5].

The year Christian's book (1963) was printed, the so-called classification of metal cations into classes A and B, according to a proposal first made by Ahrland, Chatt and Davies, was on the way to reaching its maximum consensus, thanks also to the contribution by Pearson in this field. This classification, as we all know, has been the subject of some dispute, as far as reactions in solution are concerned, as the thermodynamic data under these conditions are strongly affected by solvation effects. In other words, in the gas phase, all metal systems are hard. Even at that time Christian pointed out that, for example, the family of non-transition elements of Groups from 13 to 16 appear to behave as class B with respect to halides and sulfur-containing ligands, but not towards ammonia, amines and CN^-. In the chapter of his book dedicated to halo complexes, Christian states that "the total free energy of a given complex is an extremely intricate quantity, and the formation constants we measure and which are the fundamentals for the A- and B- classification, are small differences between huge quantities". This sentence should be taken as an encouragement to look even more deeply into the problems of energy variations along vertical sequences of the well-known periodic classification.

Christian was a really outstanding scientist. He was in a constant search for pushing back the frontiers of Science and he has had a definite influence on many colleagues around the world. He has certainly been an unforgettable person.

2
A Personal Note in Memory of Prof. Christian Jørgensen

Baldassare Di Bartolo

Christian Jørgensen was an honest, modest and incredibly knowledgeable man. I met him in the summer of 1976 at a congress in Villeurbanne organized by Madame Gaume of the University of Lyon. I remember him giving a lecture and at some point going to the blackboard and writing a long list of references without consulting any notes.

I remember a very pleasant evening at my house where Christian, Renata Reisfeld, George Blasse, and Romano Pappalardo were our guests for dinner. We all enjoyed the conviviality and the cordial conversation to which Christian contributed with his usual verve.

I remember too a similar evening some years after with Christian and Renata at the house of Georges Boulon in Lyon.

I remember his visits to my laboratory at Boston College and the lasting impression he made on my associates. During one of these visits he found my student John Flaherty working on the problem of energy transfer between manganese and erbium in manganese fluoride. Jørgensen gave him a full report on the manganese luminescence in any imaginable system. (Renata and Christian were gracious enough to cite the work of my student in their book on "Lasers and Excited States of Rare Earths.") After Jørgensen's visit, Flaherty told me that he could now see his thesis problem in a "historical context."

For Christian, life and work, science, and any other aspect of intellectual life were a continuum. Once, during a get-together with Jorgensen and other friends, the conversation turned to religion and in particular to the infallibility of the Pope, proclaimed, I said, showing off my erudition, at the First Vatican Council of 1870. I happened to know that at that time there was a group of so-called "Old Catholics" who refused to accept the decree of the Council. I thought that this was my chance to talk about something Christian knew nothing about and I informed the gathering of what I knew about these people. I was thoroughly disappointed when, as soon as I finished recounting my story, Jørgensen gave us a full account of the history of the Old Catholics, going back to their origins tied to the Giansenist Church in The Netherlands, and adding that he personally knew some Old Catholics in Switzerland.

Christian's knowledge was not a simple collection of facts, but a harmonious whole in which he had incorporated every experience and every piece of information he would come across, a whole he had molded, had meditated upon and to which he had given his personal imprint.

I will never forget Christian Jørgensen!

3
Collaboration at Cologny

Brian R. Judd

In 1962 I received an invitation from Christian Klixbüll Jørgensen to visit him at the Cyanamid European Research Institute in Cologny, where he was Director of the Theoretical Inorganic Chemistry group. He had noticed an article of mine on the intensities of optical transitions in aqueous solutions of rare-earth salts, in which I had reported that a neodymium band satisfying the selection rules for quadrupole radiation seemed peculiarly sensitive to the choice of salt. We had engaged in an active correspondence for several years on various aspects of rare-earth spectroscopy, and I was anxious to meet him.

Christian was the first to apply the recondite group-theoretical methods of Giulio Racah to the observed energy levels of rare-earth ions, and so his professorial appearance and intellectual agility did not surprise me. A theorist at heart, I thought. However, I caught a glimpse of his practical abilities at lunch in the cafeteria, where he explained how he had arranged for the tops of the tables to be used as writing surfaces. Any idea that he might be limited to a life of the mind was completely dispelled when we went into the laboratory. He produced a test-tube containing an aqueous solution of neodymium ions and invited me to inspect the band in the purple with a hand-held spectrograph. He then added some alcohol and showed me how that band intensified. I had not expected such a direct and dramatic demonstration of what we both recognized was a remarkable hypersensitivity of the neodymium ion to its environment. He then mentioned that he had investigated similar phenomena in other rare-earth ions. To my great surprise he then suddenly said, "We should write a paper." I protested that we had not considered what the underlying mechanism might be. He countered by suggesting that we could leave that problem to others. To my mind, this was not a sensible way to go. As a result of some discussion, I got him to agree that we needed time to think things over, but I quickly realized that, if I thought some explanation was called for, I would have to supply it.

At dinner, Christian's wide-ranging interests were much in evidence. I remember a waiter putting a small plate on our table, saying it was "*pour la sauce*." Or did he say, "*pour les os*"? As I pondered whether gravy or bones were in play, Christian started a lengthy disquisition on the ambiguity of language. Naturally enough, this took us (or rather, him) to digress to other topics, reminding me of Aldous Huxley's claim to be able to talk or write about anything. In Christian's case, this flexibility of mind made it difficult to have a focussed discussion with him about a single subject. His reaction to a comment would often be a polite acceptance before going off in another direction.

A few months after Christian's demonstration with the solution of neodymium ions, I came up with an explanation for the hypersensitivity, which I located (rather vaguely) in the inhomogeneity of the dielectric. I wrote a draft of an article, incorporating Christian's nine examples of hypersensitivity and using his preferred units of kilokaysers. At his request, I used "lanthanides" rather than "rare earths." I submitted the draft to him for discussion, but was taken aback by

his immediate acceptance. He generously suggested that as I had done most of the work, my name should precede his below the title. At that time I had always used a strict alphabetical ordering, and we followed my preference by settling for "Jørgensen and Judd." The paper, entitled "Hypersensitive pseudoquadrupole transitions in lanthanides," appeared in a 1964 issue of *Molecular Physics.* It was a successful collaboration: the paper started a new field of interest and has led to several interesting developments in both theory and experiment.

After this joint work, my contacts with Christian became less frequent and more casual. We met at conferences, and I was always happy to chat with him. At one such meeting, he confided to me that "ø" comes after "u" in the Danish alphabet. We had a good laugh about that. In reviewing a book of his, I once commented on how, in reading his book, one got the impression that he thought that one atom could be regarded as an analogue computer for calculating the properties of an identical atom. Christian referred to this in one of his many later writings as "a profound comment." Its profundity escaped me, but I recognized the kindness of heart and generosity of spirit that led him to compliment a colleague.

4
Christian Klixbüll Jørgensen, Some Memories and Reminiscences

George B. Kauffman

On January 9, 2001 Christian Klixbüll Jørgensen, a major contributor to the correlation of spectra with the electronic structure of coordination compounds, died in a nursing home near Paris. At the time of his death he was Professor Emeritus of Inorganic Chemistry at the Université de Genève. In 1997 he began to suffer from frequent lapses of memory and exhibited erratic behavior. As early as 1993, when the reviewers and I asked him to make changes in his reminiscences of his mentor Jannik Bjerrum (Coordination Chemistry: A Century of Progress, Kauffman, G. B., (ed); American Chemical Society: Washington, DC, 1994; pp 116-125), he uncharacteristically refus(ed) The problems that we had with our usually amiable friend and colleague at that time may have been due to the beginnings of his Alzheimer's disease.

Following an accident when a bookcase fell on him in bed, he was hospitalized and diagnosed with senile dementia, which forced him to retire in 1997. He then moved to France to be close to his son Philippe and daughter Estelle, who survive him. He was preceded in death by his wife, Micheline (née Prouvez). Considering the central role that his mind and intellectual pursuits played throughout his life from his earliest years, his final years were particularly poignant and tragic to those of us who worked with him and loved him. He will be sorely miss(ed)

I first met Christian at the 6th International Conference on Coordination Chemistry (ICCC), organized by Stanley Kirschner of Wayne State University and held in Detroit Michigan (August 27-September, 1961). Because of our common interests, we decided to collaborate on a study of isomers of iridium(III). The following year our paths crossed again when I accompanied him, his wife, and several chemists such as Erwin Weiss and Hans-Herbert Schmidtke, both of

whom were coauthors with Christian on various publications, on a Swedish Midsummer tour, beginning in Göteborg and ending in Stockholm (June 22-25, 1962), where the 7th ICCC was held, along with sessions in Uppsala (June 25-29, 1962). We both presented papers, he on absorption spectra and I on our collaborative investigation of what we thought were the *cis* and *trans* isomers of [IrCl3{(C2H5)2S}3] as well as a new binuclear iridium(III) complex. With Christian's expertise we found that the yellow isomer was indeed *cis*-(1,2,3)-[IrCl3{(C2H5)2S}3], but the red "isomer" was actually an electrolytic "polymerization" isomer, *trans*-[IrCl2{(C2H5)2S}4]+ *trans*-[IrCl4{(C2H5)2S}2]_.

Hoping to find the largest possible audience for our work, I submitted our manuscript to Science, a journal in which articles of biological interest predominat(ed) Our paper was reject(ed) Christian's letter to me (November 12, 1962), handwritten in blue ink, like all his letters, is gracious, prophetic about Science's future decision, and typifies his dry sense of humor (To keep me updated on his activities he often sent me copies of his correspondence with other scientists along with his letters to me, of which he always included Xerox copies):

"Thank you very much for the occasion to write in journals in which I would never have expected myself to write. If you do not get it accepted, write a paper demonstrating that it is not impossible that Ir(Et2S)2Cl4_ provokes an increase in female off-spring of green frogs from 49.1±0.7 to 49.3±1.8% and they will print it".

The article was published (Kauffman, G. B.; Tsai, J. H.-S.; Fay, R. C.; Jørgensen, C. K. Inorg. Chem. 1963, 2:1233-1238), and of all my experimental papers it is the one of which I am most proud. I attribute the following referee's report, which is not at all typical of those that I have received through the years, to Christian's participation in the project:

"This paper is one of the most thoroughly documented articles I have ever had the privilege to read. It has shown by a marvellously variegated number of techniques, both new and old, how a structure can be narrowly circumscribed without a final (most times extremely difficult) X-ray structure analysis. The authors are to be warmly congratulated on such a fine piece of work. Would there be more such careful research done today instead of some of the slipshod work that passes for research.

I most heartedly recommend its speedy publication in Inorganic Chemistry".

I spent my first sabbatical leave at the Universität Zürich working on my first book, a biography of Alfred Werner, during the academic year 1963-1964, which gave me another opportunity to see Christian again. He invited me to speak at the Cyanamid European Research Institute at Cologny, near Geneva, and I presented my very first seminar, "Alfred Werner: The Man and His Theory" on May 14, 1964. Following my talk Christian discreetly slipped me an envelope containing Sw. Fr. 300 ($75) – a large sum in those days – the first time that I had ever been paid for speaking, and I owe this experience to Christian!

Christian was never one to engage in "small talk". While he was serious and -intellectually active, he was never pompous or "stuffy". Following my seminar, during our walk around the old city of Geneva, I made a casual remark about phlogiston, and he seized upon it to explain how phlogiston could be equated with the electron: Oxidation corresponds to a loss of phlogiston (electrons); reduction corresponds to a gain of phlogiston (electrons).

Christian presented papers at both my symposia ((1967) Invariance and distortions of octahedral chromophores, Kauffman, G. B.(ed) Werner Centennial. American Chemical Society: Washington, 1967 DC, pp 161-177); his previously mentioned article on Jannik Bjerrum, Coordination Chemistry: A Century of Progress; Kauffman, G. B., (ed); American Chemical Society: Washington, DC, 1994; pp 116-125; "Coordination Based on Known Free Ligands, Moderate Dissociation Rate, Weaker Electron Affinity of Central Atom Than Ionization Energy of Ligand, and Quantum Paradoxes", ibid.; pp 226-239; and "Coordination Compounds of Metal Ions in Sol-Gel Glasses" (with his frequent coauthor, Renata Reisfeld), ibid.; pp 439-443). We also collaborated on a number of articles on the origin and dissemination of the term "ligand" (Ambix: 1981, 28, 171-183; J. Coord. Chem. 1982, 11:261-263; J. Chem. Inf. Comp. Sci. 1982, 22:125-129; Polyhedron 1983, 2, 1-7; J. Chem. Educ. 1983, 60:509-510; Rev. Chilena de Educación Quím. 1983, 9(1):19-21); the origin and adoption of the Stock System (J. Chem. Educ. 1985, 62:243-244); Ewens-Bassett notation (J. Chem. Educ. 1985, 62:474-476; Chimia 1987, 41, 150-151); green copper(II) chloride dihydrate (J. Chem. Educ. 1989, 66:76); and "Crookes and Marignac – A Centennial of an Intuitive and Pragmatic Appraisal of 'Chemical Elements' and the Present Astrophysical Status of Nucleosynthesis and 'Dark Matter'" (Structure and Bonding 1993, 73:227-253).

On April 29, 1983 Christian was awarded an honorary doctorate from the Philosophical Faculty II of the Universität Zürich "as a pioneer in the bridging of quantum mechanics and chemistry, which has explained in a prominent manner the electronic spectra of metal complexes and has proved fruitful for chemistry". The ceremony took place at the university's 150th anniversary celebration held in the Grossmünster, the venerable Romanesque cathedral purportedly built by Charlemagne in the 700s and from whose pulpit Huldrych Zwingli, the most important reformer in the Swiss Protestant Reformation, preached his fiery sermons beginning in 1518. With his usual wry sense of humor and dislike of pretension Christian described the ceremony to me in a letter of May 7, 1983:

"The rector, Frau Verena Meyer, spoke for an hour about relations between physics and society since 1833, and the 1100-people lunch in Kongresshaus had an indefinite number of speeches".

Christian stayed with my wife Laurie and me twice in Fresno. On January 23, 1987 he presented a seminar, "The Periodic Table as Seen by Inductive Chemists and Deductive Physicists", in which he pointed out that Mendeleev's great summarizing generalization is viewed by chemists and physicists from markedly different standpoints, which he contrasted in his lecture. He also criticized the new numbering system advocated by the International Union of Pure and Applied Chemistry (IUPAC) and eliminating A and B groups in favor of an 18-group scheme.

Christian was amused by two incidents that occurred in our work together. First, the captions for the portraits of him and Jannik Bjerrum were inadvertently switched in my "Impact" interview (J. Chem. Educ. 1985, 62:1002-1005). Second, in my role as organizer of the Coordination Chemistry Centennial Symposium (CCCS), 205th American Chemical Society National Meeting, Denver, Colorado, March 28–April 2, 1993, as soon as I discovered an error in the program proof I telephoned the ACS. I carefully and patiently explained to an ACS employee that

the last name of a speaker had been misspelled – as Jorgensen rather than Jørgensen. Unable to get across the idea of what I called a "Danish umlaut", I resorted to spelling out the name – "J and slash o rgensen". The name appeared in the program as "J&slashorgensen" both in the abstracts (HIST 002 and index) as well as in Chemical & Engineering News March 1, 1993, 71(9).73. It was at the CCCS that I last saw Christian. His legacy endures in the hearts of his friends and colleagues. We shall not forget him.

5
Recalling a Good Friend

Edwin Anthony C. Lucken

I first met Christian Jørgenson in January 1961 when we were both working at the Cyanamid European Research Institute (CERI) in Geneva. The wide breadth of his interests and the new light and often-unusual slants that he could cast on almost any subject immediately captivated me. We never actually collaborated on anything but it was always a testing and stimulating experience to try out any new ideas on Christian over the coffee table. CERI closed on 31 December 1968, by which time I had already left to take up a post at the University of Geneva, while Christian spent a year or so as a consultant to Cyanamid in the USA. I was particularly pleased when Christian was also offered a post at the University and for the many subsequent years I was able to enjoy the stimulus of his companionship.

Our two families became close friends and, in 1969 when we had both left CERI, his wife, Micheline, did us the honour of becoming the godmother of our son, Michael.

6
In Memory of Prof. Christian K. Jørgensen

Makoto Morita

It was a stormy day of November 1977 when I, while on leave from Seikei University and the University of Düsseldorf (Prof. H.-H. Schmidtke, Dr. T. Schönherr), was warmly welcomed by Professor Jørgensen in Geneva as a visiting researcher just for a month under the intra-Europe project financially supported by the Alexander-von-Humboldt Foundation. I was quickly introduced to his laboratory where I could see various chemicals put aside randomly on the desks of the lab. Suddenly he fired a white powder on a tea spoon using a Bunsen burner and passed me a small telescope-like object from his pocket. "Take a look at the flame through the microscope. You can see sharp lines of Eu^{3+} ions. Das ist Flammen reaction!" (Wie erhellend war das für den Besucher!!) He spoke to me very quickly with silent passion in English and in German to check my understanding. At lunch time, he gave me a private lecture on the spectroscopy of lanthanide complexes by writing all the equations and letters in mirror writing on a paper table-cloth. "That hand writing is quite special for a person like

Leonardo da Vinci", his secretary and a young Russian coworker told me later at a party at his home. In his room, a door and sideboards were full of his discussion notes with visitors. He did not take much care with chemicals scattered about the laboratory or piles of his papers and letters on his writing desk because he could quickly find what he wanted by simply extending his long arm. When a new theory on quarks was being discussed in the seminar in the university hall, somebody said to me: "Prof. Jørgensen was asking a sharp question to the speaker while he was busy in writing three papers at the same time!" He has been recognised as being a giant among professors. To me he was a kind navigator to spectroscopy full of intelligence and the humanities.

7
C. K. Jørgensen and Structure and Bonding

Dirk Reinen

Christian Klixbüll Jørgensen's name is closely tied to the review series *Structure and Bonding,* where the various articles honouring his scientific oevre will appear on the occasion of his tragic death. It was – without forgetting the merits of the other members of the first editorial board – mainly his initiative, which lead to the establishment of the series in 1966, meanwhile it is an accepted and renowned institution on the scientific book market. From the preface of the first volume it is worthwhile to cite specifically the last sentences, because they well reveal C. K. Jørgensens attitude toward science: *We are specially interested in the role of the "complex metal-ligand" moiety ..... and wish to direct attention towards borderline subjects. We are convinced that these borderline areas receive less attention than they justify; academic studies tend too often to be compartmentalized whereas technological interest too often lacks sufficient fundamental understanding. We hope that this series may help to bridge the gaps between some of these different fields and perhaps provide in the process some stimulation and scientific profit to the reader.* The initial volume started with an article by C. K. Jørgensen, based on contributions to the Konstanz meeting of the legendary summer school on ligand field theory in 1962 (director: H. Hartmann). Since then twenty reviews and original contributions have appeared in Structure and Bonding with C. K. Jørgensen as author or co-author, ranging from ligand field theory in its broadest sense and its various applications in complex and solid state chemistry to borderline and frontier aspects such as *quarkonium chemistry* or a *pragmatic appraisal of the chemical element concept in astrophysics* – always in line with the cited preface notes.

Christian Klixbüll Jørgensen was a thoroughly intuitive scientist with an open unencumbered mind für new developments, to whom qualitative and semiquantitative concepts were of major importance. His intimate connection with the chemical experiment – here benefiting from his fabulous memory of literature data – is possibly best characterized by the following episode, presumably better than by any other spectacular event. In a lecture, where he displayed his ideas about the nephelauxetic properties and optical electronegativities of transition metal complexes and solids, he irritated the audience by the statement: *This*

compound is so black that it does not exist – here referring to the lower-energy shift of d-d and charge transfer bands in case of strong bond covalency.

In an era, where the belief in *quantitative* theoretical treatments of chemical phenomena booms, C. K. Jørgensen's death has indeed left a gap. In 1999, after 23 years of editorial efforts, he left the board of Structure and Bonding.

The author was a member of the editorial board of Structure and Bonding from 1966 *until* 1995.

8
Christian Jørgensen: A Very Short Story of His Life and Scientific Career

Renata Reisfeld

I met Christian in 1968 when he was invited as a main speaker to Jerusalem to a conference held on coordination chemistry. At that time he was already world famous for his pioneering contributions in ligand field theory, electronic spectra of transition and rare earth elements, nephelauxetic effects and his unorthodox views of electronegativity.

Born in Aalborg, Denmark, in April 18, 1931, he started his studies of chemistry and mathematics in 1950 at the University of Copenhagen and obtained his doctorate in 1957. His thesis "Energy Levels of complexes and Gaseous ion" published in 1957 became a classic one and was taught in many universities as a basic textbook.

After serving for some years in NATO in Paris, he became the director of the group for theoretical and inorganic chemistry in Cyanamid European Research Institute in Geneva 1961-1968. For his extraordinary achievements he was elected to the Danish Academy of Science as early as 1965 and received the title of Doctor honoris causa in 1983 at the University of Zürich.

He wrote four books: "*Absorption Spectra and Chemical Bondings in Complexes*" in 1962, "*Oxidation Numbers and Oxidation States*" in 1969, "*Modern Aspects of Ligand Field Theory*" in 1971, and "*Lasers and Excited States of Rare Earth*" which was published in 1977; all of which became classics.

He published over 400 scientific publications in prestigious journals. I had the pleasure and honor to be a coauthor with him of more than 70 papers and of his fourth book.

Christian was an extraordinary man, a genius with very deep vision of the chemical phenomena which he could understand intuitively as very few people could. He was generous. His kind nature which was a gift in addition to his geniality made him to extend great assistance to his fellow scientists giving advice and sending many papers at the time where the Internet was still unavailable. He was always willing to discuss with his colleagues showing great interest and help.

In 1974 he invited me to Geneva where we started a very pleasant and productive cooperation which continued to the last moment as long as his health allowed. This cooperation was mainly focused on spectroscopy of Rare Earths, Transition Metal Ions, Uranyl Photophysics, and Solar Energy Materials in glasses. The cooperation became possible due to our frequent meetings in Geneva, Israel or at International Conferences. The impact that Christian had on

my scientific work was tremendous and I cherish his memory with great appreciation. To him I devote the chapter on "Spectroscopy of Rare Earth and their complexes in glasses" in this volume.

When we met for the first time in Jerusalem, I had just one publication on RE spectroscopy mainly of Eu(II) in alkali halides showing the charge transfer absorption in the UV and the blue emission. I was totally surprised that Christian has seen and read the paper and recited to me the entire text. I was overwhelmed by his extraordinary knowledge and the phenomenal memory. At the beginning, I hardly dared speak being confronted with the great scientist, but he kindly encouraged me and on his return to Geneva wrote me a letter that inspired me to extend my work on rare earth ions, uranyl and transition metal ions.

The first outcome of our meeting was his invitation to me to write a chapter for Structure and Bonding forwhich he was one of the editors. The outcome – Volume 13 of Structure and Bonding – was devoted to Rare Earths in which he wrote a chapter of "Inner Mechanisms of Rare Earth Elucidated by Photo Electric Spectra" and I wrote a chapter on "Spectra and Energy Transfer of Rare Earths in Inorganic Glasses". The chapter was inspired by him and resulted in an understanding in depth of mechanism of transfer in amorphous metals.

The following volume of Structure and Bonding Vol. 22 included Christian's paper on partly filled shells consisting of anti bonding orbitals and a chapter by myself on "Radiative and Nonradiative Transitions of RE Ions in Glasses".

Volume 30 of S&B included his chapter on Deep Lying Valence Orbitals and mine on Excited State and Energy Transfer from Donor Cations to RE in condensed phase.

From then on we started to write papers together. Some examples include Luminescent Solar Concentrators for Energy Conversion, S&B Vol. 49; Uranyl Photophysics, S&B Vol. 50; Excited States of Chromium(III) in Translucent Glass Ceramics, S&B Vol. 69; Optical Properties of Colorants and Luminescence Species in Sol-Gel Glass, S.B. Vol. 77.

Volume 85 of Structure and Bonding was again composed of our joint efforts and devoted to Optical and Electronic Phenomena on Sol-Gel Glasses and Modern applications. Among the many other publications I would also like to mention: C.K. Jørgensen and R. Reisfeld, Chemistry and spectroscopy of rare earth *Topics in Current Chemistry*, 100 (1982) 147-160; R. Reisfeld and C.K. Jorgensen, Excited state phenomena in vitreous materials, in K.A. Gschneidner and L. Eyring (eds) *Handbook on the Physics and Chemistry of Rare Earths* 9, chapt. 58, North-Holland, Amsterdam (1987) 1-90.

We used to discuss our work and to write the papers in most incredible places: airports when waiting for change of planes during the trips to conferences, picnic in the Alps where we met with our French colleagues. A picnic was something totally unknown to Christian, a situation he has never experienced before. He was totally absorbed in an unlimited number of books which he swallowed day and night.

His encyclopedic knowledge was unlimited and I could ask him about any subject and receive an immediate answer. I remember when I was planning with my husband a trip to Brazil he gave me a full description of the exotic places we

should visit including detailed geography, history and folklore. He was always very considerate about our security especially after my kidnapping.

During the Gulf war when we were in a closed room being afraid of Sadam Hussein rockets, he telephoned several times each day and this was certainly heart warning. I could write many more pages about our friendship and interaction that was a bright side of our life. I shall remember Christian warmly for ever.

9
In Memory of Christian Klixbüll Jørgensen

H.-H. Schmidtke

I knew Christian Klixbüll from 1961 when I joined his group which he called "Theoretical Inorganic Chemistry" of Cyanamid European Research Institute in Cologny, Canton de Geneve, Switzerland. Each of the six groups in this institute had about four scientists and in addition some laboratory technicians and secretaries, the whole being administered by a management staff. I found out very soon, that Christian was, what we call in German an "Einzelkämpfer" (individual fighter), who does his research more efficiently when working by himself. Therefore the bulk of his papers had only his name on the authors' list. In addition, he preferred working in the laboratory on his own using hundreds of glasses, beakers, flasks etc. on the bench for his experiments, the reason and meaning of which nobody could figure out because they were unlabelled. The work of the laboratory technician he had at his disposal was limited to cleaning up all the used dishes and tools which took him several days.

Christian's working habits coincided with the plans I had at that time very well. When I started to work in Geneva he asked me what kind of research I was planning to do. I told him that I would like to work on Rh(III) and probably Ir(III) chemistry in order to show the degree of parallelism to Co(III). He seemed to be surprised and answered "oh, very interesting!" – repeating it several times. Much later I found out that this phrase did not necessarily mean agreement but rather some measure of reservation. Christian rarely could say "no" when he was asked for something. Any opinion different to his views meant an instant requirement of a discussion of the topic. This was done at great length. As a consequence I could work on following my own ideas and he never interfered with my research plans and their realization. I could publish my results on my own as he did for his work. There was, however, an important exception. One day in 1963, he came early to the laboratory and made a proposal to Romano Pappalardo, the other research scientist in our group, and me that we should prepare an article on the occasion of the 50th paper of CERI-TIC (Cyanamid European Research Institute-Theoretical Inorganic Chemistry), which was a series of preprints Christian used to distribute according to a special list of possibly interested people. As usual, he had already prepared a manuscript during the week-end dealing with a subject which I immediately felt was very much worth publishing. It was the start up of a model alternate to the ligand field theory, which later was called the "Angular Overlap Model". I remember that I discussed the text of the manuscript with

Christian in much detail which took us several days. He used to submit his papers the way they were originally written without making many changes or editing for revision. Since some journals insist on certain styles and sophisticated writing, substantial changes of the text usually have to be carried out before acceptance. Christian rather preferred sending his articles somewhere else for straightforward publication instead of going through tedious revisions. Since we decided to publish our 50. CERI-TIC in a prominent journal and we chose Journal of Chemical Physics, I recall that I had to struggle with Christian for some long discussions in order to make the manuscript easily readable and understandable to the public. And I believe we succeeded: see JCP 39, 1422 (1963).

Generally Christian devoted much care to a well-ordered system of classifying his CERI-TIC papers. The surplus copies of these preprints which were not distributed from his mailing list, and the regular reprints of the published articles were piled up in an extra room under the roof of the institute and Christian spent his happy hours as our secretary heard him humming and gently singing during inspection of his written stock of intellectual achievements.

Discussing science was always his most favourite occupation. Any easy talking turned inevitably into a chemistry problem. And everybody knew about is profound knowledge on chemistry. He had a photographic memory, he had hundreds of spectra in his mind and recalled among other data all wavenumbers and intensities of bands thereof: a phenomenon nobody could compete with. For his private teaching, any audience was all right with him. He reported on his ideas during lunch in the cafeteria, in detail to colleagues in the halls or in the library of the institute no matter whether they were experts in the field or not. I even heard him teaching his wife and young children when he was absorbed in communicating or ordering his latest thoughts and ideas on chemistry.

So, for Christian Klixbüll science was his whole life, his thoughts in fact were always occupied with chemistry. Therefore he eventually had same trouble with handling the small problems of daily life. But as long as his wife was alive, a fine French lady he met when he was working in Paris with the NATO science advisor, he enjoyed great happiness with his family at home.

10
Christian Klixbüll Jørgensen – Memories of the Later Years in Geneva

Alan F. Williams

I first met Christian Jørgensen in January 1975 when I arrived in Geneva as a post-doctoral fellow, and we were office neighbours and colleagues for over twenty years until his retirement in 1997. His appearance changed remarkably little over this period: medium height, slightly stooped, but strongly built. His breadth was enhanced by his wearing a jacket which seemed a size or two too large even for his considerable build, but this was necessary since it had to act not only as an article of clothing, but also as a receptacle for a vast number of papers, index cards, pens, etc. which could be extracted in an instant to make notes or confirm some fact vital to the conversation in progress. He had a fine head, almost completely bald, with just a fringe of blond hair around the edges, and

clear grey eyes, somewhat hooded by the dome of his forehead. His Danish origins were obvious when he spoke: although his command of languages was excellent, he always kept a strong inflexion which prompted a colleague to comment that 'he speaks Danish in six languages'.

He was approachable, and happy to talk to anyone, although I noticed he always maintained a certain formality towards students. He very rarely raised his voice and in twenty years I can remember only one disparaging comment. He was a voracious reader: as a child he claimed to have read all the books in one of Copenhagen's municipal libraries, and his love of books continued, as was shown by their steady accumulation in his office. Apart from chemistry and physics, philosophy, history, astronomy, and science fiction figured prominently in his collection. His accumulation of books and papers did create certain problems in his office: as the bookcases filled up, the desk and window ledges were occupied, followed by the occupation of floor space, at first around the borders of the room, and then gradually moving in to the centre. At a certain point when there remained only a narrow path through the room, it was clear that something would have to be done, and Jørgensen's solution, of moving into the next office, was simple and effective, although it was not without apprehension that I, as his immediate neighbour, observed the second office filling up steadily.

He undoubtedly had the mentality of a collector, and had been an enthusiastic collector of stamps when younger, although in later life he turned to collecting old banknotes. My wife, upon meeting him for the first time, was somewhat surprised to be asked "As an Australian, you must remember that unusual note from 1931?"' I believe the collecting instinct was an important aspect of his intellectual character. He was aided by a truly phenomenal memory which enabled him to pluck a reprint from exactly the right pile in his office and carefully correct a misprint in the page numbers of a reference in a paper published twenty years before. The collector's capacity to accumulate and organise was one of the strengths which helped him to identify the general features of the spectra of inorganic compounds, which I believe to have been his major contribution to chemistry.

By the time I arrived in Geneva, he was reaching the end of his period of interest in X-ray photoelectron spectroscopy which had interested him from 1971. I have always felt that he was disappointed by its failure to be a more generally useful tool in the investigation of chemical bonding, although to what extent this is due to inherent weaknesses, or to the practical difficulties, notably involved with charging effects and calibration problems, remains open. After the abandon of photoelectron spectroscopy he carried out very little practical work in Geneva, although some studies on candoluminescence provided an amusing exception. Jørgensen's approach to this was quite simple: a sample of cotton (from an old pillowcase) was dipped in a solution of cerium or thorium salts, suitably laced with lanthanides, then held on a pair of tongs in the flame of a huge Bunsen burner that he had acquired somewhere. The organic matter was immediately burned off leaving an oxide matrix which shone brightly, as in a gas mantle. He would then examine the emission through a pocket spectroscope. On one occasion, his enthusiasm had led him to begin work before he had removed the wide brimmed hat that he was wearing, and as he peered through the spectroscope, he

became aware of a burning sensation as the brim of the hat dipped into the flame. He immediately ran towards his collaborator, tongs in one hand and spectroscope in the other, crying 'Je brûle, je brûle!' Fortunately his co-worker was able to extinguish the hat before major damage was done.

He never made any effort to build up a research group, and only a handful of students acquired doctorates under his supervision. While this was a consequence of his rather solitary character, it was unfortunate. In Copenhagen and at Cyanamid he had benefited from the presence of other active research groups in inorganic chemistry who undoubtedly stimulated him. When he moved to the University of Geneva in 1968, there were no other inorganic chemists and he was rather isolated. He was not particularly attracted to many of the most active fields in inorganic chemistry at that time: kinetics and mechanism, organometallic chemistry, or general structural chemistry. He remained rather sceptical of the future of calculations in quantum chemistry. It was not in his character to undertake detailed spectroscopic studies of one or two compounds, however much he appreciated this kind of work. As a result of this, his published work from 1975 onwards (just under 200 papers, nearly half the total) can be split up into his work on lanthanides in collaboration with Renata Reisfeld, where the practical work was done in Jerusalem, and a series of rather general papers, discussing general (and often almost philosophical) themes such as hardness and softness, or reviews. He was never afraid to speculate: in 1971 he published a paper on the predictable chemistry of superheavy elements such as Z=164, and in 1978 a paper on the chemistry of quarks. It seems reasonable to claim that having studied elements between Z=1/3 and Z=164, he must be regarded as the chemist having examined the widest range of elements – he would undoubtedly have appreciated the distinction. He was certainly fascinated with the developments in elementary particle theory

Jørgensen's relationship with teaching was somewhat conflictual: basically he did not greatly like it, and felt he could usefully use the time doing something else, but on the other hand he loved lecturing. Although towards the end of his life he moved over to transparencies, he was a great lover of the blackboard. He had very neat writing, and used to submit handwritten manuscripts until he was forced to move to the typewriter – I never saw him use a computer. His blackboard technique was unusual: when the board was more or less full, rather than erase, he would look to see if there were any spots which had not yet been used. When these were full he would often simply take a chalk of a different colour and write over the first. He gave the students a 80 page handout, essentially handwritten, to accompany his lectures on inorganic chemistry. This is a remarkable document as much for what it contains as for what is left out: the alkalis and alkaline earth metals never greatly interested him. I asked him about their exclusion once, and he seemed to think that they could best be assimilated to organic chemistry. The examinations in Geneva are in general oral, and were an occasion of stress. For someone who loved talking about chemistry, it was hard if not impossible to remain silent while the student struggled to find an answer. Jørgensen would try to ask the question another way, and if this elicited no response, yet another way. If an answer was forthcoming, it had to be commented. In a half-hour examination, a tongue-tied student might only speak for a few minutes. Despite

these idiosyncrasies, which would no doubt horrify a modern assessor of pedagogy, the students had a genuine respect for a professor who was quite clearly intellectually outstanding. Concerning administrative duties, the third pastime of modern academics, it may simply be said that Jørgensen and they avoided each other to their mutual satisfaction. At the few committee meetings in which he participated, he generally remained silent, but occasionally made a comment, particularly when he identified a paradox, and was a past master of the witty metaphor.

There is little doubt that the first half of his career was more significant than the period I have discussed here. His isolation, and the divergence of his interests from those of many of his former colleagues prevented the symbiosis which had proved so fruitful before. He undoubtedly was saddened by the lessening of interest of the inorganic community in his work although he never spoke of it. In general, he kept his feelings very much to himself, and had relatively few close friends. For myself, our hours of conversation opened my eyes to many previously unknown areas of chemistry, and of science in general. I will recall a deep voice saying 'As you know better than I' before telling me something of which I had no previous inkling. These discussions were always fascinating, even if, as others have remarked, it was not always obvious when they would end. However, the eccentricities and anecdotes related here should not be allowed to overshadow his major scientific achievements. His early work and his books on ligand field theory and absorption spectra will remain important references, even if they are sometimes made harder to understand by a somewhat elliptical approach to the subject matter. It is to be hoped that the chemical community will remember and honour a man who was remarkable as much for his character as for his contributions to the subject.

References to the Personal Note from F. Calderazzo

1. (a) Hoppe R, Dähne W, Mattauch H, Rödder KM (1962) Angew Chem 74:603; (b) Weeks JL, Chernick CL, Matheson MS (1962) J Am Chem Soc 84:4612
2. Claasen HH, Selig H, Malm JG (1962) J Am Chem Soc 84:3593
3. Burns JH, P. Agron A, Levy HA (1963) Science 139:1208
4. Quadrelli EA (2002) Inorg Chem 41:167 *and references therein*
5. Matonic JH, Scott BL, Neu MP (2001) Inorg Chem 40:2638